



<https://theses.gla.ac.uk/>

Theses Digitisation:

<https://www.gla.ac.uk/myglasgow/research/enlighten/theses/digitisation/>

This is a digitised version of the original print thesis.

Copyright and moral rights for this work are retained by the author

A copy can be downloaded for personal non-commercial research or study,  
without prior permission or charge

This work cannot be reproduced or quoted extensively from without first  
obtaining permission in writing from the author

The content must not be changed in any way or sold commercially in any  
format or medium without the formal permission of the author

When referring to this work, full bibliographic details including the author,  
title, awarding institution and date of the thesis must be given

Enlighten: Theses

<https://theses.gla.ac.uk/>  
[research-enlighten@glasgow.ac.uk](mailto:research-enlighten@glasgow.ac.uk)

RADIOTRACER STUDIES OF THE METAL CATALYSED  
HYDROGENATION OF UNSATURATED HYDROCARBONS

by

NIVALDO CABRAL KUHNEN, M.Sc.

A THESIS SUBMITTED FOR THE DEGREE OF

DOCTOR OF PHILOSOPHY

OF THE UNIVERSITY OF GLASGOW

February, 1981

Chemistry Department,  
University of Glasgow.

ProQuest Number: 10984238

All rights reserved

INFORMATION TO ALL USERS

The quality of this reproduction is dependent upon the quality of the copy submitted.

In the unlikely event that the author did not send a complete manuscript and there are missing pages, these will be noted. Also, if material had to be removed, a note will indicate the deletion.



ProQuest 10984238

Published by ProQuest LLC (2018). Copyright of the Dissertation is held by the Author.

All rights reserved.

This work is protected against unauthorized copying under Title 17, United States Code  
Microform Edition © ProQuest LLC.

ProQuest LLC.  
789 East Eisenhower Parkway  
P.O. Box 1346  
Ann Arbor, MI 48106 – 1346

## ACKNOWLEDGMENTS

This work was carried out in the Surface Chemistry Laboratories within the Department of Inorganic Chemistry in the University of Glasgow.

I would like to record my sincere gratitude to Professor S.J. Thomson and Dr. G. Webb, my supervisors, for their continued guidance and discussions throughout the course of this work.

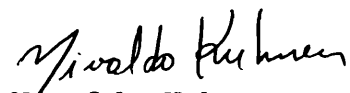
I am indebted to my colleagues and members of the academic staff of this department for their assistance during my studies in Glasgow.

I am indebted also to the technical staff of this department for the services they have provided.

I would like to acknowledge the financial support received from the British Council and the Universidade Federal de Santa Catarina - Brazil.

Finally, I wish to thank Miss E. Forbes for her patience and endeavour in typing the manuscript.

February, 1981

  
Nivaldo Kuhn,  
Chemistry Department,  
Glasgow University.

TO  
H I L D A  
AND  
Y U R I

## SUMMARY

The hydrogenation of allene over alumina-supported rhodium, iridium and palladium catalysts and the adsorption and hydrogenation of propylene over alumina-supported rhodium catalysts have been studied at ambient temperature by radiotracer techniques using a static constant volume reactor system.

The catalytic activities of the various catalysts are in the order: Palladium > Rhodium > Iridium. The hydrogenation of allene over alumina-supported rhodium and palladium showed a high selectivity for the formation of propylene in the first stage of the reaction; alumina-supported iridium gave a slightly higher production of propane than propylene.

During a series of allene hydrogenations over alumina-supported rhodium and palladium catalysts the rate of reaction progressively decreased to a "steady state" constant activity. A surface hydropolymerisation process is suggested as the most likely cause of the deactivation.

Propylene adsorption isotherms on freshly reduced alumina-supported rhodium catalysts exhibited two well-defined regions; a non-linear primary region, followed by a linear secondary region. Propylene was dissociatively adsorbed on the primary region, which, from comparison with the amounts of carbon monoxide adsorbed on the same catalyst sample, was shown to correspond to monolayer coverage of the

metal by hydrocarbon, and associatively adsorbed on the secondary region. The catalyst in the "steady state" gave rise only to secondary adsorption. Hydrogenation catalysis involved the propylene species adsorbed on the secondary region. Hydrogen treatment of the adsorbed species showed that a fraction of the [ $^{14}\text{C}$ ]propylene adsorbed on the secondary region was always retained by the catalyst as a strongly adsorbed species.

The progressive deactivation of the catalyst was accompanied by a gradual build-up of adsorbed species which could not be removed by prolonged treatment with hydrogen at ambient temperature. As the catalyst reached the "steady state" the primary region was totally covered by this permanently adsorbed species.

The role of the primary region in determining the catalytic activity of the surface is proposed to be one in which a hydrogen deficient hydrocarbon species acts as a hydrogen transfer medium for the addition of hydrogen to a propylene molecule, which is associatively adsorbed on the secondary region. Deactivation is considered to be a process whereby such a species, which is considered to be the site for the activation of hydrogen, is reduced in concentration, by participation in another surface process to a steady state value.

It was observed that during the hydrogenation of allene in the presence of [ $^{14}\text{C}$ ]propylene the amount of propane produced from the hydrogenation of propylene was very small

compared with the total propane yield. It is concluded that, in allene hydrogenation, the formation of propane occurs by a route not involving formation of propylene as an intermediate.

Similar conclusions were drawn from the results of the hydrogenation of allene over a carbon monoxide-poisoned catalyst. Over such carbon monoxide poisoned catalysts the hydrogenation of propylene was less affected than the hydrogenation of allene although the presence of adsorbed carbon monoxide resulted in an increase in selectivity.

The results of studies of the adsorption of propylene on allene precovered catalysts and of the hydrogenation of allene in the presence of [ $^{14}\text{C}$ ]propylene lead to the conclusion that three distinct types of site exist on the catalyst surface. Type I sites are active for the direct conversion of allene to propane. Type II sites are active for the hydrogenation of allene to propylene and for the hydrogenation of propylene. Type III sites are active for propylene hydrogenation, but inactive for allene hydrogenation.

A catalyst treated with carbon monoxide and then evacuated presented a reduced catalytic activity. The presence of carbon monoxide in the allene and hydrogen mixture resulted in complete poisoning of the catalyst.

An alumina-supported rhodium catalyst surface which had been totally covered with carbon monoxide and then treated with hydrogen or hydrogen/allene mixture was capable of further uptake of carbon monoxide.

## CONTENTS

	Page
Acknowledgments	
Summary	
<u>Chapter One</u> <u>Introduction</u>	1
1.1            Historical Introduction	1
1.2            Chemisorption and Physical Adsorption	3
1.2.1          Chemisorption	4
1.3            Adsorption Isotherms	5
1.4            Catalysis and Radioactive Tracer Methods	8
1.4.1          Surface Area	9
1.4.2          Catalyst Poisoning	10
1.4.3          Surface Heterogeneity	12
1.4.4          Mechanism	14
1.5            Adsorbed States of Unsaturated Hydrocarbons on Metal Catalysts	18
1.5.1          Adsorbed State of Ethylene	20
1.5.2          Adsorbed State of Acetylene	23
1.5.3          Adsorbed State of Propylene	27
1.5.4          Adsorbed State of Allene	31
1.6            The Hydrogenation of Alkynes and Dienes	32
1.6.1          The Hydrogenation of Acetylene	38

		Page
1.6.2	The Hydrogenation of Allene	41
1.7	Adsorbed State of Carbon Monoxide	45
<u>Chapter Two</u>	<u>Aims of the Present Work</u>	50
<u>Chapter Three</u>	<u>Apparatus and Experimental Procedure</u>	52
3.1	The Vacuum System	53
3.2	The Reaction Vessel and the Geiger-Müller Counters	54
3.2.1	Intercalibration of the two Geiger-Müller Counters	56
3.2.2	Determination of Gas Phase and Surface Radioactivity Using GM(A) and GM(B)	56
3.2.3	Radiation Absorption Effects	57
3.3	The Gas Chromatographic System	58
3.4	The Proportional Counter	60
3.5	The Pressure Transducer	63
3.6	Materials	64
3.6.1	Gases	64
3.6.2	Catalysts	67
3.7	Experimental Procedure	68
3.7.1	Hydrogenation Reactions	68
3.7.2	Adsorption Isotherms	69

<u>Chapter Four</u>	<u>Results</u>	Page
4.1	The Phenomenon of Self-Deactivation	70
4.1.1	Reactions over Alumina-Supported Palladium	70
4.1.2	Reactions over Alumina-Supported Iridium	73
4.1.3	Reactions over Alumina-Supported Rhodium	75
4.1.3.1	Allene Hydrogenation	75
4.1.3.2	Acetylene Hydrogenation	77
4.2	Adsorption of [ $^{14}\text{C}$ ]Propylene on Supported Rhodium Catalysts	80
4.2.1	[ $^{14}\text{C}$ ]Ethylene Adsorption Isotherms	81
4.2.2	[ $^{14}\text{C}$ ]Propylene Adsorption Isotherms on a Freshly Reduced Silica-Supported Rhodium Catalyst	82
4.2.3	[ $^{14}\text{C}$ ]Propylene Adsorption Isotherms on Alumina-Supported Rhodium Catalysts	85
4.2.3.1	[ $^{14}\text{C}$ ]Propylene Adsorption Isotherms on Freshly Reduced Alumina-Supported Rhodium Catalysts	86
4.2.3.2	[ $^{14}\text{C}$ ]Propylene Adsorption Isotherms on a Freshly Reduced Alumina-Supported Rhodium Catalyst in the presence of Allene	92

	Page	
4.2.3.3	The Effect of Self-Deactivation upon the [ $^{14}\text{C}$ ]Propylene Adsorption Isotherms	93
4.2.3.4	[ $^{14}\text{C}$ ]Propylene Adsorption Isotherms on a Steady State Alumina-Supported Rhodium Catalyst	94
4.2.3.5	[ $^{14}\text{C}$ ]Propylene Adsorption Isotherm on a Steady State Rh/alumina Catalyst in the Presence of Allene	96
4.3	[ $^{14}\text{C}$ ]Tracer Studies of Added Propylene on the Hydrogenation of Allene	97
4.3.1	Allene Hydrogenation in the Presence of 5.1 torr of [ $^{14}\text{C}$ ]Propylene	98
4.3.2	Allene Hydrogenation in the Presence of 2.01 torr of [ $^{14}\text{C}$ ]Propylene	101
4.3.3	Allene Hydrogenation in the Presence of 1.26 torr of [ $^{14}\text{C}$ ]Propylene	104
4.3.4	The Yield of [ $^{14}\text{C}$ ]Propane	104
4.4	The Effects of Carbon Monoxide Poisoning upon the Adsorption of [ $^{14}\text{C}$ ]Propylene and the Hydrogenation of Allene	106
4.4.1	The [ $^{14}\text{C}$ ]Carbon Monoxide Adsorption Isotherm on a Freshly Reduced Alumina-Supported Rhodium Catalyst	106

		Page
4.4.2	The [ $^{14}\text{C}$ ]Carbon Monoxide Adsorption Isotherm on a Freshly Reduced Alumina-Supported Rhodium Catalyst in the Presence of Allene	107
4.4.3	The [ $^{14}\text{C}$ ]Carbon Monoxide Adsorption Isotherm on a Steady State Alumina-Supported Rhodium Catalyst	108
4.4.4	The [ $^{14}\text{C}$ ]Carbon Monoxide Adsorption Isotherm on a Steady State Alumina-Supported Rhodium Catalyst in the Presence of Allene	109
4.4.5	The [ $^{14}\text{C}$ ]Propylene Adsorption Isotherm on a Freshly Reduced Alumina-Supported Rhodium Catalyst in the Presence of Carbon Monoxide	110
4.4.6	The Effect of Carbon Monoxide Poisoning upon the Catalytic Activity of a Freshly Reduced Alumina-Supported Rhodium Catalyst	111
4.4.7	The Effect of Carbon Monoxide Poisoning upon the Catalytic Activity of a Freshly Reduced Alumina-Supported Rhodium Catalyst in the Presence of Allene	113
4.4.8	The Effect of Carbon Monoxide Poisoning upon the Catalytic Activity of a Steady State Alumina-Supported Rhodium Catalyst	113

4.4.9	The Effect of Carbon Monoxide Poisoning upon the Catalytic Activity of a Steady State Alumina- Supported Rhodium Catalyst in the Presence of Allene	114
4.5	Accumulative [ $^{14}\text{C}$ ]Carbon Monoxide Adsorption on an Alumina-Supported Rhodium Catalyst	115
4.5.1	Accumulative [ $^{14}\text{C}$ ]Carbon Monoxide Adsorption on a Freshly Reduced Alumina-Supported Rhodium Catalyst	115
4.5.2	Accumulative [ $^{14}\text{C}$ ]Carbon Monoxide Adsorption on a Steady State Alumina-Supported Rhodium Catalyst	116
<u>Chapter Five</u>	<u>Discussion</u>	
5.1	The Deactivation Phenomena	117
5.2	Behaviour of [ $^{14}\text{C}$ ]Propylene Adsorbed on Supported-Rhodium Catalysts	124
5.3	Allene Hydrogenation in the Presence of [ $^{14}\text{C}$ ]Propylene	130
5.4	Carbon Monoxide Adsorption and its Effects upon Allene Hydrogenation	136
5.5	Accumulative Adsorption of Carbon Monoxide on Alumina-Supported Rhodium	139
<u>References</u>		143

## CHAPTER ONE

# C H A P T E R 1

## INTRODUCTION

### 1.1 Historical Introduction

One of the earliest recorded patterns of catalytic activity was made by H. Davy(1), when he investigated the combustion of gaseous mixtures in the presence of a platinum wire. He wrote "... the oxygen and coal gas in contact with the hot wire combined without flame, and yet produced heat enough to preserve the wire ignited, and to keep up their own combustion." Davy also discovered that a coating of sulphide poisoned the wire destroying its igniting power. Experiments on heterogeneous catalytic oxidation appeared in the literature in the following years. E. Davy(2) prepared a finely divided platinum catalyst which did not have to be hot to initiate oxidation. Dulong and Thenard(3) and Doebereiner(4) found that some metals (palladium, iridium) would bring about the hydrogen-oxygen reaction at ambient temperatures and others were active only at elevated temperatures (cobalt and nickel at 300°C and rhodium at 240°C). W. Henry(5) found that the oxidation of hydrocarbons over platinum sponge was not as easy as the oxidation of hydrogen.

To describe a series of experimental observations, which included the above mentioned oxidations, Berzelius(6) in

1836 used the words catalysis and catalytic force. The phenomenon was called catalysis and it could occur at the surface of solids which possessed a catalytic force.

The adsorption of gases at the surface of solids was known at that time and Faraday(7) proposed that the heterogeneously catalysed reactions, such as the combination of hydrogen and oxygen, occurred between adsorbed molecules of the reactants. During the first decade of this century Ostwald pointed out that a catalyst cannot change the equilibrium position in a reversible reaction, but could only increase the rate at which the equilibrium was attained. If a catalyst existed which altered the chemical equilibrium of a reversible reaction it would not obey the second law of thermodynamics.

At that time it was already established that:

- (1) a catalyst does not alter the equilibrium position in a reversible reaction, and consequently;
- (2) a catalyst must affect equally the rates of both forward and back reactions;
- (3) a catalyst cannot initiate reactions that are not thermodynamically feasible;
- (4) a catalyst may determine which path is followed when, for a given reactant, several alternative reaction paths are permissible.

In the following decades several significant contributions were made to the understanding of heterogenous

catalysis. Langmuir(8,9) developed the theoretical approach for the process of adsorption with and without dissociation. The Langmuir-Hinshelwood(10) mechanism postulated that the rate of heterogeneous reactions is controlled by the reaction of the adsorbed molecules and Rideal(11,12) proposed that surface catalytic reactions took place between a chemisorbed species and a physically adsorbed molecule. Taylor(13,14) introduced the idea of active sites and suggested that chemisorption involved an activation energy.

These were important contributions to the understanding of heterogeneous catalysis but the bulk of experiments which gave rise to our present knowledge of the phenomenon of catalysis was carried out in the last three decades.

## 1.2 Chemisorption and Physical Adsorption

The phenomenon of adsorption arises because, in a direction normal to the surface, the field of the surface lattice elements is not balanced and is capable of retaining molecules, from the gas phase, that contact the surface. The adsorption process is in most cases an exothermic process. This can be expected from the equation

$$\Delta G = \Delta H - T \Delta S,$$

since the reduction of certain degrees of freedom of the adsorbed molecules results in a decrease in entropy and, as adsorption is a spontaneous process proceeding with the decrease of the free energy of the system, the value of the

enthalpy of the system must also decrease. Endothermic chemisorption is, however, sometimes encountered(15,16).

Adsorption is commonly classified into two types, namely chemisorption and physical adsorption. The physical adsorption or van der Waals adsorption involves forces of the van der Waals type and can, in principle, occur between all gases and all solids, since it can be considered a condensation phenomenon. The heat involved in physical adsorption is small and often of the same order of magnitude as the heat of liquefaction of the adsorbate gas. A molecule physically adsorbed is not associated with any particular surface atom and it occupies an area independent of the nature of the solid. The property of physically adsorbed molecules is used in the determination of surface areas of catalysts as in the Brunauer, Emmett and Teller method(17). During the physical adsorption process formation of multilayers can take place, since the forces involved between adsorbate and adsorbent are of similar magnitude to those involved between molecules in a liquid.

### 1.2.1 Chemisorption

The free valencies present at the surface of, for example, metals provide sites for the adsorption of gas molecules and when there is a chemical reaction between the molecule being adsorbed and the metal surface the adsorption is termed chemisorption. The chemical bonds formed are, of course,

stronger than the physical forces involved in physical adsorption. The heat of chemisorption may vary between 10 and 150 kcal mol<sup>-1</sup>, although in a very few cases it may be as low as the heat of physical adsorption. Thus, for example, the heat of chemisorption of hydrogen on certain metals barely exceeds 3 kcal mol<sup>-1</sup> (18,19).

Some other characteristics of chemisorption are enumerated below:

- (1) chemisorption is highly specific and stops when a monolayer is formed;
- (2) the chemisorption process can lead to the dissociation of the adsorbate molecule;
- (3) chemisorption occurs over a wide range of temperature;
- (4) an activation energy is often involved in chemisorption.

### 1.3 Adsorption Isotherms

The relation between the quantity of material adsorbed and its equilibrium pressure at a fixed temperature is called an adsorption isotherm. The mathematical equation for an adsorption isotherm derived by Langmuir at the beginning of the century is of the form

$$\theta = \frac{bp}{1 + bp}$$

where  $\theta$  is the fraction of surface covered with adsorbed atoms or molecules,  
 $p$  is the gas pressure and,  
 $b$  is a constant proportional to  $\left[ \exp\left(\frac{-\Delta H_a}{kT}\right) \right]$   
where  $\Delta H_a$  is the heat of adsorption.

Langmuir extended this treatment to dissociative and competitive adsorption and obtained analogous equations.

Three important assumptions are made in the derivation of the Langmuir adsorption isotherm. These are as follows:

- (1) the adsorbed species are in a monolayer;
- (2) adsorption involves only one adsorbed particle per site;
- (3) the energy of an adsorbed particle is the same at any site and is unaffected by adsorption on neighbouring sites, i.e. the heat of adsorption is independent of surface coverage.

The third assumption is rarely valid. For many chemisorption systems, heats of adsorption obtained experimentally generally decrease with surface coverage(20). The reasons for the fall in the heat of adsorption with surface coverage have been discussed and three possible explanations have appeared in the literature(21-23). First, it may be due to surface heterogeneity. Adsorption on active sites is energetically more favoured than on other sites of lower adsorption potential. A second explanation is that falling heats of adsorption are due to forces of repulsion between

oriented dipoles of molecules in the adsorbed layer. The third explanation is based on the concept of work function. The greater the coverage, the greater the energy required to excite an electron from the conductivity band to the surface orbital and hence the smaller the heat of adsorption. If, on the other hand, an electron is donated by the gas the first electron will enter the lowest unoccupied level of the band system and then higher and higher levels will be used as adsorption proceeds. Again the heat will fall.

The adsorption isotherms of Freundlich(24) and Temkin (25-27) were derived to take into account the observation that the heat of adsorption is dependent on surface coverage. Table 1 shows a selection of adsorption isotherms(28).

Five different kinds of physical adsorption isotherms were first clearly recognised by Brunauer(29) and one of the most successful attempts to describe multilayer adsorption was made by Brunauer, Emmett and Teller (the BET theory)(17). The theory is not always satisfactory and has been modified by a number of investigators(30,31), but nevertheless its assumptions are sufficient for the interpretation of some experimentally observed phenomena. The BET equation offers one of the best ways to estimate the total surface areas of a solid. When it is applied to a supported metal catalyst it gives the total

Table 1

A selection of adsorption isotherms

Name	Isotherm Equation	Applicability
Langmuir	$\frac{v}{v_m} = \theta = \frac{bp}{1 + bp}$	Chemisorption and physical adsorption
Freundlich	$v = kp^{1/n}, (n > 1)$	Chemisorption and physical adsorption
Henry	$v = k'p$	Chemisorption and physical adsorption
Slygin-Frumkin Temkin	$\frac{v}{v_m} = \theta = \frac{1}{a} \ln c_0 p$	Chemisorption
Brunauer Emmett Teller (BET)	$\frac{p}{v(p_0 - p)} = \frac{1}{v_m c} + \frac{(c-1)}{v_m c} \frac{p}{p_0}$	Multilayer physical adsorption

$v$  is the volume adsorbed;

$v_m$  is the volume required to cover the adsorbent surface with a monomolecular layer of adsorbate;  $\theta$  is the fraction of the monolayer covered at an equilibrium pressure  $p$ ;  $p_0$  is the saturated vapour pressure of the adsorbate; all other symbols are constants.

area of the metal plus catalyst. To determine only the area of the metal in a supported metal catalyst by means of an adsorption method the gas used should adsorb specifically on the metal component. Carbon monoxide and hydrogen are among the gases which have been used for this purpose(32,33). Other methods of determining the metal surface area involving surface reactions have also been employed(34,35).

#### 1.4 Catalysis and Radioactive Tracer Methods

The use of radioisotopes in the study of adsorption and catalysis has been increasing in importance since the early work of Paneth(36) and it is now a well established technique. The use of isotopic tracers in studying catalysts and catalytic reactions was reviewed by Emmett(37). He discussed and illustrated the chemisorption of molecules and the nature of the catalyst surface, the measurement of the extent to which surface atoms of a catalyst participate directly in catalytic reactions and the mechanism by which the catalytic reactions take place on the catalytic surface. A review by Trimm(38) gave special attention to carbon isotopes in the study of heterogeneous catalysis. Campbell and Thomson(39), more recently reviewed selected aspects of the use of radioisotopes in studies of chemisorption and catalysis emphasising the ways in which tracers give information which would be difficult to obtain by any other means.

#### 1.4.1 Surface Area

Radiotracer methods have been used in surface area measurements. When physical adsorption occurs the standard practice in evaluation of a surface is to employ the Brunauer, Emmett and Teller method where the amount of gas adsorbed is measured by its disappearance from the gas phase. Radioactive krypton and xenon have both been used as adsorbates at 77K (40,41). It should be noted that what is actually determined by this technique is the partial pressure of a radioactive isotope which, if isotopic effects are negligible, is equal to the partial pressure of the adsorbate. In contrast to this technique Clarke(42) measured, by counting the 0.53 Mev  $\gamma$  radiation from krypton-85, the amount of krypton actually adsorbed on the solid which is a function of the surface area.

When chemisorption occurs on, for example, supported metal catalysts, it only reveals the adsorption sites on the metal and thus the area of supported metal catalysts, when measured by the two types of adsorption, will be different. Radioactively labelled gases can be used to measure the amount of gas chemisorbed on metal surfaces and Crowell and Farnsworth(43) demonstrated that such data could in fact be obtained for small area surfaces such as a face of a single metal crystal. Hughes et al.(44) used a flow system for catalyst metal surface area measurements. A known mixture of radioactive carbon monoxide and an inert carrier gas was

pumped over the catalyst at a constant rate. The concentration of unadsorbed carbon monoxide in the gas was measured by a Geiger-Müller counter. The authors applied this method to platinum, nickel, rhodium and reduced chromium oxide catalysts and investigated dispersion, sintering and correlation of catalytic activity with extent of metal surface available for carbon monoxide chemisorption.

Although radioactive carbon monoxide has been extensively used in studies of metal areas there still remain uncertainties in the stoichiometry of the chemisorption, which create difficulties in its use for absolute surface area determination. The chemisorption of carbon monoxide will be considered in more detail in section 1.7.

#### 1.4.2 Catalyst Poisoning

The poisoning of a catalyst by small amounts of impurities, usually molecules with lone pairs of electrons, has been investigated by radiotracer techniques. Campbell and Thomson(39,45) used radiotracer techniques to obtain information on whether the arrival of molecules of one species at the catalyst surface results in adsorption, and whether a previously adsorbed species is displaced during the process. These authors studied the selective poisoning of a nickel catalyst by mercury using mercury-203 and tritium. The poisoned catalyst was not active in cyclopropane hydrogenation but was active in propylene hydrogenation. They obtained evidence to show that mercury

poisons the catalyst simply by adsorbing on its surface and thereby blocking potentially active sites. They also gave an explanation for the selective poisoning based on the behaviour of the different species in adsorption and displacement.

Webb and MacNab(46) used mercury-203 as a catalyst poison to show that on supported rhodium catalysts, the hydrogenation and isomerization of 1-butene occur independently of each other and that the support may have a significant role in determining the isomerization activity of supported metal catalysts.

The poisoning effect of carbon monoxide for the hydrogenation of acetylene by supported metal catalysts was reported by Al-Ammar and Webb(47). They studied the adsorption of [ $^{14}\text{C}$ ]carbon monoxide in an attempt to understand further the poisoning effects of the carbon monoxide and concluded that the poisoning effects of carbon monoxide are not due simply to a hydrocarbon site-blocking effect but rather could be due to a hydrogen site-blocking effect.

#### 1.4.3 Surface Heterogeneity

In an ideal crystal all the atoms are arranged in a strictly regular manner. Metal catalysts are, however, normally very far from this ideal uniform state. A catalyst surface is not uniform but consists of different crystal planes involving different geometry and interatomic

distances and presents terraces, steps, kinks and vacancies. Thus a range of different strengths of adsorption and types of adsorption are possible.

Radiotracer techniques have been used to prove experimentally the existence of such surface heterogeneity, and to demonstrate the existence of active sites which form only part of the surface of catalysts. One way to study the surface heterogeneity was pointed out by Roginskii and Keier(48,49). By covering one fraction of the surface with one form of adsorbate and another part with an isotopic form the authors expected, if the surface was heterogeneous, to observe during a thermally assisted desorption the first adsorbate to desorb last. This has been applied satisfactorily by Schuit(50) and Gundry(51) to nickel surfaces. This method suffers from the disadvantage that heating may increase the probability of surface migration of atoms and thus obscure the heterogeneity by scrambling the isotopes. A displacement technique was used by Cranstoun and Thomson(52). This involved the desorption of a gas from the surface by adsorption of a more strongly adsorbed species. Hydrogen and tritiated hydrogen were adsorbed on a nickel surface. The isotopes were slowly displaced by mercury and the displaced gas was examined. It was found that at 298K nickel films were heterogeneous; the "last on, first off" phenomenon was observed.

Altham and Webb(53) using a microcatalytic reactor coupled to a radio-gas chromatograph system studied the

chemisorption of [ $^{14}\text{C}$ ]ethylene and [ $^{14}\text{C}$ ]propylene between 20°C and 350°C on alumina-supported platinum. They obtained quantitative data on extents of adsorption and simultaneous production of methane, ethane and propane. The injection of inactive ethylene on to [ $^{14}\text{C}$ ]ethylene precovered surface showed limited exchange and the amount of exchangeable ethylene decreased with increasing temperature. When ethylene was injected onto the surface of an alumina-supported platinum catalyst, which was precovered with [ $^{14}\text{C}$ ]propylene, it was observed that ethylene adsorption could still occur and that at 200°C and below no radioactivity was displaced from the surface. The authors concluded that different types of site are involved in the retention of ethylene and propylene.

The participation of chemisorbed molecules in catalytic reactions has also been studied by radiotracer techniques (54-60). Thomson and Wislade(54,55) examined the behaviour of [ $^{14}\text{C}$ ]ethylene on the catalyst surface during a catalytic reaction. A specially designed Geiger-Müller counter detected radiation from [ $^{14}\text{C}$ ]ethylene preadsorbed on nickel films on which hydrogenation of inactive ethylene, subsequently, took place. They concluded that in ethylene hydrogenation on nickel films not all chemisorbed species were active in the hydrogenation process, that is the ethylene-nickel surface was heterogeneous. They also concluded that attempts to relate heats of adsorption, conductivity and magnetic changes in films, surface

potentials, adsorption isotherms, etc.... , to the process of catalysis, can only be valid if they apply to that fraction of adsorbed molecules, or surface, active in the catalytic process.

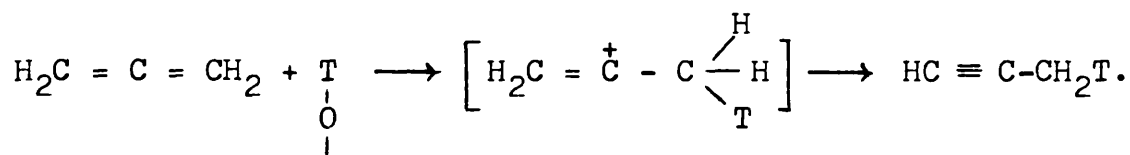
Al-Ammar and Webb(58) studied the behaviour of [ $^{14}\text{C}$ ]acetylene and [ $^{14}\text{C}$ ]ethylene over silica-supported rhodium, iridium and palladium catalysts. They showed that the adsorption occurred irreversibly at 298K in two distinct stages; a non-linear primary region, in which the species were predominantly dissociatively adsorbed and a linear secondary region in which the species were associatively adsorbed. They also showed that the hydrogenation reaction was associated with the hydrocarbon species adsorbed on the secondary region.

#### 1.4.4 Mechanism

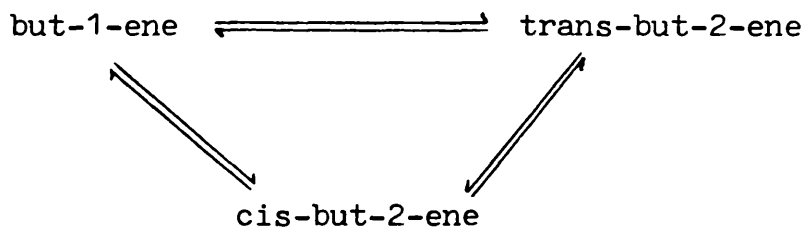
The application of radiotracers to the elucidation of the mechanism of catalytic reactions is widespread. The study by Kummer et al.(61) of the mechanism of the Fischer-Tropsch synthesis of hydrocarbons is an example of the use of radiotracers. It was shown that a carbide mechanism was not the principal path in the reaction. A series of studies followed this early work and led to the conclusion that primary alcohols were involved as principal intermediates over Fischer-Tropsch catalysts.

The isomerization of allene to methylacetylene on

silica gel at 250°C has been investigated by labelling the catalyst with tritium(62). The exchange of acetylenic hydrogen takes place fairly rapidly, independently of the isomerization. The incorporation of tritium atoms into the methyl group of methylacetylene formed from allene suggested the following scheme:-



Hightower and Hall(63), using mixtures of two butenes, one of which was labelled with [<sup>14</sup>C], showed that on catalysts based on alumina, all possible transformations of the three butenes take place according to the scheme



Thus when a mixture of cis-but-2-ene and [<sup>14</sup>C]but-1-ene was used, the specific radioactivity of the trans-but-2-ene was not greater or equal to that of the but-1-ene, indicating direct formation of trans-but-2-ene from cis-but-2-ene.

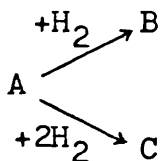
In the hydrogenation of di-unsaturated hydrocarbons it is possible that, in the initial stages of the reaction, the products may be the corresponding monoolefin, or the alkane, or a mixture of both the alkene and alkane. Thus, in such reactions we have the phenomenon of selectivity, whereby one

reaction product may be formed preferentially.

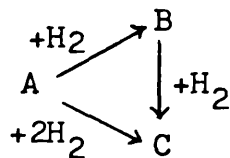
Since the monoolefin may be an intermediate in the production of the corresponding saturated hydrocarbon, it is possible to distinguish two types of selectivity for olefin formation in the hydrogenation of a di-unsaturated hydrocarbon. The first type is represented in the reaction scheme



where A is an acetylene or diolefin, B is a monoolefin and C is the corresponding saturated hydrocarbon. The second type arises with the simultaneous production of two products from a single reactant and the reaction scheme is



In the hydrogenation of di-unsaturated hydrocarbons, the two types of selectivity may occur simultaneously. Thus the full scheme must be written as:



The relative importance of the two possible routes to selective behaviour was investigated by Al-Ammar and Webb (47) for the hydrogenation of acetylene using [ $^{14}\text{C}$ ]ethylene

as radiotracer. They studied the hydrogenation of acetylene in the presence of various pressures of [ $^{14}\text{C}$ ]ethylene over silica-supported palladium, rhodium and iridium catalysts. The results showed that with each catalyst the yield of ethane from the hydrogenation of ethylene was small; the major route to ethane formation was by direct hydrogenation of acetylene. Direct surface monitoring during the hydrogenation reaction showed that ethylene did not adsorb on the acetylene hydrogenation sites. The increase in rate observed when all the acetylene had reacted was not due to an increase in ethylene surface coverage, but was interpreted in terms of an increase in hydrogen availability for ethylene hydrogenation.

Guczi et al.(64) obtained similar results when investigating acetylene deuteration in the presence of [ $^{14}\text{C}$ ]ethylene. They applied a double labelling method using [ $^{14}\text{C}$ ]ethylene and deuterium gas simultaneously, to investigate the surface reaction path in the deuteration of unlabelled acetylene. The results showed that the ethane formed initially was a result of a parallel reaction of acetylene to ethane and ethylene, and that the rate of ethylene desorption was much faster than its further reaction on the surface to form ethane.

There are many other examples of the use of radio-tracers in mechanistic studies. A review of [ $^{14}\text{C}$ ] studies of the mechanisms in heterogeneous catalysis with particular reference to hydrocarbon transformations has been published

by Derbentsev and Isagulyants(65). Ozaki, in a monograph(66), reviewed the fields of application of isotopes in studies of heterogeneous catalysis and particular attention was paid to mechanistic studies of isomerization of olefins, olefin disproportionation, dehydration and dehydrogenation, hydrogenation and oxidation reactions.

### 1.5 Adsorbed States of Unsaturated Hydrocarbons on Metal Catalysts

It is not inappropriate that, at this stage, the subject matter of this thesis is outlined in order that this and subsequent sections of this chapter may be seen in better perspective.

The work to be described in subsequent chapters of this thesis is concerned with the hydrogenation of allene over supported metal catalysts. The deactivation of catalysts and their selectivity for propylene formation will be described, as will the behaviour of [ $^{14}\text{C}$ ]propylene adsorbed on the catalysts and the use of [ $^{14}\text{C}$ ]propylene as a tracer in the study of the mechanism of allene hydrogenation.

Whereas the adsorption of propylene and allene, and the mechanism of allene hydrogenation has been relatively little studied, extensive and relevant studies of the adsorption and metal-catalysed hydrogenation of ethylene and acetylene have been reported. It is, therefore, pertinent that these studies should be reviewed to provide a basis for the studies described subsequently in this thesis.

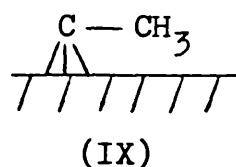
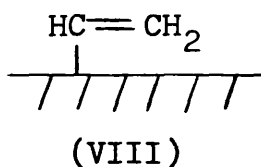
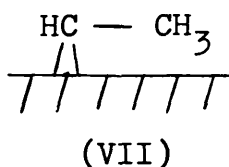
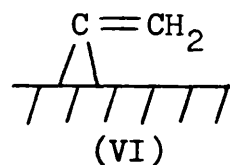
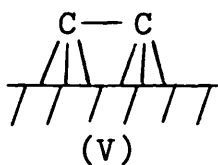
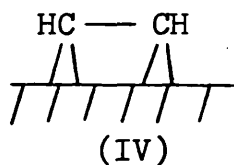
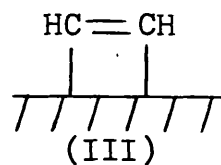
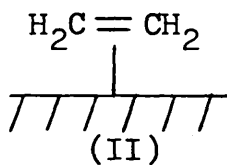
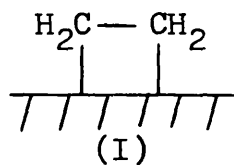
The mechanism of catalytic action is intrinsically related to the mechanism of chemisorption and a complete understanding of the mechanism of chemisorption is essential to the understanding of catalysis. Much attention has been given to the nature of the adsorbed state as it has a direct bearing upon the mechanism of chemisorption. Information regarding the nature of the adsorbed states of hydrocarbons has traditionally been obtained from three main sources: (i) indirectly from studies of surface processes such as hydrocarbon-deuterium exchange(67), self-hydrogenation and self-poisoning(68,69); (ii) from changes in the properties of the metal, e.g. magnetic susceptibility and work function during and after adsorption(70); and (iii) by direct observation using infrared spectroscopy(71).

Surface analysis techniques are now increasingly being used in the determination of the molecular structure of adsorbed species on well-characterized transition metal surfaces. Electron spectroscopy for chemical analysis (ESCA), photoelectron spectroscopy (PES), Auger electron spectroscopy (AES), low energy electron diffraction (LEED) and many other complementary techniques have been applied not only to well-defined single crystal metal surfaces but also to clean polycrystalline metals and to selected non-metallic catalysts. The role of these fundamental studies in understanding heterogeneous catalysis has been the subject of recent reports(72 - 75).

When unsaturated hydrocarbons interact with a metal surface, both dissociatively and associatively adsorbed species are formed(76). Although it has generally been assumed that the associatively adsorbed species is responsible for processes such as hydrogenation and isomerization, recent studies have suggested that dissociatively adsorbed species may also play an important role in processes such as alkene isomerization(77,78) and in alkene and alkyne hydrogenation(60,79,80).

### 1.5.1 Adsorbed State of Ethylene

The adsorption of ethylene has been extensively studied by a number of different methods and under a variety of conditions. The interpretations of the results have led to proposals of one or more of the structures below.



The associative species (I, II) have been reported from magnetic studies using nickel-silica catalysts at 0°C(70). When the temperature is raised, dissociation occurs giving rise to self-hydrogenation and, above 130°C, the formation of surface carbide occurs. These conclusions are also supported by volumetric studies of ethylene adsorption on nickel(69) and palladium(81).

Infrared studies revealed that the adsorption of ethylene on a bare platinum-silica catalyst at room temperature leads to spectra in which the associatively bonded species (I) is predominant(82,83).

The nature of the ethylene-metal bonding in the associatively adsorbed state is still much in debate. The major differences between structures(I) and (II) lie in the geometries of the two species. Thus, whereas the di- $\sigma$ -bonded species (structure I) requires two metal atoms at a suitable distance apart and has  $sp^3$ -hybridised carbon atoms, the  $\pi$ -complex (structure II) requires only one surface site, although others may be obscured, and retains some double bond character depending upon the extent of the metal-ethylene interaction.

The  $\sigma$ -diadsorbed species has been well characterized by infrared techniques(82). It is, however, only recently that i.r. spectroscopic evidence for the existence of  $\pi$ -adsorbed species has been reported. It was necessary to use an extremely sensitive interferometry technique(84,85), or a

low temperature measurement(86) to demonstrate the existence of the  $\pi$ -adsorbed species.

It is well established that, when ethylene is adsorbed on to a freshly prepared evaporated metal film or on to a freshly reduced supported metal catalyst, self-hydrogenation resulting in the production of ethane is observed(87-89). A plausible mechanism for self-hydrogenation of ethylene may be pictured as the reaction of adsorbed ethylene with hydrogen atoms released by dissociation of associatively adsorbed ethylene or by disproportionation of two associatively adsorbed ethylene molecules. Infrared studies (71) of adsorbed ethylene on palladium-silica catalysts show the presence of dissociatively adsorbed species (structure III).

Results from radioactive tracer studies are consistent with the formation of multiply bonded hydrogen-deficient surface species (structures III, IV, V, VI). These structures were postulated from studies of adsorption of [ $^{14}\text{C}$ ]ethylene over a series of supported Group VIII metal catalysts in the temperature range 20 - 350°C(53,87,90).

Low energy electron diffraction (LEED) studies of ethylene adsorption on the (111) face of platinum at room temperature suggest that the adsorbed ethylene occupies four sites(91), thereby supporting the postulate of species such as structure (IV).

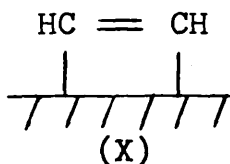
Ethylidene (structure VII), ethylidyne (structure IX) and vinyl species (structure VIII) have been recently

reported as the chemisorbed species formed during ethylene adsorption on platinum(111) surface at room temperature. Low energy electron diffraction (LEED) gives ethynidyne species as the species most consistent with the experimental data(92). The formation of vinyl species is proposed by Demuth(93) using temperature-programmed thermal desorption spectroscopy and UV photoemission spectroscopy (UPS) studies. Ibach(94) based on data from electron energy loss spectroscopy (ELS) proposed the formation of an ethynidene species.

The LEED results and UPS results are contradictory in relation to the adsorption of ethylene on Pt(111) at room temperature. The LEED results do not support a vinyl species nor the UPS results an ethynidyne species. Neither of these two methods is conclusive and this contradiction emphasizes the importance of the cautionary remarks made by Thomson(72) in his report about the contributions of surface science to heterogeneous catalysis in which he states "much of interest and significance does emerge from a subject which has not yet reached maturity".

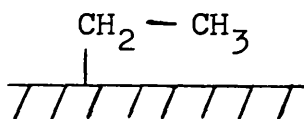
### 1.5.2 Adsorbed State of Acetylene

Associatively bonded acetylene (structure X) has been proposed on the basis of volumetric studies(69,95).



Infrared spectra support the existence of the associatively bonded species (structure X). On silica-supported nickel a band near  $3020\text{cm}^{-1}$  is assigned to this species(96) and more recently magnetic and infrared results (97) again indicated the presence of this surface species on silica-supported nickel.

The presence of a surface alkyl group (structure XI) has also been identified from infrared studies(96,98). The



(XI)

admission of hydrogen(96,98) resulted in an intensification of the bands ascribed to olefinic species (structure X) and the appearance of new bands ascribable to surface alkyl groups of average structure  $\text{CH}_3(\text{CH}_2)_n$ , where  $n = 3$  with nickel and  $n \geq 4$  with platinum.

Acetylene, when adsorbed on active nickel catalysts, undergoes self-hydrogenation with the production of ethylene (99), although the extent of this process is less than with ethylene. Similar behaviour has been observed with alumina-supported palladium and silica-supported palladium, iridium and rhodium(58), although with these metals ethane is the sole self-hydrogenation product. No ethylene was ever observed as a self-hydrogenation product from the adsorption of acetylene on any of these catalysts. During adsorption

of acetylene over a 25% nickel/SiO<sub>2</sub> catalyst ethane was the sole self-hydrogenation product. There was no formation of ethylene(100).

[<sup>14</sup>C]tracer studies of acetylene adsorption on alumina- and silica-supported palladium(58,90), platinum(53) and iridium(58) show the coexistence of at least two adsorbed states, one of which is retained on the surface, the other being reactive undergoing molecular exchange and reaction with hydrogen. Acetylene adsorption exhibits the same general characteristics as those observed with ethylene. However, there are important differences. The extent of adsorption and retention is substantially greater with acetylene than with ethylene. Furthermore, the amounts of acetylene retained by "clean" and ethylene-precovered surfaces is identical. The results have been interpreted as showing that the adsorbate states of acetylene involved in retention and hydrogenation are different and that the sites involved in acetylene and ethylene adsorption are different. This latter conclusion is substantiated by field emission microscopic studies of acetylene and ethylene adsorbed on iridium and tungsten(101,102) which have shown that, while acetylene is most readily adsorbed on the (110)planes, ethylene is preferentially adsorbed on the (111)planes.

The existence of several adsorbed states of acetylene on palladium has been demonstrated in a particularly elegant study by Inoue and Yasumori(103). In this study, it was demonstrated that the catalytic activity of a cold-worked

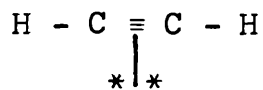
palladium foil showed a marked variation with the annealing temperature. [ $^{14}\text{C}$ ]acetylene adsorption demonstrated the existence of four types of adsorbed acetylene: one which underwent desorption on evacuation; one which was removed from the surface during hydrogenation; another which was not removed during hydrogenation, but could be removed by treatment with hydrogen at  $150^\circ\text{C}$ ; and one which was retained even after reduction at  $150^\circ\text{C}$ .

It is generally assumed that the acetylenic species active in catalytic hydrogenation is associatively bonded to the surface. However, as with ethylene, there is still doubt as to the precise formulation of the surface-acetylene bonding. In the early work(104), it was assumed that the associatively adsorbed complex was adequately represented as a di- $\sigma$ -bonded olefin (structure X).

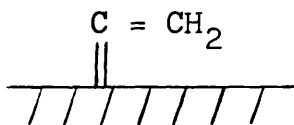
This postulate led to the conclusion that the (111)faces would be inactive in acetylene adsorption, but in a study of the adsorption of acetylene on platinum single crystals by low energy electron diffraction(105), it has been shown that acetylene adsorbs on the (111)planes. No evidence was found for the existence of a  $\pi$ -complex species, although it was stated that such species may possibly be located in a less stable overlayer which had been observed.

Following the proposals of Rooney et al.(106-108), it has generally been assumed that the adsorbed species active in hydrogenation is a  $\pi$ -complex formed by the interaction of the  $\pi$ -orbitals of the acetylenic bond with two metal atoms.

The  $\pi$ -complex may be represented as structure (XII)

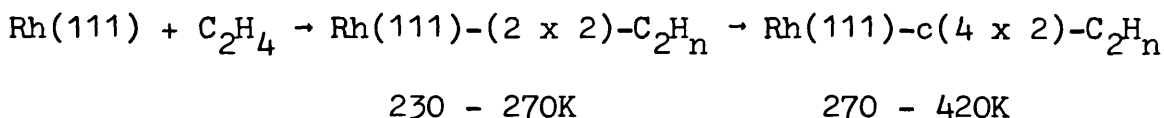


(XII)



(XIII)

The adsorption of acetylene on Pt(111) has been studied, at room temperature, by energy-loss spectroscopy (ELS) (94), low energy electron diffraction (LEED) (92). The formation of vinylidene species (structure XIII) on Pt(111) has been proposed by Demuth(93) using UV photoemission spectroscopy studies. The chemisorption of acetylene on Rh(111) studied by LEED, ELS and thermal desorption mass spectrometry (TDS) has recently been reported(109). This combination of techniques allowed the authors to observe ordered structures on the surface and follow their molecular rearrangement as a function of temperature.

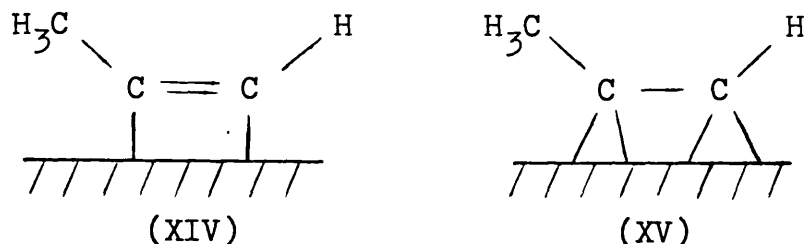


$\text{C}_2\text{H}_n$  stands for the stable hydrocarbon species with an undetermined hydrogen content.

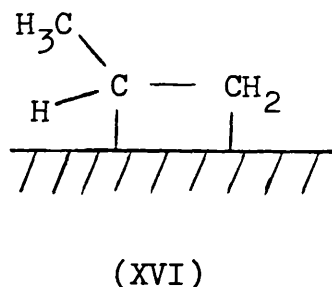
### 1.5.3 Adsorbed State of Propylene

Sheppard(110) presented infrared results for the chemisorption of propylene on silica-supported platinum. Propylene was considered to be adsorbed by a dissociative

mechanism to yield species such as structures(XIV) and (XV),

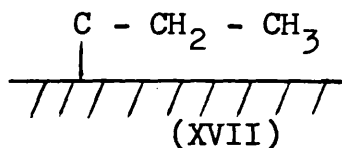


rather than the associatively adsorbed species (structure XVI).

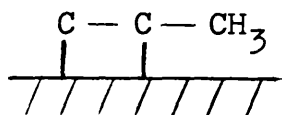


Hydrogenation of the surface species produced a much more intense methyl band at  $2980\text{cm}^{-1}$ , which was ascribed to an isopropyl group.

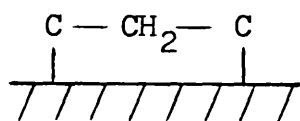
Avery(111) studied the chemisorption of propylene on silica-supported palladium. Initial adsorption of propylene produced infrared bands due to methyl and methylene groups. However, as hydrogenation of the surface species produced a large increase in absorption intensity the adsorbed species was unlikely to be due to species represented as structure (XVII).



It was suggested that the species likely to be present were those represented by structures (XVIII) and (XIX).



(XVIII)



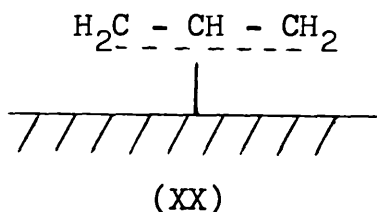
(XIX)

It should be noted that in structures (XVII), (XVIII) and (XIX) no information about the hydrogen content of the adsorbed carbon atoms is given.

By monitoring the infrared spectrum during the hydrogenation of propylene over silica-supported nickel, Erkelens(112) obtained information on the nature of the reacting system on the catalyst surface. The spectra consisted mainly of one intense band at about  $2950\text{cm}^{-1}$  indicating a chemisorbed secondary propyl group. Dissociative adsorption was not observed, but the author did not rule out the possibility that a band, due to a dissociatively adsorbed species, could be overlapped by the main adsorption band of the spectrum.

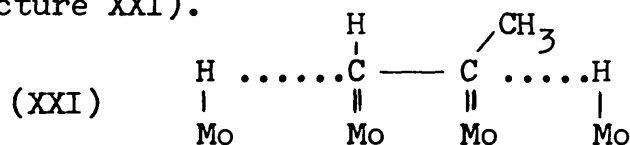
$[^{14}\text{C}]$ propylene adsorption on alumina and silica-supported platinum catalysts was studied in the temperature range  $20^\circ\text{C}$  to  $200^\circ\text{C}$  (53). A fraction of the initially retained  $[^{14}\text{C}]$ propylene will undergo molecular exchange with gas-phase propylene. This fraction is 35% with platinum-alumina and 26% with platinum-silica. These fractions are greater than the fractions obtained when initially retained

[<sup>14</sup>C]ethylene undergoes molecular exchange with gas-phase ethylene. The greater ease of exchange of propylene relative to ethylene suggests that a different type of adsorbed species may be in part responsible for propylene retention. With propylene surfaces species of the π-allyl type (structure XX) may be formed, which are not possible with ethylene.



Further evidence for this proposal comes from the observation that ethylene adsorption can still occur on surfaces which have been effectively saturated with propylene, although the extent of ethylene adsorption is less than on a clean surface.

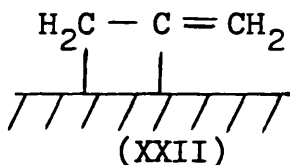
Calorimetric studies(113) of propylene adsorption on molybdenum films at room temperature suggest that propylene undergoes dissociation of the carbon-carbon π bond and of two C-H bonds. The proposed structure for the adsorbed species is Mo=(CH)-C(CH<sub>3</sub>)=Mo. The hydrogen atoms dissociated from propylene are not freely mobile on the surface, but are coordinated around the hydrocarbon residue forming a surface complex (structure XXI).



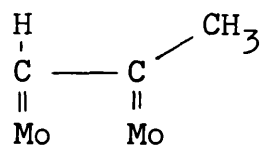
Low energy electron diffraction (LEED) and work function studies of adsorbed propylene on the (100) and (111) crystal faces of platinum have been reported by Gland and Somorjai(114). The diffraction pattern of propylene adsorbed on the Pt(111) surface corresponds to a (2 x 2) structure. The work function decreases with adsorption of propylene. The authors, based on their LEED and work function data, suggest a partial dissociation of propylene.

#### 1.5.4 Adsorbed State of Allene

Almost no studies of the adsorption of allene have been reported. Khulbe and Mann(115) have obtained infrared spectra of allene adsorbed on silica-supported cobalt, nickel, palladium, platinum, and rhodium. The spectra were similar for all the metals, although variations in band intensity from metal to metal were observed. Evacuation for two hours at room temperature had no effect on the spectra. New bands appeared on the addition of hydrogen suggesting the formation of methyl groups. The spectra obtained for the hydrogenated species of allene resemble those obtained for the surface-hydrogenated product of chemisorbed propylene, which was thought to be an adsorbed prop-1-yl group. The authors concluded that the initial allene spectrum was consistent with the adsorbed species being a 1:2-di- $\sigma$ -bonded allene (structure XXII).



Calorimetric studies(113) of allene adsorption on molybdenum films at room temperature suggest that allene probably first rearranges into methylacetylene and then undergoes dissociation of two carbon-carbon bonds. It is proposed that allene and propylene give surface species of the same basic structure (XXIII).



(XXIII)

## 1.6 The Hydrogenation of Alkynes and Dienes

The metal-catalysed hydrogenation of multiply unsaturated hydrocarbons presents many features and poses many problems of a kind essentially different from those encountered in monoolefin hydrogenation. Thus, an acetylene or a diolefin will generally hydrogenate to give both monoolefin and alkane, and the system may show any degree of preference for either product. This gives rise to selectivity in catalytic hydrogenation.

### Selectivity

Throughout this work the term selectivity will be used to denote the extent to which an alkyne or diene will yield

the corresponding monoolefin as opposed to the corresponding alkane; thus

$$\text{Selectivity, } S = \frac{P_{C_n H_{2n}}}{P_{C_n H_{2n}} + P_{C_n H_{2n+2}}}$$

So defined,  $S$  may take values between zero and unity. The factors affecting the degree of selectivity which may be achieved in the catalytic hydrogenation of alkynes and other di-unsaturated hydrocarbons are a thermodynamic factor and a mechanistic factor(23). The thermodynamic factor is based upon the assumption that the same surface sites are responsible for both alkene and alkyne adsorption. Thus, the rate of reaction of either species will depend on its degree of occupation of the surface, which in turn will depend on its partial pressure, and its free energy of adsorption, so that

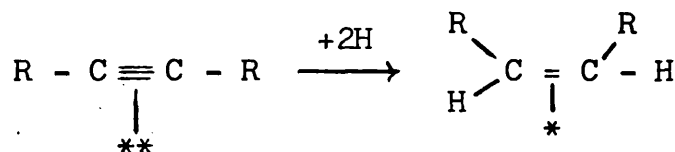
$$\frac{\theta_A}{\theta_B} = \frac{P_A}{P_B} \exp - \delta \Delta G/RT$$

$\theta_A$  and  $\theta_B$  are the fractional surface coverage of A and B respectively, where A is an acetylene or a diolefin and B is a monoolefin.  $P_A$  and  $P_B$  are the pressures in equilibrium with the surface,  $\delta \Delta G$  is the difference in the free energies of adsorption of A and B. A difference of only a few kilojoules per mole in the free energies of adsorption would result, therefore, in a very high surface coverage of the more strongly adsorbed species. The thermodynamic approach

may not be completely justified with supported metal hydrogenation catalysts(58,90). The mechanistic factor has its origin not in the thermodynamics of the adsorption of reactants but rather in the mechanism of the process. If both the alkene and the alkane are formed during one residence of the parent molecule on the surface the selectivity will depend upon the specific properties of the catalyst.

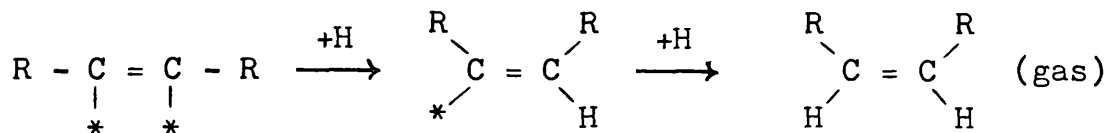
### Mechanism

The interpretation of the experimentally observed selectivity depends to some extent on the assumed nature of the adsorbed alkyne and alkadiene. If the alkyne is adsorbed as a di- $\pi$ -complex (structure XII), the product olefin will be formed as an adsorbed species, which must, therefore, undergo desorption before appearing in the gas phase. Consequently the selectivity will, in part, be dependent upon the relative abilities of the olefin to desorb, which may be aided by displacement by the more strongly adsorbed acetylene, or undergo further hydrogenation (mechanism 1).



mechanism 1

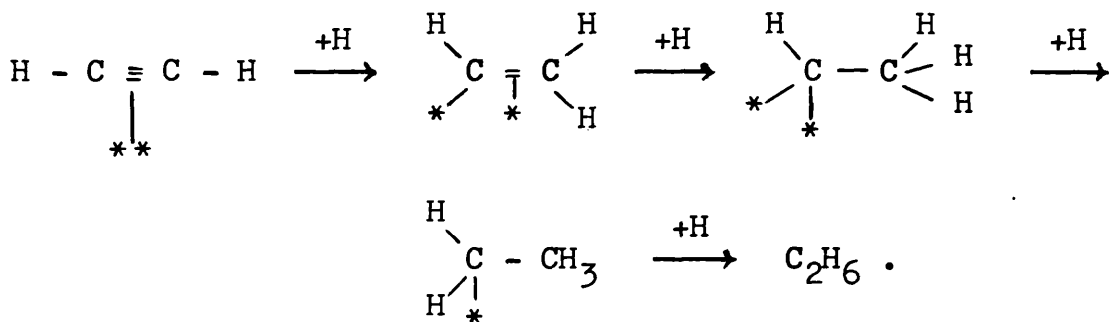
Alternatively if, as was originally envisaged(23), the alkyne is adsorbed as a di- $\sigma$ -bonded complex (structure X), hydrogenation will lead to the direct formation of olefin in the gas phase (mechanism 2).



mechanism 2

Further hydrogenation of the monoolefin, and hence the selectivity, would depend upon the re-adsorption of the olefin in competition with the alkyne.

In either of the above cases the selectivity will also depend upon the existence, or otherwise, and the relative importance of a direct route from the diunsaturated hydrocarbon to the alkane, not involving the monoolefin as an intermediate. For example, a possible route to the direct formation of ethane from acetylene could be envisaged as shown in mechanism 3 below. Similar mechanisms can be



mechanism 3

envisaged for other alkynes and dienes.

The source of hydrogen atoms for the above mechanisms is not readily established. There are several possibilities:

- (a) dissociative adsorption of molecular hydrogen, which may occur either competitively or non-competitively with the adsorbed hydrocarbon;
- (b) interaction of molecular hydrogen with chemisorbed hydrocarbon;
- (c) hydrogen transfer between associatively adsorbed hydrocarbon species;
- (d) hydrogen transfer between associatively adsorbed hydrocarbon and a dissociatively adsorbed hydrocarbon residue, which may be represented as  $C_xH_y$ (79).

### Carbonaceous Overlayer

In recent literature there is a growing body of evidence to suggest that a carbonaceous overlayer is an important source of hydrogen in hydrogenation reactions and that carbonaceous overlayers can have an important effect in determining both the catalytic activity and selectivity of a metal surface. Gardner and Hansen(116) suggested that the hydrogenation of ethylene on tungsten occurred by hydrogen transfer from ethylene adsorbed on tungsten to molecules of ethylene adsorbed in an upper layer. Weinberg et al.(117) have postulated that the carbonaceous overlayer is the catalytic site for the hydrogenation of ethylene on the

Pt(111) surface.

Dus in a capacitor study of adsorption and hydrogenation of ethylene over evaporated palladium films(118, 119) and nickel, and platinum films(119) has found two adsorbed ethylene layers. The first layer was formed by dissociatively adsorbed ethylene and the second layer was formed by 'undissociatively' adsorbed ethylene. Ethylene adsorbed in the second layer reacted readily with hydrogen, whereas that from the first layer did not so react.

Evidence for overlayer formation with supported metal catalysts has been obtained from [ $^{14}\text{C}$ ]acetylene and [ $^{14}\text{C}$ ]ethylene adsorption studies by Al-Ammar and Webb(58). On the basis of the results obtained from radiochemical studies Thomson and Webb(79) proposed a general mechanism for metal-catalysed hydrogenation of unsaturated hydrocarbons. They suggested that such reactions should be interpreted as a hydrogen transfer between an adsorbed hydrocarbon and the adsorbed olefin, rather than addition of hydrogen direct to the latter. Such a mechanism has the merit that it allows a satisfactory interpretation of such observations as the facile non-structure sensitivity of hydrogenation(120), the small variation of activation energy with change in metal and the apparent lack of any correlation between hydrogenation activity and electronic, magnetic or geometrical features of metals.

Although some authors take the view that a carbonaceous overlayer is not catalytically active(121) or reduces the

catalytic activity(122) it is clear from the above observations that the role of a carbon overlayer in hydrocarbon-metal catalysis is not only to act as catalyst poison but to participate actively in the catalytic process; it is worthy of further investigations.

#### 1.6.1 The Hydrogenation of Acetylene

All the metals of Group VIII catalyse the hydrogenation of acetylene. Among the early systematic studies of the metal-catalysed hydrogenation of acetylene were those of Sheridan and Reid(123-125) who discussed and compared the catalytic effects of all the metals of Group VIII. Subsequently, Bond et al.(126-132) extensively investigated the reaction over pumice- and alumina-supported metals and metal powders. The reaction of acetylene with deuterium over nickel(133,134) and alumina-supported noble Group VIII metals(135,127) has also been investigated in detail.

From these studies the following generalization may be made. The initial rate order in hydrogen has always been observed to lie in the range 1.0 - 1.5, while orders in acetylene are zero or negative. When deuterium is used all possible isotopic isomers of ethylene are always observed, acetylene exchange is absent or only very slow, but the extent of hydrogen exchange, during acetylene deuteration varies from metal to metal. Ethylene, ethane, and higher hydrocarbons are always observed as initial products of the reaction.

The selectivities for ethylene formation during the hydrogenation of acetylene over the noble Group VIII metals are always indirectly dependent upon hydrogen pressure and directly dependent upon temperature(67).

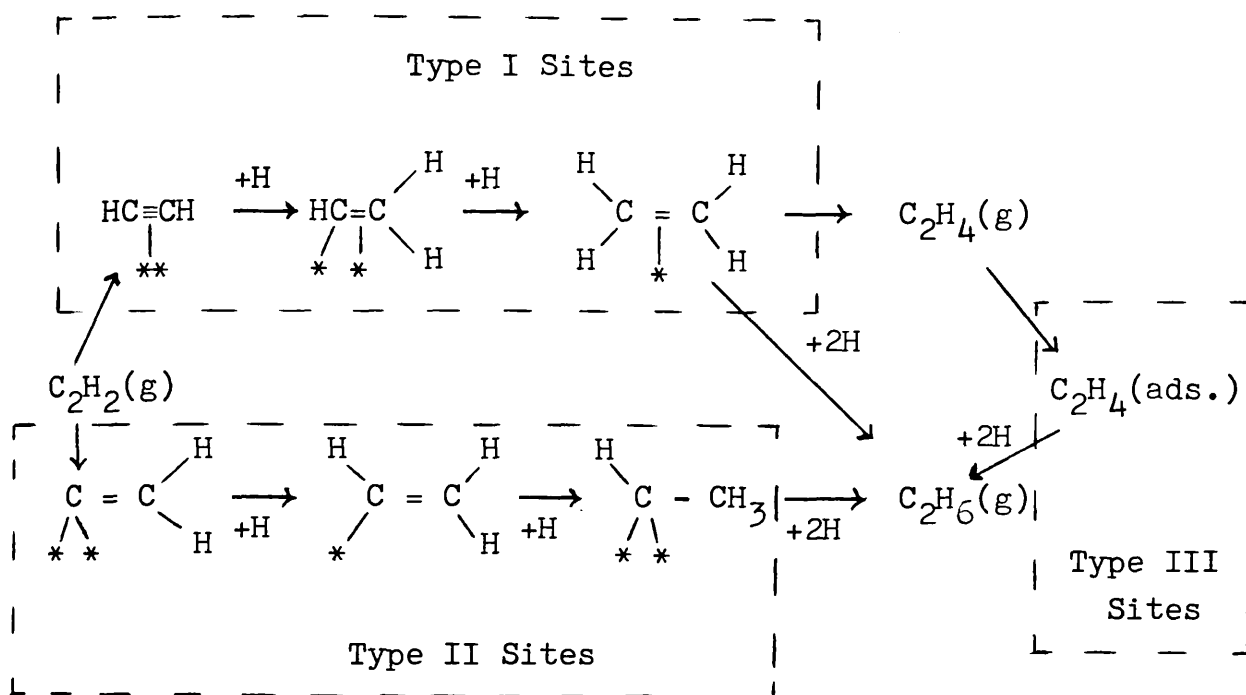
For reactions carried out in a constant volume reactor, the shapes of the pressure fall against time curves are dependent upon the initial hydrogen:acetylene ratio, but in general the reaction takes place in two distinct stages. During the first stage the main product is ethylene, with small yields of ethane. The onset of the second stage is generally accompanied by a sharp increase in rate. After the rapid acceleration the main process occurring is the further hydrogenation of ethylene to ethane.

The shapes of the pressure-time curves together with the observation that the selectivity remains constant or nearly so until the acceleration point is reached has been taken to indicate that the thermodynamic factor is predominant, that is the presence of acetylene effectively prevents the readsorption of ethylene from the gas phase and also aids the desorption of ethylene. Such a conclusion makes the implicit assumption that the same sites are involved in acetylene and ethylene adsorption. Studies using [ $^{14}\text{C}$ ]tracers(47,58,136) have shown that, with alumina-supported palladium and silica-supported palladium, iridium and rhodium, the admission of acetylene to [ $^{14}\text{C}$ ]ethylene-precovered surfaces results in the displacement of only a

small fraction of the [ $^{14}\text{C}$ ]ethylene, although a further fraction will undergo hydrogenation to [ $^{14}\text{C}$ ]ethane. Furthermore, the addition of [ $^{14}\text{C}$ ]ethylene to an acetylene-hydrogen reaction mixture shows that the added [ $^{14}\text{C}$ ]ethylene undergoes hydrogenation independently of the hydrogenation of acetylene. These results show that earlier interpretations of selectivity in terms of a thermodynamic factor and a mechanistic factor are inadequate. A full understanding of the factors which influence the selectivity must include the following: (i) the relative amounts of acetylene and ethylene adsorbed on independent sites; (ii) the relative amounts of different forms of adsorbed intermediates which can only lead to the formation of the alkane.

Studies, by McGown et al.(137), of acetylene hydrogenation in the presence of excess ethylene over alumina-supported palladium catalysts, using [ $^{13}\text{C}$ ]labelled acetylene and deuterium, indicated the existence of two distinct types of surface site. One (type X) that is active for both acetylene and ethylene hydrogenation and on which acetylene is adsorbed  $\sim 2200$  times more strongly than ethylene at 293K and one (type Y) that can be easily poisoned by carbon monoxide, can hydrogenate ethylene in the presence of acetylene, but is inactive for acetylene hydrogenation.

From the [ $^{14}\text{C}$ ]tracer results, a general reaction scheme for acetylene hydrogenation involving three types of surface site can be envisaged(138).



Reaction scheme for acetylene hydrogenation

### 1.6.2 Hydrogenation of Allene

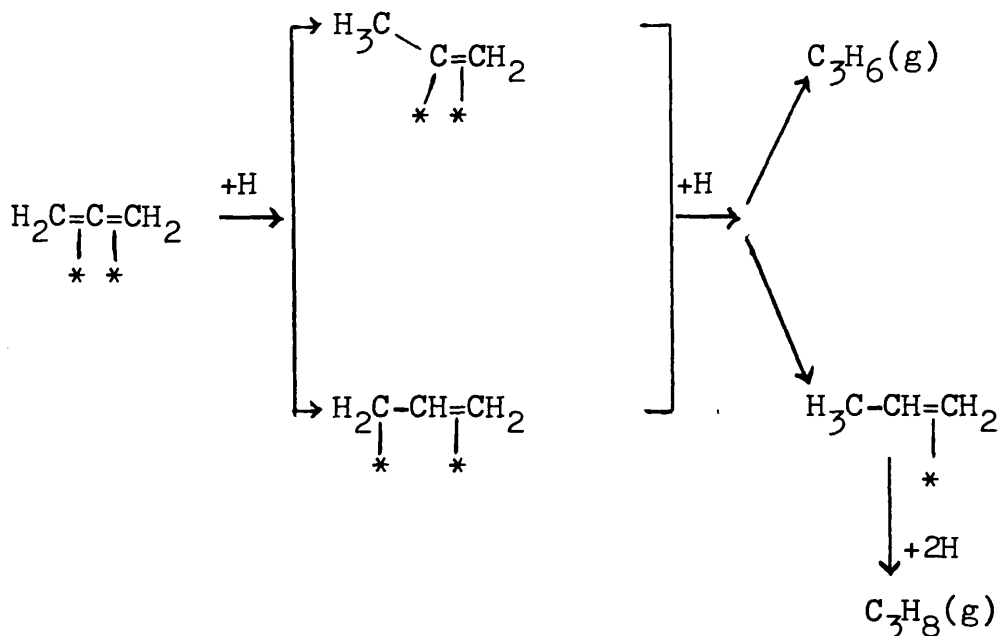
All the metals of Group VIII catalyse the hydrogenation of allene. The reaction was first systematically studied over pumice-supported platinum, nickel or palladium catalysts(139). Subsequently, studies for all the Group VIII metals either when supported on pumice(140) or silica(115) or as unsupported metal powders(141,142) have been reported. The hydrogenation of allene over alumina-supported metal catalysts has been reported only for the noble metals of Group VIII (143). The initial rate orders of reaction are first, or slightly higher, and zero with respect to hydrogen and allene respectively over all catalysts.

A comparative study of catalytic activities for silica-supported metals was presented by Khulbe and Mann(115). They found that the specific activity, calculated as the rate coefficient at 100°C referred to unit area of metal, decreased in the order Pd > Rh > Pt > Ni > Co > Ru > Ir. The catalytic activities of the unsupported metals are in the sequence Pd > Ir > Rh > Ru, Os (142), whilst for pumice-supported metals, the corresponding sequence is Pt > Pd > Rh > Ir > Ni > Co > Fe > Ru > Os (140).

All the allene hydrogenation studies mentioned above were carried out in a constant volume reactor and the pressure-fall against time curves for reactions with initial hydrogen:allene ratios of two or greater exhibit two distinct stages. Over the noble Group VIII metals the first stage, one in which there is selective propylene formation, is slower than the second stage, which follows when almost all the allene has been removed(139,115). Over unsupported nickel, iron and cobalt the rate of the first stage is higher than that of the second stage(141). The selectivity, as defined in section 1.6 is dependent upon the initial hydrogen pressures and temperature. The selectivity decreases with increasing initial hydrogen pressure and increases with increasing temperature in all cases. Palladium(139,143) is the most selective catalyst for propylene formation and iridium(139) distinguishes itself by providing more propane than propylene in the initial stage of reaction.

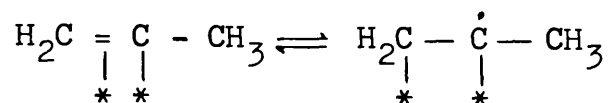
The reaction of allene with hydrogen over supported and unsupported metal catalysts yields small amounts of reduced polymers of allene. The chemical identity of the polymeric products has not been established.

Allene hydrogenation in almost all respects closely resembles the acetylene-hydrogen reaction. By analogy with the mechanism proposed for acetylene hydrogenation, allene hydrogenation has been postulated as occurring by the mechanism shown below.



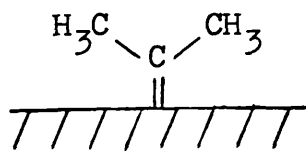
The addition of the first hydrogen atom must be assumed to occur in one of two ways, giving two possible half-hydrogenated states. The addition of a second hydrogen atom gives either propylene in the gas phase or an adsorbed species which reacts further with hydrogen to form propane.

The hydropolymerization of allene has been explained by postulating that the half-hydrogenated state can isomerize to form a free radical.



The radical either reacts further with adsorbed hydrogen to form adsorbed propylene or combines with adsorbed allene to form polymers(140).

The reaction of allene with deuterium over alumina-supported palladium at 293K has been reported(144). The reaction products were analyzed by mass and nmr spectroscopy and were propane, hexenes, hexane and branched C<sub>6</sub>-hydrocarbons. Deuterium did not appear in the allene reactant and no isomers of allene were detected in the products. The results from the allene deuteration led to the conclusion that a species represented by structure (XXIV) is an important intermediate in propane formation and that a specific region of the surface may be involved in production of propane.



(XXIV)

## 1.7 Adsorbed State of Carbon Monoxide

Part of the work described in this thesis will be concerned with carbon monoxide adsorption isotherms and the poisoning effects of carbon monoxide upon the hydrogenation of allene and propylene. Thus, this section presents a survey of studies of carbon monoxide interactions with transition metal surfaces.

The interaction of carbon monoxide with transition metal surfaces is one of the most studied chemisorption systems in surface chemistry. One of the best ways to study the structure of chemisorbed carbon monoxide involves the use of vibrational spectroscopy. This has been effectively carried out on single crystals using electron energy loss spectroscopy (ELS)(145,146), as well as reflection-absorption infrared spectroscopy(147). On dispersed metals, inelastic electron tunnelling spectroscopy has been employed(148), although most vibrational work to date using dispersed metals has been done using transmission infrared spectroscopy(149).

The molecular orbital picture of carbon monoxide bonding to metals involves electron transfer from the  $\sigma$ -orbital of carbon monoxide to the metallic d-orbitals and back-donation of metallic d-electrons into the empty  $\pi^*$ -orbital of the adsorbate. This approach has been used to explain the infrared spectra of chemisorbed carbon monoxide. In early work on the infrared absorption by surface species Eischens &

Pliskin(150) ascribed the observed infrared bands to a linear and a bridged form of adsorbed carbon monoxide (structures XXV and XXVI).



Using a molecular orbital model Blyholder(151) suggested that the whole range of infrared bands may be interpreted in terms of only one structure, the linear form. The lowest frequency bands, previously assigned to bridged species, were explained by the idea that exposed metal atoms on edges and corners of metal crystallites would have the highest electron density for backbonding from the metal d-orbital into the  $\pi^*$ -orbital of carbon monoxide. In a recent review of the vibrational spectra of chemisorbed carbon monoxide Sheppard and Nguyen(149) presented experimental evidence from a variety of sources in support of Eischen's interpretation.

The system of carbon monoxide on alumina-supported rhodium has been extensively studied. More than twenty years ago Yang and Garland(152) performed the first infrared studies using 2% unsintered rhodium supported on alumina. They produced evidence for a species of the form  $\text{Rh}(\text{CO})_2$ , a gem-dicarbonyl, whose infrared spectrum showed a doublet at 2095 and 2027 $\text{cm}^{-1}$ , due to coupling of the vibrations of the

two equivalent CO groups. The presence of linear ( $\sim 2060\text{cm}^{-1}$ ) and bridge bonded ( $1925\text{cm}^{-1}$ ) forms were also observed. More recent investigations (149, 153-155) agree extremely well with the early results presented by Yang and Garland. The thermostability of these adsorbed species is in the sequence  $\text{Rh}_2\text{CO} > \text{RhCO} > \text{Rh}(\text{CO})_2$  (154). Similar results have been obtained in infrared studies of carbon monoxide adsorption on evaporated rhodium films. However, due to the high density of rhodium atoms, no species of the form  $\text{Rh}(\text{CO})_2$  were formed in this case.

In the low frequency range (below  $1000\text{cm}^{-1}$ ) infrared spectroscopy is of little use because of strong substrate absorption, although this region of the spectrum may be investigated by inelastic electron tunnelling spectroscopy (IETS), which covers a range down to  $250\text{cm}^{-1}$  or less. IETS (148) measurements on alumina-supported rhodium particles add little new structural information except that the low frequency modes, due to the Rh-CO bond, are observed.

The structure of carbon monoxide adsorbed on rhodium(111) surface studied by low energy electron diffraction was first reported by Grant and Haas (156). Recently a study of the chemisorption of carbon monoxide on rhodium(111) by techniques of high resolution electron energy loss spectroscopy (ELS), thermal desorption mass spectroscopy (TDS) and low energy electron diffraction (LEED) has been reported (146) and a fairly complete picture of carbon monoxide chemisorption

on Rh(111) was presented. At very low exposures only the linear species is present on the surface and the diffraction pattern corresponds to a  $(\sqrt{3} \times \sqrt{3}) R30^\circ$  structure. Above this coverage the bridged species begin to form. At a pressure of  $\sim 1 \times 10^{-6}$  torr a  $(2 \times 2)$  LEED pattern is formed with two different CO species per unit cell. The ratio of linear and bridge sites is two to one. The bridged species has a lower binding energy to the surface than the linear species. A set of force constants for the two species of chemisorbed carbon monoxide was also presented.

Hydrogen and carbon monoxide chemisorption are commonly used to determine metal surface area in supported metal catalysts. The stoichiometry with which the gas and metal interact must be known and it is assumed that there is no chemisorption on the support. Platinum, in particular, has been extensively studied. There is good evidence in the literature that the H/Pt ratio is close to unity for supported platinum catalysts(157). Surface area measurements of supported rhodium catalysts obtained from adsorption of hydrogen and carbon monoxide have been reported(153-158). A summary of H/M and CO/M ratios are shown in table 2.

Table 2  
Comparison of Hydrogen and Carbon Monoxide  
Adsorption on Supported Rhodium

Rhodium conc. (wt %)	H/M			CO/M		
	A	B	C	A	B	C
10	0.48	-	0.54	0.44	-	0.46
5	0.59	0.75	0.51	0.52	0.75	0.44
1	0.94	1.0	1.06	1.01	1.45	1.46

A - Rhodium/silica (ref. 158)

B - Rhodium/alumina (ref. 159)

C - Rhodium/alumina (ref. 153)

H/M - Hydrogen atoms per rhodium atom in the catalyst

CO/M - Carbon monoxide molecules per rhodium atom in the catalyst.

The H/M and CO/M values are not very different at 10% and 5% rhodium on silica or alumina. Much larger differences are evident with the 1% rhodium samples. For the silica supported catalyst the CO/M ratio is only a little larger than the H/M ratio, while for both alumina supported samples the CO/M ratio is about 40% more than the H/M ratio. Such values indicate that a considerable amount of species of the form  $\text{Rh}(\text{CO})_2$  is present on the alumina supported rhodium, while only small amounts are present on the silica-supported rhodium.

## CHAPTER TWO

C H A P T E R 2

AIMS OF THE PRESENT WORK

Many studies of the adsorption and hydrogenation of ethylene and acetylene, as reviewed in chapter 1, have been carried out, but relatively little work has been reported concerning the adsorption and hydrogenation of C<sub>3</sub>-hydrocarbons.

The work described in this thesis was undertaken with the aim of obtaining information concerning;

- (1) the adsorption of propylene on alumina-supported rhodium catalysts, using carbon-14 as tracer, in an attempt to understand further the nature and reactivity of adsorbed species at metal surfaces;
- (2) the deactivation of alumina-supported palladium, rhodium and iridium catalysts during the hydrogenation of allene and the effects of catalyst deactivation upon the selectivity for propylene formation during the hydrogenation of allene;
- (3) the mechanism of the selective hydrogenation of allene. In particular, to determine the relative contributions of the so-called thermodynamic and mechanistic factors to the observed selectivity.

In order to obtain this information the following investigations have been carried out:

- (a) The determination of adsorption isotherms at room temperature of [ $^{14}\text{C}$ ]propylene on clean and on allene and carbon monoxide precovered catalysts.
- (b) The evaluation of the effect of various treatments, such as evacuation, molecular exchange and hydrogenation upon adsorbed [ $^{14}\text{C}$ ]propylene.
- (c) The determination of [ $^{14}\text{C}$ ]propylene adsorption isotherms after varying numbers of allene hydrogenations have been carried out.
- (d) The determination of catalytic activity and selectivity for propylene formation during a series of allene hydrogenations over freshly reduced metal catalysts.
- (e) The evaluation of the production of propane direct from allene by using [ $^{14}\text{C}$ ]propylene as a tracer during the hydrogenation of allene.
- (f) The determination of catalytic activity and selectivity for propylene formation during allene hydrogenation over carbon monoxide poisoned catalysts.

## CHAPTER THREE

### C H A P T E R 3

#### APPARATUS AND EXPERIMENTAL PROCEDURE

The radiotracer studies of the metal catalysed hydrogenation of unsaturated hydrocarbons carried out in this work required a system in which it was possible;

- (1) to follow the reaction in order to obtain information about the velocity of reaction and about the distribution of the reaction products throughout the course of the reaction;
- (2) to determine adsorption isotherms by measuring the amount of radioactive material adsorbed on the surface of the catalyst as a function of the pressure of the hydrocarbon adsorbate in the gas phase;
- (3) to determine the chemical composition of the gas phase in contact with the surface during the adsorption of the hydrocarbon at the catalyst surface;
- (4) to analyse the products of the hydrogenation of radioactively labelled hydrocarbons, to determine the extent of incorporation of radioactivity in the various components of the product mixture and
- (5) to effect the in situ reduction of catalysts at elevated temperatures.

### 3.1 The Vacuum System

A conventional high vacuum system (figure 1), to which was attached a constant volume reactor, hereafter referred to as the reaction vessel (R.V.), was constructed.

The vacuum system, which was maintained at a pressure of  $\leq 10^{-4}$  torr by means of a mercury diffusion pump (D) backed by an oil rotary pump (R), incorporated four two litre vessels (G) for the storage of hydrogen and reactant hydrocarbons and three 250ml vessels (g) for storage of the diluted radioactive gases. Reaction mixtures of the required compositions were pre-mixed and stored in the mixing vessel (M.V.).

A [ $^{14}\text{C}$ ]carbon dioxide converter (C) for producing carbon monoxide and a hydrogen purification system, incorporating a silver-palladium thimble (P), were also attached to the vacuum system.

Pressures in the system were measured using either a mercury manometer, a calibrated differential pressure transducer (see section 3.5) or a Pirani type vacuum gauge (Edwards High Vacuum, model 8/2). The pressures in the reaction vessel were measured using either the pressure transducer or, for pressures below  $10^{-1}$  torr, the Pirani gauge, thereby reducing the possibility of catalyst poisoning by mercury vapour. The mercury manometer was only used to measure pressures in the gas storage vessels.

### 3.2 The Reaction Vessel and the Geiger-Müller Counters

The reaction vessel was designed in such a way that it permitted the simultaneous determination of surface and gas phase radioactive count rates during the adsorption of [ $^{14}\text{C}$ ]labelled hydrocarbons at ambient temperature. It also contained the facility for the in situ reduction of catalysts at elevated temperatures. It was of similar design to that originally developed by Cormack(57) and subsequently modified and improved by Reid(160).

The reaction vessel (figure 2) was connected to the vacuum line via a 4mm tap ( $T_1$ ), to the sample-handling unit via a 1mm tap ( $T_2$ ) and to the pressure transducer via another 1mm tap ( $T_3$ ). The catalyst was evenly spread on the walls of a glass boat (b), which was divided into two compartments by a 3mm thick glass wall, and which could be moved from position (1) to position (2) by the use of an external magnet applied to the glass-enclosed metal bar (m). The boat could be removed from the reaction vessel via a B34 joint. The catalyst boat was always in position (1) during the experiments and only during the reduction of the catalyst was it moved to position (2) where high temperatures up to 350°C, necessary during the reduction, were attained by the use of an electric furnace (F). The hydrogen used to reduce the catalyst flowed through the reaction vessel entering through tap ( $T_1$ ) and leaving through tap ( $T_4$ ).

The reaction vessel was fitted with two Geiger-Müller

counters, GM(A) and GM(B), which were held in position by means of extended B34 cones to which the counters were attached with Araldite.

The Geiger-Müller tubes (Mullard ZP 1481) were end-window counters filled with a mixture of neon, argon and halogen gases. Each counter was connected to a probe unit (EKCO - type 110A) which in turn was connected to a scaler (EKCO-type N 59 D). The discriminator, which was required to cut out pulses due to electronic noise, was set at 15. The dead time was set at a constant value by setting the paralysis time of the probe unit at 300 $\mu$  sec.; this being greater than the dead time (120  $\mu$  sec.) of the Geiger-Müller counter. Count rates higher than one thousand counts per minute were corrected for dead time losses according to the equation

$$N = \frac{N_o}{(1 - N_o t)}$$

where  $N_o$  = counts per minute recorded on the scaler  
N = corrected count rate  
t = dead time in minutes.

The plateau region, where the count rate is nearly independent of applied voltage, was determined for each Geiger-Müller tube using a  $^{60}\text{Co}$  source. A typical plateau is shown in figure 3. The voltage in the middle of the plateau was chosen as the working voltage during the

experiments. During use the working voltage was checked at frequent intervals by redetermination of the plateau region.

### 3.2.1 Intercalibration of the two Geiger-Müller Counters

In order that the count rates recorded by the two Geiger-Müller tubes could be directly compared, it was necessary to intercalibrate them. The intercalibration was performed by adding small amounts of a radioactive gas into the reaction vessel in the absence of any catalyst, with the boat in the counting position (1). The count rate was determined using each counter after each addition of radioactive gas. The count rates were corrected for dead time and background and the intercalibration factor was determined from a plot (figure 4) of the count rate recorded by Geiger-Müller (A) against the count rate recorded by Geiger-Müller (B).

### 3.2.2 Determination of Gas Phase and Surface Radioactivity Using GM(A) and GM(B)

The catalyst was slurried with water and was spread thinly and evenly on the walls of the compartment of the catalyst boat, which was to be under Geiger-Müller (B), when the boat was in position (1). The other compartment of the boat was always empty. With the boat in position (1),

during the determination of an adsorption isotherm, Geiger-Müller (A) recorded only the gas phase radioactivity and Geiger-Müller (B) recorded the gas phase radioactivity in a similar volume of gas to that sensed by counter GM(A) together with the radioactivity from the material adsorbed on the catalyst surface. Thus, the amount of radioactive material on the catalyst surface, in equilibrium with the radioactively labelled gas phase, was obtained as the difference between the count rate recorded by GM(A) and that recorded by GM(B), after the individual count rates had been corrected for background and, where necessary, dead-time.

In order to check that the radioactivity from the material adsorbed on the catalyst surface was not being recorded by Geiger-Müller (A), a [ $^{14}\text{C}$ ]poly(methyl- $^{14}\text{C}$ -) methacrylate sheet was used in the place of the catalyst. With the boat in the counting position (1), Geiger-Müller (A) did not record any emissions from the [ $^{14}\text{C}$ ]-emitter showing that Geiger-Müller (A) recorded only gas phase radioactivity during the adsorption experiments.

### 3.2.3 Radiation Absorption Effects

The possible occurrence of self-absorption of radiation from the radioactively labelled gas phase and from adsorbed material on the catalyst was examined either by introducing into the reaction vessel different pressures of a

radioactive gas and recording the count rate, or by placing a  $^{60}\text{Co}$  source beneath Geiger-Müller (B) inside the reaction vessel and introducing various pressures of non-radioactive gases into the evacuated reaction vessel.

No self-absorption occurred when different pressures, within the pressure range used in the present work, of a radioactive gas was introduced into the reaction vessel. A linear relationship was observed between the gas pressures and the radioactive count rates (figure 5).

The variation in the count rate was negligible when, with the  $^{60}\text{Co}$  source placed beneath Geiger-Müller (B), various pressures, within range used in the present work, of hydrogen, air or propylene were introduced into the evacuated reaction vessel.

### 3.3 The Gas Chromatographic System

Analysis of reaction products was performed by gas chromatography. The sample-handling unit (figure 6), volume  $5.2\text{cm}^3$ , was connected directly to the reaction vessel. This permitted analysis of the products throughout the course of the reaction.

A column consisting of 30% w/w dimethylsulpholane supported on chromosorb P was used for the separation of the products of the hydrogenation of allene(161). The column was 20 feet long and was constructed of 3mm internal diameter copper tubing. 30g of dimethylsulpholane

(B.D.H. Ltd.) were dissolved in 250ml of ethanol and 100g of 30 - 60 mesh chromosorb P (Perkin Elmer Ltd.) were added with constant stirring. The ethanol was removed by vacuum distillation and, when the chromosorb P was dry and free running, it was packed into the column.

The column was operated at ambient temperature using helium at a flow rate of  $60\text{ml min}^{-1}$  as carrier gas. A typical trace is shown in figure 7.

For the separation of the products of the hydrogenation of acetylene a column containing 44 - 60 mesh activated silica-gel was used. The column was 3 feet long and was constructed of 3mm internal diameter copper tubing. This column was operated at  $80^{\circ}\text{C}$  using helium at a flow rate of  $60\text{ml min}^{-1}$  as carrier gas. A typical trace is shown in figure 8.

A hot wire (Gow-Mac 10 285) detector, operated at a filament current of 200mA, was used. The detector output was fed to a Servoscribe potentiometric chart recorder type RE 520.

The chromatograph operating conditions were kept as constant as possible, however fluctuations in ambient conditions and instrumental response did occur. Standard analyses were incorporated in each experiment to eliminate errors due to day to day fluctuations. The standard samples contained all the components to be found in the reaction products. Peak areas were determined by direct

measurement on the chromatogram. To determine a peak area, the product of the peak height and its width at half-height was generally used. However, when the peaks had a sufficiently large area a fixed arm planimeter was used for area determination.

### 3.4 The Proportional Counter

Radio-gas chromatography has been an important analytical tool for many years. The ability to measure quantitatively both the mass and radioactivity of compounds emerging from the gas chromatograph permits one to identify the labelled fractions and determine their specific activities in a single pass through the system.

Various studies of the use of radio-gas chromatography for [ $^{14}\text{C}$ ]labelled compounds have been described in the literature(162). The methods described have included the use of Geiger-Müller counters, proportional flow counters, ion chambers and liquid scintillation counters. In the present work a proportional counter was selected as the detector for a number of reasons. It is capable of high count rates without coincidence loss, it is an internal counting system which is free of window problems and it is basically simple in design so that it is readily coupled to a flowing gas system.

The proportional flow counter (figure 9) was constructed using a design similar to that described by

Schmidt-Bleek and Rowland(163), with minor alterations to accommodate different connectors, both for the gas inlet and the high voltage supply. The anode was a stainless steel wire of diameter 0.0025cm. The internal volume of the counter was ca. 26cm<sup>3</sup>. The proportional counter was connected to a pre-amplifier (ESI 425), which was in turn connected to a scaler-ratemeter (ESI type 5350). The output from the scaler-ratemeter was fed to a Servoscribe potentiometric chart recorder type RE 520 (figure 10).

The proportional counter was operated with a helium-methane filling. Methane (Air Products Ltd.) was introduced into the helium carrier gas stream at the exit from the chromatographic system, the flow rate of the methane being controlled by a Nupro (L series) fine metering needle valve.

Using a <sup>60</sup>Co external source placed adjacent to the counter, it was found that the location and the length of the counter plateau (figure 11) was very dependent upon the composition of the helium-methane mixture. Optimum operating conditions were obtained when a 10:1; helium:methane mixture was used. Under these conditions a plateau length in excess of 100 volts, with a variation of less than 4 per cent in the count rate over the length of the plateau, was obtained. During use the operation of the counter was checked at frequent intervals by redetermination of the plateau region.

When [ $^{14}\text{C}$ ]hydrocarbon samples were passed through the counter, the output from the latter was recorded as peaks on a recorder trace. Simultaneously, the total integrated counts comprising the peak were measured on the scaler. The total radioactivity in the hydrocarbon component was obtained by subtracting from the total integrated counts, the background counts integrated over the time of passage of the sample through the counter. The average background count rate was determined immediately before and after the passage of the sample. Initially, background count rates of approximately 65 counts per minute were recorded. However, with usage, this value increased slightly to around 120 counts per minute.

Possible quenching effects of the presence of the hydrocarbon samples in the counter were investigated by introducing various pressures of propylene into the helium-methane gas flow and examining the variation in counts from an external  $^{60}\text{Co}$  source as the propylene passed through the counter(164). Whilst quenching was observed with high pressures of propylene (figure 12), it did not occur to any measurable extent in the pressure range used in the present reaction system. Over the pressure range 0 - 7 torr, the total integrated counts observed were directly proportional to the pressure of [ $^{14}\text{C}$ ]propylene admitted, as shown in figure 13.

### 3.5 The Pressure Transducer

The pressure in the reaction vessel was measured using a differential pressure transducer (figure 1). This eliminated the possibility of catalyst poisoning by mercury vapour. The use of the pressure transducer also allowed the continuous recording of the pressure fall during a hydrogenation reaction, by feeding the output from the transducer directly to a Servoscribe potentiometric chart recorder.

The pressure transducer was supplied by S.E. Laboratories (EMI) Ltd., type SE/V/10D. It comprised a piezo-resistive half-bridge element. The input circuit of the measuring electronics and the transducer formed a Wheatstone bridge configuration. The bridge output was a voltage proportional to the applied pressure differential. The pressure transducer was calibrated over the pressure range 0 - 100 torr against a mercury manometer. A linear relationship was observed between the applied pressure and the output signal from the pressure transducer. An output signal of 1mV corresponded to a pressure variation of 0.50(7) torr.

### 3.6 Materials

#### 3.6.1 Gases

##### Hydrogen

For catalyst reduction cylinder hydrogen (B.O.C. Ltd.) was used without further purification. The hydrogen used in the hydrogenation reactions was purified by diffusion through an electrically heated silver-palladium alloy thimble (50mm long, 1.6mm O.D.).

##### Acetylene

Cylinder acetylene (B.O.C. Ltd.) contained acetone as the major impurity. This was removed by three successive bulb to bulb distillations, the acetone being trapped in the storage vessel cold finger at acetone/solid CO<sub>2</sub> bath temperature and the acetylene being trapped at liquid nitrogen temperature. The middle fraction was retained each time.

##### Allene and Propylene

Cylinder allene and cylinder propylene (Matheson Co. Inc.) were found to contain no impurities detectable by gas chromatography and were merely degassed before use.

[<sup>14</sup>C]carbon Monoxide

[<sup>14</sup>C]carbon monoxide was prepared by the reduction of [<sup>14</sup>C]carbon dioxide (1mCi batches, specific activity = 59.1 mCi/mmol), supplied by the Radiochemical Centre, Amersham, with metallic zinc(165). The apparatus used is shown in figure 14. Small pellets, about 6mm in diameter, were made from a moistened mixture composed of 95 per cent w/w zinc dust (Analar) and 5 per cent w/w Aerosil silica, the silica being used to give greater porosity and prevent clogging. The zinc pellets were dried at 120°C in an air oven for 24 hours before being placed in the converter. With the [<sup>14</sup>C]carbon dioxide ampoule in place the converter was evacuated for 24 hours at 400°C. Temperature control was effected by surrounding part of the converter with an electrical furnace, the current being controlled by a Variac transformer. Temperatures were measured using a Comark electronic thermometer whose thermocouple hot junction was in contact with the side of the converter. After evacuating the converter for 24 hours the [<sup>14</sup>C]carbon dioxide was introduced into the converter by breaking the breakseal on the ampoule. Convection up through the converter acted to circulate the gas from the ampoule through the zinc pellets. Almost complete conversion was obtained by circulating the [<sup>14</sup>C]carbon dioxide through the converter at 400°C for 36 hours. After freezing out any non-converted [<sup>14</sup>C]carbon dioxide in the cold finger at

liquid nitrogen temperature, the [ $^{14}\text{C}$ ]carbon monoxide was diluted with non-radioactive carbon monoxide (Air Products Ltd.) before use. In order that dilution of the [ $^{14}\text{C}$ ]-carbon monoxide could be carried out in an accurate manner the volume ( $336\text{cm}^3$ ) of the [ $^{14}\text{C}$ ]carbon monoxide storage vessel was determined.

### [ $^{14}\text{C}$ ]ethylene

50 $\mu\text{Ci}$  [ $^{14}\text{C}$ ]ethylene (The Radiochemical Centre, Amersham) with a specific activity of 95mCi/mmol was diluted with non-radioactive ethylene to the required specific activity before use.

### [ $^{14}\text{C}$ ]propylene

[ $^{14}\text{C}$ ]propylene was prepared by the catalytic dehydration of [1,3- $^{14}\text{C}$ ]propan-2-ol (0.25mCi, specific activity = 9.1 mCi/mmol) supplied by The Radiochemical Centre, Amersham. The apparatus used is shown in figure 15. The catalytic dehydration was performed over 7.2g alumina H (Spence) containing 10 per cent w/w potassium chloride at 400°C. Before dehydration the [ $^{14}\text{C}$ ]propan-2-ol was diluted with non-active propan-2-ol (Hopkins-Williams Co.) to the required specific activity. The diluted [ $^{14}\text{C}$ ]propan-2-ol was injected in small quantities (0.1ml) through a heated injection port in a flow (ca.  $15\text{cm}^3/\text{min}$ ) of nitrogen, which was previously dried by passage through a concentrated

sulphuric acid bubbler. The products of the catalytic dehydration, namely water and propylene, were collected in traps cooled in ice-water and liquid nitrogen respectively. The trap containing the [ $^{14}\text{C}$ ]propylene was connected to the vacuum line and the nitrogen was pumped away. Further purification was effected by three successive bulb to bulb distillations. The purity of the [ $^{14}\text{C}$ ]propylene produced was found by radio-gas chromatography to be  $> 97\%$ . Propane was present to an extent of  $\leq 0.7\%$ . Overall the process was about 70% efficient, mainly because only the fraction collected in the first 15 minutes after the injection of [ $^{14}\text{C}$ ]propan-2-ol was used. The remaining fraction, collected over a period of about 4 hours, contained a greater percentage of impurity and was not used.

[ $^{14}\text{C}$ ]propylene (New England Nuclear Corporation), which had an activity of 0.25 mCi and a specific activity of 5 mCi/mmol, was used in those experiments where a high specific activity was required.

### 3.6.2 Catalysts

All the catalysts used in the present work were prepared in a similar manner using  $\gamma$ -alumina (aluminium oxide C, supplied by Degussa Ltd.) as support and a metal loading of 5% w/w.

Following the procedure described by Reid(166), a concentrated solution of the appropriate weight of the metal

salt ( $\text{RhCl}_3 \cdot 3\text{H}_2\text{O}$ ,  $\text{IrCl}_3$  or  $\text{PdCl}_2$ ) was stirred carefully into a slurry of the support material ensuring even mixing. The slurry was then evaporated slowly to dryness with constant stirring and finally dried in an air oven at  $120^\circ\text{C}$  overnight. After being ground to a fine powder, the catalyst was stored as the supported salt until required.

Before use the supported salt was reduced inside the reaction vessel in a stream of hydrogen (ca.  $10 \text{ cm}^3 \text{ min}^{-1}$ ) at  $200^\circ\text{C}$  for 12 hours. Further reduction was achieved by leaving the catalyst under a purified hydrogen atmosphere for a further 6 hours at  $350^\circ\text{C}$ . The catalyst was then evacuated for 6 hours at  $350^\circ\text{C}$ , before it was cooled down to ambient temperature under vacuum.

The silica-supported rhodium catalyst was from the same batch as that previously used by Al-Ammar(167). It was a 5% rhodium supported on Aerosil silica (Degussa Ltd.) catalyst and was prepared and reduced under similar conditions to those described above.

The catalysts were never exposed to air and were used as soon as possible after reduction.

### 3.7 Experimental Procedure

#### 3.7.1 Hydrogenation Reactions

A mixture of hydrocarbon and hydrogen was prepared by admitting a measured pressure of hydrocarbon into the

mixing vessel and condensing it in the cold finger. Hydrogen was then admitted until the desired ratio of hydrogen:hydrocarbon was obtained. The two gases were allowed to mix at room temperature for at least one hour before use.

Hydrogenation reactions were carried out by admitting 48 torr of the reaction mixture (hydrogen:hydrocarbon = 3:1) into the reaction vessel. The reaction was monitored by measuring the pressure fall recorded by the differential pressure transducer and samples were extracted from the reacting mixture at any desired time into the sample-handling unit and injected into the radio-gas chromatographic system, where the relative yields of the products and the amount of radioactivity in each of them was determined. In a typical reaction five samples were taken for analysis at different intervals throughout the course of the reaction.

### 3.7.2 Adsorption Isotherms

The adsorption isotherms were determined by admitting aliquots of the radioactive gas into the reaction vessel. After each aliquot had been added the radioactivity in the gas phase and on the catalyst surface was determined. An interval of at least five minutes was allowed between each addition.

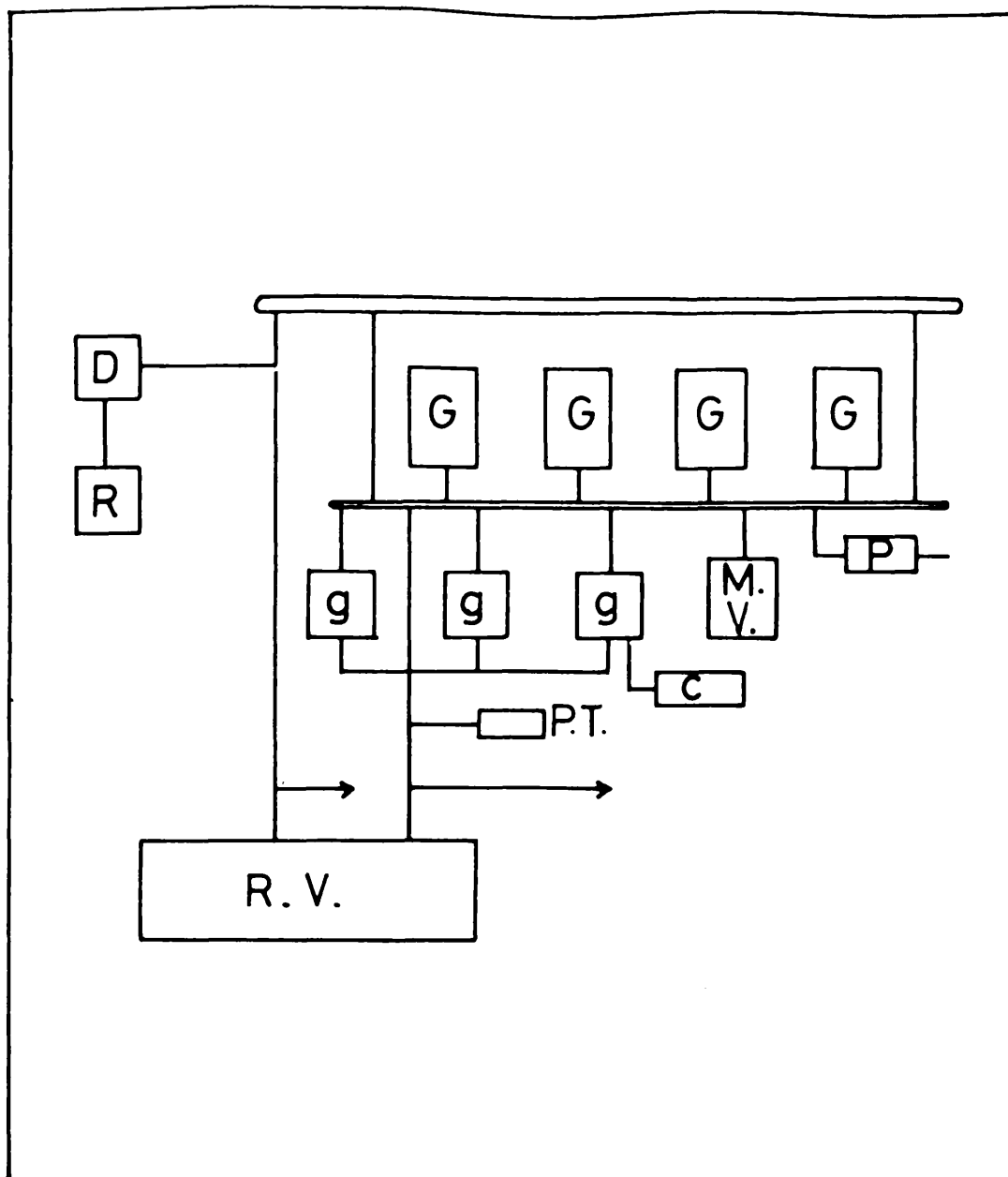


Figure 1. - Vacuum line diagram.

- G, g = gas storage vessels
- R.V. = reaction vessel
- M.V. = mixing vessel
- P = palladium thimble
- C = carbon dioxide converter
- D = diffusion pump
- R = rotary pump
- P.T. = pressure transducer.

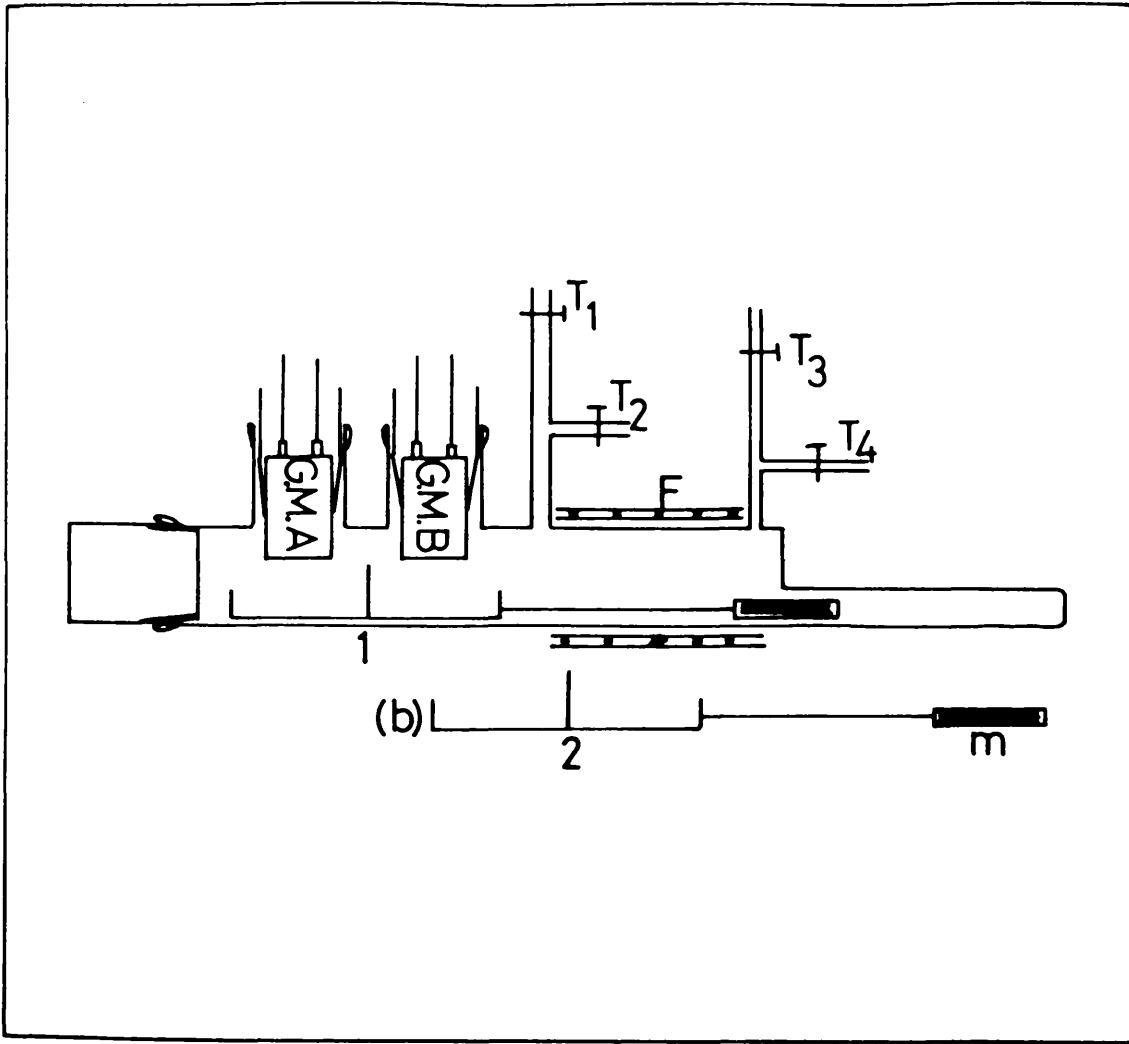


Figure 2. - The reaction vessel and the Geiger-Müller counters.

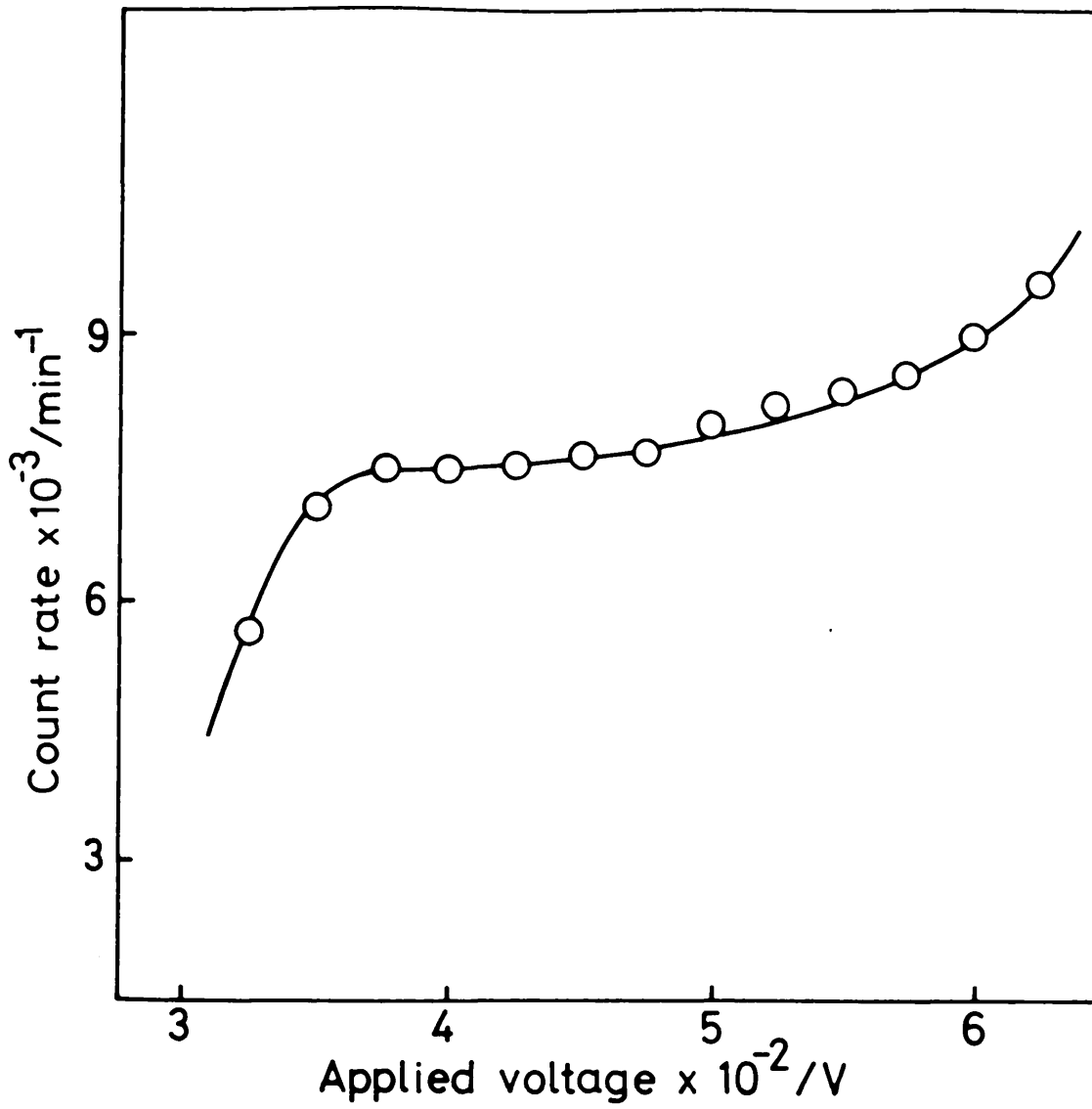


Figure 3. - A typical Geiger-Müller plateau region.

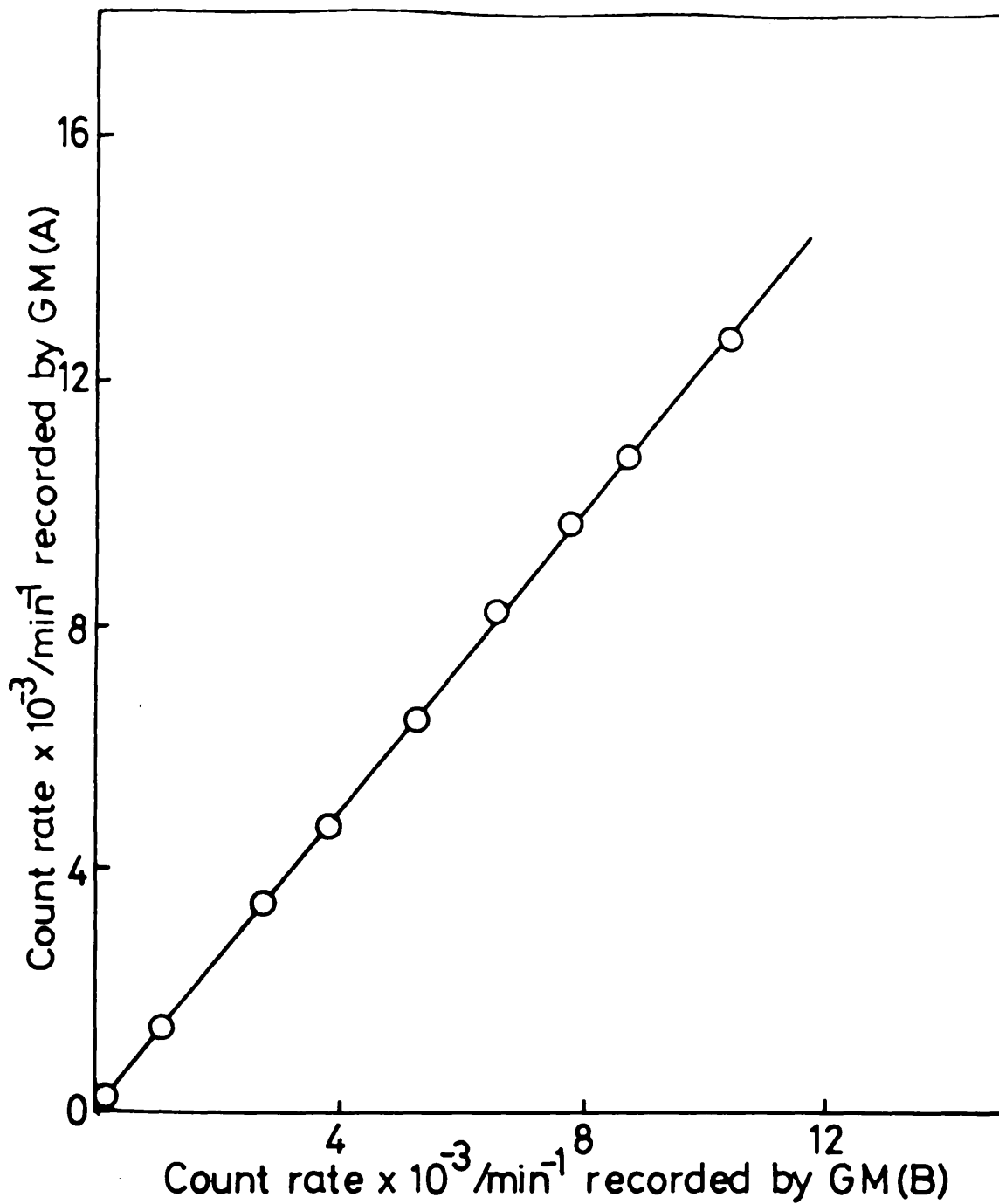


Figure 4. - Intercalibration of the two Geiger-Müller counters GM(A) and GM(B) when different pressures of [<sup>14</sup>C]carbon monoxide were present in the reaction vessel.

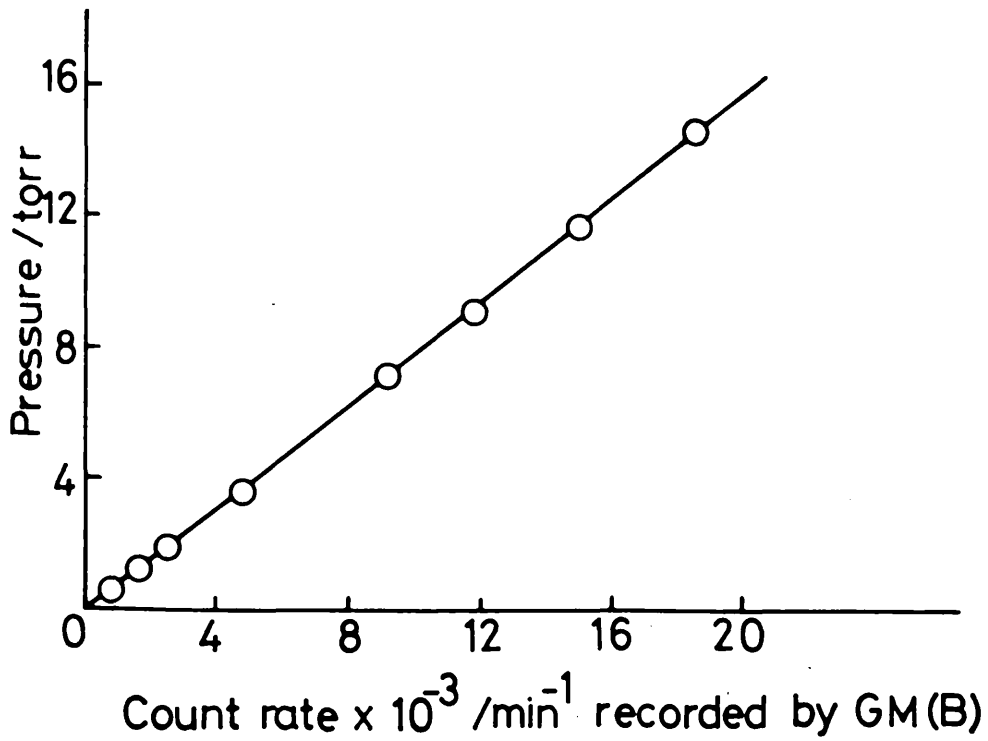
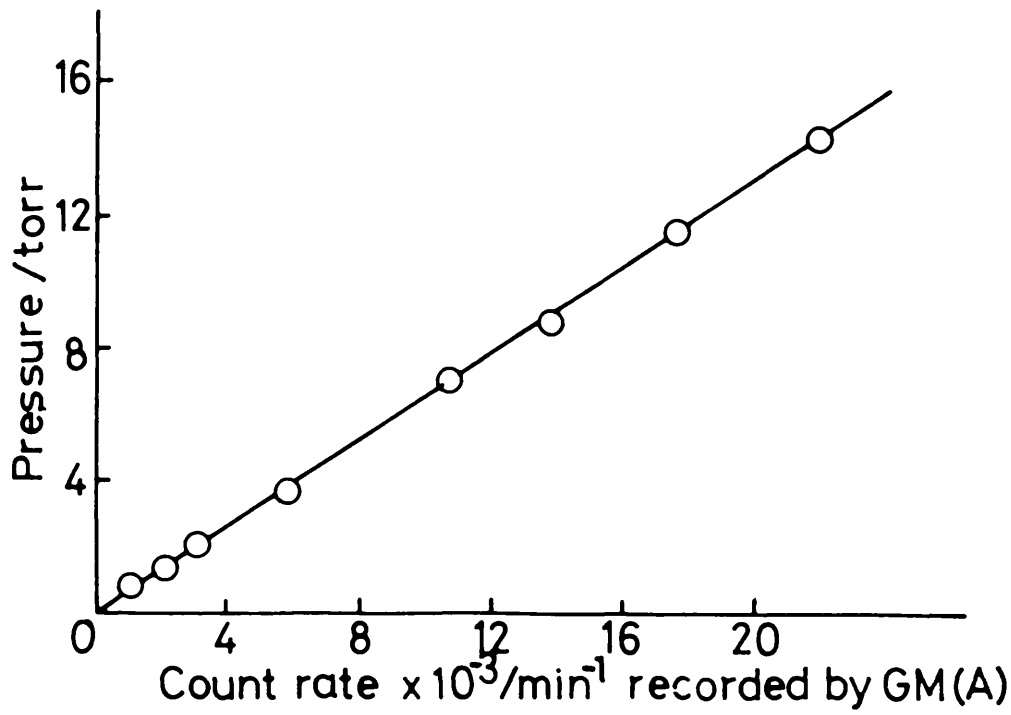


Figure 5. - Plots of count rates recorded by GM(A) and GM(B) against pressures of radioactive gas.

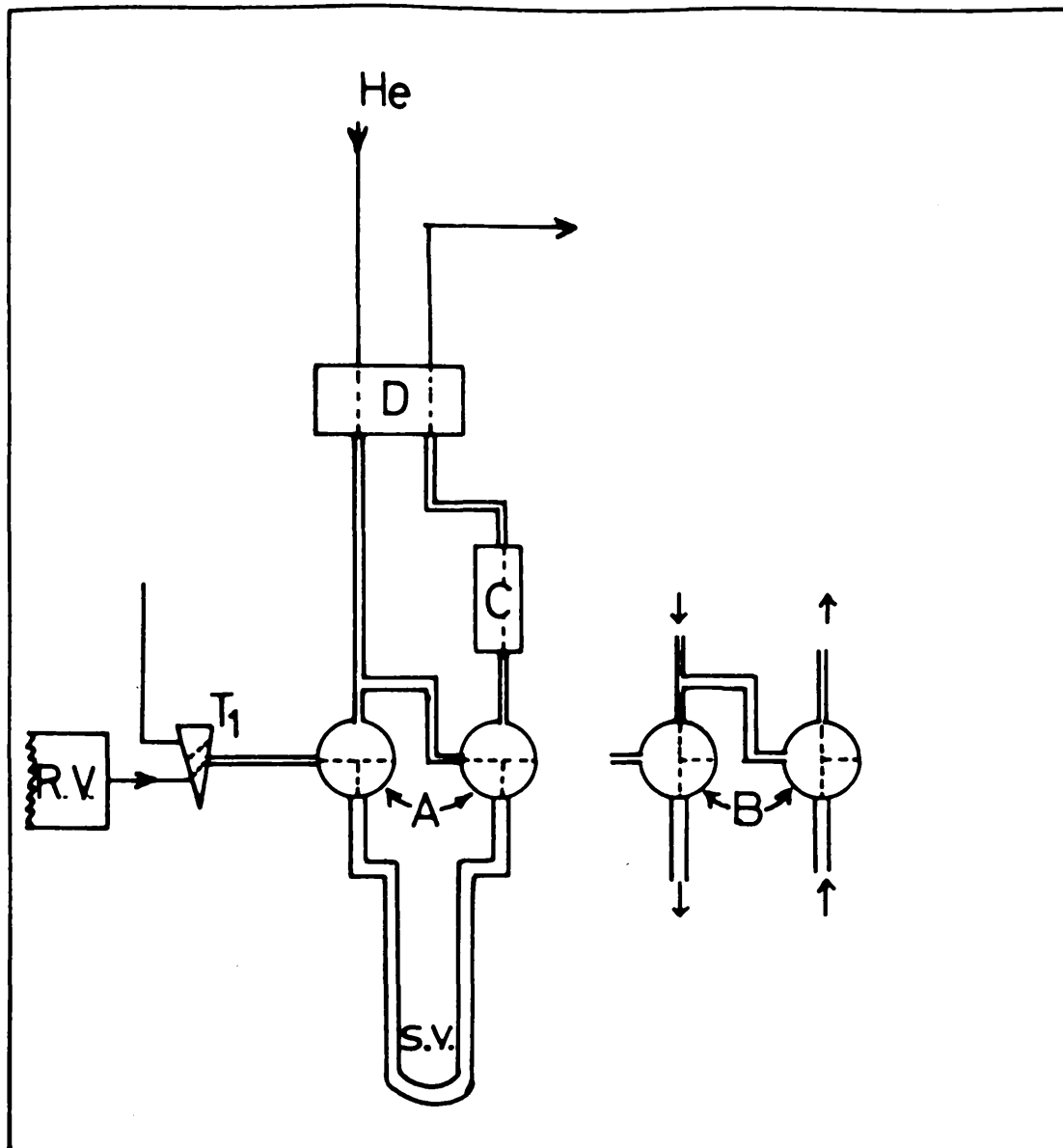


Figure 6. - Sample handling unit.

When the taps were in position (A) a sample of reaction mixture was introduced into the sampling vessel (S.V.) and when the taps were in position (B) the sample was flushed into the column (C). Tap (T<sub>1</sub>) was used either to evacuate the sampling vessel or to remove samples from the reaction vessel

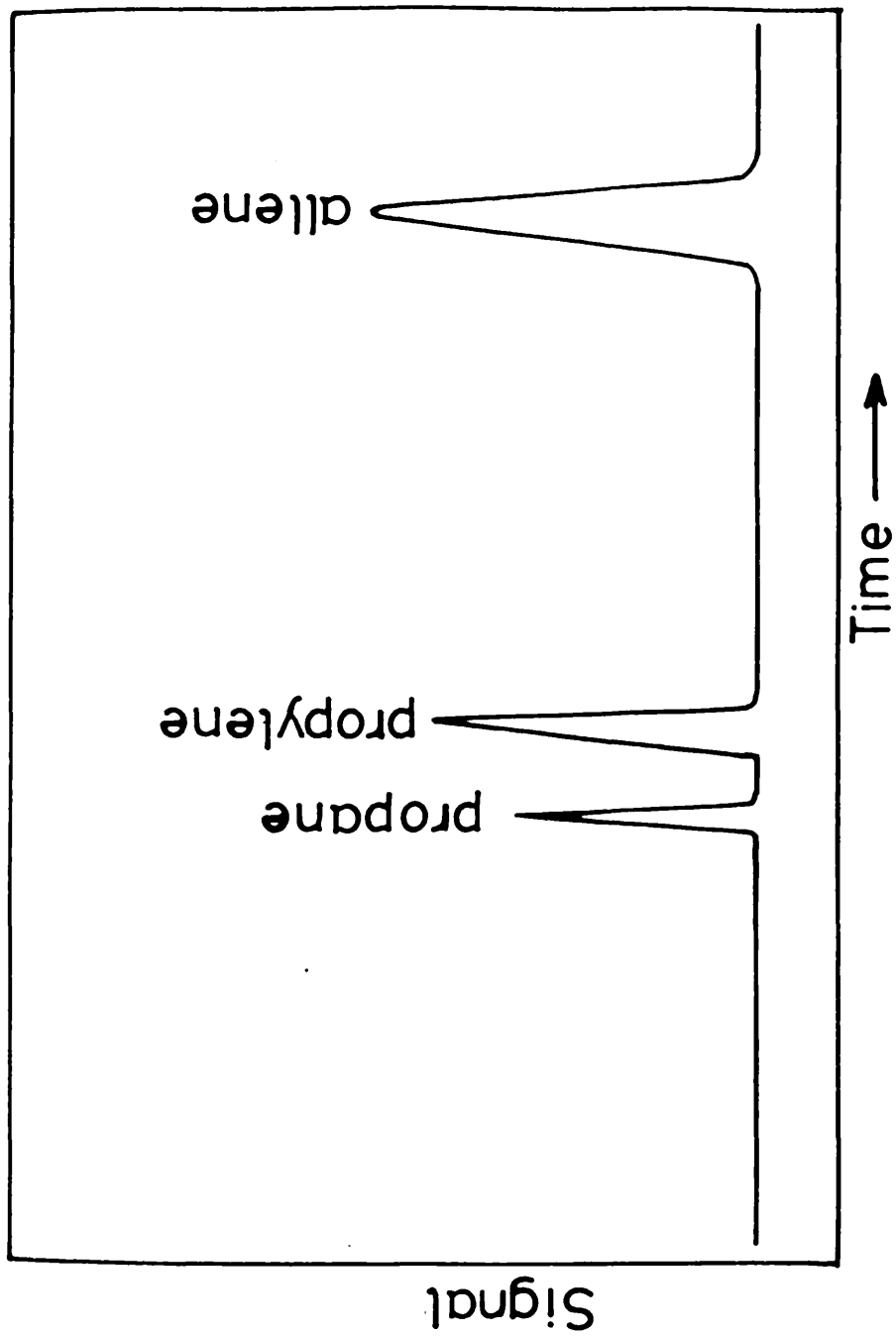


Figure 7. - A typical chromatograph trace from a mixture of propane, propylene and allene.

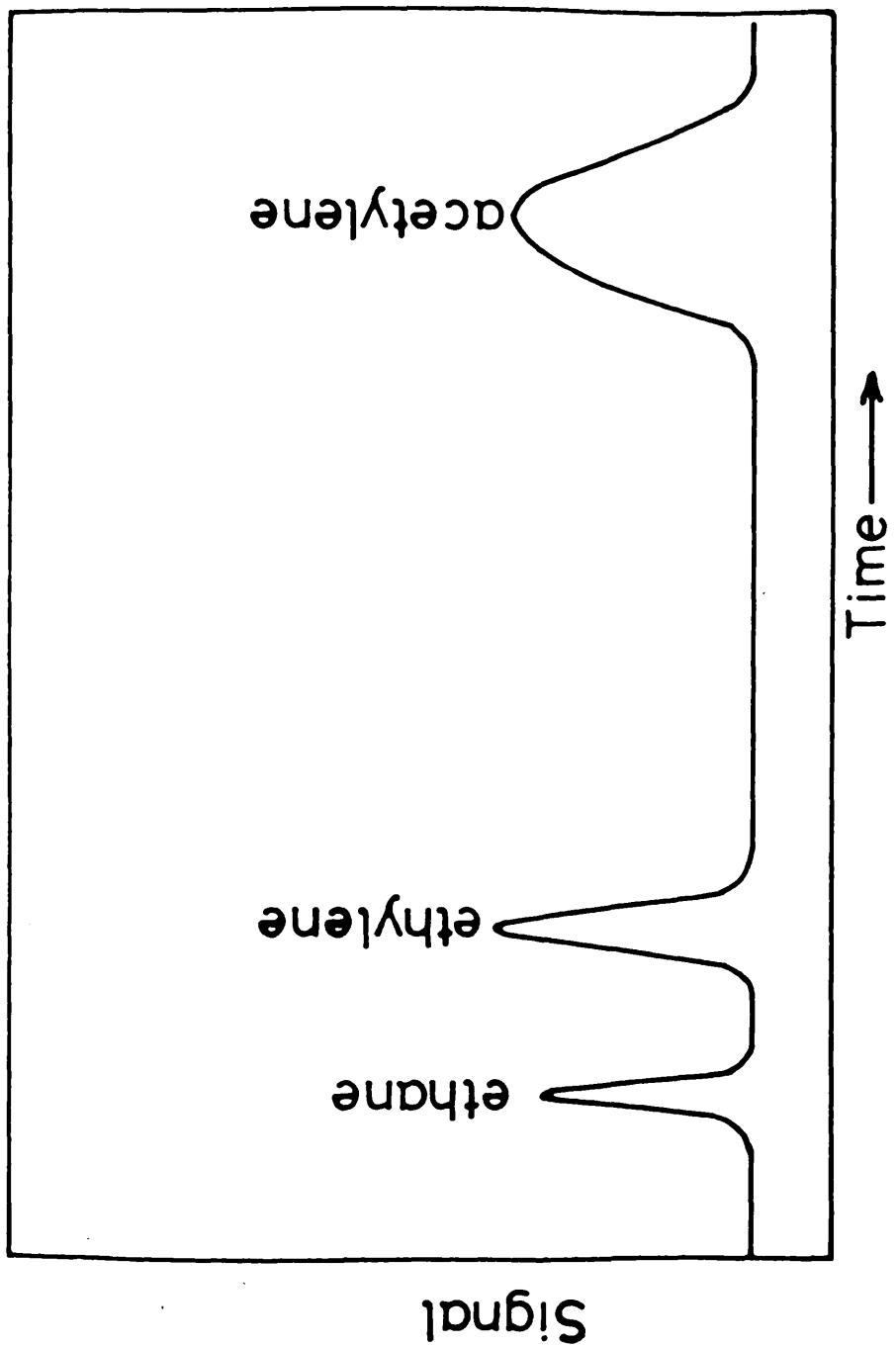


Figure 8. - A typical chromatograph trace from a mixture of ethane, ethylene and acetylene.

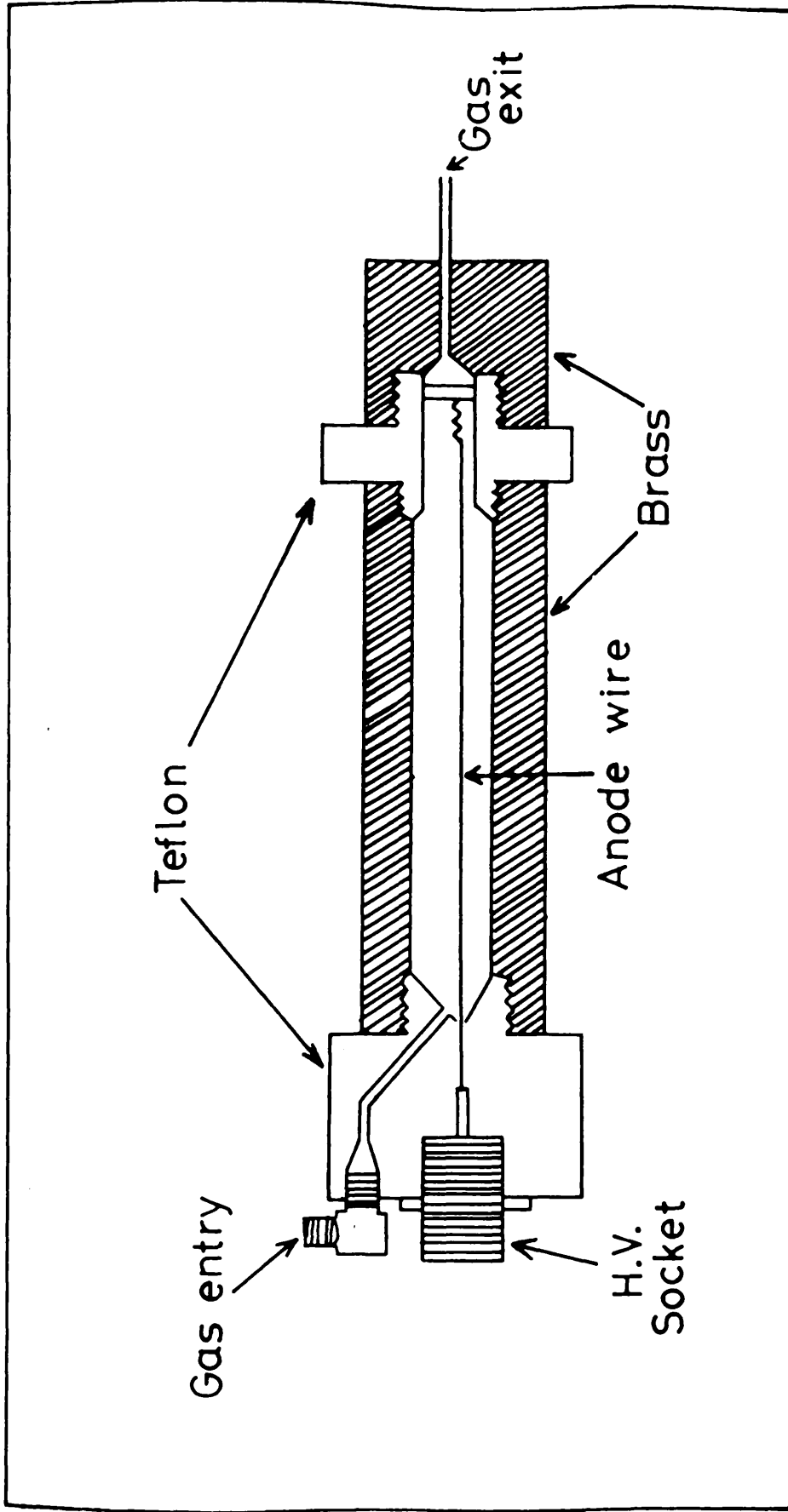


Figure 9. - The Proportional Counter

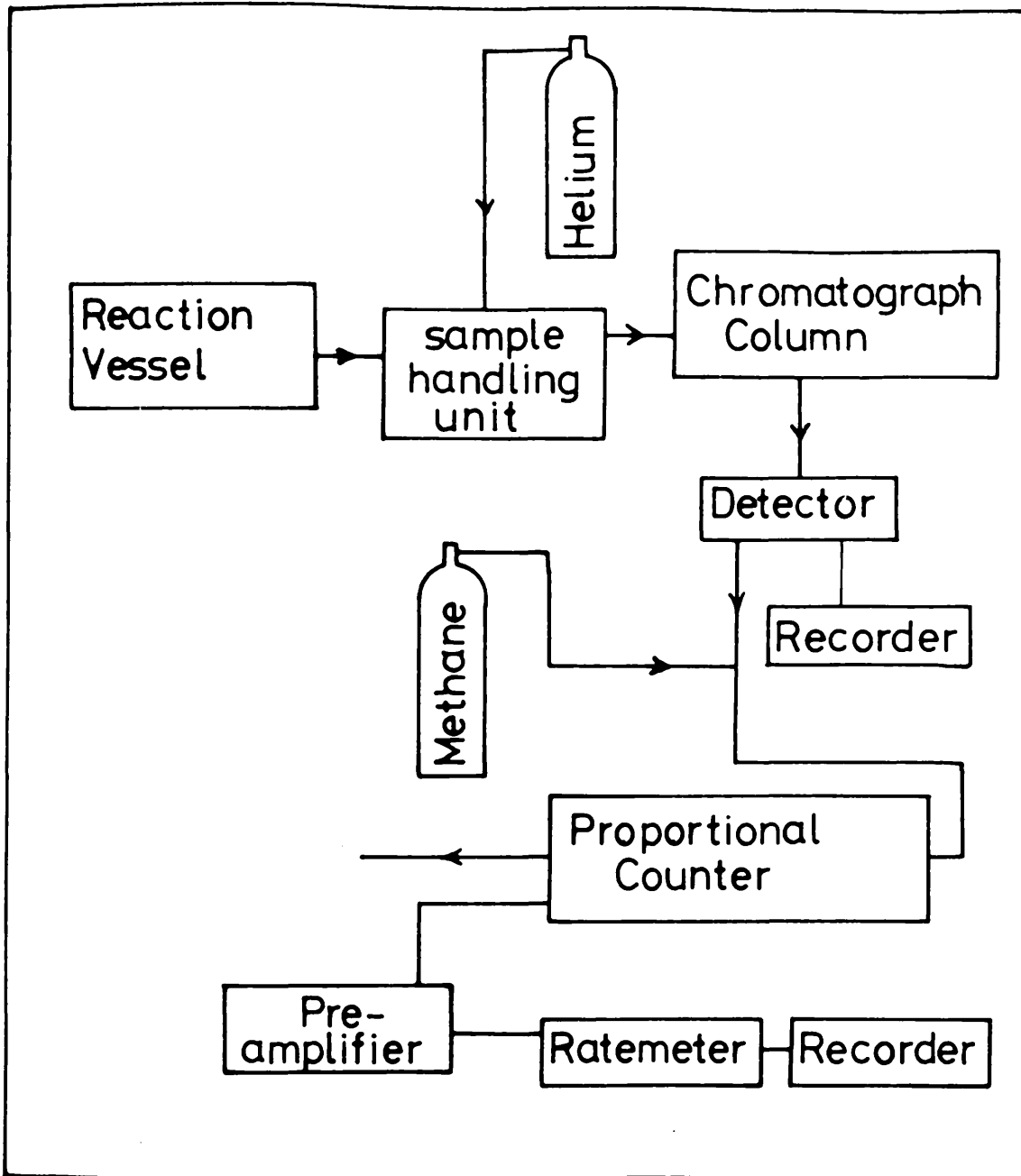


Figure 10. - Block diagram of the gas chromatographic system and proportional counter.

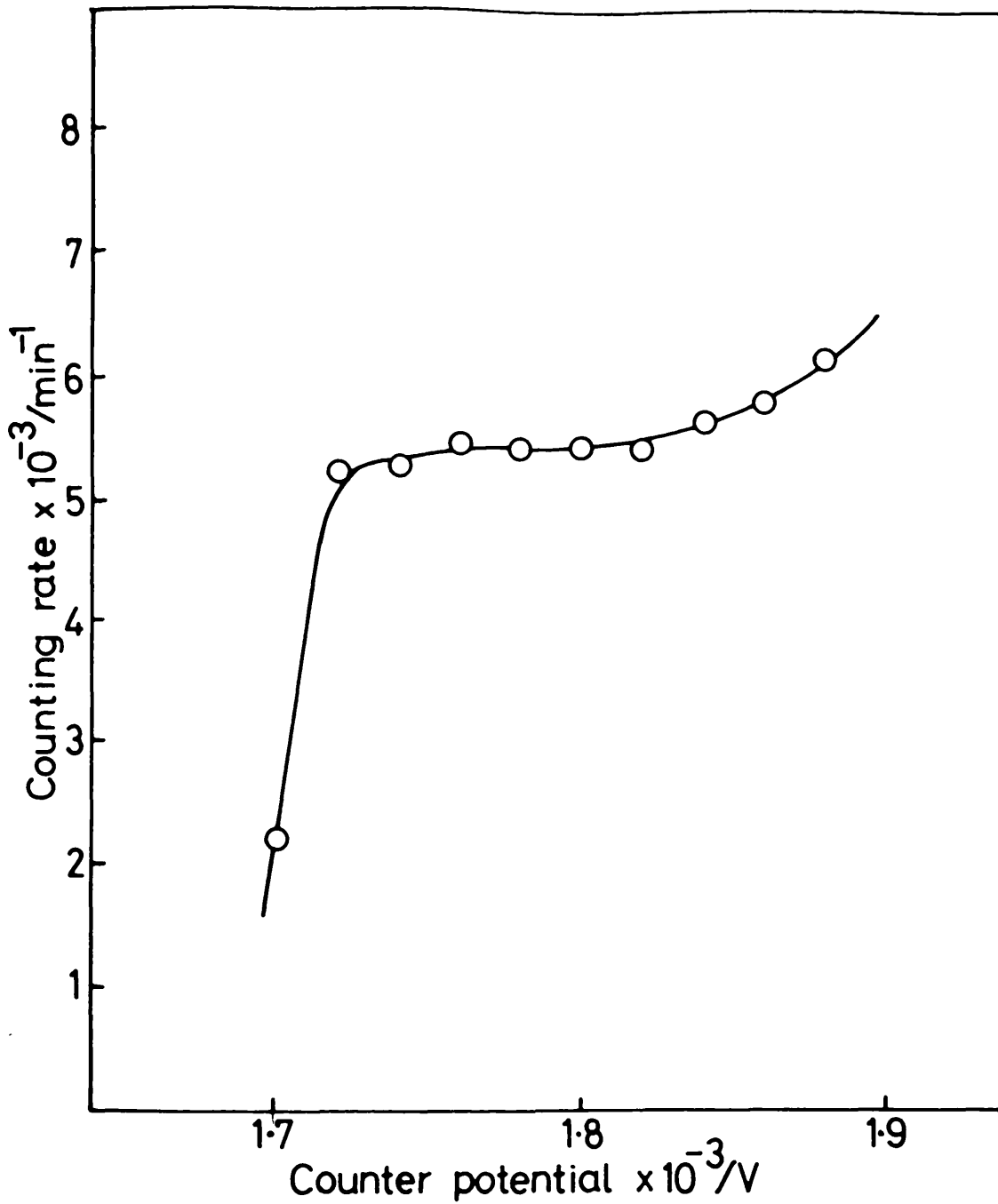


Figure 11. - Counting characteristics of the gas flow proportional counter (helium:methane = 10:1) obtained with a  $^{60}\text{Co}$  external source of radiation. Flow rate  $66 \text{ cm}^3 \text{ min}^{-1}$ . Lower discrimination = 150. Gain = 32.

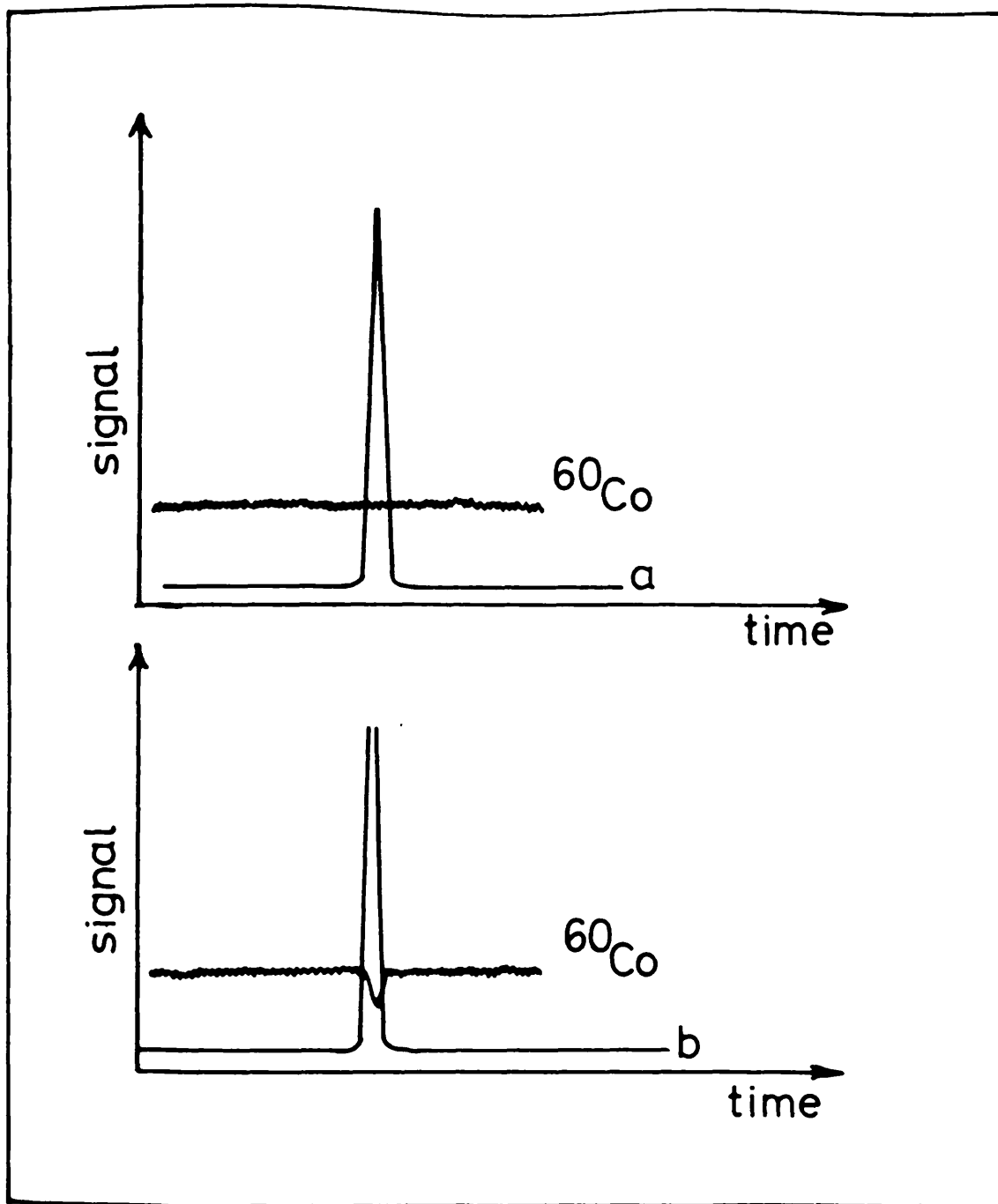


Figure 12. - Investigation of the influence of propylene (a) 14.0 torr and (b) 25.0 torr on activity counting of proportional counter. External [ $^{60}\text{Co}$ ]cobalt source.

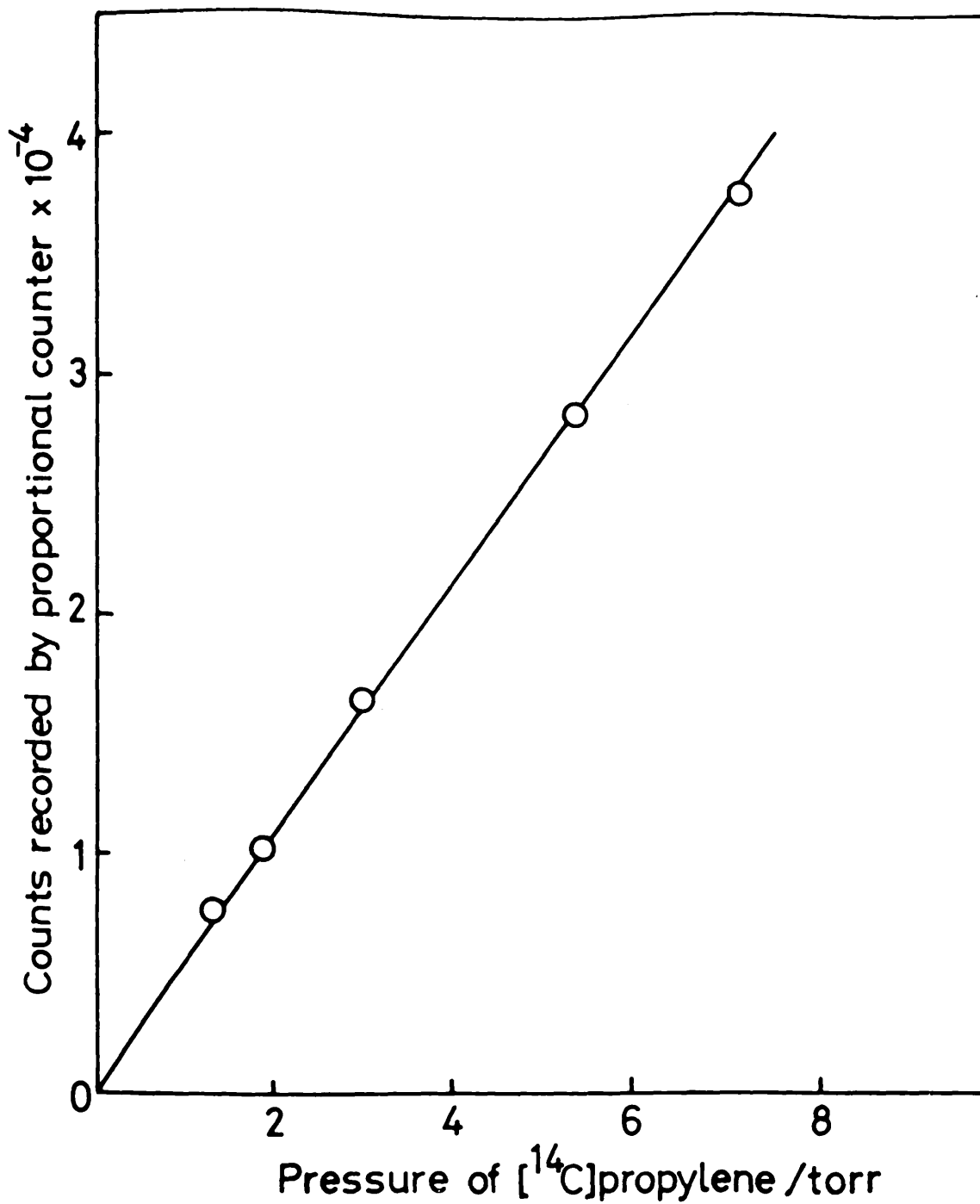


Figure 13. - Calibration curve. Radioactivity recorded by the proportional counter versus pressure of [<sup>14</sup>C]propylene. [<sup>14</sup>C]propylene specific activity was 0.031 mCi/mmol.

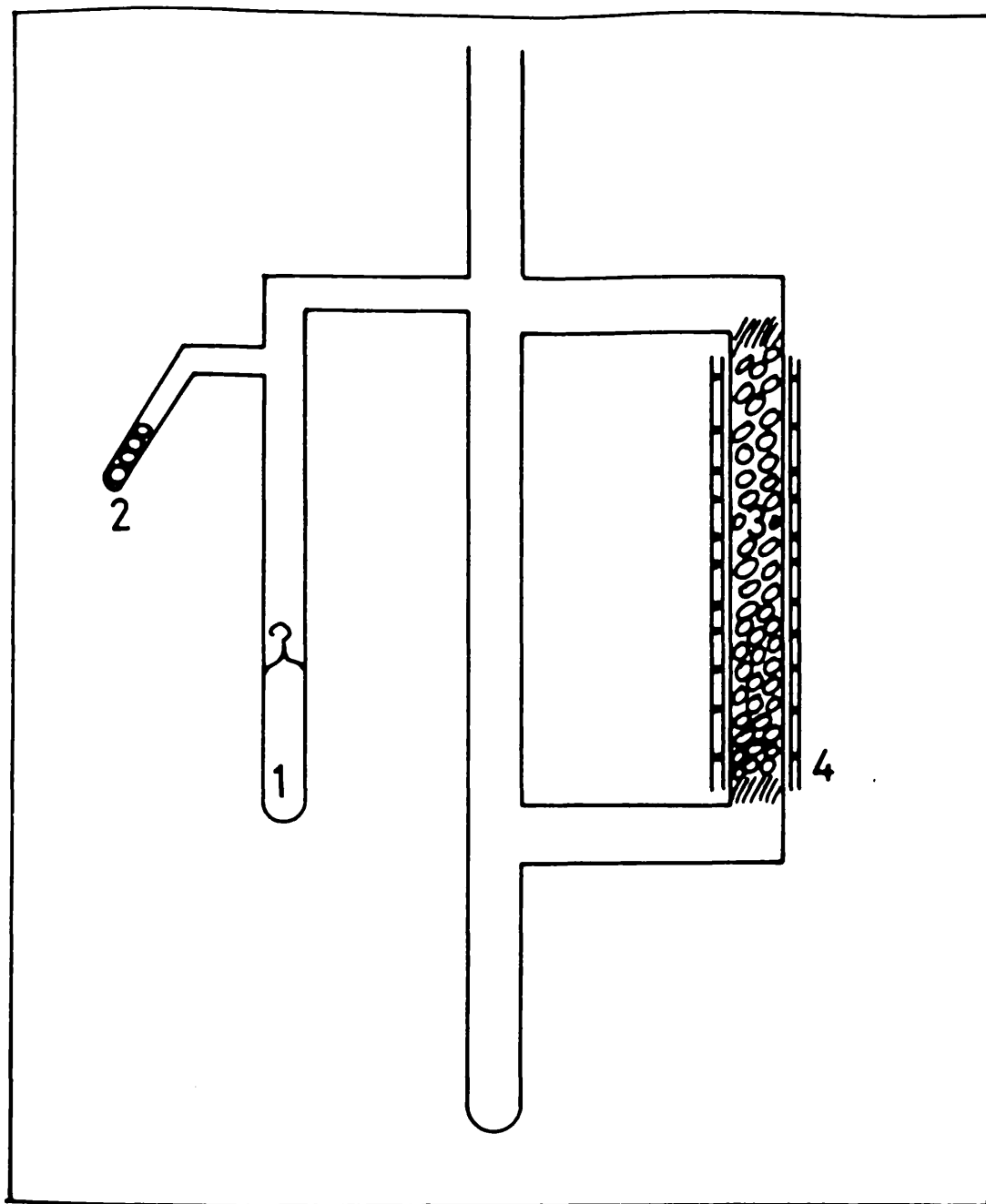


Figure 14. - Apparatus for the conversion of [ $^{14}\text{C}$ ]carbon dioxide to [ $^{14}\text{C}$ ]carbon monoxide.

1. [ $^{14}\text{C}$ ]Carbon dioxide in glass break-seal ampoule.
2. Stainless steel balls.
3. Zinc pellets.
4. Electrical furnace.

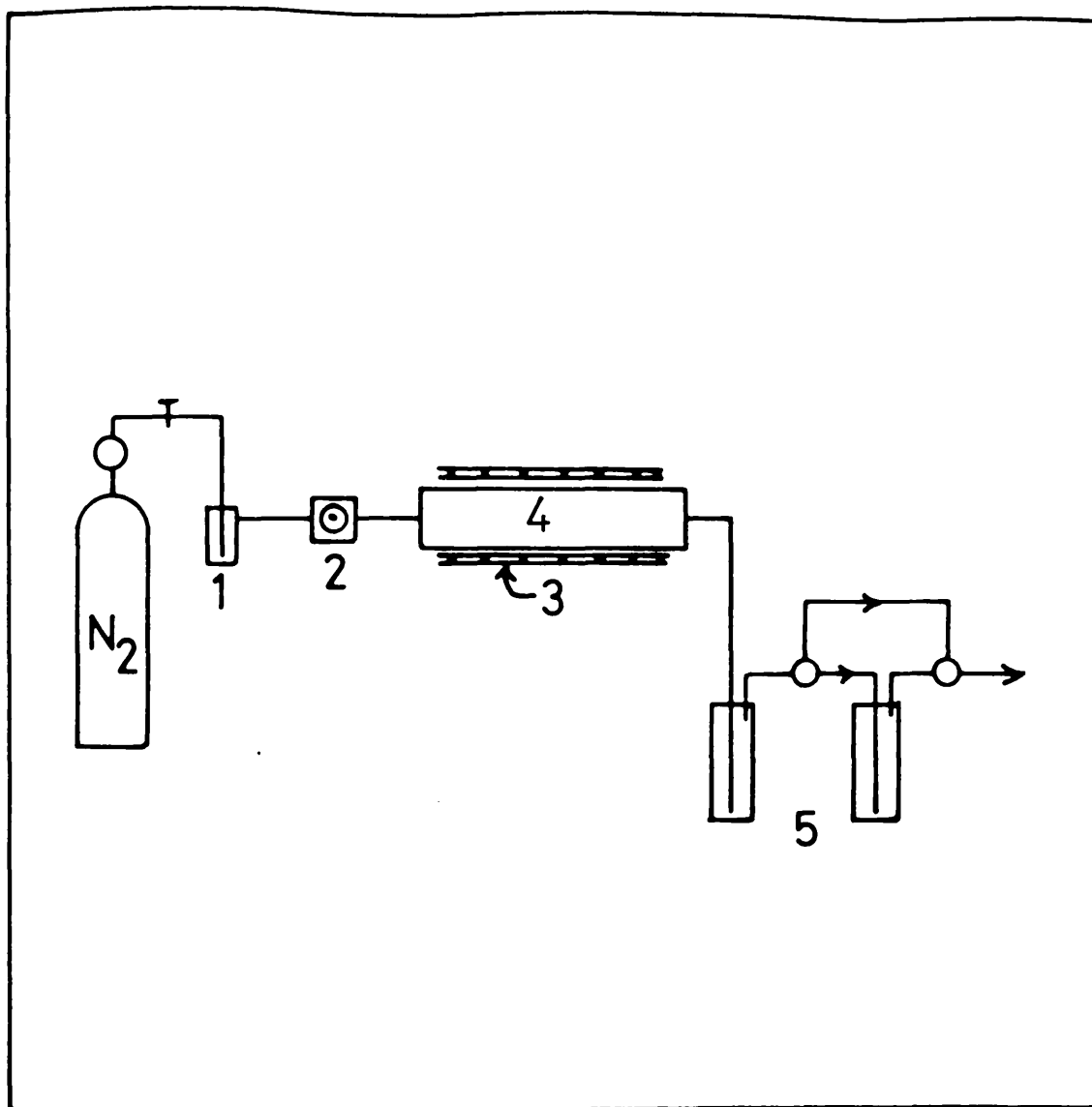


Figure 15. - Preparation of  $[^{14}\text{C}]$ propylene.

1. Bubbler containing concentrated  $\text{H}_2\text{SO}_4$ .
2. Heated injection port.
3. Electrical furnace.
4. Alumina.
5. Traps.

## CHAPTER FOUR

## CHAPTER 4

### RESULTS

#### 4.1 The Phenomenon of Self-Deactivation

It has been reported that in the hydrogenation of unsaturated hydrocarbons over supported metal catalysts the rates of reaction of the freshly reduced catalysts progressively decrease to a steady state constant activity (136,168). A systematic study of the self-deactivation phenomenon during a series of allene hydrogenations was carried out with the aims of examining the possible effects of the deactivation upon the kinetics and upon the selectivity of the catalysts for propylene formation.

##### 4.1.1 Reactions Over Alumina-Supported Palladium

The reaction of 12.0 torr of allene with 36.0 torr of hydrogen was examined using 0.01g of the palladium catalyst. 48.0 torr of the pre-mixed sample ( $H_2:C_3H_4 = 3:1$ ) was introduced into the reaction vessel containing a freshly reduced catalyst at room temperature. The progress of the reaction was followed by monitoring the variation of pressure fall with time. Figure 16 shows some typical pressure fall against time curves. The first reactions proceeded in two distinct stages, the onset of the second stage being accompanied by an increase in rate. The second

stage gradually disappeared as more reactions were performed over the catalyst.

The acceleration point, denoted as  $-\Delta P_a$  is defined as the pressure fall at the obtained point of intersection by extrapolating the first and second stages of the reaction. The acceleration point was dependent upon the reaction number and its value ( $-\Delta P_a$ ) increased from 6.5 torr for the first reaction to 12.3 torr for reactions with a rate of reaction approaching the steady state activity. The acceleration point disappeared when the catalyst reached the steady state activity.

Up to a pressure fall corresponding to the acceleration point the pressure-time curves were always accurately first order in total pressure (figure 17).

The rate of hydrogenation decreased with successive reactions until a constant steady state activity was eventually attained. The reaction rate did not tend to zero. Figure 18 shows the variation of the first order rate constant with reaction number for 0.01g of the palladium catalyst. Once the steady state had been achieved the catalytic activity could be partially restored by leaving the catalyst in contact with the reaction mixture for an extended period ( $\geq 2$  hours) (figure 18). The original activity could be reproducibly restored by heating the catalyst in an atmosphere (760 torr) of hydrogen at 623K for 6 hours.

The analysis of the reaction products during the deactivation process was performed by extracting samples from the reaction mixture at 40% conversion. When the steady state was attained, samples were extracted from the reaction mixture at different percentages of conversion. (% conversion = 100 x moles of hydrogen consumed per mole of allene present).

The variation of the amount of propane, propylene and allene with conversion for the hydrogenation of allene over 0.01g alumina-supported palladium is shown in figure 19. The selectivity for propylene formation, defined as

$$\text{selectivity} = S = \frac{P_{C_3H_6}}{P_{C_3H_6} + P_{C_3H_8}}$$

was independent of pressure fall up to approximately 70% conversion (figure 20). The effect of reaction number upon selectivity for propylene formation can be seen in figure 21. The selectivity fell slightly from an initial value of 0.932 to a limiting value of 0.902 when the steady state activity was achieved (table 3).

A study of the deactivation phenomenon during a series of hydrogenation reactions over a freshly reduced palladium catalyst was also carried out using 0.02g of catalyst and a reaction mixture with a 2 to 1 hydrogen (24.0 torr):allene (12.0 torr) ratio. The results were similar to those obtained when a reaction mixture with a 3 to 1 hydrogen:allene

ratio was used. Up to a pressure fall corresponding to the acceleration point, the pressure-time curves were always accurately first order in total pressure. The catalytic activity decreased with reaction number until a constant steady state activity was eventually attained (figure 22). The selectivity was independent of pressure fall up to approximately 70% conversion (figure 23). The variation of selectivity with reaction number can be seen in figure 24. The selectivity fell slightly from an initial value of 0.943 to a limiting value of 0.896 when the steady state activity was achieved (table 3).

#### 4.1.2 Reactions over Alumina-Supported Iridium

The allene hydrogenation was examined using 0.25g of the alumina-supported iridium catalyst. A premixed sample containing hydrogen (36.0 torr) and allene (12.0 torr) was admitted to a freshly reduced iridium catalyst at room temperature. The pressure fall against time curves, recorded by the differential pressure transducer, showed that the reaction proceeded in two distinct stages, the onset of the second stage being accompanied by an increase in rate (figure 25).

The acceleration point ( $-\Delta P_a$ ), obtained by extrapolating the first and second stages of the reaction, occurred at a pressure fall of  $18.6 \pm 0.5$  torr and was independent of the number of reactions performed over the catalyst.

Up to the acceleration point the pressure against time curves were always accurately first order in total pressure (figure 26).

Figure 27 shows the variation of the first order rate constant with reaction number for the hydrogenation of allene over 0.25g of the iridium catalyst. It can be seen that the catalytic activity remained constant as the reaction number increased. The catalyst did not undergo self-poisoning; the catalyst activity remained approximately constant for several days.

Storage of the catalyst under the hydrogen-rich reaction products for several hours had no effect upon the catalytic activity. After a series of allene hydrogenations, further treatment of the catalyst in a hydrogen atmosphere for 6 hours at 623K did not affect the catalytic activity.

The analysis of the reaction products during a series of reactions was performed by extracting samples from the reaction mixture at different percentage conversions. The variation of the amount of propane, propylene and allene with conversion can be seen in figure 28.

The selectivity for propylene formation was dependent upon the progress of the reaction. The selectivity decreased slightly with conversion up to the acceleration point (figure 29). After the acceleration point, the selectivity decreased rapidly because the main process occurring was further hydrogenation of propylene to propane. Table 4 shows the selectivity obtained during a series of hydrogenation

reactions. The sample was, in each reaction, extracted from the reaction vessel at approximately 90% conversion. It can be seen from table 4 that the selectivity remained approximately constant as the reaction number increased.

#### 4.1.3 Reactions over Alumina-Supported Rhodium

##### 4.1.3.1 Allene Hydrogenation

The reaction of 12.0 torr of allene with 36.0 torr of hydrogen was examined using 0.05g or 0.10g of the rhodium catalyst. Reactions were carried out by admitting a pre-mixed sample of hydrogen and allene ( $H_2:C_3H_4 = 3:1$ ) to the reaction vessel containing a freshly reduced catalyst at room temperature. The pressure fall against time curves, recorded by the pressure transducer, showed that the reaction proceeded in two distinct stages, the onset of the second stage being accompanied by an increase in rate. Figure 30 shows a typical pressure fall against time curve obtained using 0.05g of the rhodium catalyst.

The acceleration point ( $-\Delta P_a$ ) was independent of the catalytic activity for reactions occurring at a rate of less than 0.5 torr per minute and had a value of  $12.0 \pm 0.5$  torr. For reactions occurring at a faster rate the acceleration point decreased with increasing catalytic activity.

Up to the acceleration point the pressure against time curves were always accurately first order in total pressure (figure 31).

The catalytic activity decreased with successive reactions until a constant steady state activity was eventually attained. The first order rate constant for reactions at constant steady state activity was  $k = 3.2 \times 10^{-3} \text{ min}^{-1}$  for the 0.05g Rh/alumina catalyst sample and  $k = 7.0 \times 10^{-3} \text{ min}^{-1}$  for the 0.10g Rh/alumina catalyst sample. For both samples the reaction rate did not tend to zero. It was also observed that the catalytic activity increased after the first reaction. The second reaction was faster than the first one and after reaching a maximum the catalytic activity fell with successive reactions to the steady state value (figure 32).

With both samples of catalyst the deactivation process was dependent only upon the number of hydrogenation reactions performed on the catalyst. The catalytic activity, for allene hydrogenation, of the 0.05g sample of rhodium catalyst, previously used for a series of acetylene hydrogenations (see section 4.1.3.2) was  $k = 3.5 \times 10^{-3} \text{ min}^{-1}$ . This catalytic activity was approximately the same as when the catalyst reached the steady state after successive reactions of allene hydrogenation. Therefore, the steady state catalytic activity for allene hydrogenation, could be reached by either a series of successive allene hydrogenations or successive acetylene hydrogenations. Pretreatment of the catalyst with 200 torr of allene for two hours and storage of the catalyst under the reaction products up

to twelve hours had no effect upon either the progress of the catalyst deactivation or the steady state catalytic activity. The original activity could, however, be reproducibly restored by heating the catalyst in an atmosphere (760 torr) of hydrogen at 623K for one hour. During this regeneration process only propane was produced, although, because of the small amounts involved, accurate quantitative analysis of the amount of propane could not be achieved.

The variation of the amounts of propane, propylene and allene with conversion for the hydrogenation of allene over the 0.10g sample of alumina-supported rhodium catalyst is shown in figure 33. The selectivity for propylene formation was independent of the progress of the reaction up to the acceleration point (figure 34). The effect of reaction number upon selectivity can be seen in figure 35. The selectivity increased slightly from an initial value of 0.940 to a limiting value of 0.950 when the steady state activity had been achieved (table 5).

#### 4.1.3.2 Acetylene Hydrogenation

The reaction of 12.0 torr of acetylene with 36.0 torr of hydrogen was examined using 0.05g or 0.10g of the rhodium catalyst. Reactions were carried out by admitting a premixed sample of hydrogen and acetylene ( $H_2:C_2H_2 = 3:1$ ) to the reaction vessel containing a freshly reduced catalyst at room temperature. The pressure fall against time curves showed

that the reaction proceeded in two distinct stages, the onset of the second stage being accompanied by an increase in rate. Figure 36 shows a typical pressure fall against time curve obtained using 0.10g of the rhodium catalyst.

The acceleration point ( $-\Delta P_a$ ) occurred at a pressure fall of  $16.4 \pm 0.5$  torr and was independent of the number of reactions performed over the catalyst.

Up to the acceleration point the pressure against time curves were always accurately first order in total pressure (figure 37).

The rate of hydrogenation decreased with successive reactions until a constant steady state activity was eventually attained. The reaction rate did not tend to zero. Figure 38 shows the variation of the first order rate constant with reaction number for the hydrogenation of acetylene over the 0.10g sample of rhodium catalyst.

Analysis of the reaction products during the deactivation process was performed by extracting samples from the reaction mixture at approximately 60% conversion. When the steady state was attained, samples were extracted from the reaction mixture at different conversions. (% conversion =  $100 \times$  moles of hydrogen consumed per mole of acetylene present).

The variation of the amounts of ethane, ethylene and acetylene with conversion for the hydrogenation of acetylene over the 0.10g sample of alumina-supported rhodium catalyst

is shown in figure 39. The selectivity for ethylene formation, defined as

$$\text{selectivity} = S = \frac{P_{C_2H_4}}{P_{C_2H_4} + P_{C_2H_6}}$$

was independent of the progress of reaction up to the acceleration point (figure 40). The effect of reaction number upon selectivity can be seen in figure 41. The selectivity fell slightly from an initial value of 0.737 to a limiting value of 0.701 when the steady state activity was achieved (table 6).

Table 3

Effect of Self-Poisoning on Selectivity

Reaction Number	Selectivity	
	0.01g Pd/alumina (H <sub>2</sub> :allene = 3:1)	0.02g Pd/alumina (H <sub>2</sub> :allene = 2:1)
1	0.932	-
2	0.941	-
3	0.940	0.943
4	0.930	0.943
5	0.929	0.936
6	0.920	0.912
7	0.912	0.913
8	0.906	0.911
9	0.905	0.908
10	0.905	0.904
11	0.905	0.900
12	0.905	0.899
13	0.902	0.898
14	0.904	0.896

Table 4

Selectivity for Propylene Formation During a  
Series of Allene Hydrogenations over 0.25g  
Alumina-Supported Iridium Catalyst

Reaction Number	Selectivity
1	0.436
2	0.440
-	-
4	0.439
5	0.441
6	0.441
-	-
14	0.441

Table 5

Selectivity for Propylene Formation During a Series of Allene Hydrogenations over 0.10g Alumina-Supported Rhodium Catalyst

Reaction Number	Selectivity
1	-
2	0.941
3	0.940
4	0.944
5	0.944
6	0.947
7	0.951
8	-
9	0.947
10	-
11	0.948
12	-
13	0.950
14	-
15	0.950
16	-
17	0.949
18	-
19	-
20	0.949
21	-
22	0.952
23	-
24	0.950
25	-
26	-
27	0.952
28	0.954
29	0.948
30	-
31	-
32	-
33	0.950

Table 6

Selectivity for Ethylene Formation During  
a Series of Acetylene Hydrogenations over  
0.10g Alumina-Supported Rhodium Catalyst

Reaction Number	Selectivity
1	0.737
2	0.730
3	0.731
4	0.719
5	0.719
6	0.717
7	0.708
8	0.706
9	0.708
10	0.708
11	0.701
12	0.704

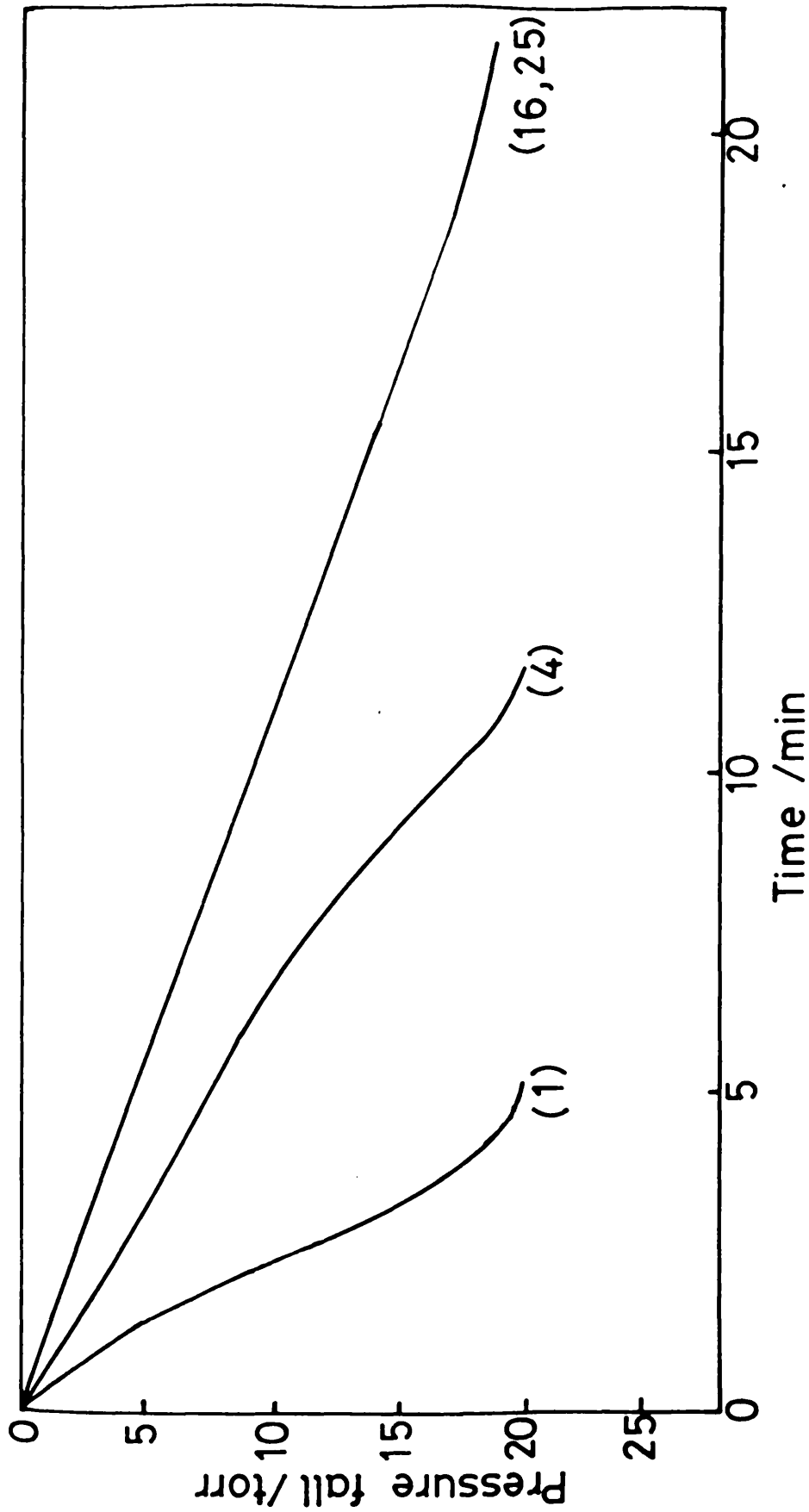


Figure 16. - Pressure fall against time curves for the hydrogenation of 12.0 torr allene with 36.0 torr hydrogen over 0.01g Pd/alumina catalyst at 294 K. Numbers refer to the reaction sequence.

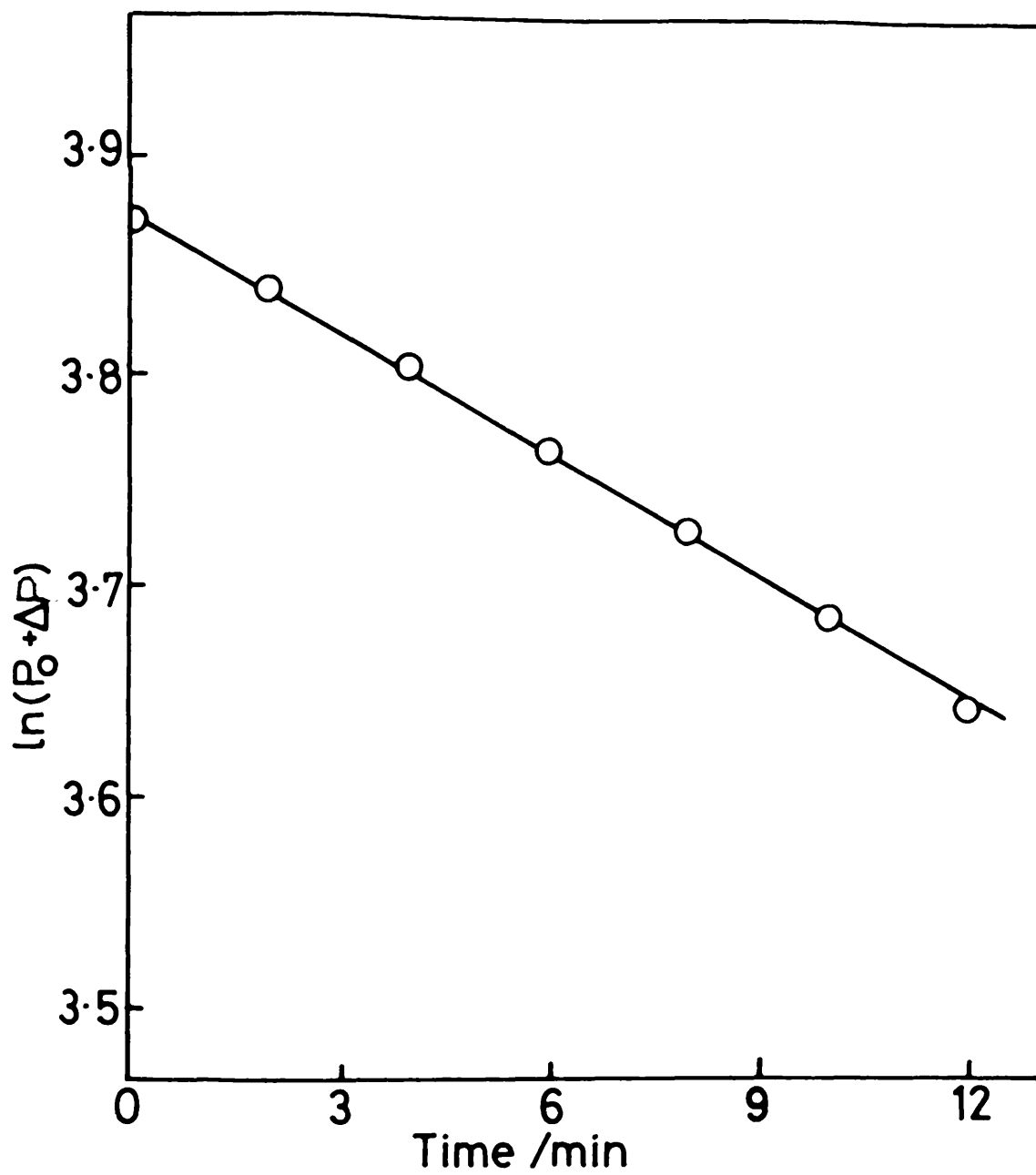


Figure 17. - Variation of  $\ln(P_0 + \Delta P)$  with time for the hydrogenation of allene over 0.01g Pd/alumina.

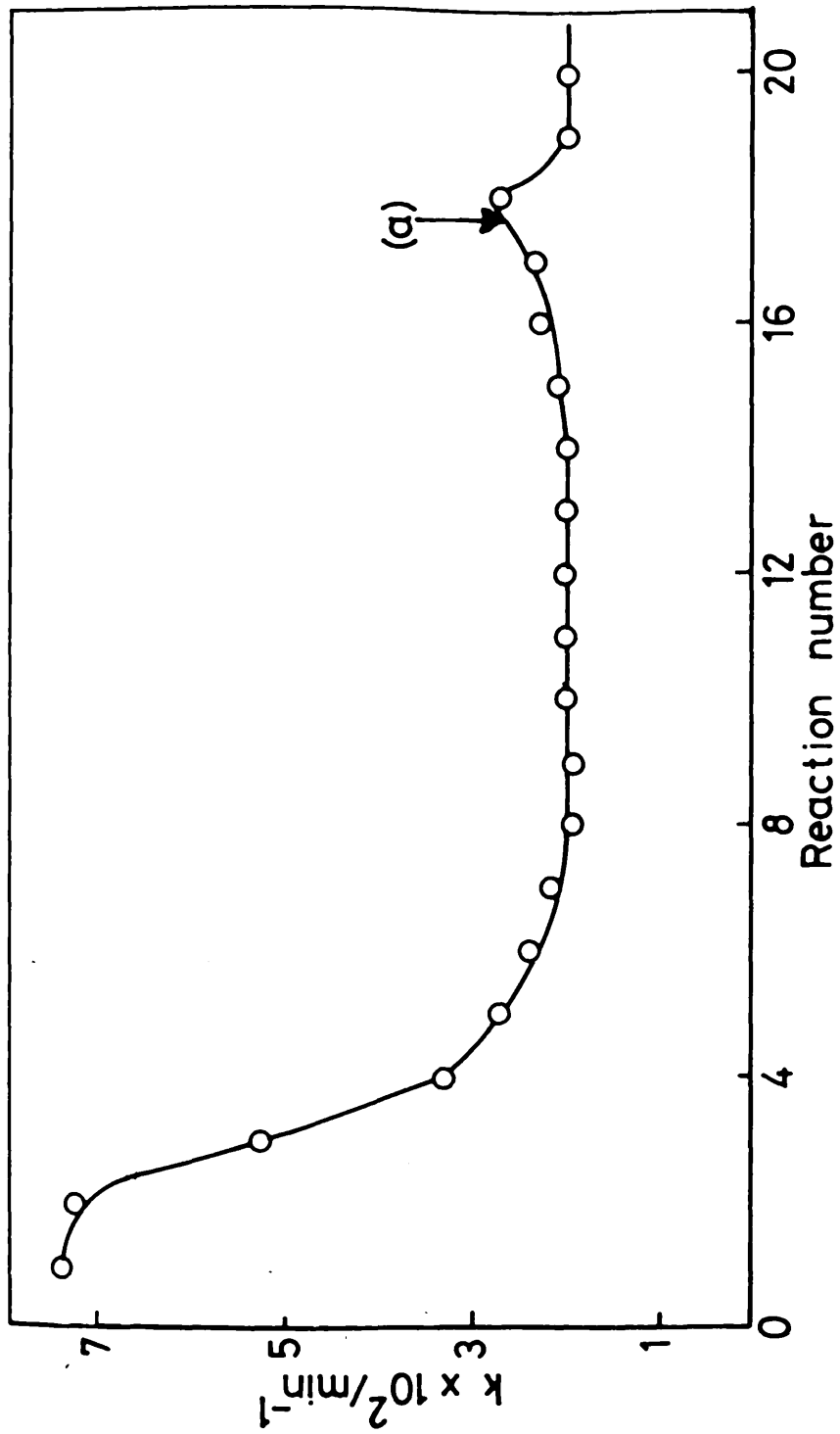


Figure 18. - Variation of the first order rate constant with reaction number for 0.01g Pd/alumina catalyst at 294 K. The point (a) corresponds to the treatment of the catalyst in the hydrogen rich reaction products for 2 hours.  $[(P_{C_3H_4})_0 = 12.0 \text{ torr}; (P_{H_2})_0 = 36.0 \text{ torr}]$ .

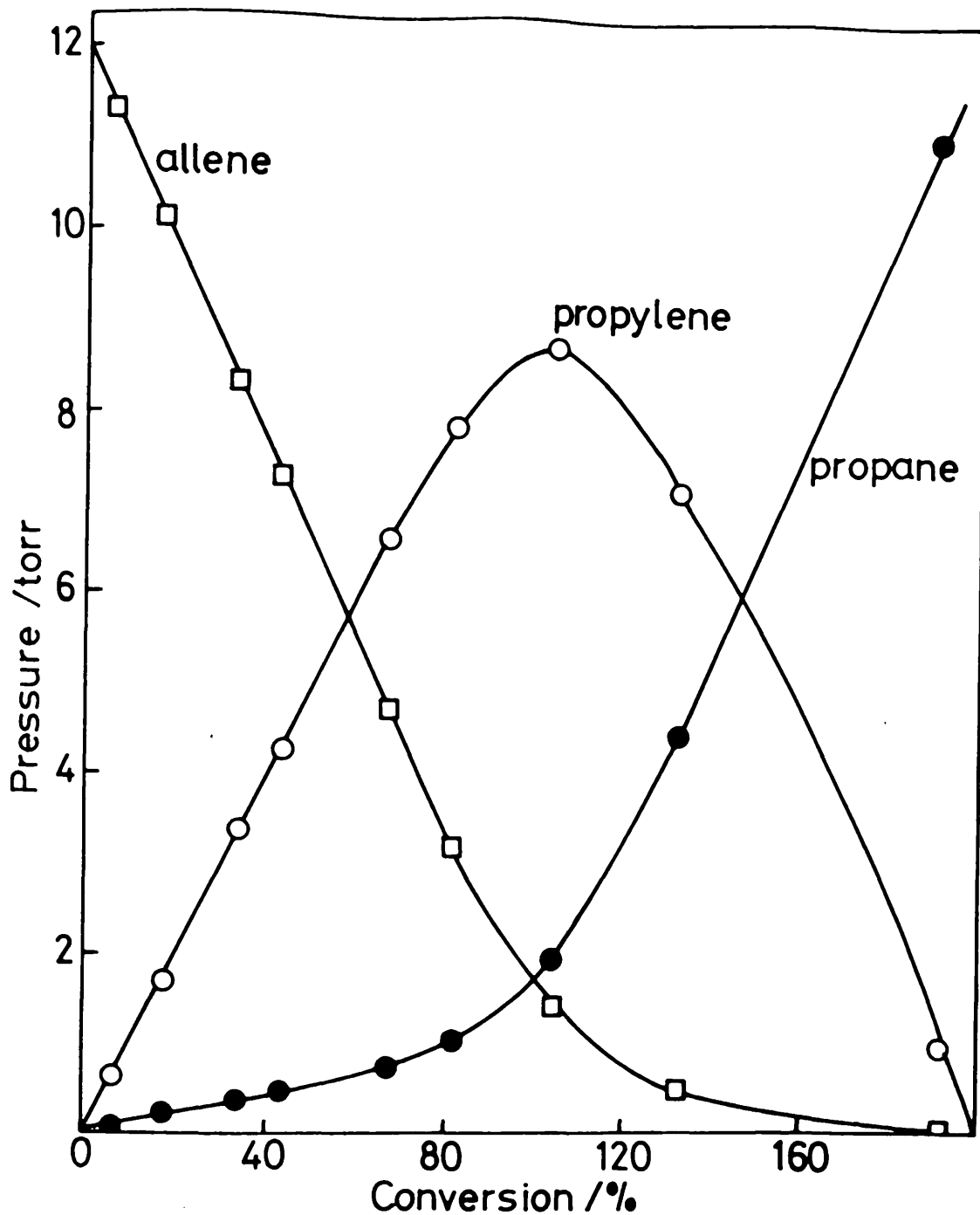


Figure 19. - Variation of the amount of propane (●), propylene (○) and allene (□) with conversion for the hydrogenation of a mixture of hydrogen (36.0 torr) and allene (12.0 torr) over 0.01g Pd/alumina catalyst.

(% conversion =  $100 \times \text{moles of H}_2 \text{ consumed per mole of allene present}$ ).

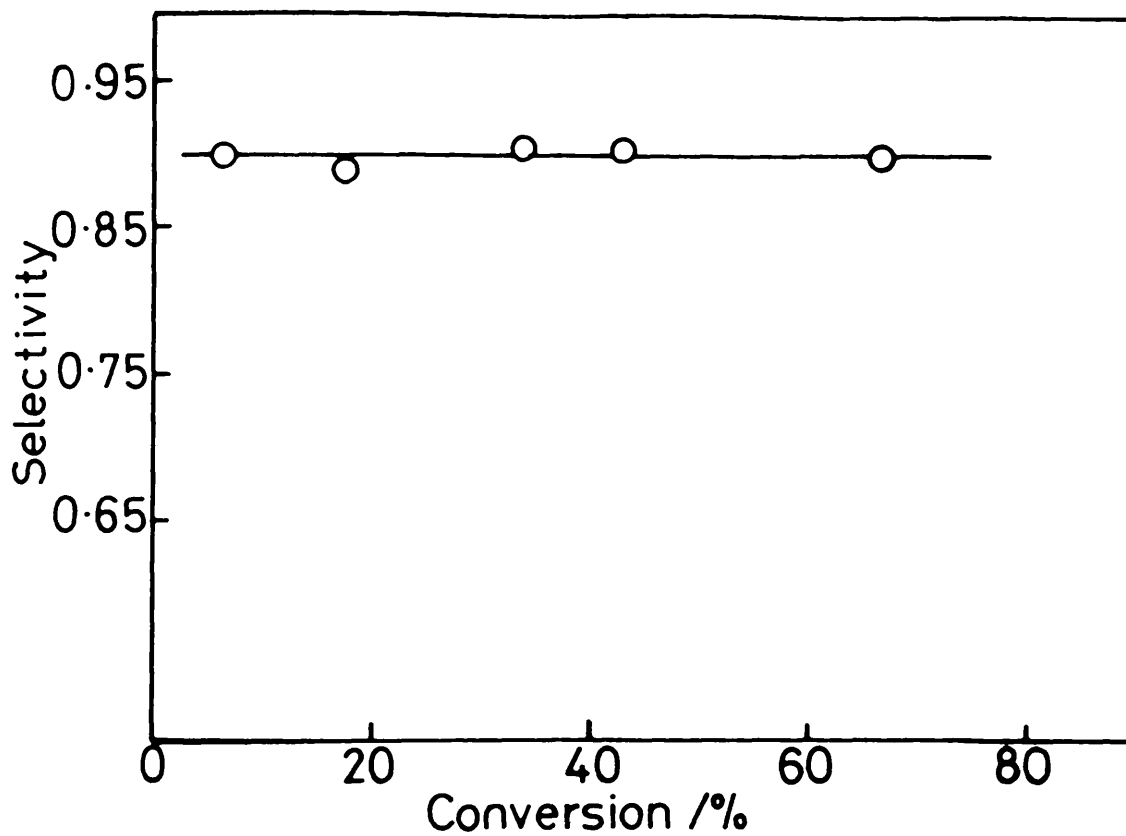


Figure 20. - Variation of selectivity with conversion for the hydrogenation of 12.0 torr allene with 36.0 torr hydrogen over 0.01g Pd/alumina catalyst at 294 K.

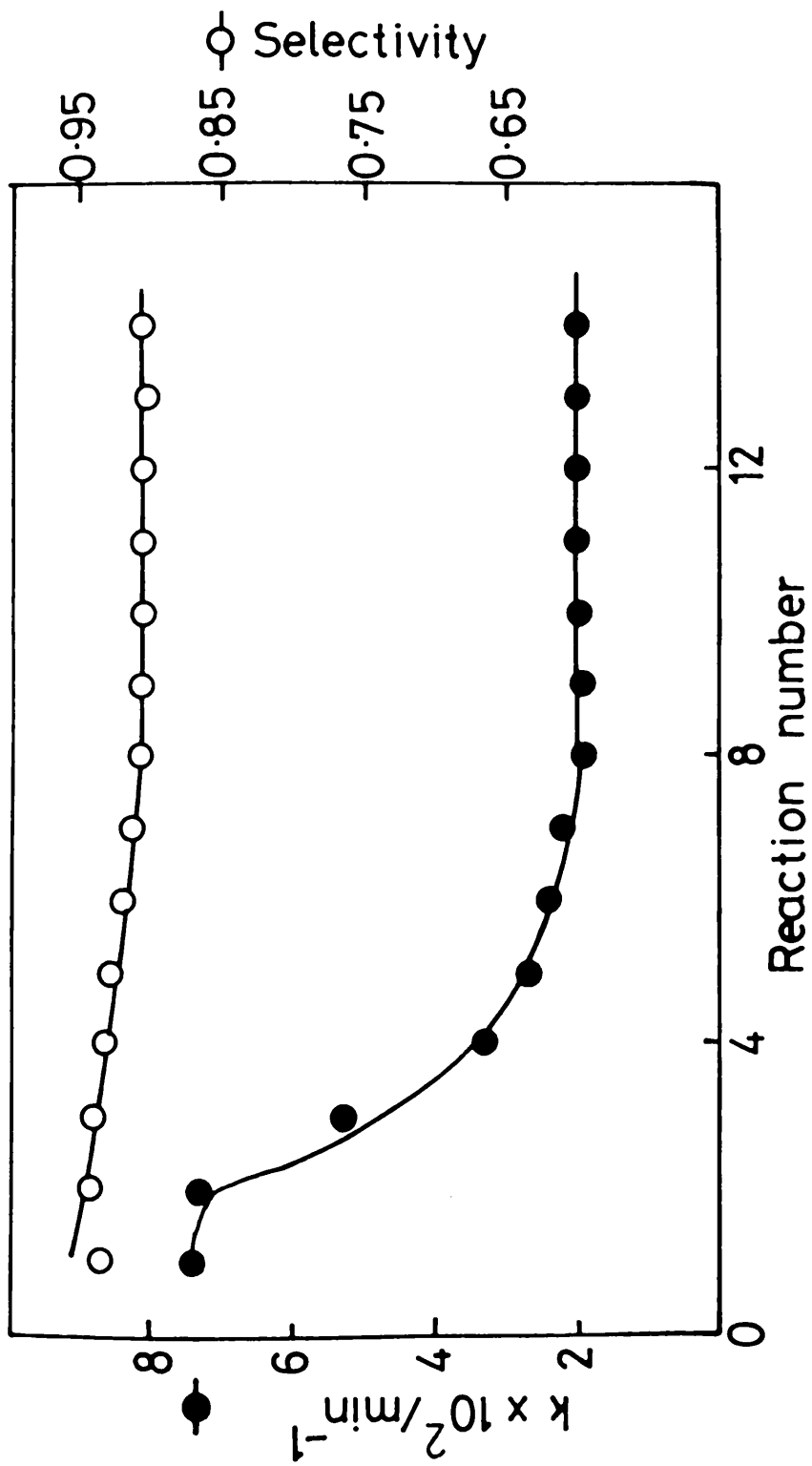


Figure 21. - The effect of the deactivation process upon selectivity for propylene formation during a series of allene hydrogenations over 0.01g Pd/alumina catalyst at 294 K.  $[(\text{C}_3\text{H}_4)_0 = 12.0 \text{ torr}; (\text{P}_{\text{H}_2})_0 = 36.0 \text{ torr}]$

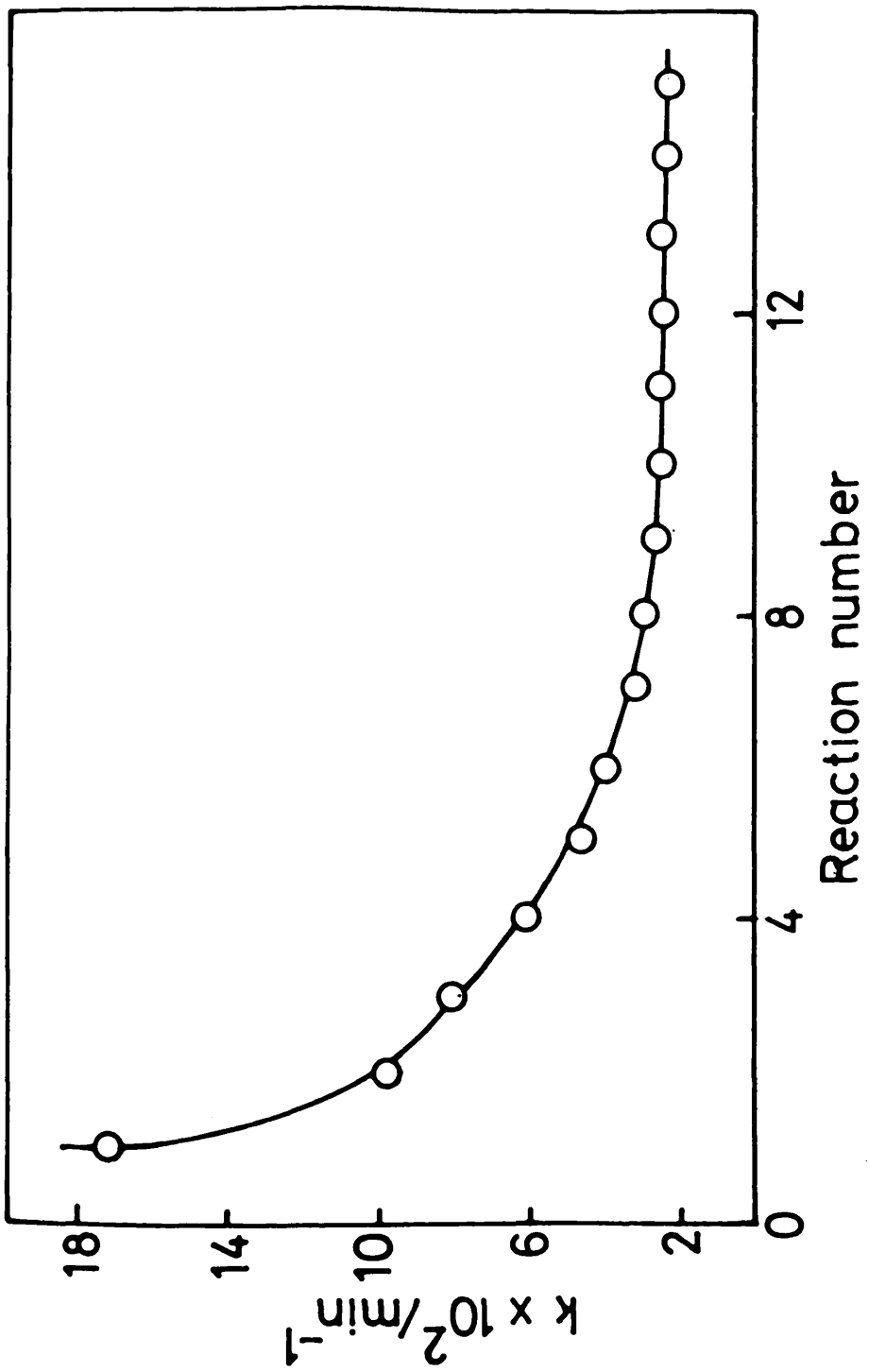


Figure 22. - Variation of the first order rate constant with reaction number for 0.02g Pd/alumina catalyst at 293 K.  $[(\text{C}_3\text{H}_4)_0 = 12.0 \text{ torr}; (\text{P}_{\text{H}_2})_0 = 36.0 \text{ torr}]$

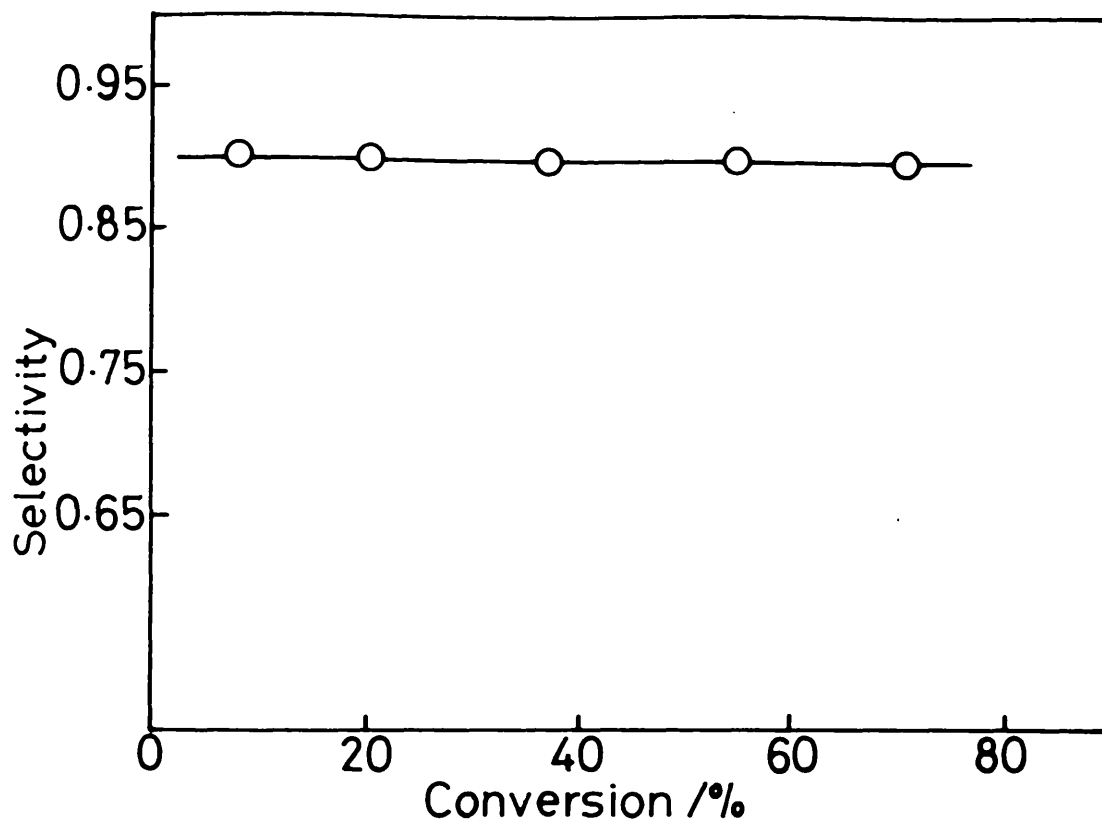


Figure 23. - Variation of selectivity with conversion for the hydrogenation of 12.0 torr allene with 24.0 torr hydrogen over 0.02g Pd/alumina catalyst.

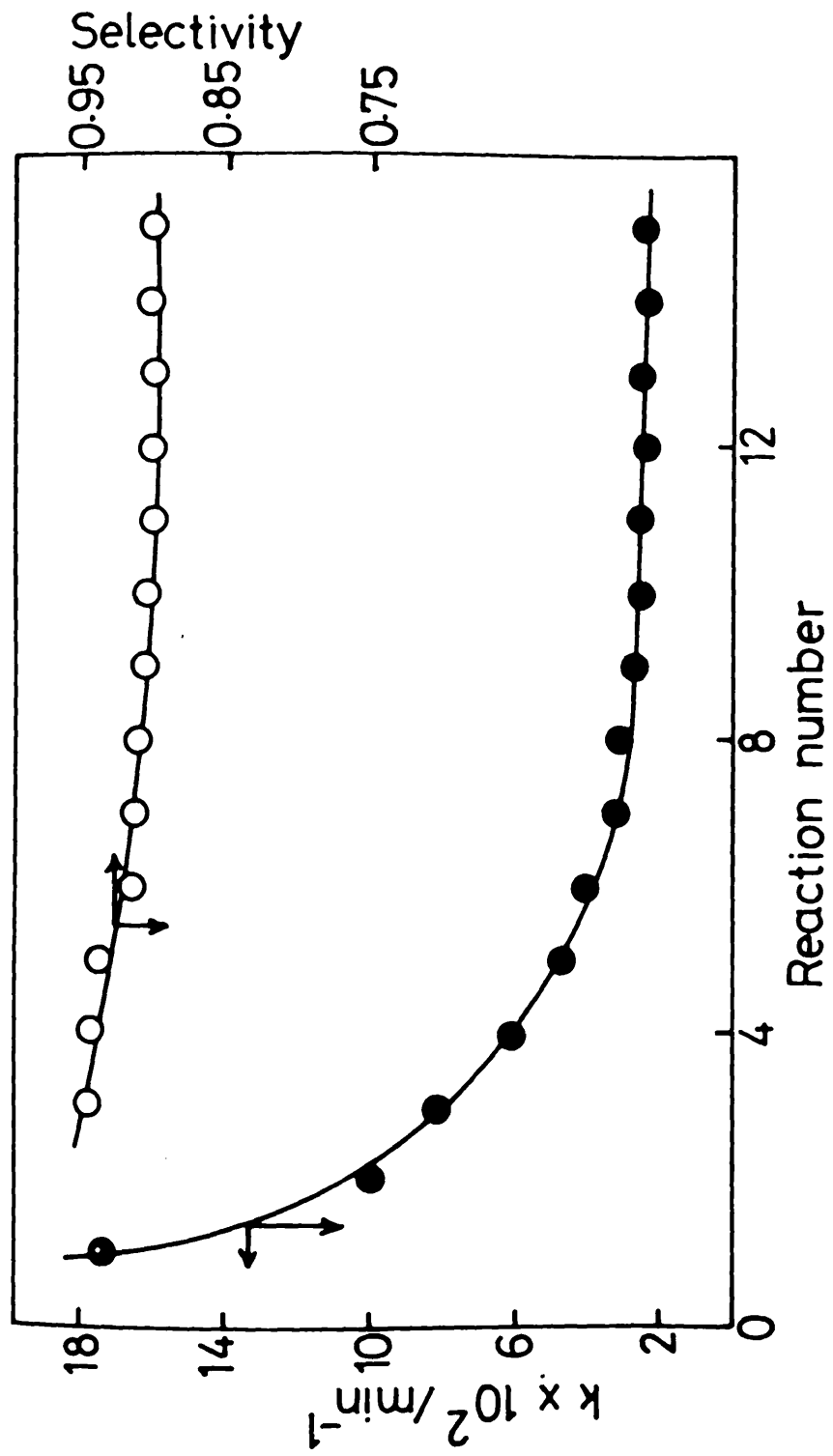


Figure 24. - The effect of the deactivation process upon selectivity for propylene formation during a series of allene hydrogenations over 0.02g

Pd/alumina catalyst at 293 K.  $[(\text{P}_{\text{C}_3\text{H}_4})_0 = 12.0 \text{ torr}; (\text{P}_{\text{H}_2})_0 = 24.0 \text{ torr}]$

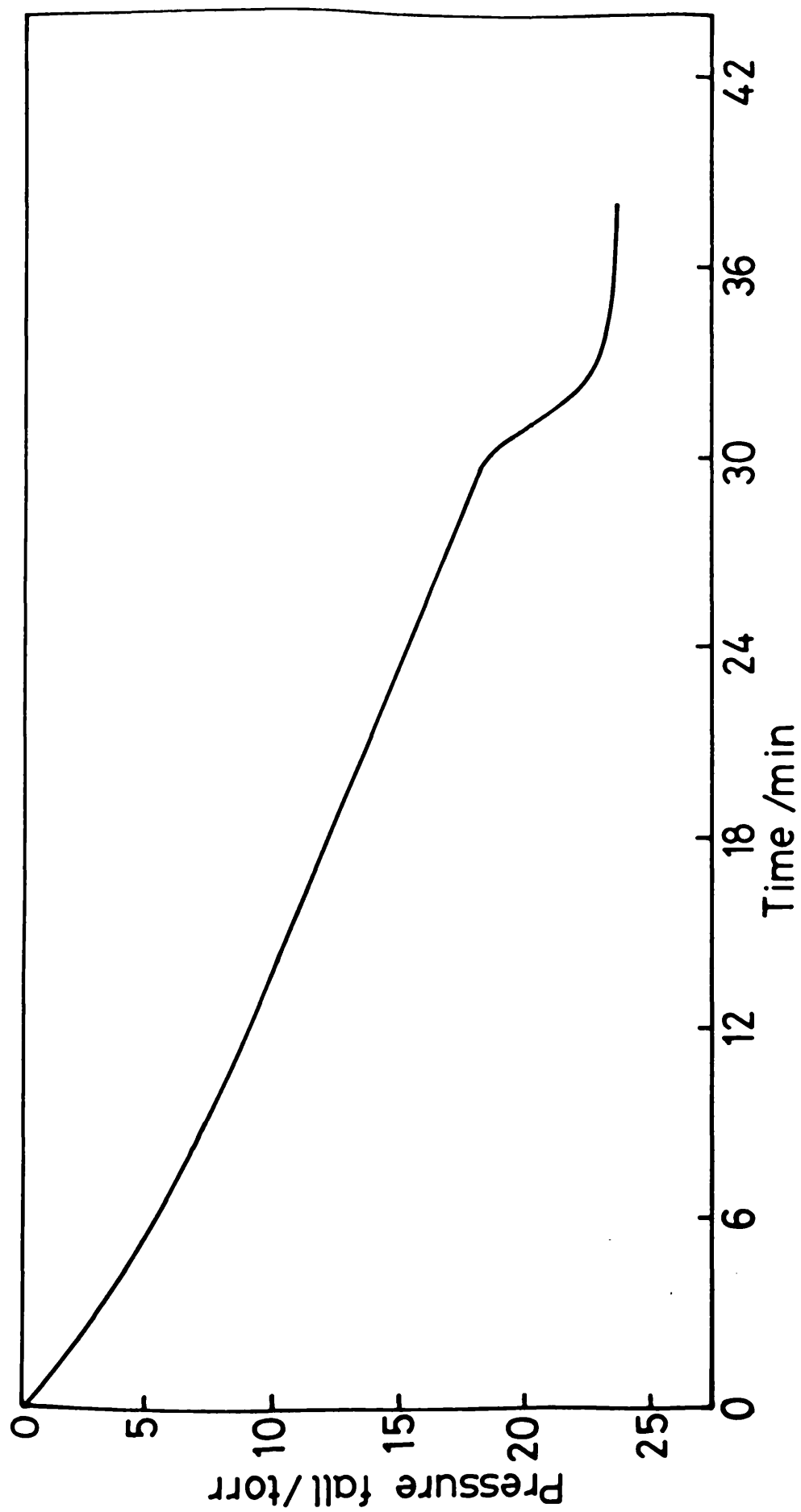


Figure 25. - Pressure fall against time curve for the hydrogenation of 12.0 torr allene with 36.0 torr hydrogen over 0.25g Ir/alumina catalyst at 293 K.

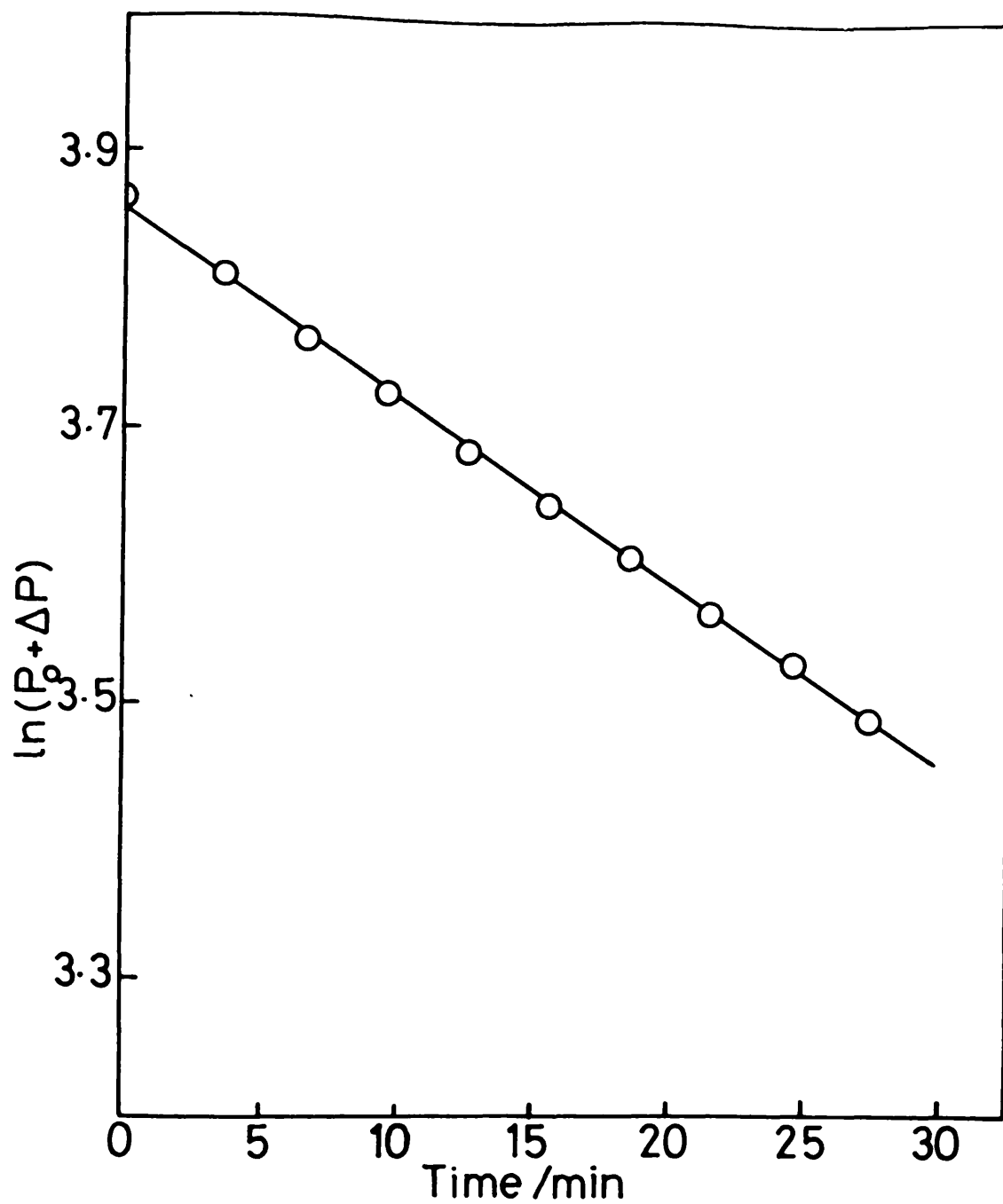


Figure 26. - Variation of  $\ln(P_0 + \Delta P)$  with time for the hydrogenation of allene over 0.25g Ir/alumina catalyst at 293K.

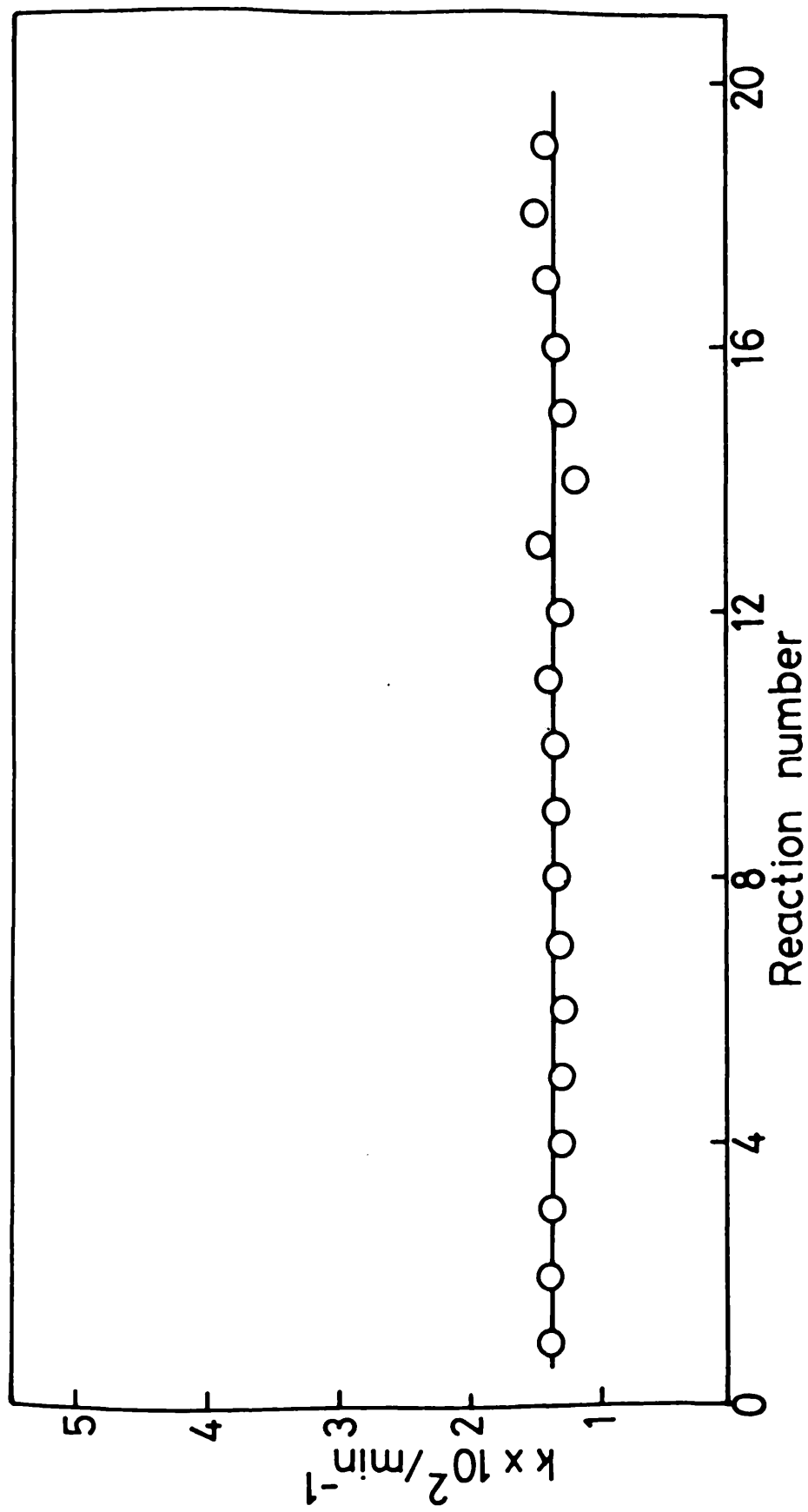


Figure 27. - Variation of the first order rate constant with reaction number for 0.25g Ir/alumina catalyst at 293 K.  $[(\text{C}_3\text{H}_4)_0 = 12.0 \text{ torr}; (\text{P}_{\text{H}_2})_0 = 36.0 \text{ torr}]$

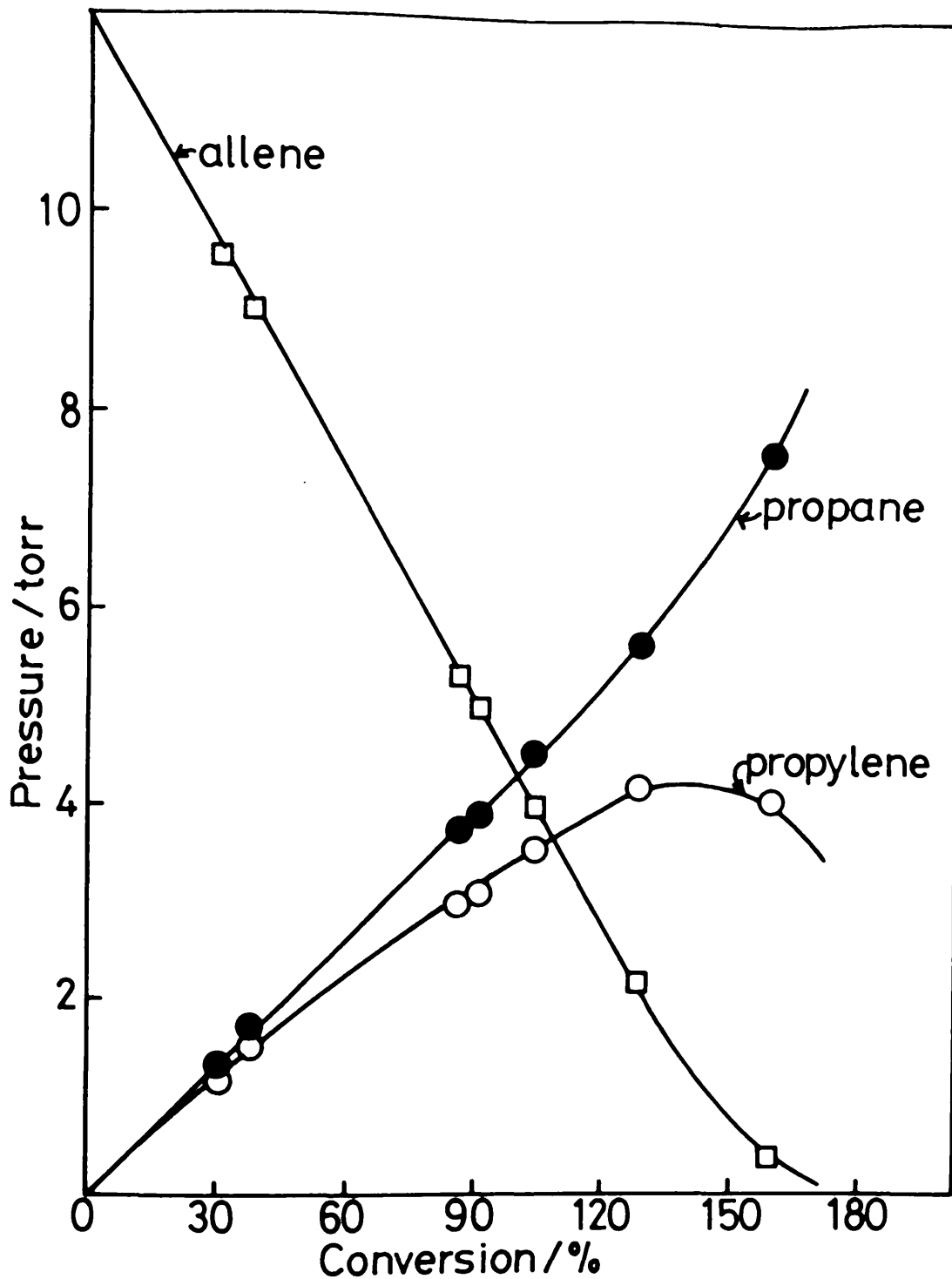


Figure 28. - Variation of the amount of propane (●), propylene (○) and allene (□) with conversion for the hydrogenation of a mixture of hydrogen (36.0 torr) and allene (12.0 torr) over 0.25g Ir/alumina catalyst.

(% conversion = 100 x moles of H<sub>2</sub> consumed per mole of allene present.)

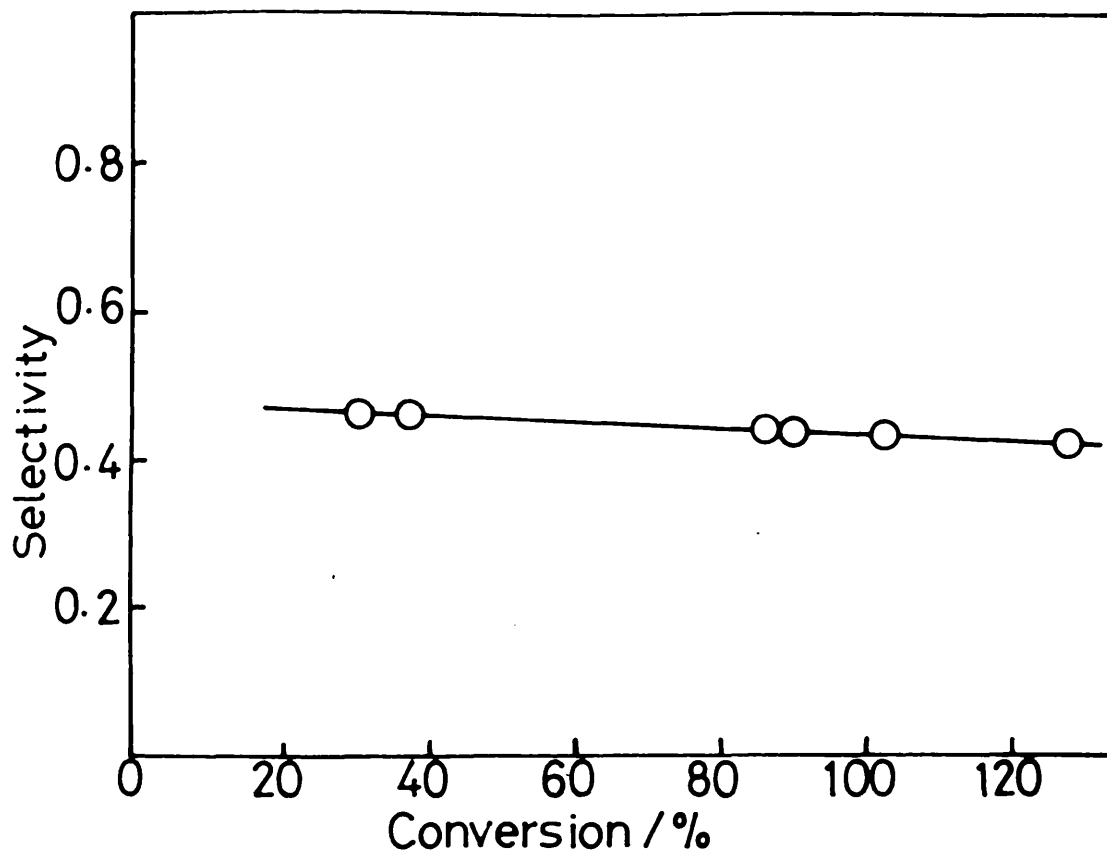


Figure 29. - Variation of selectivity with conversion for the hydrogenation of 12.0 torr allene with 36.0 torr hydrogen over 0.25g Ir/alumina catalyst at 293 K.

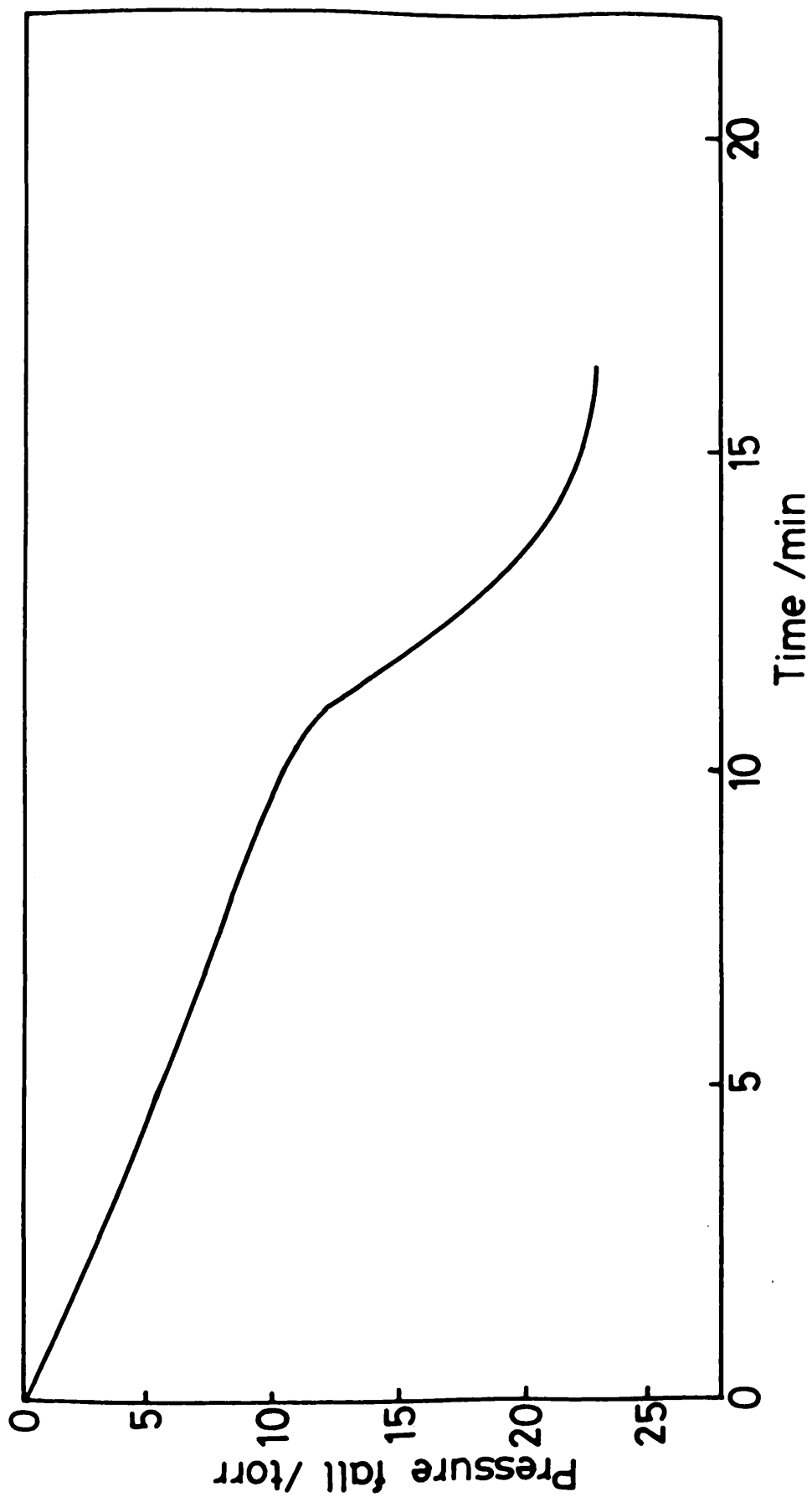


Figure 30. - Pressure fall against time curve for the hydrogenation of 12.0 torr allene with 36.0 torr hydrogen over 0.05g Rh/alumina at 293 K.

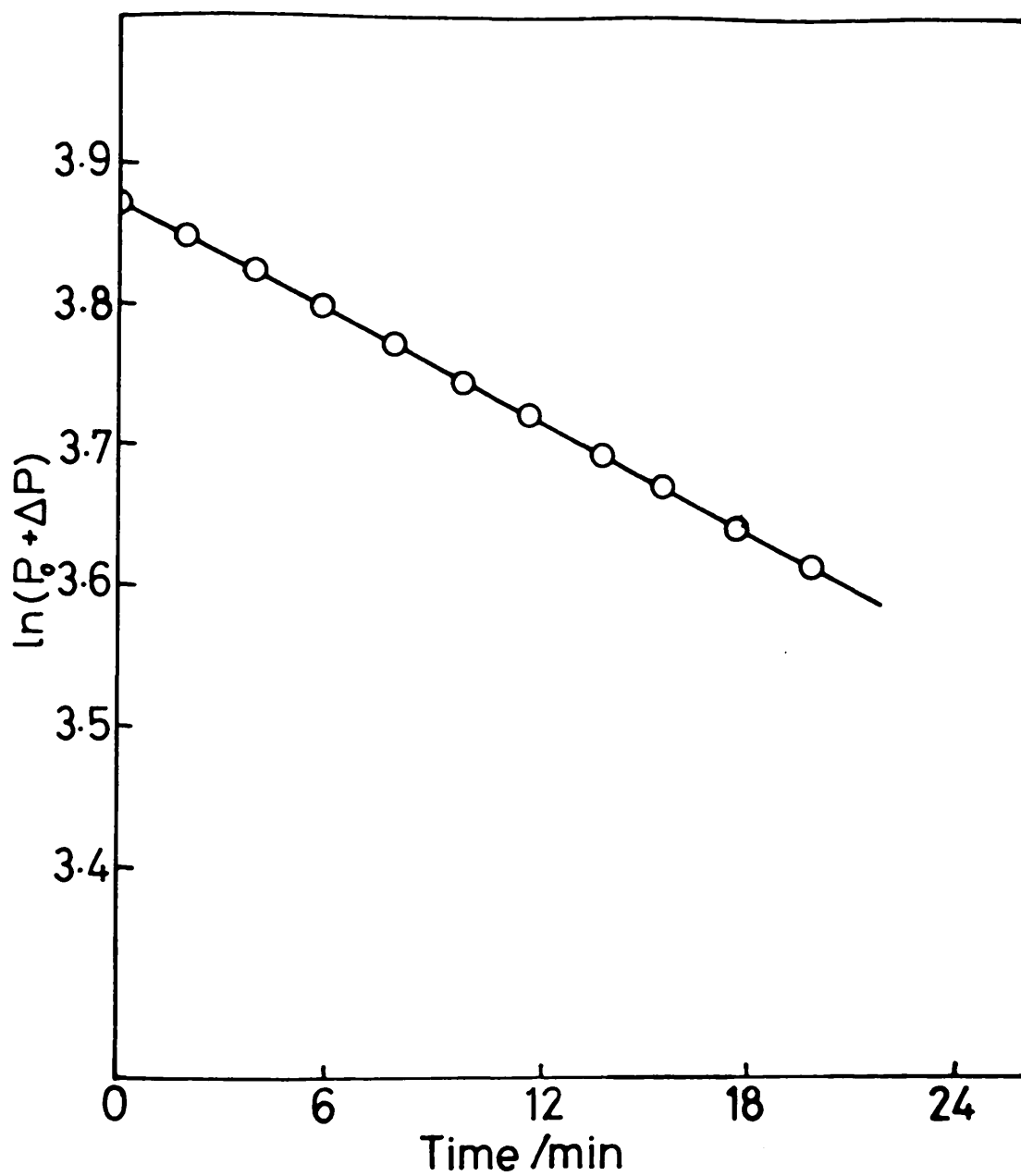


Figure 31. - Variation of  $\ln(P_0 + \Delta P)$  with time for the hydrogenation of allene over 0.05g Rh/alumina catalyst at 293 K.

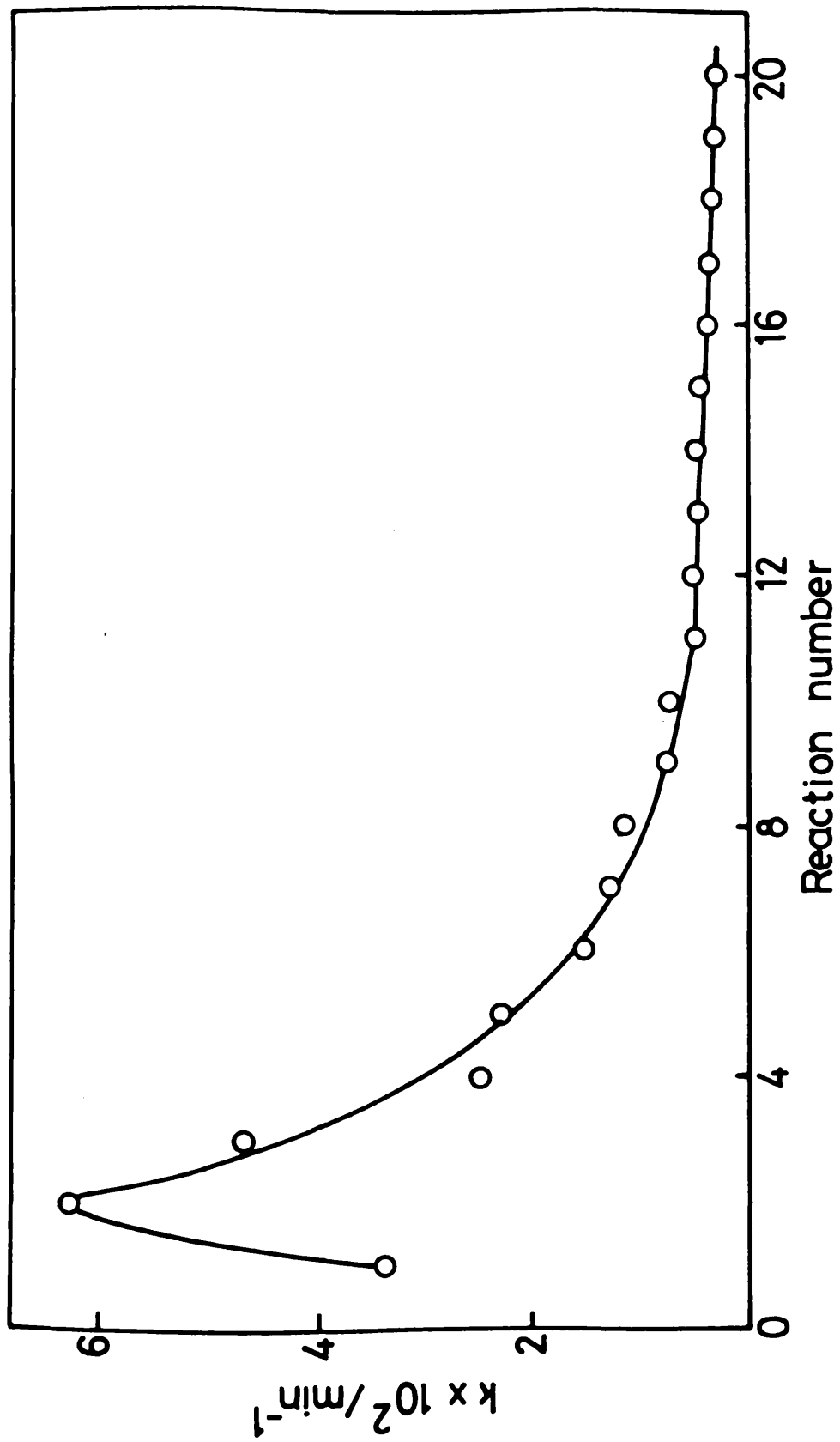


Figure 32. - Variation of the first order rate constant with reaction number for 0.05g Rh/alumina at 293 K.  $[(\text{PC}_3\text{H}_4)_0 = 12.0 \text{ torr}; (\text{P}_{\text{H}_2})_0 = 36.0 \text{ torr}]$

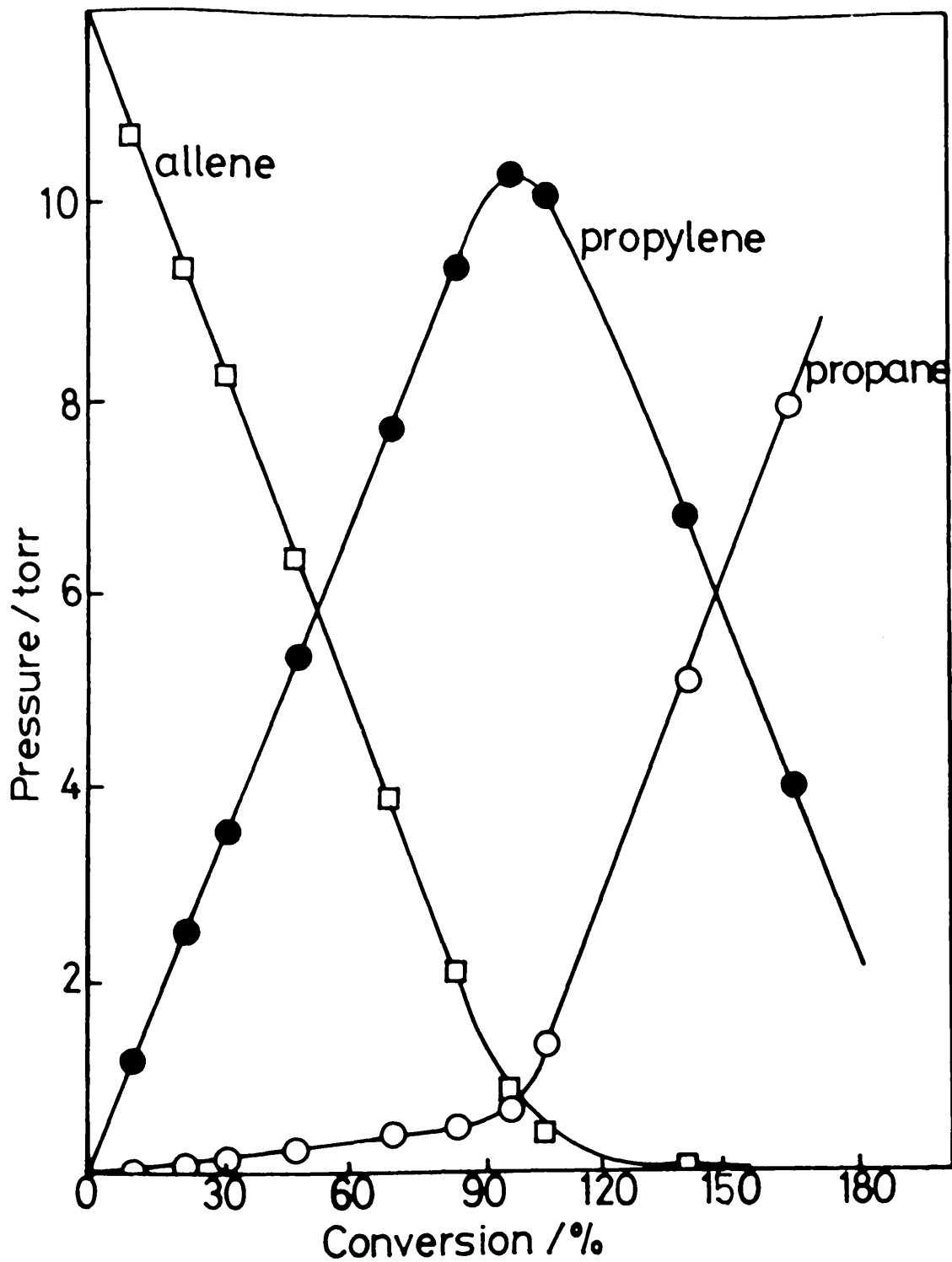


Figure 33. - Variation of the amount of propane (○), propylene (●) and allene (□) with conversion for the hydrogenation of a mixture of hydrogen (36.0 torr) and allene (12.0 torr) over 0.10g Rh/alumina catalyst. (% conversion = 100 x moles of H<sub>2</sub> consumed per mole of allene present)

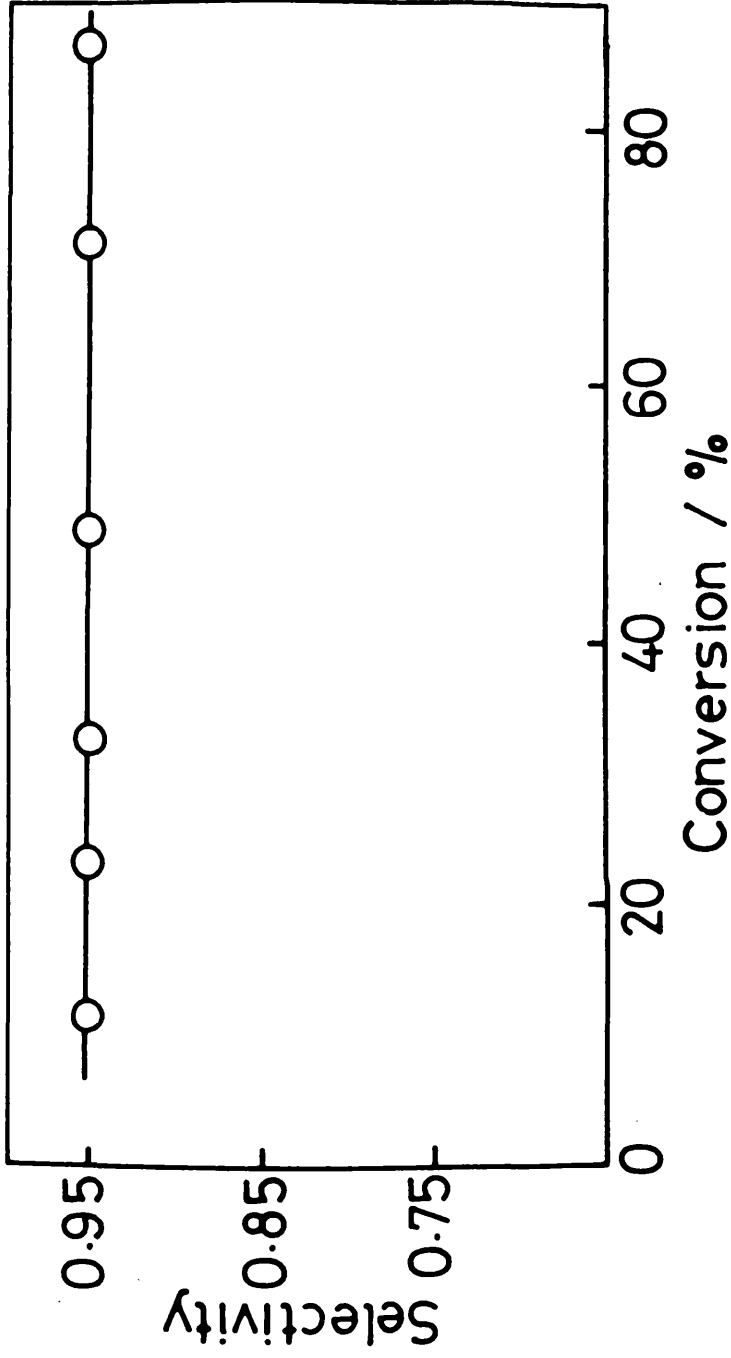


Figure 34. - Variation of selectivity with conversion for the hydrogenation of 12.0 torr allene with 36.0 torr hydrogen over 0.10g Rh/alumina catalyst at 293 K.

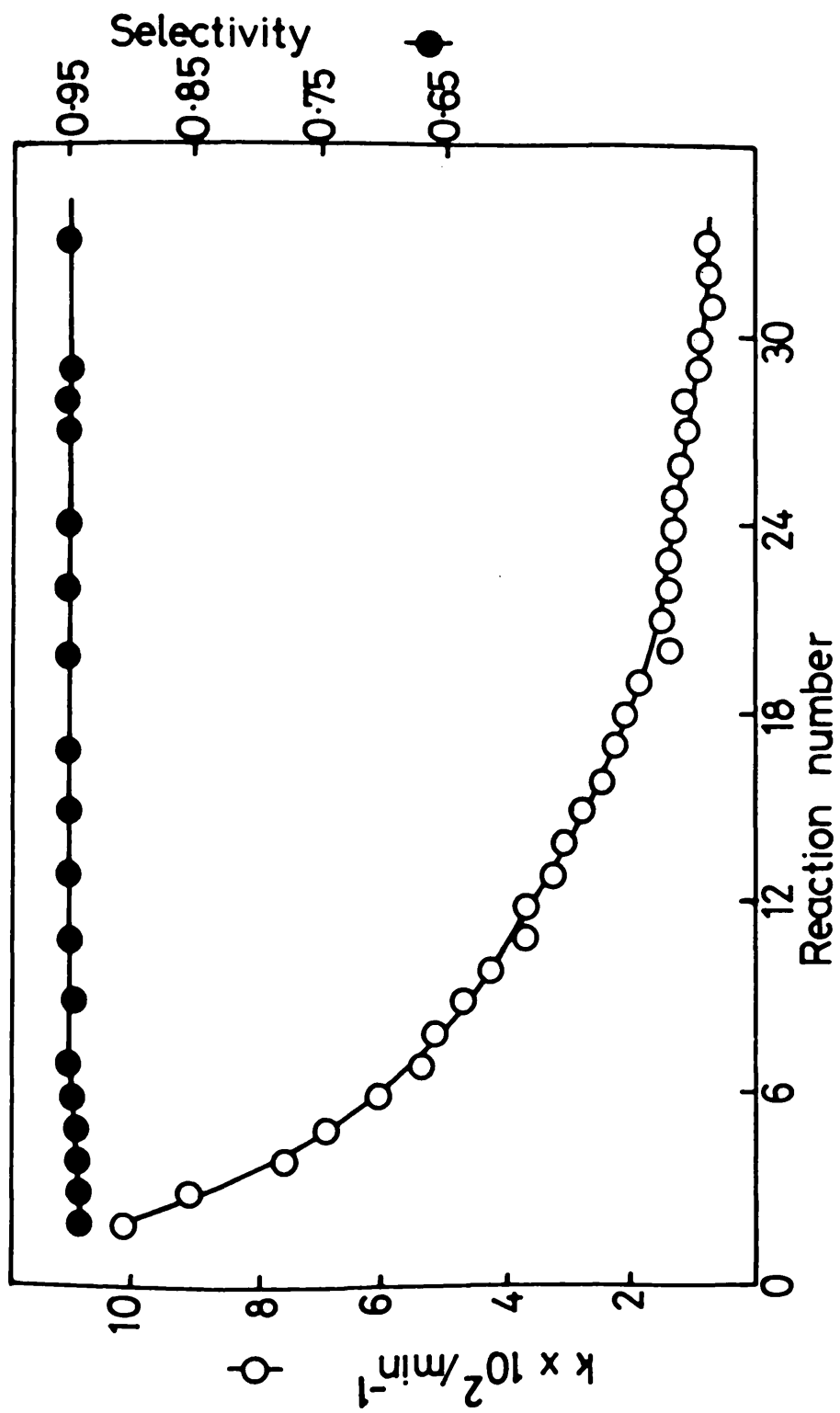


Figure 35. - The effect of the deactivation process upon selectivity during a series of allene hydrogenations over 0.10g Rh/alumina catalyst at 293 K.  
 $[(\text{P}_{\text{C}_3\text{H}_4})_0 = 12.0 \text{ torr}; (\text{P}_{\text{H}_2})_0 = 36.0 \text{ torr}]$

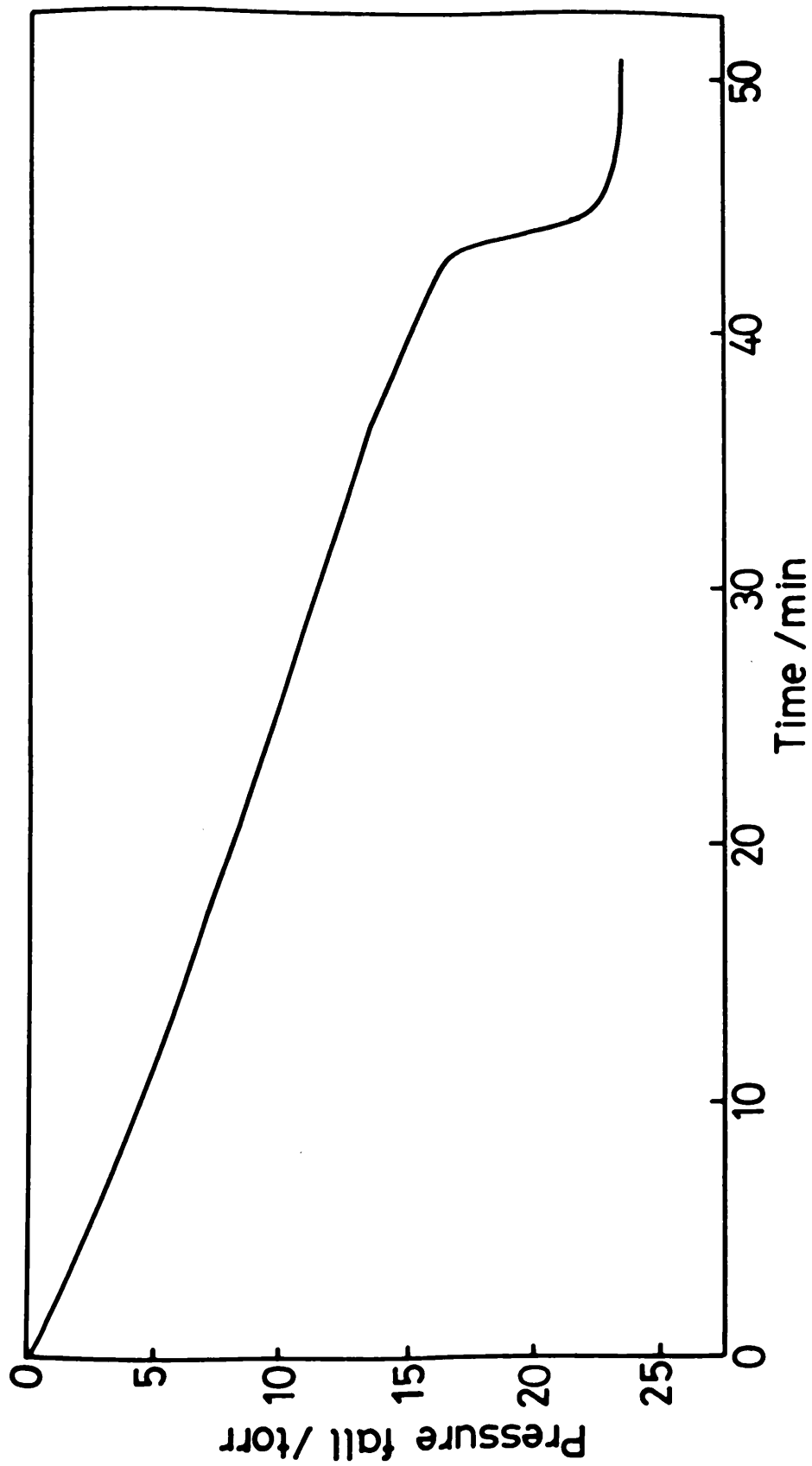


Figure 36. - Pressure fall against time curve for the hydrogenation of 12.0 torr acetylene with 36.0 torr hydrogen over 0.10g Rh/alumina catalyst at 293 K.

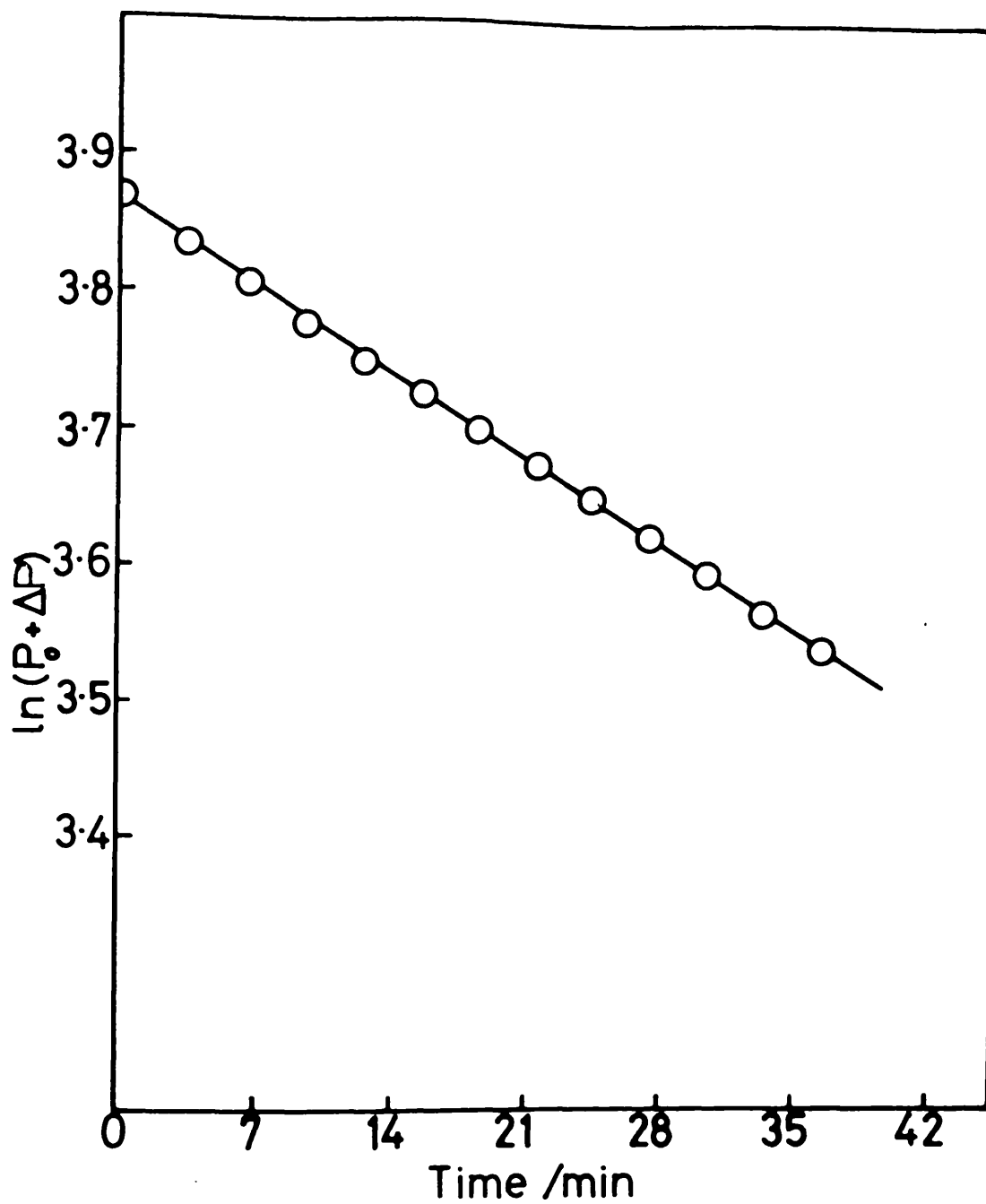


Figure 37. - Variation of  $\ln(P_0 + \Delta P)$  with time for the hydrogenation of acetylene over 0.10g Rh/alumina catalyst at 293 K.

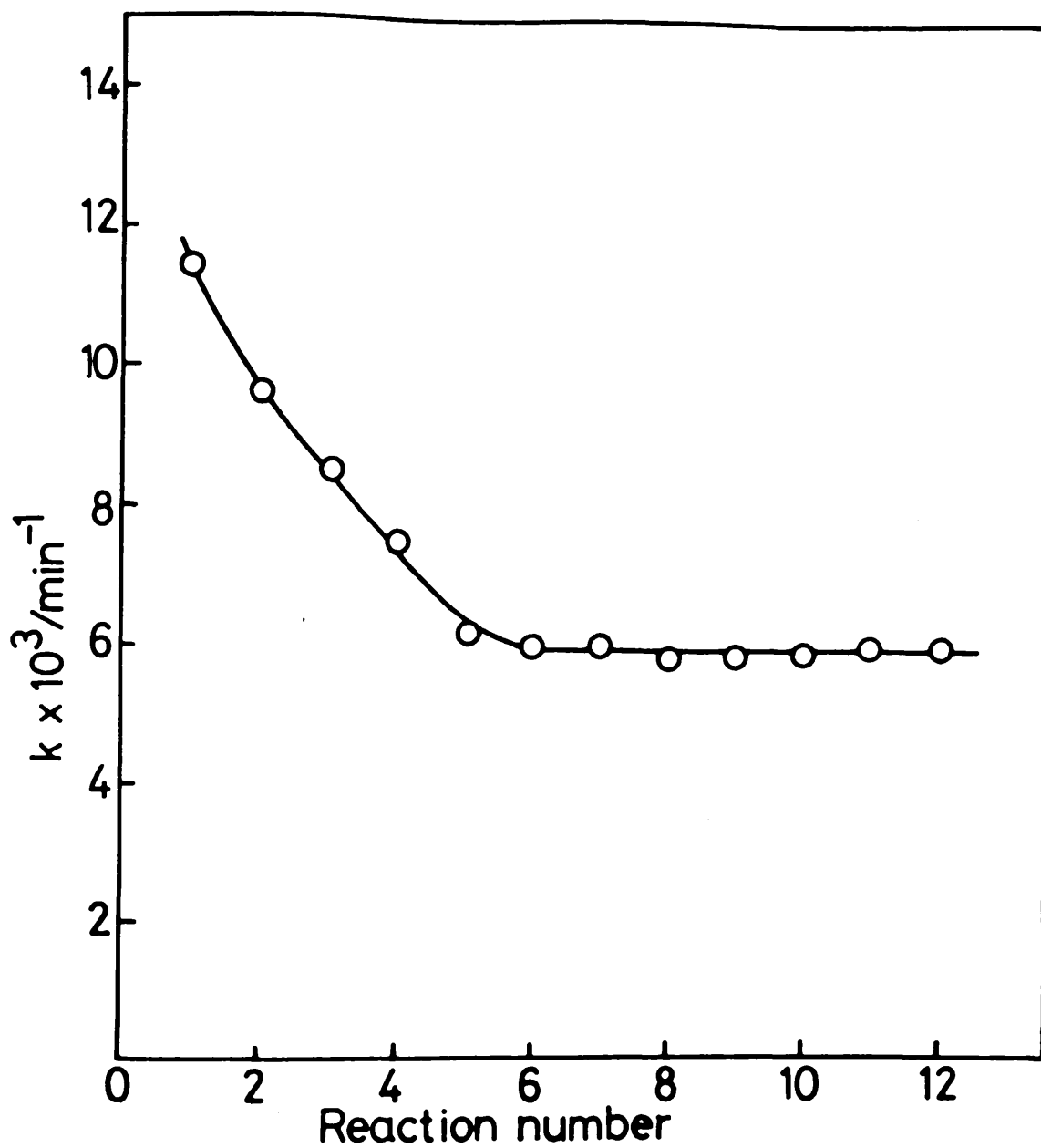


Figure 38. - Variation of the first order rate constant with reaction number for 0.10g Rh/alumina at 293 K.

$[(P_{\text{C}_2\text{H}_2})_0 = 12.0 \text{ torr}; (P_{\text{H}_2})_0 = 36.0 \text{ torr}]$

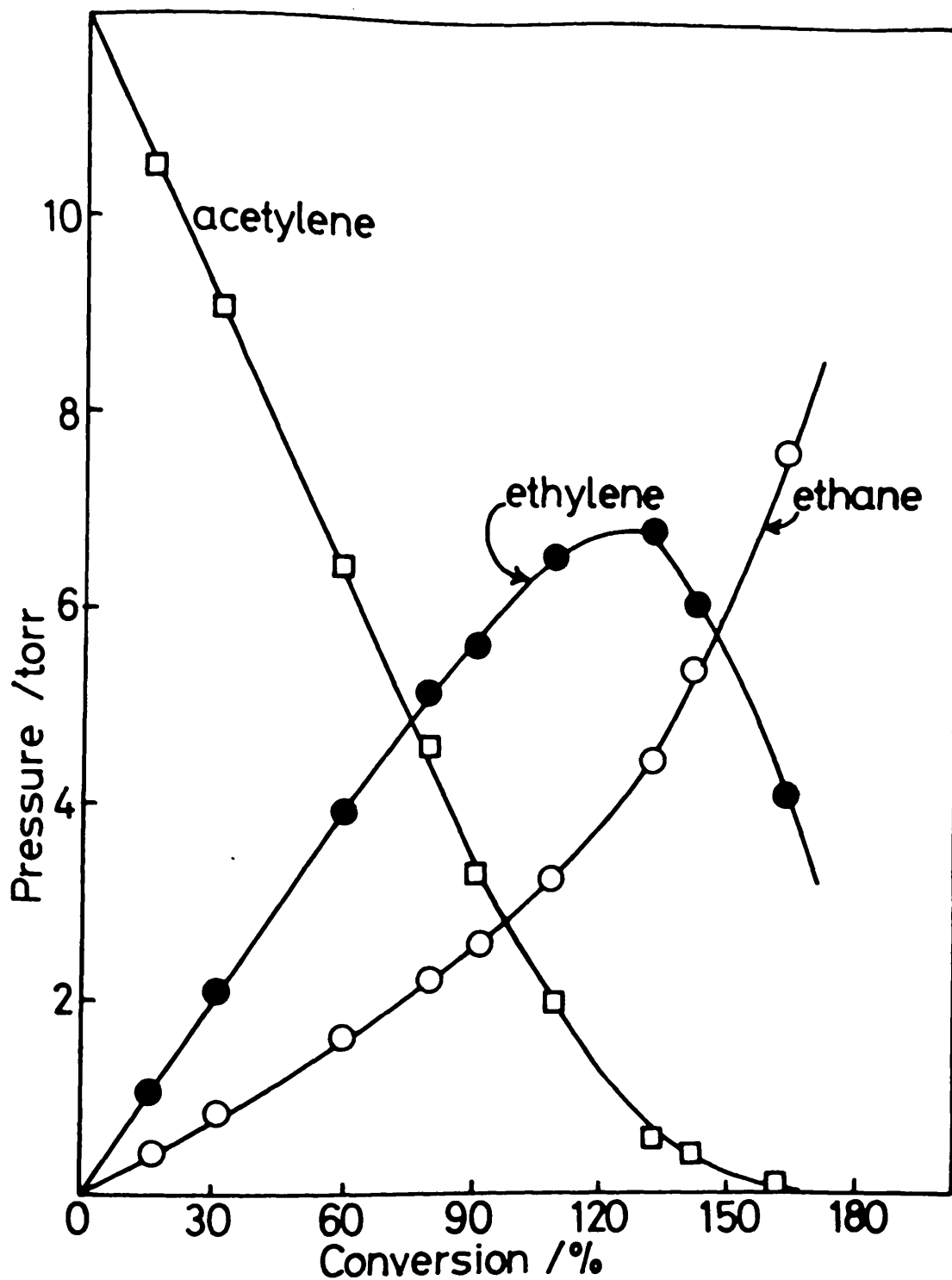


Figure 39. - Variation of the amount of ethane (O), ethylene (●) and acetylene (□) with conversion for the hydrogenation of a mixture of hydrogen (36.0 torr) and acetylene (12.0 torr) over 0.10g Rh/alumina catalyst at 293 K.

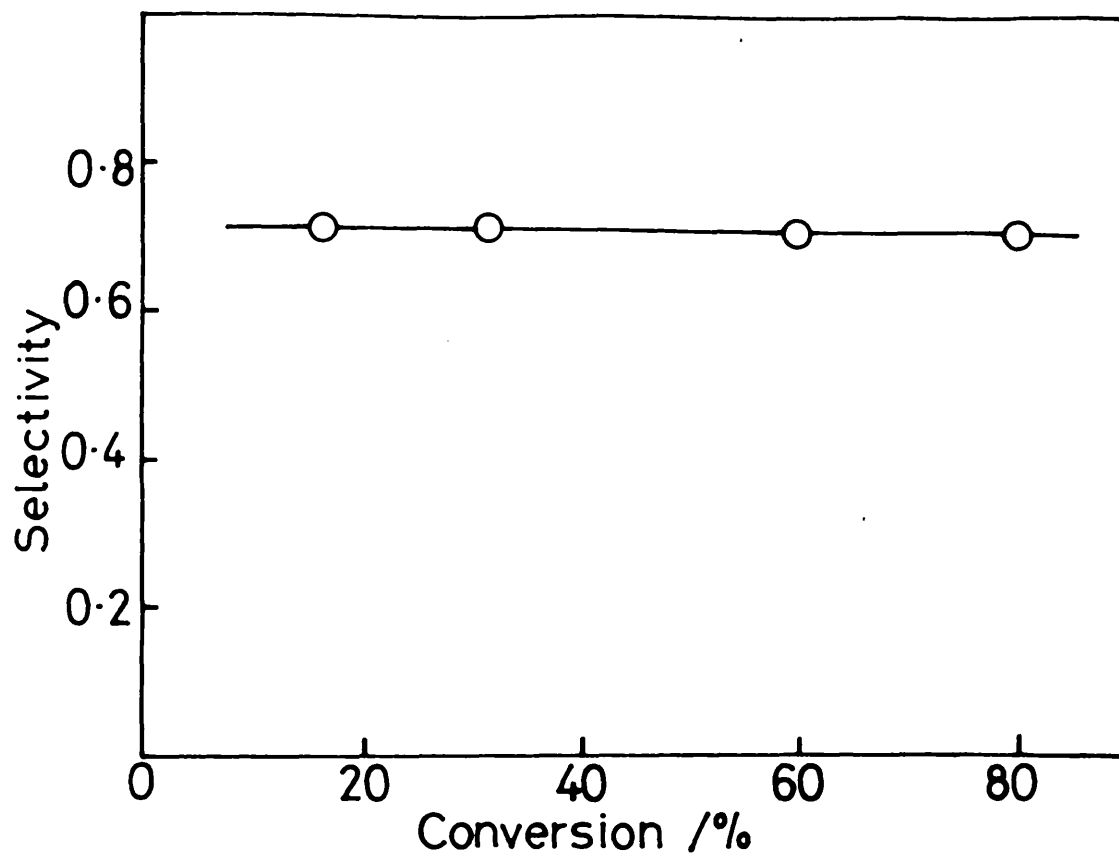


Figure 40. - Variation of selectivity with conversion for the hydrogenation of 12.0 torr acetylene with 36.0 torr hydrogen over 0.10g Rh/alumina catalyst at 293 K.

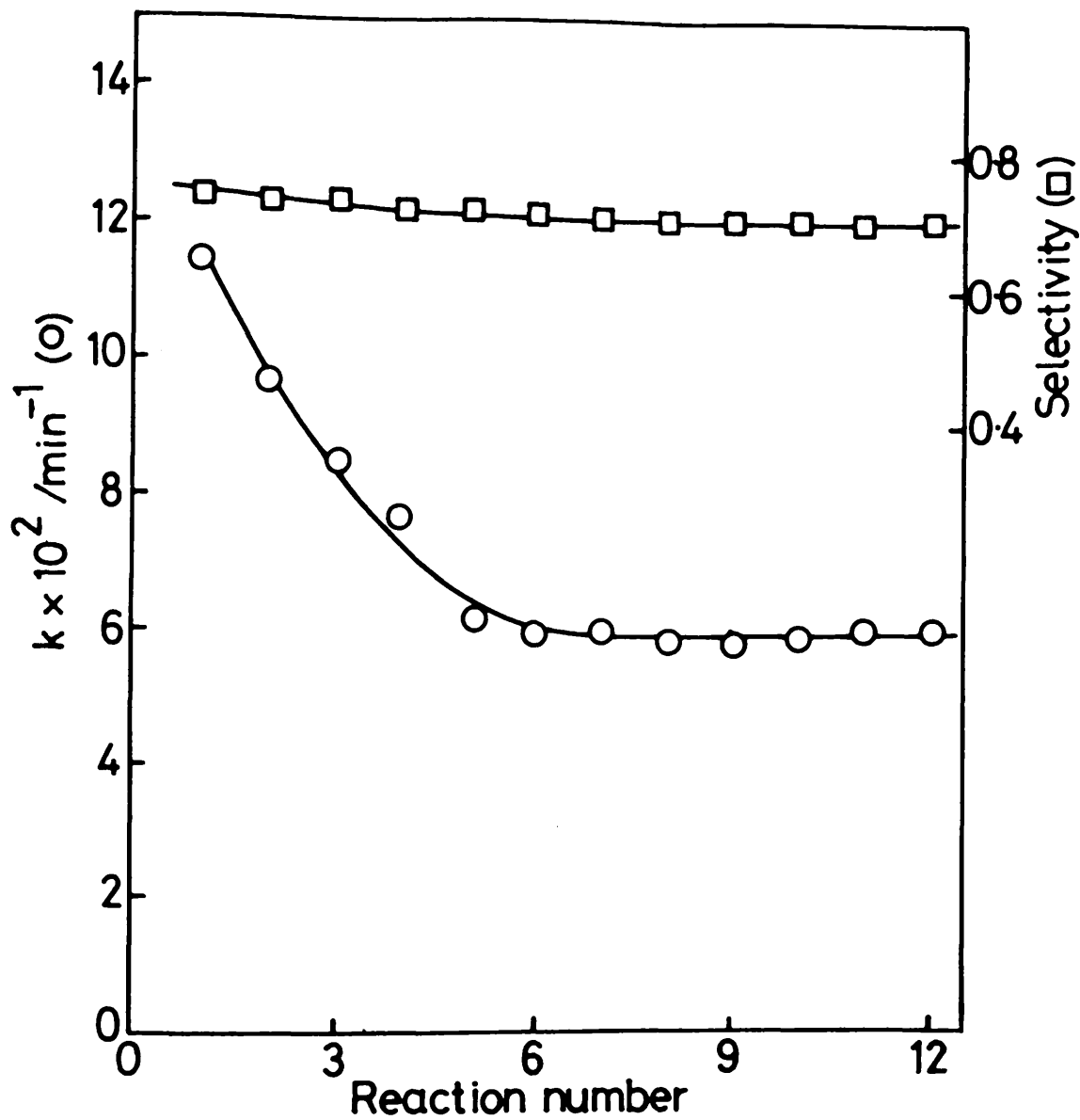


Figure 41. - The effect of the deactivation process upon selectivity for ethylene formation during a series of acetylene hydrogenations over 0.10g Rh/alumina catalyst at 293 K.  $[(P_{C_2H_2})_0 = 12.0 \text{ torr}; (P_{H_2})_0 = 36.0 \text{ torr}]$

#### 4.2 Adsorption of [<sup>14</sup>C]Propylene on Supported Rhodium Catalysts

In a previous study of the adsorption of [<sup>14</sup>C]acetylene and [<sup>14</sup>C]ethylene on supported rhodium catalysts, Reid et al. (169) reported the effect of evacuation, exchange with non-radioactive gas-phase material and hydrogenation on the radioactively labelled pre-adsorbed gases. It was shown that the supported rhodium catalysts retained a fraction of the adsorbed [<sup>14</sup>C]ethylene and [<sup>14</sup>C]acetylene when these processes were allowed to occur. Reid also reported that the adsorption isotherms showed two distinct regions: a steep primary region and a less steep linear secondary region.

These studies were extended to the adsorption of propylene. Adsorption isotherms were determined as described in section 3.7.2. In order to test the reproducibility of the adsorption isotherms, it was necessary to find a method whereby all the radioactivity from a previous adsorption could be removed from the surface. It was found that heating the catalyst in a stream of hydrogen (ca. 10 cm<sup>3</sup> min<sup>-1</sup>) at 623K for 6 hours removed all the surface radioactivity.

#### 4.2.1 [<sup>14</sup>C]Ethylene Adsorption Isotherms

Adsorption isotherms using radioactively labelled ethylene were determined in order to compare our system with that of Reid. Typical adsorption isotherms for [<sup>14</sup>C]-ethylene on a freshly reduced 0.30g sample of rhodium/alumina catalyst are shown in figure 42. The shape of these isotherms is similar to that observed previously (169). They differ in shape from the [<sup>14</sup>C]carbon monoxide adsorption isotherm (figure 58) in that surface adsorption continues to rise with increasing gas-phase pressure. A steep primary region was followed by a less steep secondary region. Uptake of [<sup>14</sup>C]ethylene continued up to a gas pressure of about 6 torr, this being the maximum pressure studied.

Radioactively labelled ethylene, approximately five times less dilute than the material used to construct the isotherms shown in figure 42, was employed to obtain the adsorption isotherm shown in figure 43 for a 0.10g sample of the rhodium catalyst. Again two adsorption regions were observed.

Evacuation of the reaction vessel for one hour removed very little of the ethylene adsorbed on the rhodium/alumina catalysts (table 7).

Table 7

The Effect of Evacuation on Adsorbed [<sup>14</sup>C]Ethylene

catalyst	turning point	evacuation	
		before	after
	count rate (min <sup>-1</sup> )	count rate (min <sup>-1</sup> )	count rate (min <sup>-1</sup> )
0.10g Rh/alumina	2440	3215	3136
0.30g Rh/alumina	1430	2204	1920
	1500	2324	2089

The "turning point" was obtained by extrapolating the linear secondary region to zero pressure.

Figure 42 shows two adsorption isotherms for the same catalyst sample, from which it can be seen that [<sup>14</sup>C]-ethylene isotherms were reproducible.

4.2.2 [<sup>14</sup>C]Propylene Adsorption Isotherms on a Freshly Reduced Silica-Supported Rhodium Catalyst

Adsorption isotherms for [<sup>14</sup>C]propylene on a freshly reduced 0.30g sample of the silica-supported rhodium catalyst are shown in figure 44. The shape of the [<sup>14</sup>C]propylene adsorption isotherm was similar to that

observed with [ $^{14}\text{C}$ ]ethylene over an alumina-supported rhodium catalyst. It showed two distinct regions, a non-linear primary region followed by a linear secondary region. The extent of adsorption of [ $^{14}\text{C}$ ]propylene on the secondary region continued to increase linearly with increasing gas pressure and no plateau region was observed although gas pressures in excess of 4 torr were used. The specific activity of the [ $^{14}\text{C}$ ]propylene was  $0.031 \text{ mCi (mmole)}^{-1}$ .

The amount of adsorbed [ $^{14}\text{C}$ ]propylene removed from the surface of the catalyst by evacuation of the reaction vessel for one hour is shown in table 8.

Table 8

The Effect of Evacuation on Adsorbed [ $^{14}\text{C}$ ]Propylene

catalyst	turning point count rate ( $\text{min}^{-1}$ )	evacuation	
		before	after
		count rate ( $\text{min}^{-1}$ )	count rate ( $\text{min}^{-1}$ )
Freshly reduced 0.3g Rh/silica	1400	2321	1760
	1400	2567	1841

Figure 44 shows two adsorption isotherms for the same catalyst sample, from which it can be seen that [ $^{14}\text{C}$ ]-propylene adsorption isotherms over the silica-supported rhodium catalyst were reproducible.

In the interpretation of the adsorption phenomena it was thought to be important that any molecular exchange between [ $^{14}\text{C}$ ]labelled and unlabelled hydrocarbon which occurred be determined. This was done by carrying out an adsorption isotherm, using radioactive gas, well into the secondary adsorption region. The displacing gas, in non-radioactive form, was admitted to the reaction vessel and the extent of displacement determined from the fall in surface count rate.

From figure 45 it can be seen that very little molecular exchange occurred if the reaction vessel was previously evacuated for one hour. The amount of radioactivity removed from the surface by molecular exchange was similar to that removed by evacuation, provided the non-radioactive hydrocarbon was admitted to the reaction vessel before evacuation (figure 45).

Adsorption of [ $^{14}\text{C}$ ]propylene was followed, after evacuation for one hour, by the introduction of about 36 torr of hydrogen. The fall in surface count rate with time was then recorded (table 9). An initial fast fall in surface count rate was followed by a very slow one. More than 25% of the adsorbed [ $^{14}\text{C}$ ]propylene was retained by the catalyst

and could not be removed by treatment with hydrogen at room temperature.

Table 9

The Effect of Hydrogen on Adsorbed [ $^{14}\text{C}$ ]Propylene

Catalyst: 0.30g Rh/silica

time (min)	addition of 36.0 torr $\text{H}_2$ surface count rate ( $\text{min}^{-1}$ )
0	1770
10	848
30	742
60	714
120	631
2880	490

4.2.3 [ $^{14}\text{C}$ ]Propylene Adsorption Isotherms on  
Alumina-Supported Rhodium Catalysts

The adsorption of [ $^{14}\text{C}$ ]propylene over an alumina-supported rhodium catalyst was studied first over a freshly reduced catalyst and then over a catalyst which had been brought to the steady state by a series of allene hydrogenations. After determining the adsorption isotherm over

a freshly reduced catalyst the effect of evacuation, exchange with non radioactive gas-phase hydrocarbon and addition of hydrogen upon the adsorbed [ $^{14}\text{C}$ ]propylene was studied. The results of these studies are presented below.

#### 4.2.3.1 [ $^{14}\text{C}$ ]Propylene Adsorption Isotherms on Freshly Reduced Alumina-Supported Rhodium Catalysts

Adsorption isotherms for [ $^{14}\text{C}$ ]propylene on a freshly reduced 0.30g sample of the alumina-supported rhodium catalyst are shown in figure 46. The shape of the [ $^{14}\text{C}$ ]propylene adsorption isotherm was similar to that observed with [ $^{14}\text{C}$ ]ethylene over alumina-supported rhodium and with [ $^{14}\text{C}$ ]propylene over silica-supported rhodium catalysts. It again showed two distinct regions, a non-linear primary region followed by a linear secondary region. The extent of adsorption of [ $^{14}\text{C}$ ]propylene on the secondary region continued to increase linearly with increasing gas pressure and no plateau region was observed although gas pressures in excess of 4 torr were used. The specific activity of the [ $^{14}\text{C}$ ]propylene was  $0.031 \text{ mCi (mmole)}^{-1}$ .

The amount of adsorbed [ $^{14}\text{C}$ ]propylene removed from the surface of the alumina-supported rhodium catalyst by evacuation of the reaction vessel for one hour can be seen in table 10.

Table 10

The Effect of Evacuation on Adsorbed [<sup>14</sup>C]Propylene

catalyst	evacuation	
	before count rate (min <sup>-1</sup> )	after count rate (min <sup>-1</sup> )
Freshly reduced 0.30g Rh/alumina	2074	1688
	1587	1444
	2515	2318

Figure 46 shows that the [<sup>14</sup>C]propylene adsorption isotherms over a 0.30g sample of alumina-supported rhodium catalyst were reproducible.

After building up the [<sup>14</sup>C]propylene adsorption isotherm the reaction vessel was evacuated for one hour. 12.5 torr non-radioactive propylene was then admitted to the reaction vessel and the extent of displacement determined from the fall in surface count rate.

From figure 47 it can be seen that very little molecular exchange occurred if the catalyst was previously evacuated for one hour. Some molecular exchange occurred if the non-radioactive propylene was admitted before evacuation of the reaction vessel, but the amount of adsorbed material that underwent exchange was less than the amount removed by evacuation.

Adsorption of [ $^{14}\text{C}$ ]propylene was followed by evacuation, addition of non-radioactive propylene and evacuation again for one hour. 36.0 torr of hydrogen was then admitted to the reaction vessel and the fall in surface count rate with time was recorded. An initial fast fall in surface count rate was followed by a very slow one (table 11).

Table 11

The Effect of Hydrogen upon the Adsorbed [ $^{14}\text{C}$ ]Propylene

catalyst: 0.30g Rh/alumina

time (min)	addition of 36.0 torr $\text{H}_2$ surface count rate ( $\text{min}^{-1}$ )
0	1611
1	1209
5	998
60	737
120	676

From figure 47 it can be seen that, even after 24 hours under hydrogen at room temperature, about 20% of the adsorbed material remained on the surface of the catalyst.

Table 12 shows the fall in surface count rate on admission of a 1:1 mixture of propylene and hydrogen. It was also observed, during the recording of this removal, that a pressure fall, as indicated on the pressure transducer, was taking place, that is, hydrogenation of the propylene was occurring. Table 12 also shows the fall in surface count rate on admission of 36.0 torr of hydrogen after evacuation of the 1:1 mixture of propylene and hydrogen.

Table 12

Variation of Adsorbed [<sup>14</sup>C]Propylene Count Rate on Admission of C<sub>3</sub>H<sub>6</sub>/H<sub>2</sub> Mixture and Hydrogen

catalyst: freshly reduced 0.30g Rh/alumina	
	count rate (min <sup>-1</sup> )
(A) surface count rate after adsorption isotherm build-up	2033
(B) admission of 24.0 torr C <sub>3</sub> H <sub>6</sub> /H <sub>2</sub> (1:1) to A	1415
(C) surface count rate of B after evacuation for one hour	1509
(D) admission of 36.0 torr H <sub>2</sub> to C	583
Adsorption isotherm turning point	1400

Table 13 shows the fall in surface count rate on admission of a mixture of allene and hydrogen ( $H_2:C_3H_4 = 2:1$ ). It also shows the fall in surface count rate on admission of 36.0 torr of hydrogen after evacuation of the allene and hydrogen mixture.

Table 13

Variation of Adsorbed [ $^{14}C$ ]Propylene Count Rate on Admission of  $C_3H_4/H_2$  Mixture and Hydrogen over Freshly Reduced Catalyst

catalyst: freshly reduced 0.30g Rh/alumina	
	count rate ( $min^{-1}$ )
(A) surface count rate after adsorption isotherm build-up	2515
(B) surface count rate of A after evacuation for one hour	2318
(C) admission of 36.0 torr $C_3H_4/H_2$ (1:2) to B	1412
(D) surface count rate of C after 24 hours	1320
(E) surface count rate of C after evacuation for one hour	1350
(F) admission of 36.0 torr $H_2$ to E	953

Adsorption of [ $^{14}\text{C}$ ]propylene on a freshly reduced 0.20g sample of the alumina-supported rhodium catalyst was followed by evacuation of the reaction vessel for one hour. 48 torr of a premixed sample of allene and hydrogen ( $\text{C}_3\text{H}_4:\text{H}_2 = 1:3$ ) was then admitted to the reaction vessel. After evacuating the reaction products for one hour the surface count rate was determined. This process (admission of allene and hydrogen mixture, evacuation and counting) was repeated forty times. The effect of this series of allene hydrogenations upon the amount of adsorbed [ $^{14}\text{C}$ ]-propylene is shown in table 14.

Table 14  
Removal of Adsorbed [ $^{14}\text{C}$ ]Propylene by a Series  
of Allene Hydrogenations

reaction number	surface count rate ( $\text{min}^{-1}$ )
0	2479
1	617
2	473
3	435
-	-
5	342
-	-
10	269
-	-
20	221
-	-
29	208
-	-
40	209

The gas phase hydrocarbon in contact with the surface during the build-up of the adsorption isotherm was analysed after the addition of aliquots of [ $^{14}\text{C}$ ]propylene. The analysis is shown in figure 48, for a freshly reduced 0.20g sample of the Rh/alumina catalyst and [ $^{14}\text{C}$ ]propylene of specific activity  $0.08 \text{ mCi (mmol)}^{-1}$ . The analysis showed that during the build-up of the primary region the gas phase was solely propane. The formation of propane ceased at the onset of the secondary region. Propylene only appeared in the gas phase at the commencement of the secondary region.

#### 4.2.3.2 [ $^{14}\text{C}$ ]Propylene Adsorption Isotherms on a Freshly Reduced Alumina-Supported Rhodium Catalyst in the Presence of Allene

The extent to which [ $^{14}\text{C}$ ]propylene would adsorb on a catalyst sample already exposed to allene was determined as follows:

The same 0.30g sample of the Rh/alumina catalyst which was used in section 4.3.2.1 was cleaned by treatment with a stream of hydrogen for 12 hours at 623K. The catalyst was then evacuated at 623K for 6 hours and allowed to cool down in vacuo to ambient temperature. The catalyst was then exposed to 12.0 torr non-radioactive allene for 1 hour. Without removing allene from the gas phase the [ $^{14}\text{C}$ ]-propylene adsorption isotherm was determined on the allene precovered surface. Figure 46 shows that [ $^{14}\text{C}$ ]propylene

adsorption on the allene precovered surface could take place, although the amount adsorbed was considerably reduced compared to that on a "clean" surface. No primary adsorption was observed and the secondary gradient was less than in the case of a "clean" surface. Evacuating the reaction vessel for one hour removed little of the adsorbed [ $^{14}\text{C}$ ]propylene.

#### 4.2.3.3 The Effect of Self-Deactivation upon the [ $^{14}\text{C}$ ]Propylene Adsorption Isotherms

The adsorption of [ $^{14}\text{C}$ ]propylene was investigated on a freshly reduced 0.10g sample of the Rh/alumina catalyst and at various stages during the deactivation process. After each reaction, before an adsorption isotherm was determined, the catalyst was allowed to stand under the reaction products, containing excess hydrogen, for a minimum of 2 hours. The catalyst was then evacuated and the adsorption isotherm determined. The isotherms are shown in figure 49. For each adsorption isotherm the surface count rates have been corrected for the background activity arising from permanently retained propylene. The effect of the deactivation of the catalyst upon the adsorption isotherms was to reduce the extent of the primary adsorption until it disappeared completely as the steady state activity was attained. It can also be seen that the deactivation had no effect on the secondary adsorption process.

Figure 50 shows that a linear relationship exists

between the extent of primary adsorption, as determined from the turning points in the isotherms at different stages during the deactivation, and the rate of allene hydrogenation at the corresponding points on the deactivation curve.

#### 4.2.3.4 [<sup>14</sup>C]Propylene Adsorption Isotherms on a Steady State Alumina-Supported Rhodium Catalyst

Investigation with [<sup>14</sup>C]propylene showed that, although only a part of preadsorbed [<sup>14</sup>C]propylene participated in a subsequent hydrogenation reaction, a further fraction of the preadsorbed propylene could be removed by allowing the catalyst to stand under either hydrogen alone or under the hydrogen-rich reaction product mixture following the hydrogenation of 48.0 torr of a premixed sample of allene and hydrogen ( $C_3H_4:H_2 = 1:3$ ). Consequently, the adsorption isotherms for the deactivated steady state catalyst were determined after the catalyst had been allowed to stand under the hydrogen-rich reaction products for a minimum of 2 hours in order to remove most of the "removable" preadsorbed propylene. Comparison of the isotherms given in figure 51 shows that rhodium/alumina catalyst, in the steady state, showed no primary region and a much reduced capacity for [<sup>14</sup>C]propylene adsorption, when compared with the adsorption capacity of the freshly reduced catalyst. The [<sup>14</sup>C]propylene specific activity was 0.08 mCi/mmol for the

results presented in this section.

After the determination of the [ $^{14}\text{C}$ ]propylene isotherm on the steady state catalyst the reaction vessel was evacuated for one hour. Table 15 shows the amounts of adsorbed [ $^{14}\text{C}$ ]propylene removed from the steady state surface by this evacuation. Subsequent admission of 12.0 torr non-radioactive propylene to the [ $^{14}\text{C}$ ]propylene pre-covered surface had little effect on the surface count rate. The results in table 15 also show that no molecular exchange took place. The reaction vessel was again evacuated and 12.0 torr of non-radioactive allene was admitted to the reaction vessel. The non-radioactive allene had little effect on the surface count rate (table 15).

Table 15  
Variation of Adsorbed [ $^{14}\text{C}$ ]Propylene Count Rate on  
Admission of Non-Radioactive Propylene and Allene

catalyst: steady state 0.20g Rh/alumina	
	count rate ( $\text{min}^{-1}$ )
(A) surface count rate after adsorption isotherm build-up	576
(B) surface count rate of A after evacuation for one hour	398
(C) admission of 12.0 torr propylene to B	384
(D) surface count rate of C after evacuation for one hour	384
(E) admission of 12.0 torr allene to D	372

Adsorption of [ $^{14}\text{C}$ ]propylene on the steady state surface was followed by evacuation of the residual gas phase for one hour and then admission of hydrogen (36.0 torr). The fall in surface count rate with time was monitored. There was a rapid initial removal of the secondary adsorbed species, followed by a further slow decrease in the surface count rate (figure 52). Approximately 31.9% of the adsorbed [ $^{14}\text{C}$ ]-propylene was removed in the initial 20 minutes and only a further 7.5% was removed over a period of 2 hours.

#### 4.2.3.5 [ $^{14}\text{C}$ ]Propylene Adsorption Isotherm on a Steady State Rh/alumina Catalyst in the Presence of Allene

In order to examine the adsorption of propylene in the presence of allene, thereby obtaining information regarding the possible thermodynamic effect in determining the selectivity in allene hydrogenation, [ $^{14}\text{C}$ ]propylene (specific activity = 0.24 mCi/mmol) was admitted to a steady state catalyst in the presence of 12.0 torr of gas-phase allene. As shown in figure 53, the presence of the allene reduced the adsorptive capacity of the steady state surface for propylene by approximately 40%.

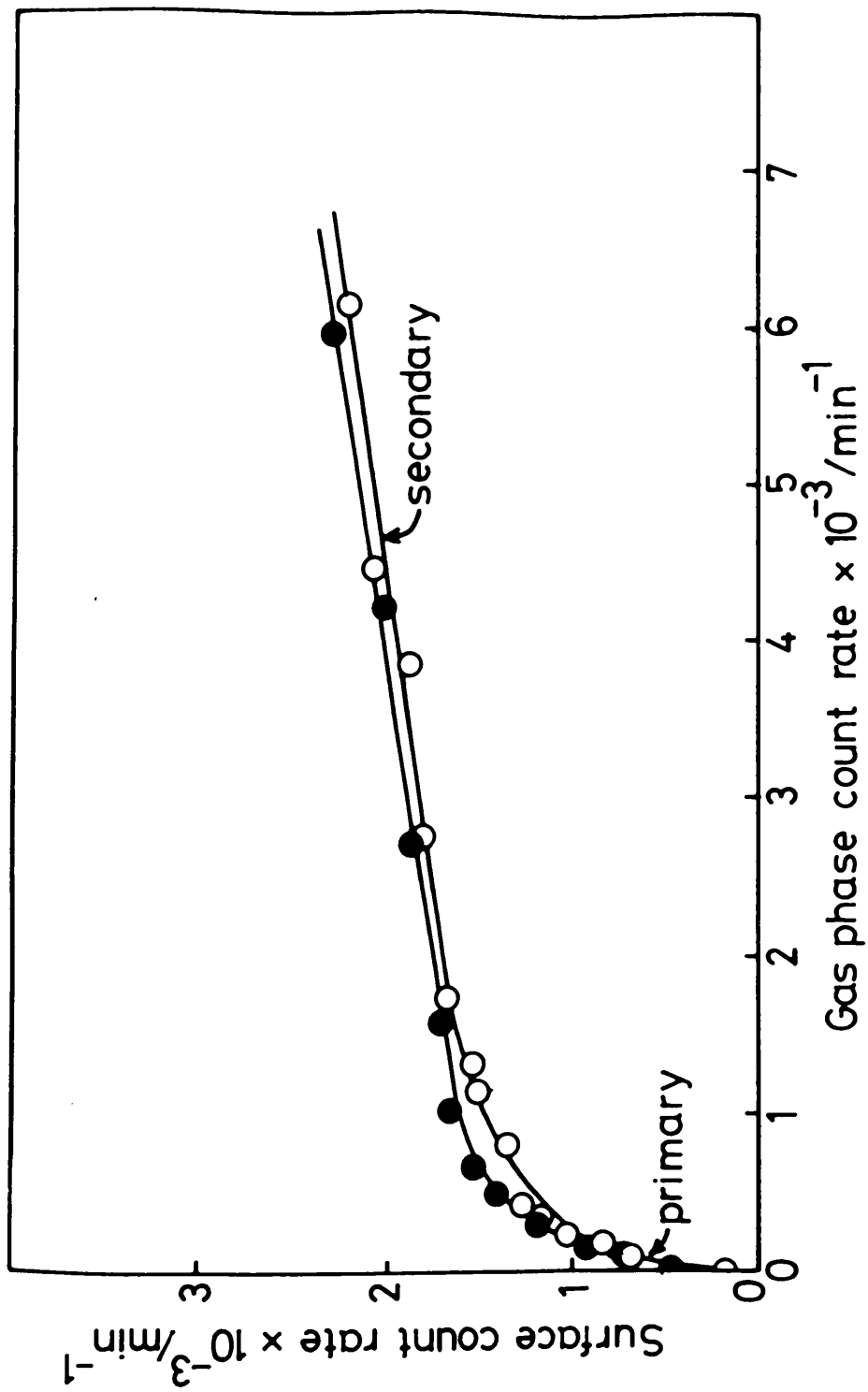


Figure 42. - Adsorption isotherms for [ $^{14}\text{C}$ ]ethylene on a freshly reduced 0.30g Rh/alumina catalyst. Two adsorptions on the same catalyst sample are shown.

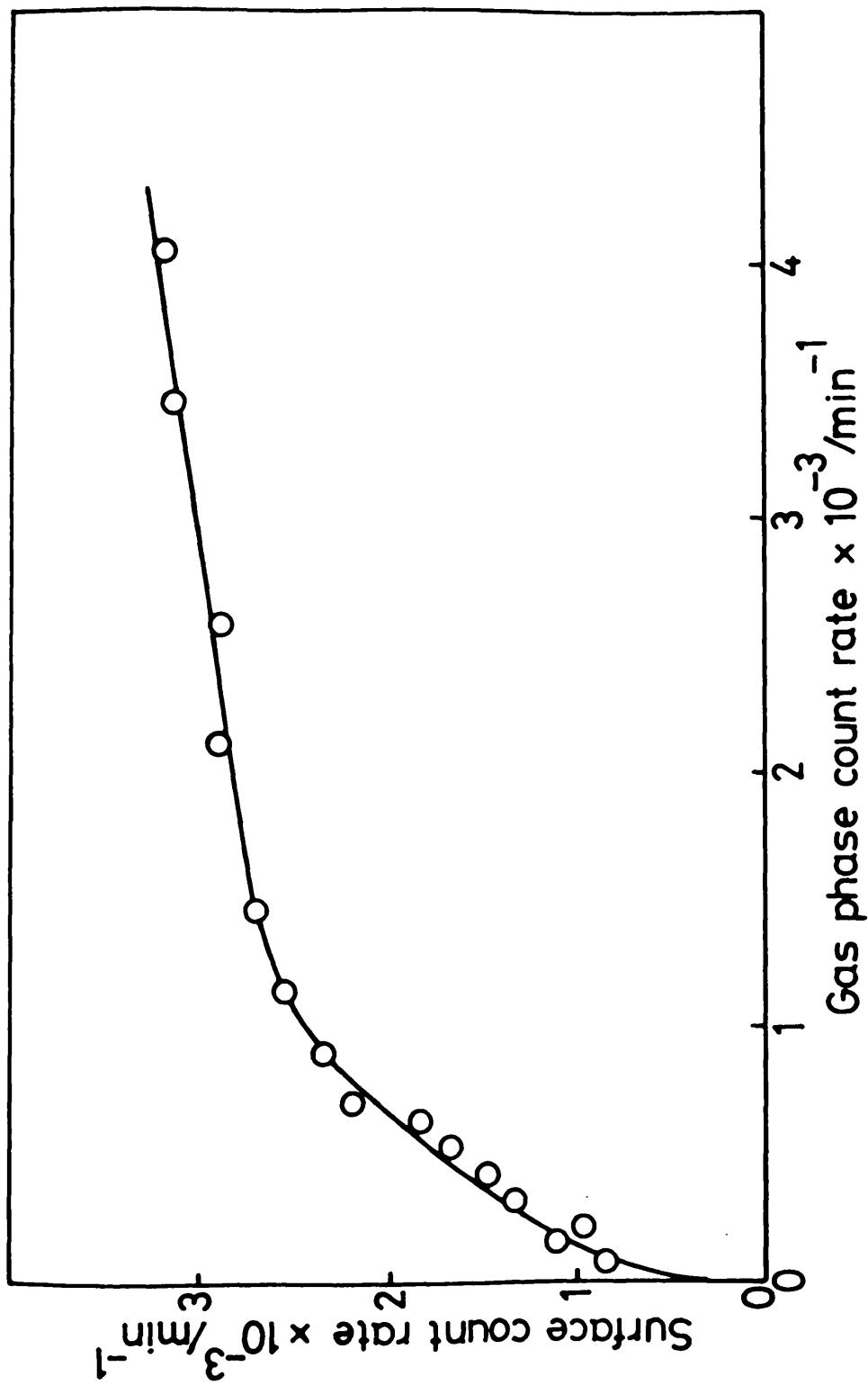


Figure 43. - Adsorption isotherm for  $[^{14}\text{C}]$ ethylene on a freshly reduced 0.10g Rh/alumina catalyst.  $[^{14}\text{C}]$  specific activity was 0.1 mCi ( $\text{mmol}^{-1}$ )

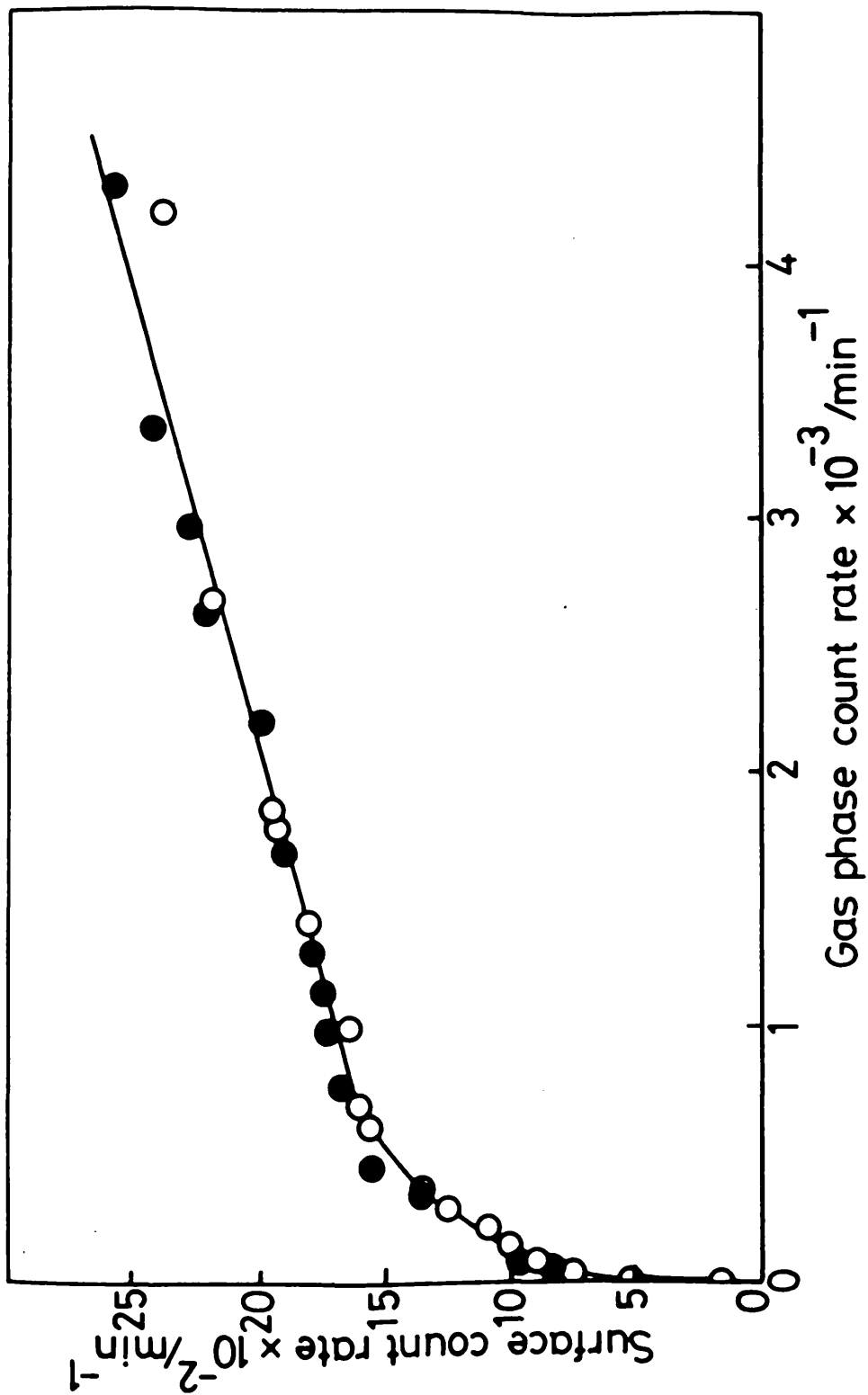


Figure 44. - Adsorption isotherms for [<sup>14</sup>C]propylene on a freshly reduced 0.30g Rh/silica catalyst. Two adsorptions on the same catalyst sample are shown.

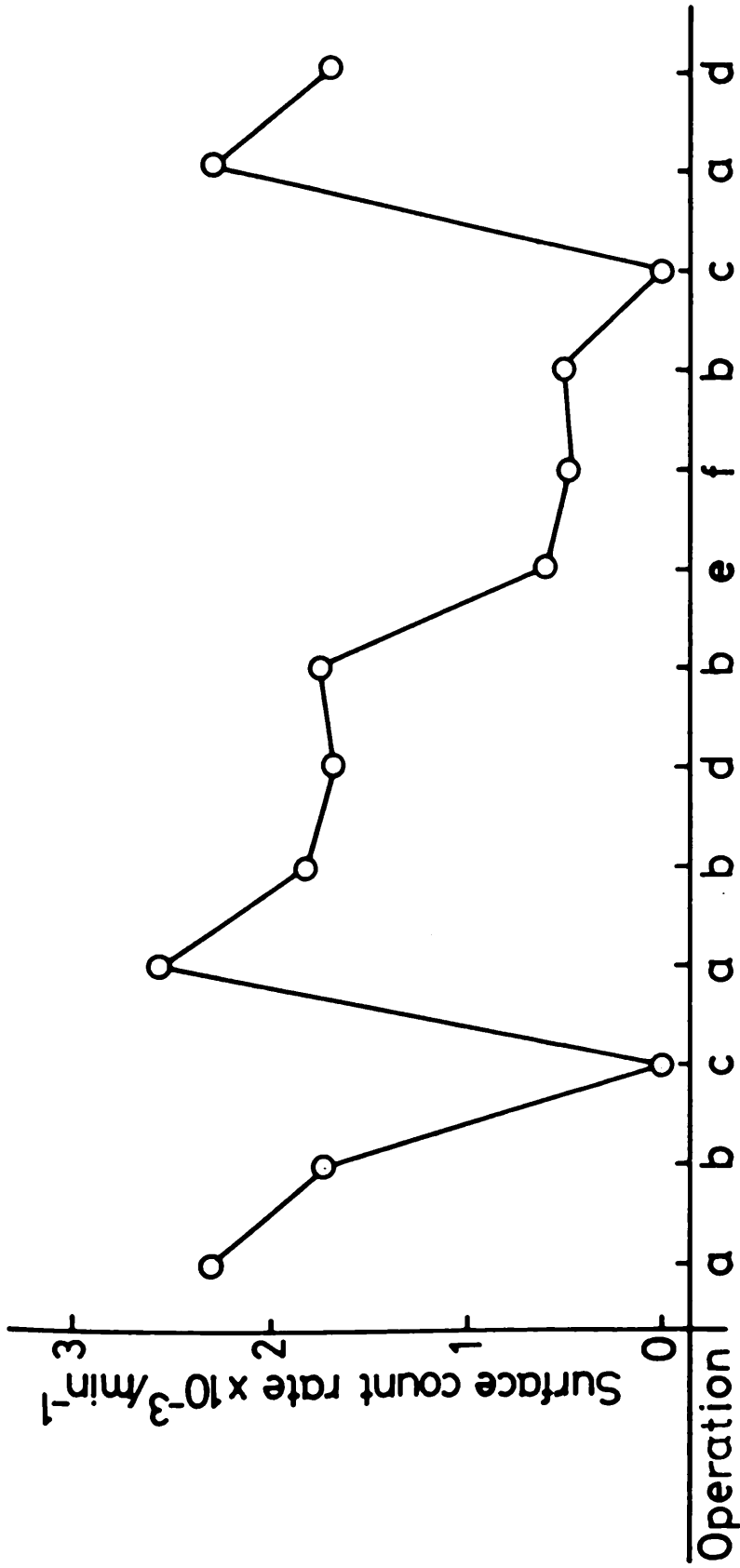


Figure 45. - The effect of various treatments upon adsorbed [ $^{14}\text{C}$ ]propylene on a 0.30g Rh/silica catalyst. Operations: (a) adsorption isotherm build-up; (b) evacuation; (c) catalyst reactivation; (d) 50.0 torr propylene admitted; (e) 36.0 torr  $\text{H}_2$  for 1 hour; (f) 36.0 torr hydrogen for 48 hours.

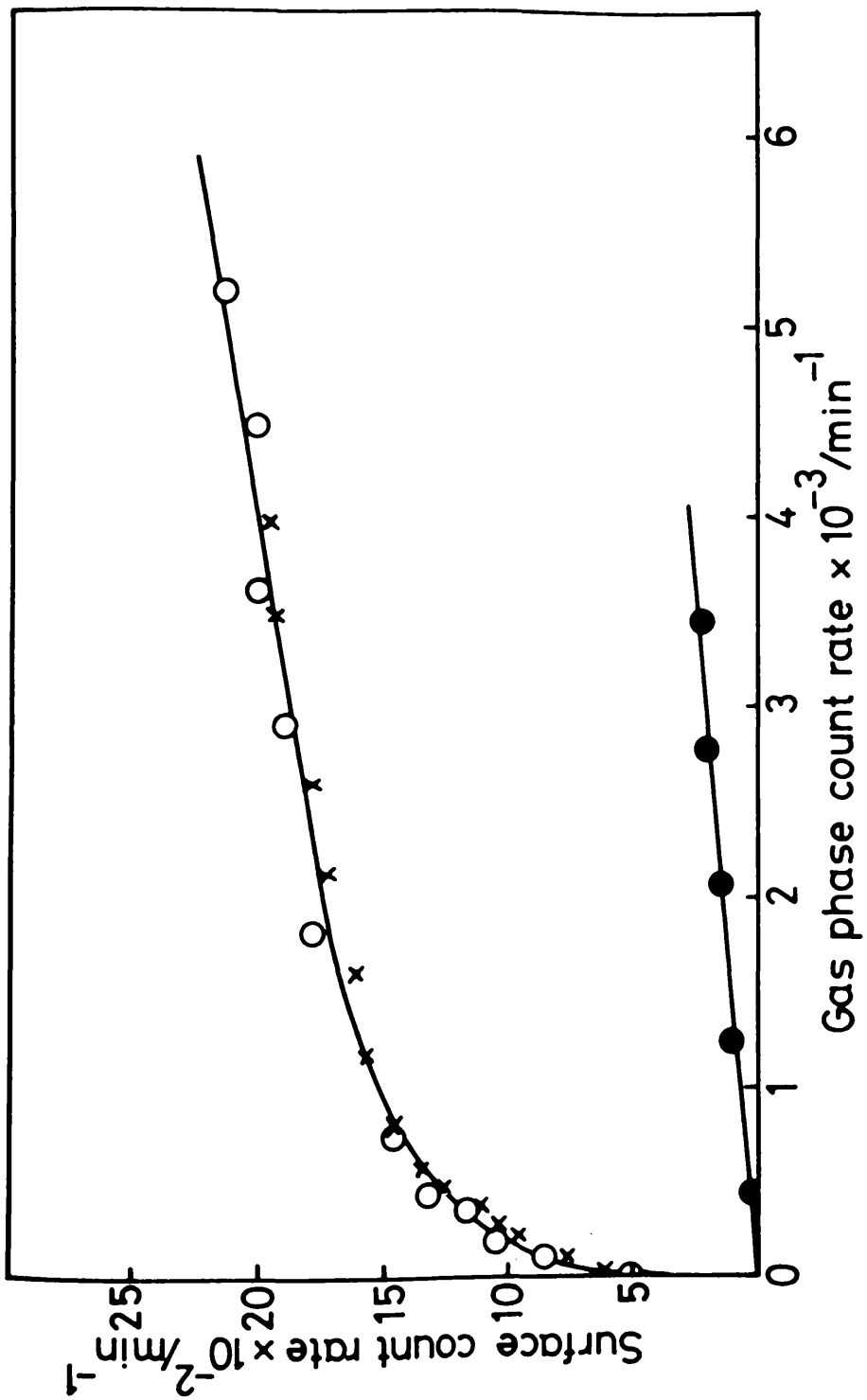


Figure 46. - Adsorption isotherm for [ $^{14}\text{C}$ ]propylene on a freshly reduced 0.30g Rh/alumina catalyst. Two adsorptions on the same catalyst sample are shown (O,X). (●) shows the [ $^{14}\text{C}$ ]propylene adsorption isotherm in presence of 12.0 torr allene.

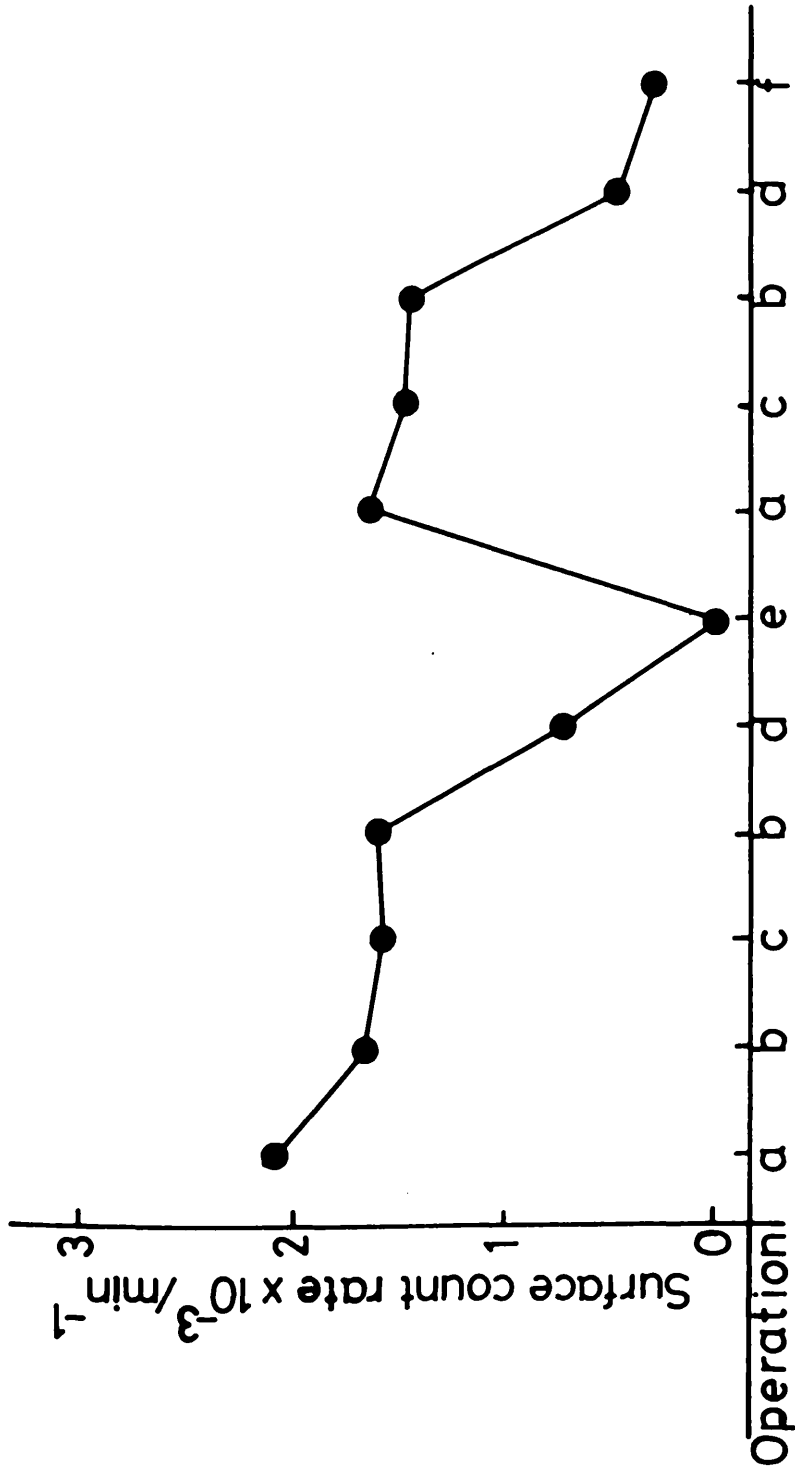


Figure 47. - The effect of various treatments upon adsorbed [ $^{14}\text{C}$ ]propylene on a 0.30g Rh/alumina catalyst. Operations: (a) adsorption isotherm build-up; (b) evacuation; (c) 12.5 torr propylene admitted; (d) 36.0 torr  $\text{H}_2$  for 1 hour; (e) catalyst reactivation; (f) 36.0 torr  $\text{H}_2$  for 24 hours.

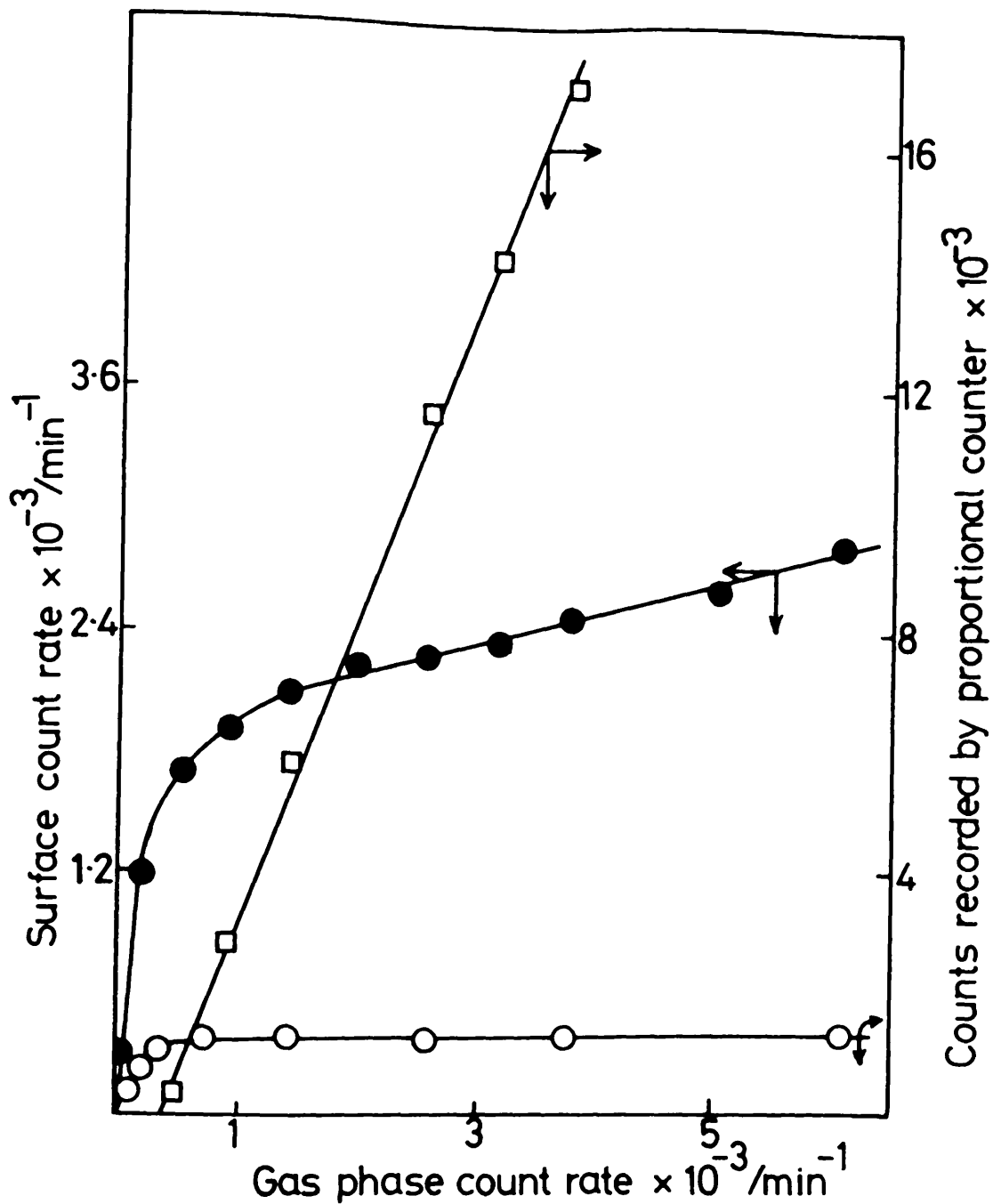


Figure 48. - Adsorption isotherm for [ $^{14}\text{C}$ ]propylene (●) and analysis, by the proportional counter, of the gas phase. [ $^{14}\text{C}$ ]propane (○) and [ $^{14}\text{C}$ ]propylene (□) ; on a freshly reduced 0.20g Rh/alumina catalyst. (1 torr = 12990 counts in proportional counter)

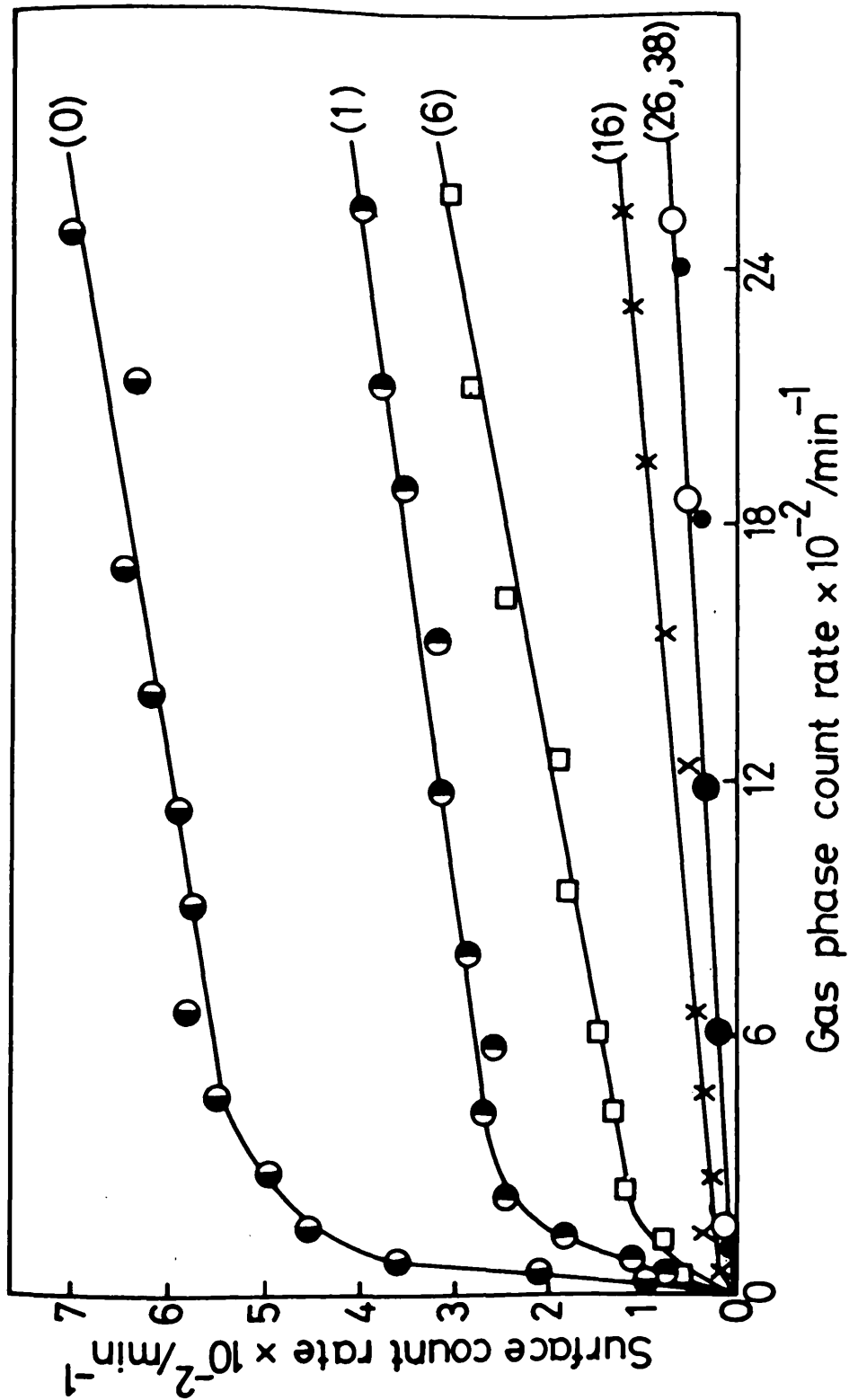


Figure 49. - Adsorption isotherms for [<sup>14</sup>C]propylene on 0.10g Rh/alumina catalyst after varying numbers of reactions have been carried out.

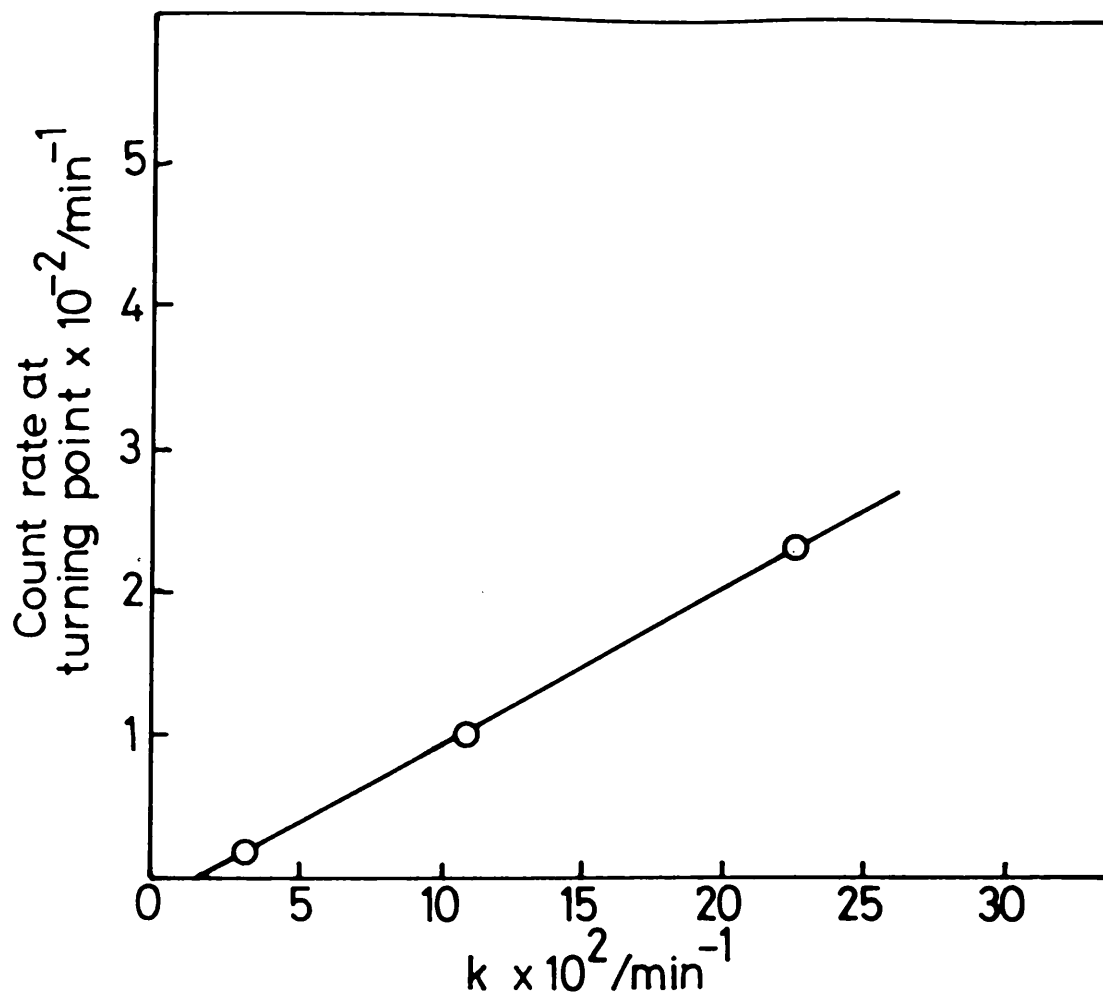


Figure 50. - Variation of the extent of [ $^{14}\text{C}$ ]propylene primary adsorption with catalytic deactivation for 0.10g Rh/alumina catalyst at 293 K.

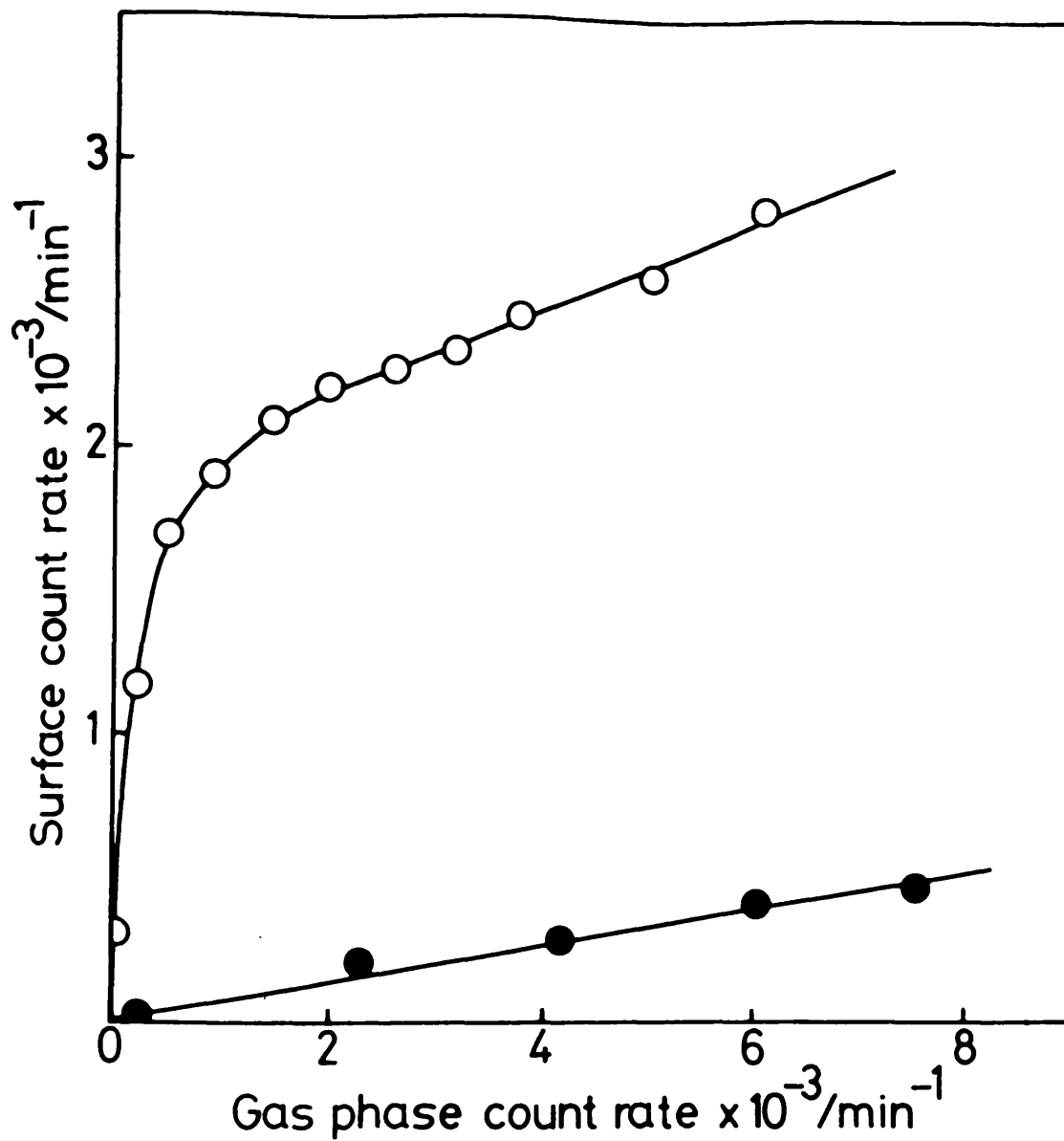


Figure 51. - The adsorption of [ $^{14}\text{C}$ ]propylene on freshly reduced (O) and constant activity (●) catalysts, for a 0.20g Rh/alumina

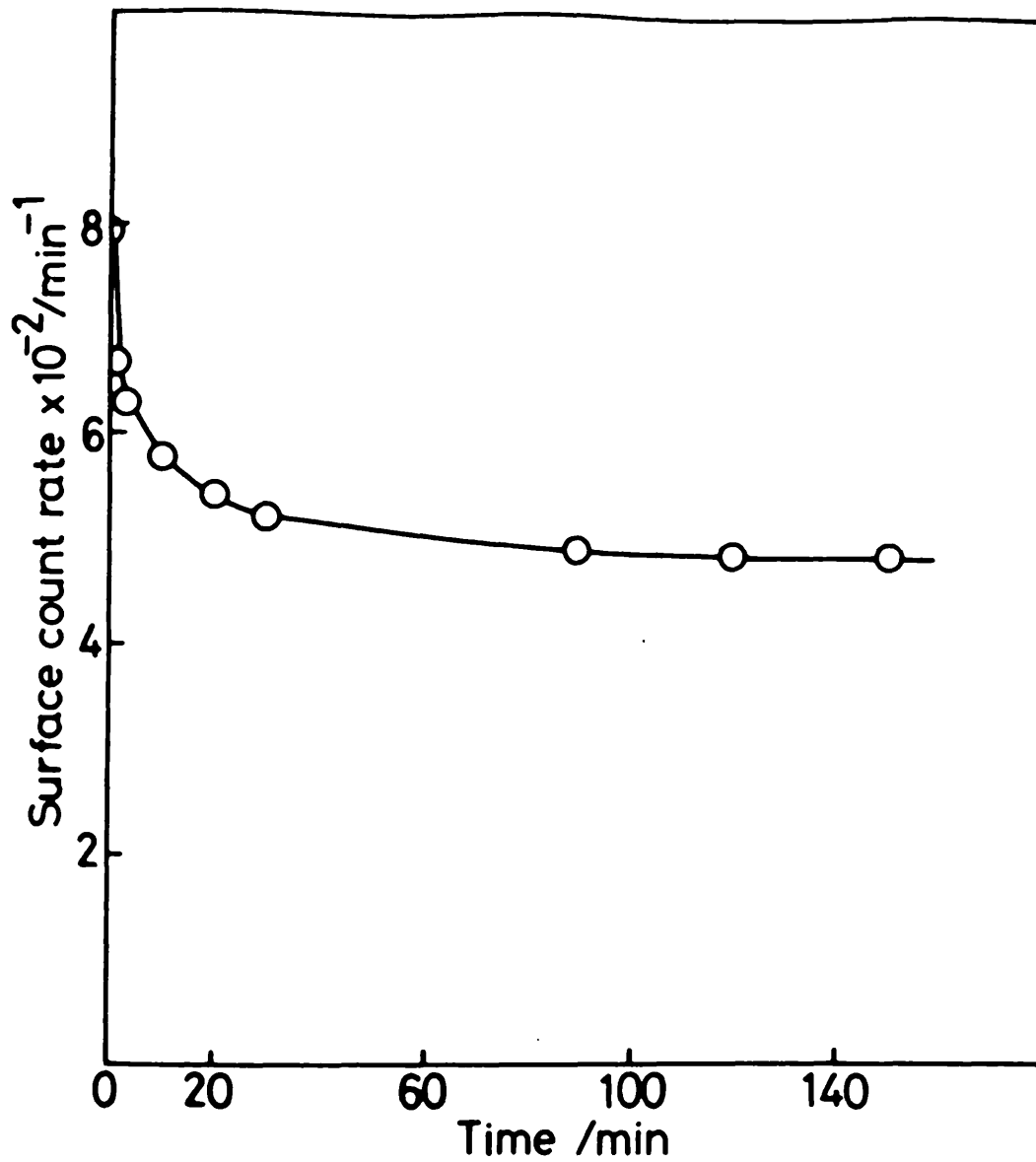


Figure 52. - The effect of 36.0 torr hydrogen on the adsorbed [<sup>14</sup>C]propylene adsorption isotherm for 0.20g Rh/alumina catalyst in the steady state.

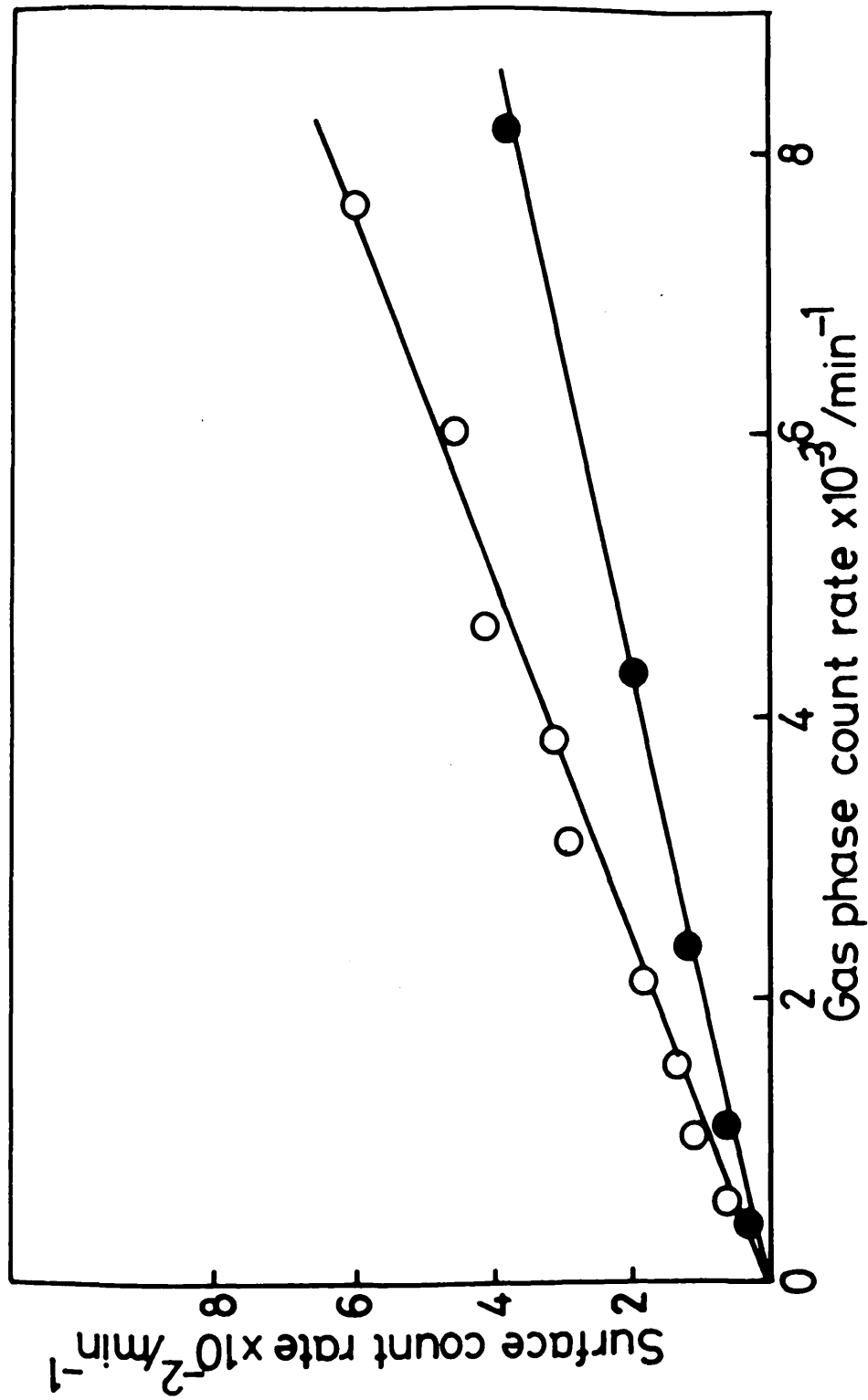


Figure 53. - Adsorption of [ $^{14}\text{C}$ ]propylene on a steady state 0.20g Rh/alumina catalyst in the absence (O) and presence (●) of 12.0 torr allene

#### 4.3 [<sup>14</sup>C]Tracer Studies of Added Propylene on the Hydrogenation of Allene

The addition of [<sup>14</sup>C]propylene to the reaction mixture of allene and hydrogen was used in this work to gain further insight into the mechanism of selective hydrogenation, in particular to determine the relative contributions of the so-called thermodynamic and mechanistic factors to the observed selectivity.

0.10g of alumina-supported rhodium catalyst was used in these experiments. The [<sup>14</sup>C]propylene specific activity was 0.031 mCi/mmol which gave 5390 counts per torr in the proportional counter.

A series of allene hydrogenations (38 reactions) was performed over the freshly reduced catalyst until it reached a steady state activity. Once the steady state activity was reached the selectivity (S) for propylene formation, defined as:

$$S = \frac{P_{C_3H_6}}{P_{C_3H_6} + P_{C_3H_8}}$$

was determined. The results are shown in table 16.

Table 16

Variation of Selectivity with Conversion for Allene Hydrogenation over 0.10g Rh/alumina in the Steady State

conversion (%)	selectivity (S)
11.3	0.952
23.3	0.952
33.0	0.950
49.2	0.949
71.2	0.948
86.7	0.949

4.3.1 Allene Hydrogenation in the Presence of 5.1 torr of [<sup>14</sup>C]Propylene

A premixed sample of 5.1 torr of [<sup>14</sup>C]propylene, 12.0 torr of allene and 36.0 torr of hydrogen was admitted to the reaction vessel containing the rhodium catalyst in its steady state. The progress of the reaction was followed by the fall in pressure recorded by the pressure transducer. Samples were extracted from the reaction vessel, at different pressure falls, and analysed in the radio-gas chromatographic system. The total amount (radioactive plus

non-radioactive) of propylene and propane was determined by measuring the areas of the respective chromatographic peaks. The amount of [ $^{14}\text{C}$ ]propane and [ $^{14}\text{C}$ ]propylene were determined from the gas proportional counter trace.

The results, after correction for the losses of material due to the withdrawal of samples for analysis, are shown in table 17.

The selectivity ( $S^*$ ), termed the "inherent" selectivity shown in table 17 is defined as:

$$S^* = \frac{P_{\text{C}_3\text{H}_6}}{P_{\text{C}_3\text{H}_6} + P_{\text{C}_3\text{H}_8}^*}$$

where  $P_{\text{C}_3\text{H}_8}^*$  is the pressure of propane produced directly from allene.

Figure 54 shows the variation of the yield of [ $^{14}\text{C}$ ]propane and non-radioactive propane with conversion during the first stage of the allene hydrogenation in the presence of 5.10 torr [ $^{14}\text{C}$ ]propylene.

Table 18 shows that the ratio [ $^{14}\text{C}$ ]propane/[ $^{12}\text{C}$ ]propane is much smaller than the [ $^{14}\text{C}$ ]propylene/[ $^{12}\text{C}$ ]propylene ratio.

Table 17

Distribution of C<sub>3</sub>-Products from the Hydrogenation  
of 12.0 torr of Allene in the Presence of 5.1 torr

[<sup>14</sup>C]Propylene over 0.10g Rh/alumina

(P<sub>H<sub>2</sub></sub>)<sub>0</sub> = 36.0 torr

Temp. = 294 ± 1 K

conversion (%)	[ <sup>12</sup> C]propane (torr)	[ <sup>12</sup> C]propylene (torr)	selectivity (S)
26.7	0.159	2.888	0.948
43.9	0.242	4.784	0.952
64.8	0.349	7.069	0.953
71.3	0.408	7.742	0.950
87.7	0.562	10.420	0.949

conversion (%)	[ <sup>14</sup> C]propane (torr)	[ <sup>12</sup> C]propane direct (torr)	selectivity (S*)
26.7	0.015	0.150	0.951
43.9	0.028	0.216	0.957
64.8	0.040	0.294	0.960
71.3	0.044	0.342	0.958
87.7	0.052	0.456	0.958

Table 18

[<sup>14</sup>C]Propane/[<sup>12</sup>C]Propane and [<sup>14</sup>C]Propylene/[<sup>12</sup>C]Propylene

Ratios During the Hydrogenation of 12.0 torr

[<sup>12</sup>C]Allene and 5.1 torr [<sup>14</sup>C]Propylene

conversion (%)	$\frac{[^{14}\text{C}]\text{propane}}{[^{12}\text{C}]\text{propane}}$	$\frac{[^{14}\text{C}]\text{propylene}}{[^{12}\text{C}]\text{propylene}}$
26.7	0.094	1.76
43.9	0.116	1.06
64.8	0.115	0.72
71.3	0.108	0.65
87.7	0.093	0.48

4.3.2 Allene Hydrogenation in the Presence of  
2.01 torr of [<sup>14</sup>C]Propylene

A premixed sample of 2.01 torr of [<sup>14</sup>C]propylene, 12.0 torr of allene and 36.0 torr of hydrogen was admitted into the reaction vessel containing the rhodium catalyst in its steady state. Samples were extracted from the reaction vessel, at different percentage conversions and analysed in the radio-gas chromatographic system. The results, after correction for the losses of material due to the withdrawal of samples for analysis, are shown in table 19.

Table 19

Distribution of C<sub>3</sub>-Products from the Hydrogenation  
of Allene in the Presence of 2.01 torr [<sup>14</sup>C]Propylene  
over 0.10g Rh/alumina

(P<sub>H<sub>2</sub></sub>)<sub>0</sub>

Temp. = 294 ± 1 K

conversion (%)	[ <sup>12</sup> C]propane (torr)	[ <sup>12</sup> C]propylene (torr)	selectivity (S)
10.3	0.065	1.108	0.945
23.8	0.131	2.592	0.952
38.9	0.228	4.168	0.948
57.5	0.317	6.263	0.952
96.2	0.606	10.296	0.944

conversion (%)	[ <sup>14</sup> C]propane (torr)	[ <sup>12</sup> C]propane direct (torr)	selectivity (S*)
10.3	0.002	0.064	0.945
23.8	0.006	0.123	0.955
38.9	0.008	0.211	0.952
57.5	0.012	0.280	0.957
96.2	0.020	0.504	0.953

Figure 55 shows the variation of the yield of  $[^{14}\text{C}]$ propane and  $[^{12}\text{C}]$ propane with conversion during the first stage of allene hydrogenation in the presence of 2.01 torr  $[^{14}\text{C}]$ propylene.

Table 20 shows that the  $[^{14}\text{C}]$ propane/ $[^{12}\text{C}]$ propane ratio is much smaller than the  $[^{14}\text{C}]$ propylene/ $[^{12}\text{C}]$ propylene ratio.

Table 20

$[^{14}\text{C}]$ Propane/ $[^{12}\text{C}]$ Propane and  $[^{14}\text{C}]$ Propylene/ $[^{12}\text{C}]$ Propylene

Ratios During the Hydrogenation of 12.0 torr

$[^{12}\text{C}]$ Allene and 2.01 torr  $[^{14}\text{C}]$ Propylene

conversion (%)	$\frac{[^{14}\text{C}]\text{propane}}{[^{12}\text{C}]\text{propane}}$	$\frac{[^{14}\text{C}]\text{propylene}}{[^{12}\text{C}]\text{propylene}}$
10.3	0.031	1.81
23.8	0.046	0.77
38.9	0.035	0.48
57.5	0.038	0.319
96.2	0.033	0.193

#### 4.3.3 Allene Hydrogenation in the Presence of 1.26 torr of [<sup>14</sup>C]Propylene

A premixed sample of 1.26 torr of [<sup>14</sup>C]propylene, 12.0 torr of allene and 36.0 torr of hydrogen was admitted into the reaction vessel containing the rhodium catalyst in its steady state activity. Samples were extracted from the reaction vessel, at different percentage conversions and analysed in the radio-gas chromatographic system. The results are shown in table 21.

#### 4.3.4 The Yield of [<sup>14</sup>C]Propane

From the results in sections 4.3.1, 4.3.2 and 4.3.3 it can be seen that the yield of [<sup>14</sup>C]propane only constitutes a small proportion of the total propane yield. Another interesting feature that emerged from the results was the linearity of the increase in the yield of [<sup>14</sup>C]propane as the reaction proceeded. The variation of the yield of [<sup>14</sup>C]propane with conversion for the hydrogenation of allene in the presence of various pressures of [<sup>14</sup>C]propylene added is shown in figure 56.

The variation of the yield of [<sup>14</sup>C]propane at 50% conversion against pressures of added [<sup>14</sup>C]propylene is shown in figure 57. It can be seen that the yield of [<sup>14</sup>C]propane was directly proportional to the initial pressure of added [<sup>14</sup>C]propylene.

Table 21

Distribution of C<sub>3</sub>-Products from the Hydrogenation  
of 12.0 torr of Allene in the Presence of 1.26 torr  
[<sup>14</sup>C]Propylene over 0.10g Rh/alumina

(P<sub>H<sub>2</sub></sub>)<sub>0</sub> = 36.0 torr

Temp. = 294 ± 1 K

conversion (%)	[ <sup>12</sup> C]propane (torr)	[ <sup>12</sup> C]propylene (torr)	selectivity (S)
18.1	0.103	1.975	0.950
40.7	0.242	4.579	0.950
64.8	0.390	7.012	0.947
93.3	0.541	9.345	0.945

conversion (%)	[ <sup>14</sup> C]propane (torr x 10 <sup>-2</sup> )	[ <sup>12</sup> C]propane direct (torr)	selectivity (S*)
18.1	0.28	0.099	0.952
40.7	0.6	0.224	0.953
64.8	0.9	0.339	0.954
93.3	1.5	0.431	0.956

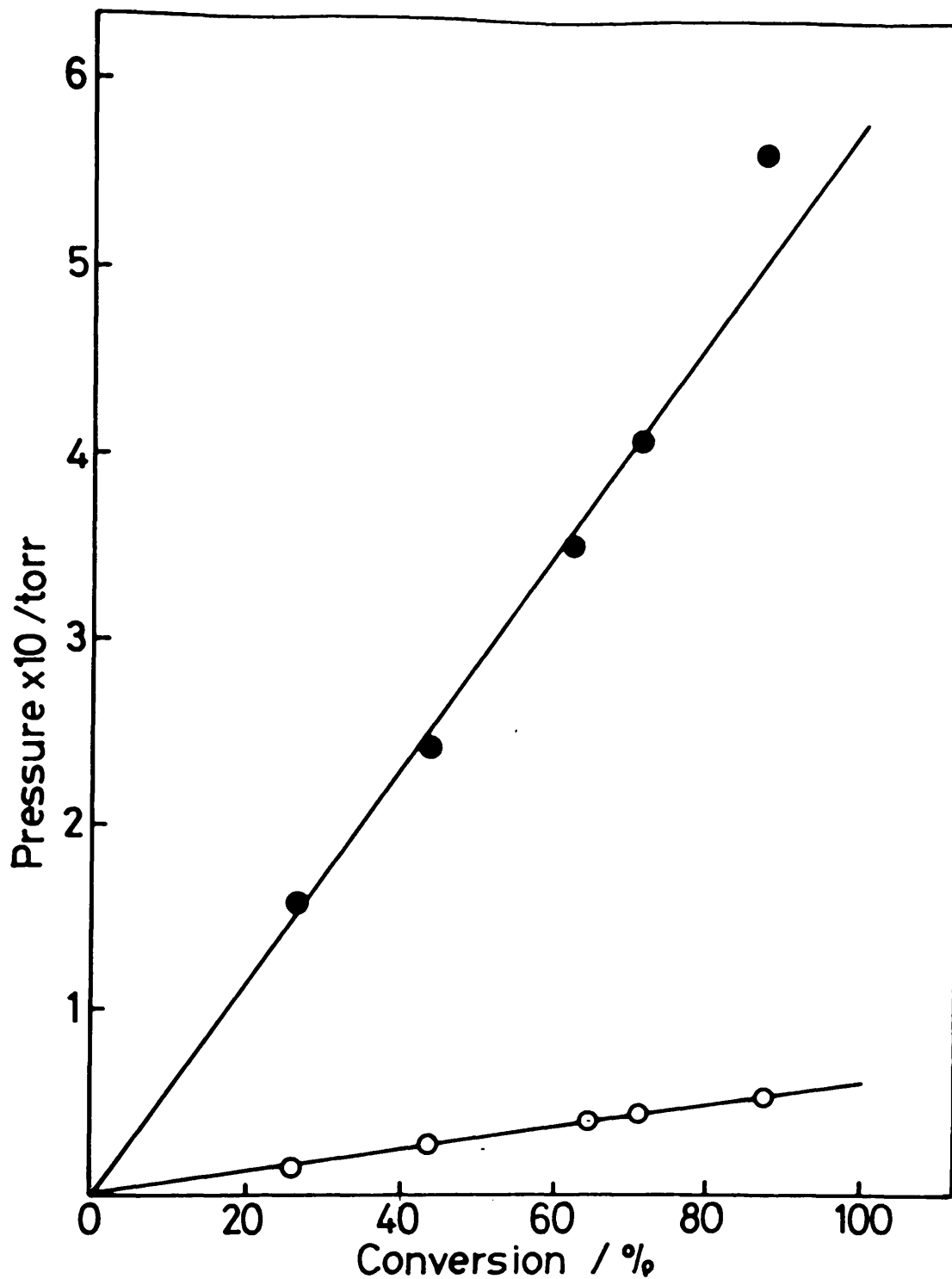


Figure 54. - Variation of the yield of [<sup>14</sup>C]propane (O) and [<sup>12</sup>C]propane (●) with conversion during the first stage of 12.0 torr allene and 5.1 torr [<sup>14</sup>C]propylene hydrogenation over a 0.10g Rh/alumina catalyst.

$$(P_{H_2})_0 = 36.0 \text{ torr}$$

$$T = 294 \pm 1 \text{ K}$$

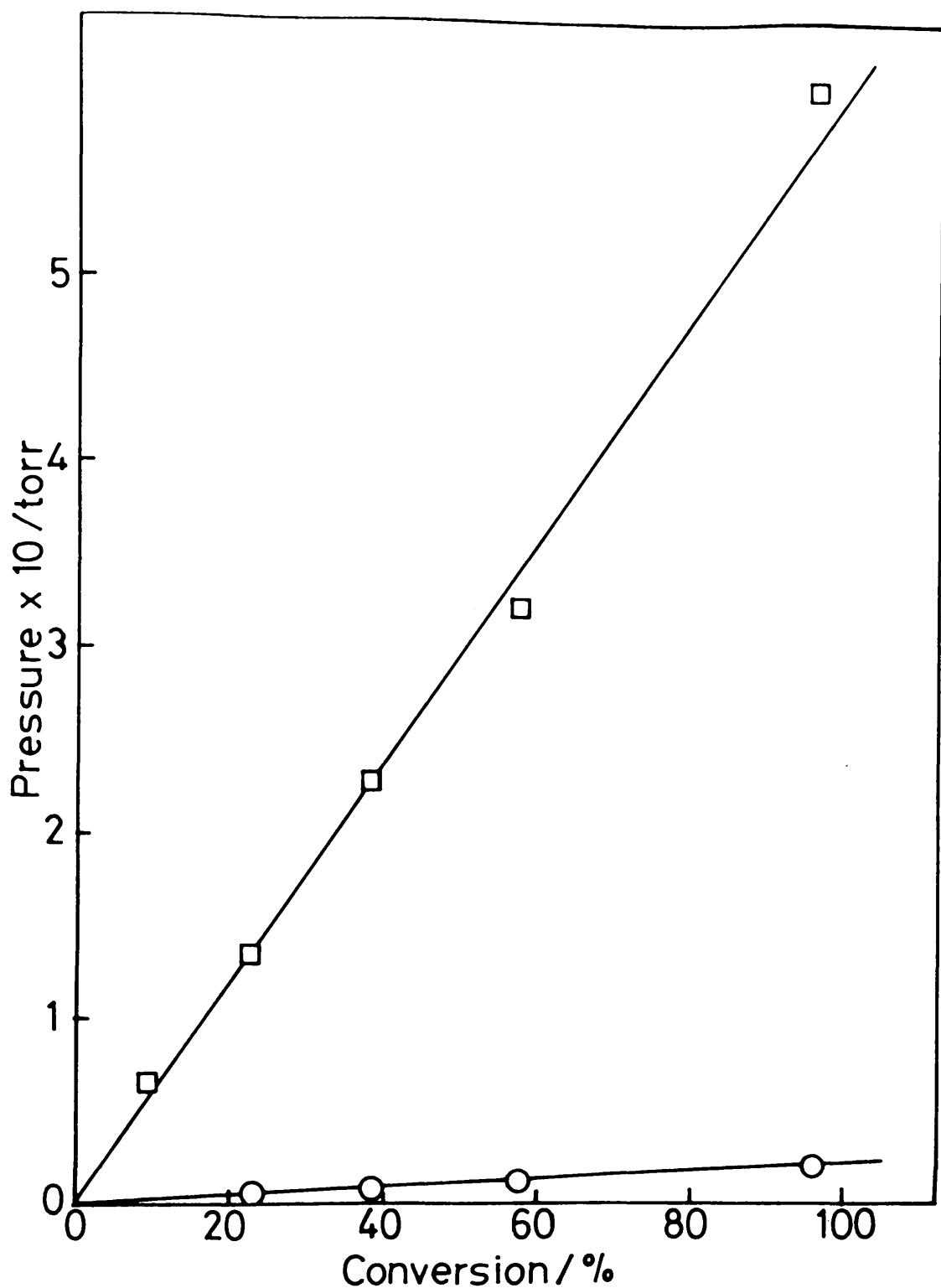


Figure 55. - Variation of the yield of [<sup>14</sup>C]propane (○) and [<sup>12</sup>C]propane (□) with conversion during the first stage of 12.0 torr allene and 2.01 torr [<sup>14</sup>C]propylene hydrogenation over 0.10g Rh/alumina catalyst.

$$(P_{H_2})_0 = 36.0 \text{ torr}$$

$$T = 294 \pm 1 \text{ K}$$

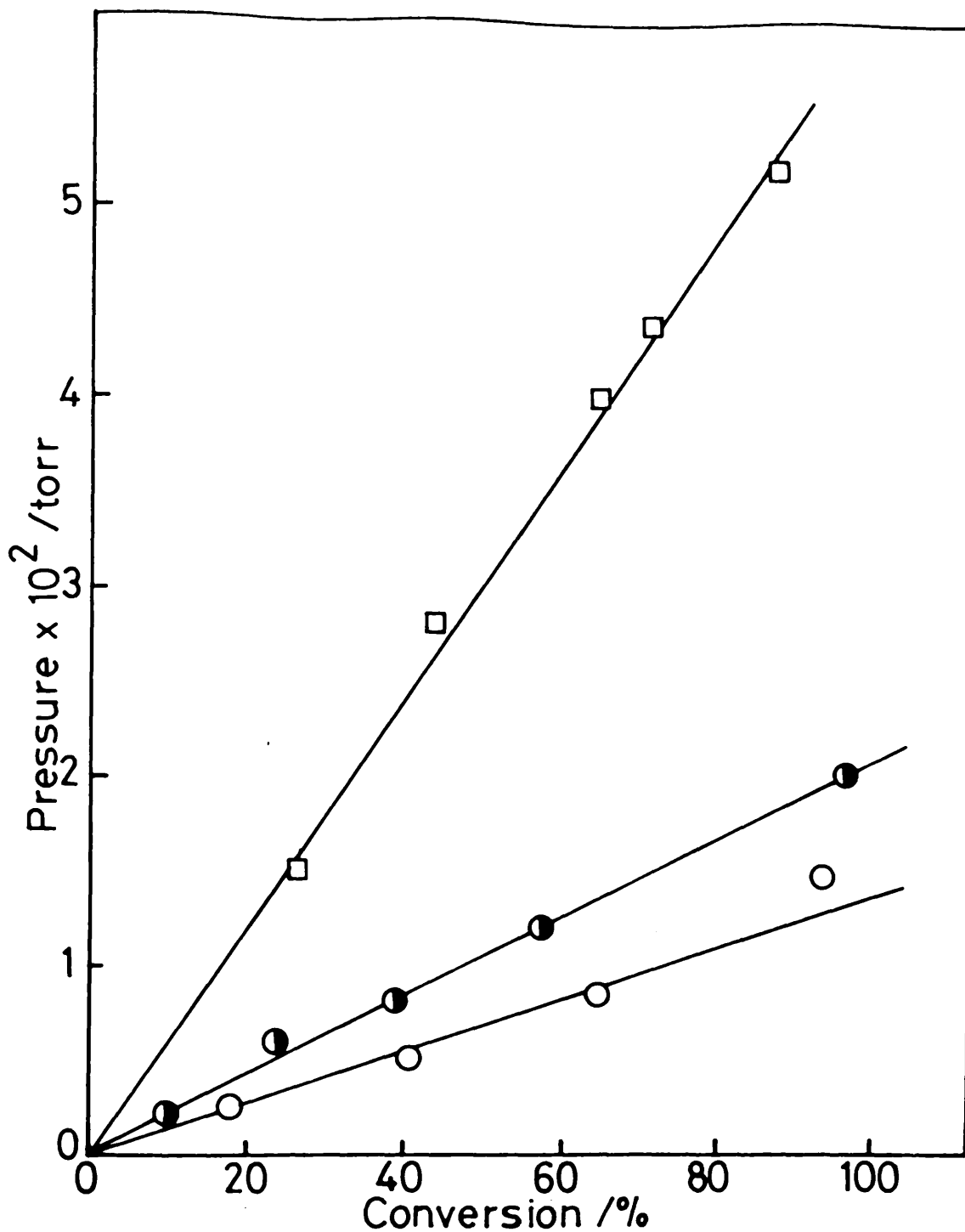


Figure 56. - Variation of the yield of [<sup>14</sup>C]propane with conversion for the hydrogenation of 12.0 torr allene and 1.26 torr (○), 2.01 torr (●) and 5.1 torr (□) [<sup>14</sup>C]propylene over 0.10g Rh/alumina catalyst.

$$(P_{H_2})_0 = 36.0 \text{ torr.}$$

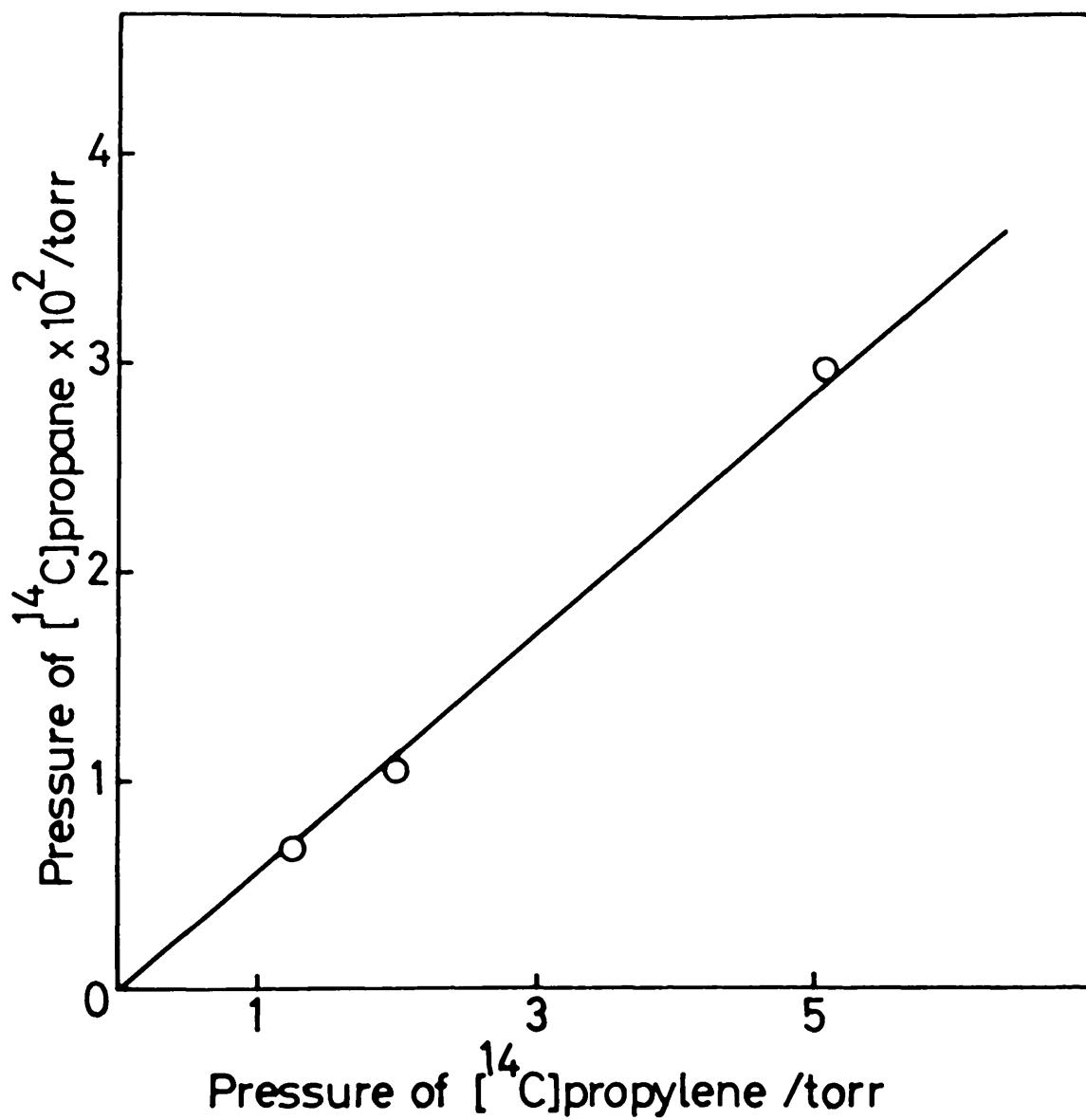


Figure 57. - Variation of the yield of  $[^{14}\text{C}]$ propane with pressure of added  $[^{14}\text{C}]$ propylene at a constant uptake of hydrogen corresponding to 50% conversion.

4.4 The Effects of Carbon Monoxide Poisoning upon the Adsorption of [ $^{14}\text{C}$ ]Propylene and the Hydrogenation of Allene

This section presents the results of a detailed investigation of the effects of the presence of carbon monoxide upon the hydrogenation of allene. The effect of the presence of carbon monoxide upon the [ $^{14}\text{C}$ ]propylene adsorption isotherm is also presented. The same sample of catalyst was often used for many experiments. It was cleaned of adsorbed material by use of the procedure described in section 4.2. This procedure was found to efficiently remove both [ $^{14}\text{C}$ ]propylene and [ $^{14}\text{C}$ ]carbon monoxide from the catalyst surface.

4.4.1 The [ $^{14}\text{C}$ ]Carbon Monoxide Adsorption Isotherm on a Freshly Reduced Alumina-Supported Rhodium Catalyst

The [ $^{14}\text{C}$ ]carbon monoxide adsorption isotherm was determined by admitting aliquots of the radioactive carbon monoxide (specific activity = 0.08 mCi/mmol) to the reaction vessel containing a 0.20g sample of freshly reduced rhodium/alumina catalyst. The adsorption isotherm is shown in figure 58. It is a typical monolayer adsorption isotherm, which shows no secondary region.

Evacuation of the reaction vessel for one hour resulted in the removal of only 2.7% of the preadsorbed radioactive

material on the surface of the catalyst (table 22). The displacement of [ $^{14}\text{C}$ ]carbon monoxide by allene was observed by introducing 12.0 torr of allene into the reaction vessel. 13.9% of the adsorbed radioactive carbon monoxide was replaced by allene (table 22). After the evacuation of the allene 36.0 torr of hydrogen was admitted into the reaction vessel. Only a very small amount of the radioactive material adsorbed on the catalyst was removed by the hydrogen (less than 0.25%)(table 22). After the evacuation of the hydrogen, 48.0 torr of a premixed sample of hydrogen and allene ( $\text{H}_2:\text{C}_3\text{H}_4 = 3:1$ ) was admitted into the reaction vessel. After evacuating the products of reaction the amount of radioactive material adsorbed on the catalyst had only decreased by 0.3% (table 22).

#### 4.4.2 The [ $^{14}\text{C}$ ]Carbon Monoxide Adsorption Isotherm on a Freshly Reduced Alumina-Supported Rhodium Catalyst in the Presence of Allene

The catalyst used in this experiment was the same as that used in section 4.6.1. After removing all radioactivity from the catalyst surface a pressure of 12.0 torr of allene was introduced into the reaction vessel. After one hour, without removing the allene from the gas phase, the [ $^{14}\text{C}$ ]carbon monoxide isotherm was determined on the allene precovered surface. The adsorption isotherm is shown in figure 58. This adsorption isotherm had the same shape

as the adsorption isotherm on the freshly reduced catalyst, but the amount of radioactive material adsorbed on the surface of the catalyst was considerably reduced (table 22). The reaction vessel was evacuated for one hour and the amount of radioactive material on the surface of the catalyst was again determined. The evacuation removed only 2.7% of the radioactive material adsorbed on the surface of the catalyst. After the evacuation of the allene, 48.0 torr of a premixed sample of hydrogen (36.0 torr) and allene (12.0 torr) was admitted into the reaction vessel. The evacuation of the products of reaction had no effect upon the amount of radioactive material adsorbed on the catalyst surface (table 22).

#### 4.4.3 The [ $^{14}\text{C}$ ]Carbon Monoxide Adsorption Isotherm on a Steady State Alumina-Supported Rhodium Catalyst

A series of allene hydrogenations (forty reactions) was performed over the catalyst until it reached a steady state activity. The catalyst was evacuated for one hour and then the [ $^{14}\text{C}$ ]carbon monoxide isotherm was determined (figure 58). This adsorption isotherm had the same shape as the adsorption isotherm built on a freshly reduced catalyst, although the amount of radioactive material adsorbed on the surface of the catalyst was considerably less (table 22). The reaction vessel was evacuated for one hour. This evacuation removed 12.5% of the adsorbed radio-

active material. A pressure of 12.0 torr of allene was introduced into the reaction vessel to observe the displacement of [ $^{14}\text{C}$ ]carbon monoxide by allene. The amount of [ $^{14}\text{C}$ ]carbon monoxide adsorbed on the surface of the catalyst remained the same after the addition of allene, indicating that no displacement took place. After the evacuation of the allene, 48.0 torr of a premixed sample of hydrogen (36.0 torr) and allene (12.0 torr) was admitted into the reaction vessel. After evacuating the products of reaction the amount of radioactive material adsorbed on the catalyst was decreased by only 2.1% (table 22).

#### 4.4.4 The [ $^{14}\text{C}$ ]Carbon Monoxide Adsorption Isotherm on a Steady State Alumina-Supported Rhodium Catalyst in the Presence of Allene

A pressure of 12.0 torr of allene was introduced into the reaction vessel containing 0.20g Rh/alumina catalyst in its steady state. After one hour, without removing allene from the gas phase, the [ $^{14}\text{C}$ ]carbon monoxide isotherm was determined on the allene precovered surface. The adsorption isotherm is shown in figure 58. This adsorption isotherm had the same shape as the adsorption isotherm built on the clean freshly reduced catalyst, but the amount of radioactive material adsorbed on the surface of the catalyst was considerably reduced (table 22). Figure 58 shows that the amount of [ $^{14}\text{C}$ ]carbon monoxide adsorbed on a steady state

rhodium/alumina catalyst in the presence of allene is approximately half of the amount of [ $^{14}\text{C}$ ]carbon monoxide adsorbed on a steady state rhodium/alumina catalyst when allene is not present and it is approximately the same as the amount of [ $^{14}\text{C}$ ]carbon monoxide adsorbed on a freshly reduced catalyst in presence of allene.

Evacuation for one hour resulted in the removal of 1.2% of the adsorbed [ $^{14}\text{C}$ ]carbon monoxide. After evacuation of the allene, 48.0 torr of a premixed sample of hydrogen (36.0 torr) and allene (12.0 torr) was admitted into the reaction vessel. After evacuating the products of reaction the amount of radioactive material adsorbed on the catalyst was reduced by 1.6% (table 22).

The amount of radioactive carbon monoxide adsorbed on the surface of the catalyst could be increased by admitting to the reaction vessel [ $^{14}\text{C}$ ]carbon monoxide (3.0 torr) mixed with allene (12.0 torr) and hydrogen (36.0 torr). After one hour this mixture was evacuated and the surface count rate recorded. The amount of adsorbed radioactive material increased from 1133 to 4089 counts per minute.

#### 4.4.5 The [ $^{14}\text{C}$ ]Propylene Adsorption Isotherm on a Freshly Reduced Alumina-Supported Rhodium Catalyst in the Presence of Carbon Monoxide

0.20g Rh/alumina catalyst was used to determine the extent to which [ $^{14}\text{C}$ ]propylene would adsorb on a catalyst

exposed to carbon monoxide. The freshly reduced catalyst was exposed to 5.0 torr non-radioactive carbon monoxide. Without removing carbon monoxide from the reaction vessel the [ $^{14}\text{C}$ ]propylene adsorption isotherm was determined on the carbon monoxide precovered surface. Figure 59 shows that [ $^{14}\text{C}$ ]propylene adsorption on carbon monoxide precovered surface can take place, although the amount adsorbed was considerably less than that on a clean surface. No primary adsorption region was observed and evacuating the reaction vessel for one hour removed approximately 30% of the adsorbed [ $^{14}\text{C}$ ]propylene.

#### 4.4.6 The Effect of Carbon Monoxide Poisoning upon the Catalytic Activity of a Freshly Reduced Alumina-Supported Rhodium Catalyst

When a premixed sample of carbon monoxide (1.0 torr), allene (12.0 torr) and hydrogen (36.0 torr) was admitted into the reaction vessel containing a freshly reduced 0.20g sample of Rh/alumina catalyst no reaction occurred over a period of 12 hours. However, the catalyst revealed some activity after the reaction vessel had been evacuated for one hour and a new reaction mixture (12.0 torr allene and 36.0 torr hydrogen) admitted to the reaction vessel. This activity was approximately five hundred times less than the catalytic activity of the non-poisoned catalyst (table 23).

In another experiment, carbon monoxide (1.0 torr) was first introduced into the reaction vessel containing a freshly reduced 0.2g sample of Rh/alumina catalyst. The reaction vessel was then evacuated for one hour at 294K. When 48.0 torr of a premixed sample of allene (12.0 torr) and hydrogen (36.0 torr) was admitted into the reaction vessel, reaction occurred but again the catalytic activity was very low. While the reaction was taking place, a pressure of one torr of carbon monoxide was introduced into the reaction vessel. This resulted in complete poisoning of the catalyst. The reaction stopped as soon as the carbon monoxide was introduced into the reaction vessel.

The hydrogenation reaction over the carbon monoxide poisoned catalyst is also first order with respect to the total pressure. The pressure fall versus time curve was of the same shape as when the catalyst was not poisoned. The only difference was that the first stage of the reaction was more affected (approximately ten times more), by the presence of carbon monoxide than the second stage of the reaction.

The selectivity (table 24) was also affected by the presence of carbon monoxide. The amount of propane produced was considerably less than that obtained with a non-poisoned catalyst (figure 60).

4.4.7 The Effect of Carbon Monoxide Poisoning upon the Catalytic Activity of a Freshly Reduced Alumina-Supported Rhodium Catalyst in the Presence of Allene

A pressure of 12.0 torr of allene was introduced into the reaction vessel containing a freshly reduced 0.20g sample of Rh/alumina catalyst. After one hour, without removing allene from the reaction vessel, 2.0 torr of carbon monoxide was admitted into the reaction vessel and left for two hours. The reaction vessel was then evacuated for one hour. After the evacuation 48.0 torr of a premixed sample of hydrogen (36.0 torr) and allene (12.0 torr) was admitted into the reaction vessel. The catalyst was still active (table 23). After evacuating the reaction products a premixed sample containing carbon monoxide (1.0 torr), allene (12.0 torr) and hydrogen (36.0 torr) was admitted into the reaction vessel, but no reaction occurred over a period of 12 hours.

4.4.8 The Effect of Carbon Monoxide Poisoning upon the Catalytic Activity of a Steady State Alumina-Supported Rhodium Catalyst

A series of allene hydrogenations (forty reactions) was performed over a 0.20g sample of Rh/alumina catalyst until it reached its steady state. 2.0 torr of carbon monoxide

was admitted into the reaction vessel for one hour followed by evacuation for one hour. When 48.0 torr of a premixed sample of allene and hydrogen was admitted into the reaction vessel, reaction occurred, but the catalytic activity was very low (table 23). After evacuating the reaction products a premixed sample containing carbon monoxide (1.0 torr), allene (12.0 torr) and hydrogen (36.0 torr) was admitted into the reaction vessel, but no reaction occurred over a period of 12 hours.

4.4.9 The Effect of Carbon Monoxide Poisoning upon the Catalytic Activity of a Steady State Alumina-Supported Rhodium Catalyst in the Presence of Allene

A pressure of 12.0 torr of allene was admitted into the reaction vessel containing a steady state 0.20g sample of the Rh/alumina catalyst. After one hour, without removing allene from the reaction vessel, 2.0 torr of carbon monoxide was admitted and left for two hours. After evacuation for one hour, 48.0 torr of a premixed sample of hydrogen (36.0 torr) and allene (12.0 torr) was admitted into the reaction vessel. The catalyst was still active (table 23).

#### 4.5 Accumulative [ $^{14}\text{C}$ ]Carbon Monoxide Adsorption on an Alumina-Supported Rhodium Catalyst

During the experiments carried out in section 4.4 it was observed that the surface of a catalyst, on which a [ $^{14}\text{C}$ ]carbon monoxide adsorption isotherm had been built, could adsorb more [ $^{14}\text{C}$ ]carbon monoxide after being treated with a mixture of allene (12.0 torr) and hydrogen (36.0 torr).

It was decided to investigate this accumulative [ $^{14}\text{C}$ ]carbon monoxide adsorption phenomena.

##### 4.5.1 Accumulative [ $^{14}\text{C}$ ]Carbon Monoxide Adsorption on a Freshly Reduced Alumina-Supported Rhodium Catalyst

After the determination of a [ $^{14}\text{C}$ ]carbon monoxide adsorption isotherm on a freshly reduced 0.10g sample of Rh/alumina catalyst, the reaction vessel was evacuated. A premixed sample of allene (12.0 torr) and hydrogen (36.0 torr) was then allowed into the reaction vessel. When the products of reaction were evacuated and a new [ $^{14}\text{C}$ ]carbon monoxide isotherm determined, it was observed that the amount of [ $^{14}\text{C}$ ]carbon monoxide adsorbed on the surface of the catalyst had increased (table 25). This process (allene hydrogenation, evacuation, [ $^{14}\text{C}$ ]CO isotherm) was repeated twice. The extent of the adsorption of carbon monoxide increased each time. Table 25 also shows the

increase in the amount of carbon monoxide after the catalyst had been left under the reaction products for twelve hours.

Figure 61 shows the successive [ $^{14}\text{C}$ ]carbon monoxide adsorption isotherms described in this section.

It should be noted that practically no accumulative carbon monoxide adsorption occurred, when the only treatment between two isotherms was the evacuation of the reaction vessel (tables 26 and 27).

Table 27 also shows the accumulative adsorption of carbon monoxide on a 0.20g sample of Rh/alumina catalyst after treatment with 36.0 torr of hydrogen for 12 hours.

#### 4.5.2 Accumulative [ $^{14}\text{C}$ ]Carbon Monoxide Adsorption on a Steady State Alumina-Supported Rhodium Catalyst

A [ $^{14}\text{C}$ ]carbon monoxide adsorption isotherm was determined using a steady state 0.10g sample of Rh/alumina catalyst. The reaction vessel was evacuated and a premixed sample of allene (12.0 torr) and hydrogen (36.0 torr) was allowed into the reaction vessel. When the products of reaction were evacuated from the reaction vessel and a new [ $^{14}\text{C}$ ]carbon monoxide isotherm determined, it was observed that the amount of [ $^{14}\text{C}$ ]CO adsorbed on the surface of the catalyst had increased by approximately 35% (table 28).

Table 22

Effect of Evacuation, Allene, Allene Hydrogenation and Hydrogen upon the

Amount of [<sup>14</sup>C]Carbon Monoxide Adsorbed on 0.20g Rh/alumina Catalyst

Catalyst (0.20g Rh/alumina)	[ <sup>14</sup> C]Carbon monoxide saturation surface count rate	[ <sup>14</sup> C]Carbon monoxide removed by evacuation	[ <sup>14</sup> C]Carbon monoxide removed by 12.0 torr allene	[ <sup>14</sup> C]Carbon monoxide removed by 36.0 torr hydrogen	[ <sup>14</sup> C]Carbon monoxide removed by 48.0 torr H <sub>2</sub> /allene mixture
	(counts/ min.)	(counts/ min.) (%)	(counts/ min.) (%)	(counts/ min.) (%)	(counts/ min.) (%)
A - freshly reduced catalyst	9366	251 2.7	1265 13.9	18 0.2	25 0.3
B - freshly reduced catalyst precovered by 12.0 torr of allene	1246	34 2.7	- -	- -	zero zero
C - steady state catalyst	2500	313 12.5	zero zero	- -	46 2.1
D - steady state catalyst precovered by 12.0 torr of allene	1165	14 1.2	- -	- -	18 1.6

Table 23

Catalytic Activity for the Hydrogenation of Allene

on an Alumina-Supported Rhodium Catalyst

Catalyst Condition (0.20g Rh/alumina)	Catalytic Activity (k) (min <sup>-1</sup> )
Freshly reduced	4.29 x 10 <sup>-1</sup>
Freshly reduced, treated with carbon monoxide and evacuated	8.9 x 10 <sup>-4</sup>
Freshly reduced in presence of 1 torr of CO	zero
Freshly reduced, treated with carbon monoxide in presence of 12 torr allene and evacuated	4.6 x 10 <sup>-2</sup>
Steady state	6.0 x 10 <sup>-2</sup>
Steady state, treated with carbon monoxide and evacuated	3.1 x 10 <sup>-3</sup>
Steady state in presence of 1 torr of CO	zero
Steady state, treated with carbon monoxide in presence of 12 torr of allene and evacuated	1.2 x 10 <sup>-2</sup>

Table 24

Variation of Selectivity with Conversion for the  
Hydrogenation of 12.0 torr Allene with 36.0 torr  
Hydrogen over 0.20g Rh/alumina Catalyst Poisoned  
by Carbon Monoxide

Conversion (%)	Propane (torr)	Propylene (torr)	Selectivity (S)
13.7	0.034	1.397	0.976
19.6	0.036	1.964	0.982
40.4	0.080	3.361	0.978
74.7	0.120	6.598	0.982
84.8	0.135	7.355	0.982
90.9	0.153	7.840	0.981

Table 25

Accumulative [ $^{14}\text{C}$ ]Carbon Monoxide Adsorption  
on 0.10g Rh/alumina Catalyst

Adsorption isotherm number	Treatment of catalyst between isotherms	[ $^{14}\text{C}$ ]CO surface count rate  (counts/min)	[ $^{14}\text{C}$ ]CO adsorbed in each isotherm  (counts/min)
1	Freshly reduced	5973	5973
2	Evacuation, allene hydrogenation, evacuation	6516	543
3	Evacuation, allene hydrogenation, evacuation	7039	523
4	Evacuation, allene hydrogenation, evacuation	7200	161
5	Evacuation, allene hydrogenation, reaction product left for 12 hours in reaction vessel, evacuation	8567	1367
6	Evacuation, allene hydrogenation, evacuation, $\text{H}_2$ (36.0 torr) for 12 hours, evacuation.	10090	1523

Table 26

The Extent of Adsorption of [ $^{14}\text{C}$ ]Carbon Monoxide  
on 0.1g Rh/alumina Catalyst after Consecutive  
Adsorption Isotherms

Adsorption isotherm number	Treatment of catalyst before isotherms were carried out	[ $^{14}\text{C}$ ]CO surface count rate (counts/min)	[ $^{14}\text{C}$ ]CO adsorbed in each isotherm (counts/min)
1	Freshly reduced	5492	5492
2	Evacuation	5495	3
3	Evacuation	5562	67

Table 27

Accumulation [<sup>14</sup>C]Carbon Monoxide

Adsorption on 0.20g Rh/alumina Catalyst

Adsorption isotherm number	Treatment of catalyst before isotherms were carried out	[ <sup>14</sup> C]Carbon monoxide surface count rate (counts/min)	[ <sup>14</sup> C]CO adsorbed in each isotherm (counts/min)
1	Freshly reduced	10035	10035
2	Evacuation, H <sub>2</sub> (36.0 torr) for twelve hours, evacuation	11227	1192
3	Evacuation	11262	35

Table 28

Accumulative [<sup>14</sup>C]Carbon Monoxide Adsorption  
on a Steady State Rh/Alumina Catalyst

catalyst (0.10g Rh/alumina)	
	(counts/min)
(A) saturation surface count rate	2243
(B) surface count rate of A after evacuation for one hour	2001
(C) surface count rate of B after allene hydrogenation followed by evacuation and admission of [ <sup>14</sup> C]carbon monoxide	2832
(D) surface count rate of C after evacuation for one hour	2710

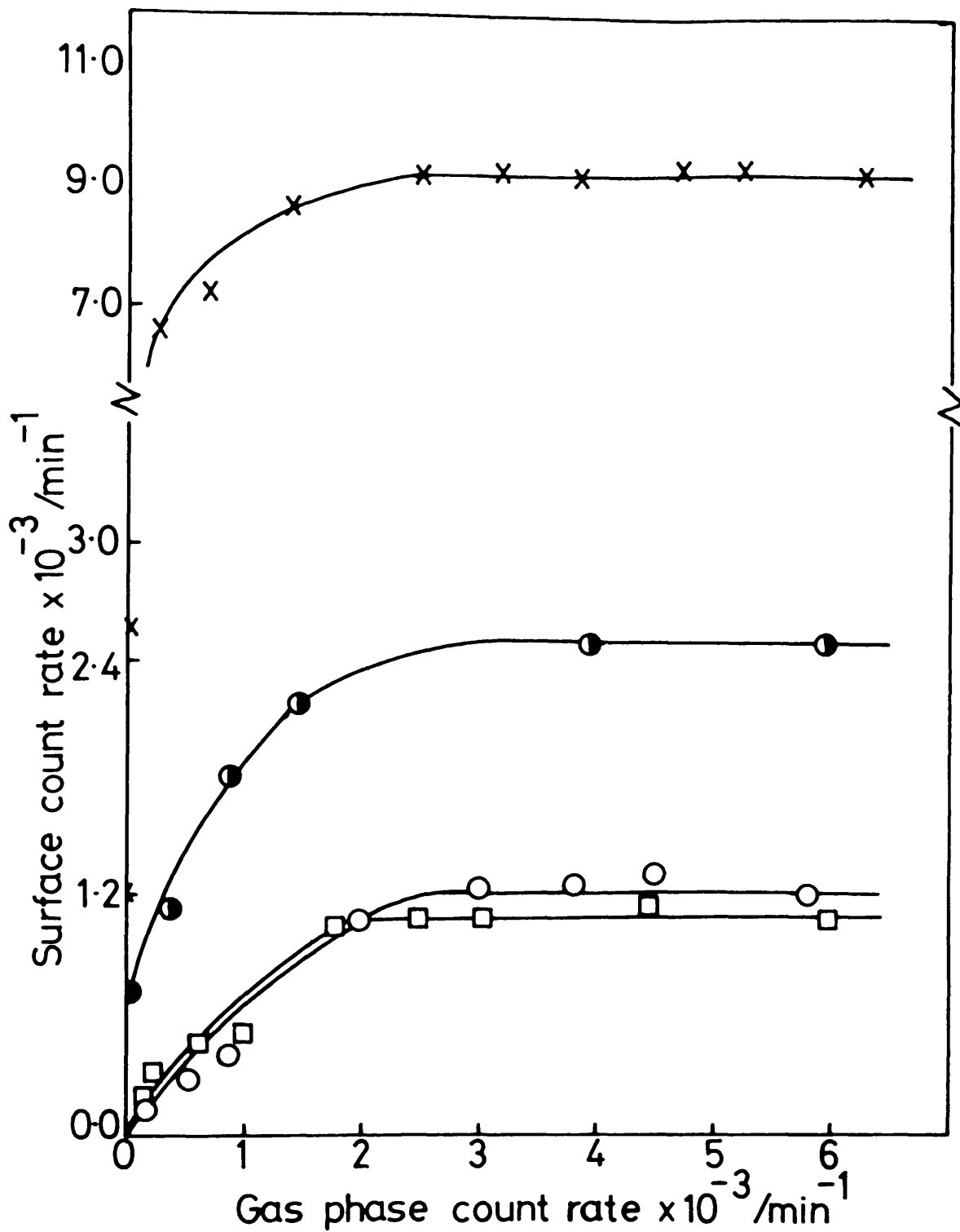


Figure 58. - Adsorption isotherms for  $[^{14}\text{C}]\text{CO}$  on freshly reduced 0.20g Rh/alumina catalyst in the absence (X) and presence (O) of 12.0 torr allene and on steady state 0.20g Rh/alumina catalyst in the absence (●) and presence (□) of 12.0 torr allene.

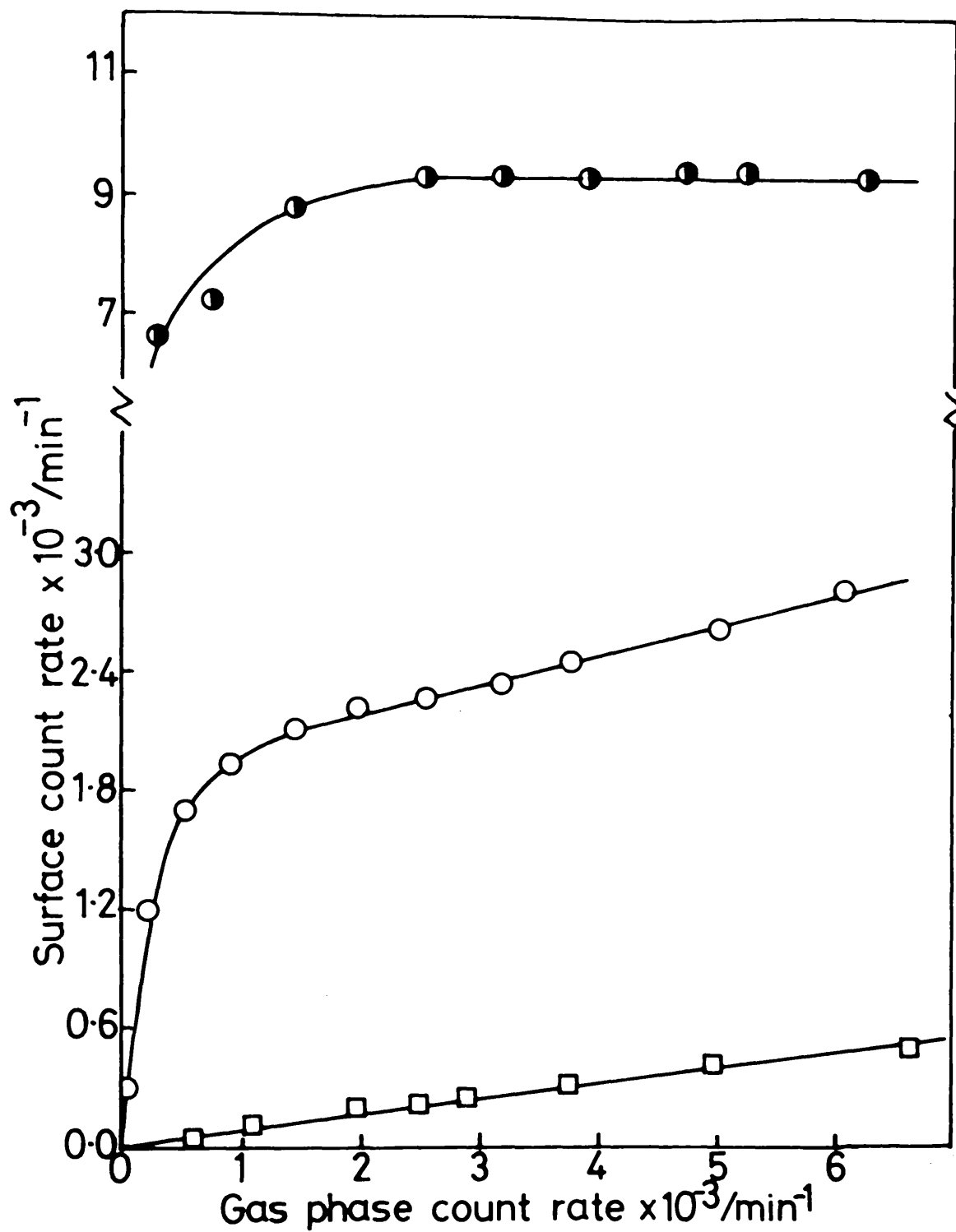


Figure 59. - Adsorption isotherms for [ $^{14}\text{C}$ ]CO (●) and [ $^{14}\text{C}$ ]C $_3$ H $_6$  in the absence (○) and presence (□) of 5.0 torr CO on freshly reduced 0.20g Rh/alumina catalyst. [ $^{14}\text{C}$ ]CO and [ $^{14}\text{C}$ ]C $_3$ H $_6$  specific activities were 0.08 mCi/mmol in each case.

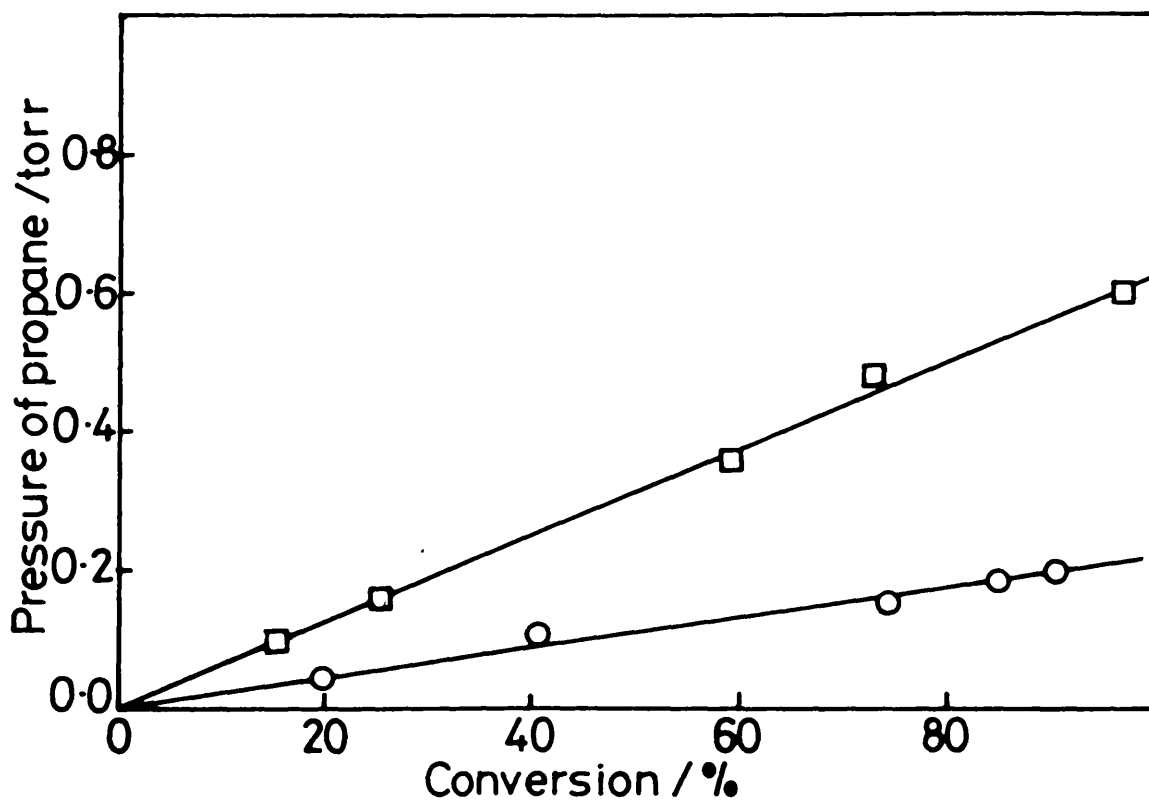


Figure 60. - Variation of the amount of propane from a CO-poisoned catalyst (○) and the amount of propane from a non-poisoned catalyst (□) with conversion for the hydrogenation of 12.0 torr of allene over Rh/alumina catalyst.  $(P_{H_2})_0 = 36.0$  torr

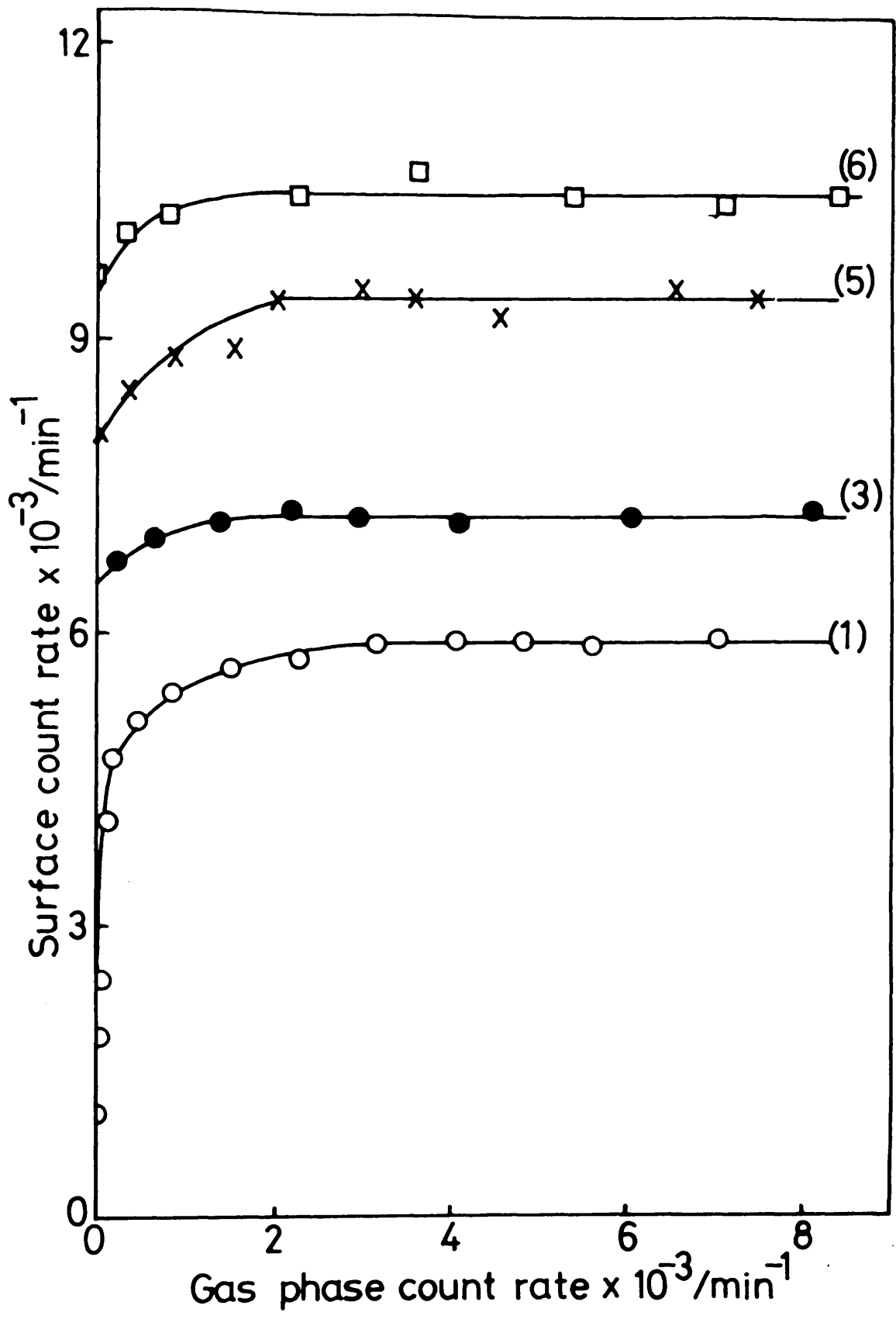


Figure 61. - Accumulative [ $^{14}\text{C}$ ]carbon monoxide adsorption isotherms on 0.10g Rh/alumina catalyst. Numbers refer to adsorption isotherm sequence (see table 25).

CHAPTER FIVE

## C H A P T E R 5

### DISCUSSION

#### 5.1 The Deactivation Phenomena

The results presented in section 4.1 provide information about the tendencies of rhodium, iridium and palladium to undergo deactivation during a series of allene hydrogenations.

Palladium and rhodium catalysts exhibited appreciable deactivation, whereas the catalytic activity of iridium remained constant during a series of allene hydrogenations at ambient temperature.

The catalytic activities were in the sequence:

Pd > Rh > Ir. This sequence was found to apply to both the initial and the steady state activities.

The deactivation phenomena can not be ascribed to poisoning of the catalyst due to external factors such as impurities in the reactants or the presence of air in the reaction vessel, since the catalytic activity did not tend to zero, but rather to a limiting value. For the purpose of this work a steady state catalyst is defined as a catalyst which has been deactivated, by successive allene hydrogenations, to this limiting value.

It was observed that, when the catalysts were treated with allene alone, no significant effect upon the progress of the deactivation occurred. The deactivation could only be

achieved by treating the catalyst with a mixture of allene and hydrogen, that is, by carrying out a series of hydrogenation reactions. These observations rule out the possibility that surface carbides or other hydrogen-deficient surface species resulting from simple dissociative adsorption of the hydrocarbon are themselves responsible for the catalyst deactivation process.

The experimental results in section 4.4 and the discussion in section 5.4 show that there are sites, located on the metal, which are left vacant following the adsorption of allene and which may be responsible for hydrogen adsorption. It is significant that the amounts of carbon monoxide adsorbed on freshly reduced and steady state catalysts in the presence of gas phase allene are experimentally identical. Thus, assuming the validity of identity of the carbon monoxide and hydrogen adsorption sites on each catalyst under hydrogenation conditions, the deactivation phenomena cannot be ascribed to blocking of the hydrogen adsorption sites located on the metal.

The deactivation phenomena must result from a reduction in the number of active sites on the surface of the catalyst and the "steady state" activity corresponds to the establishment of a "steady state" concentration of the active sites.

Thomson and Webb (79) recently proposed a mechanism for the catalytic hydrogenation of unsaturated hydrocarbons in which they suggest that the hydrogenation occurs through a hydrogen transfer mechanism between an associatively

adsorbed hydrocarbon and a dissociatively adsorbed hydrocarbon residue, which may be represented as  $C_xH_y$ . The observation that the deactivation required the presence of hydrogen suggests that a surface hydropolymerisation reaction is the most likely cause of deactivation. By considering that, during the allene hydrogenation reaction, a surface hydropolymerisation reaction occurs, a decrease in the concentration of hydrogen-transfer species, for example, an adsorbed  $C_3H_x$  species can be envisaged. The surface hydropolymerisation could be considered to involve this  $C_3H_x$  species, thereby decreasing its concentration. Thus, the steady state activity would correspond to the establishment of a steady state concentration of the  $C_3H_x$  hydrogen-transfer species. The detailed evidence for such a  $C_3H_x$  species will be discussed in section 5.2.

Similar studies (136) of the deactivation phenomena over silica-supported rhodium, iridium and palladium during acetylene hydrogenation have also concluded that the deactivation of the catalysts is due to formation of surface polymers.

The pressure-time curves obtained for allene hydrogenation over alumina-supported rhodium and iridium catalysts exhibited two distinct stages in the reaction, with an acceleration point ( $-\Delta P_a$ ), corresponding to the start of the second stage. Similar types of pressure-time curves have been reported for the acetylene hydrogenation

over alumina-supported platinum (126) and for acetylene hydrogenation over silica-supported rhodium, iridium and palladium and alumina-supported palladium (136). The pressure-time curves obtained during a series of allene hydrogenations over the freshly reduced alumina-supported palladium catalysts also featured an acceleration point during the first few reactions. However, the acceleration point gradually disappeared during the deactivation process. The catalyst in the steady state did not show any acceleration point.

During the first stage of the allene hydrogenation over alumina-supported rhodium, iridium and palladium catalysts the pressure-time curves were always accurately first order in total pressure (figures 17, 26, 31).

It was observed from the pressure fall against time curves that the second stage of reaction also underwent a deactivation process. Figure 62 shows the extension of the deactivation process for the first and second stage of a series of allene hydrogenations over a 0.10g sample of alumina-supported rhodium catalyst. The rate of reaction obtained from the linear section of the second stage of reaction, decreased with successive reactions until a constant steady value was eventually obtained. It can be concluded that the formation of polymeric species during the allene hydrogenations affected both the first and second stages of the reaction.

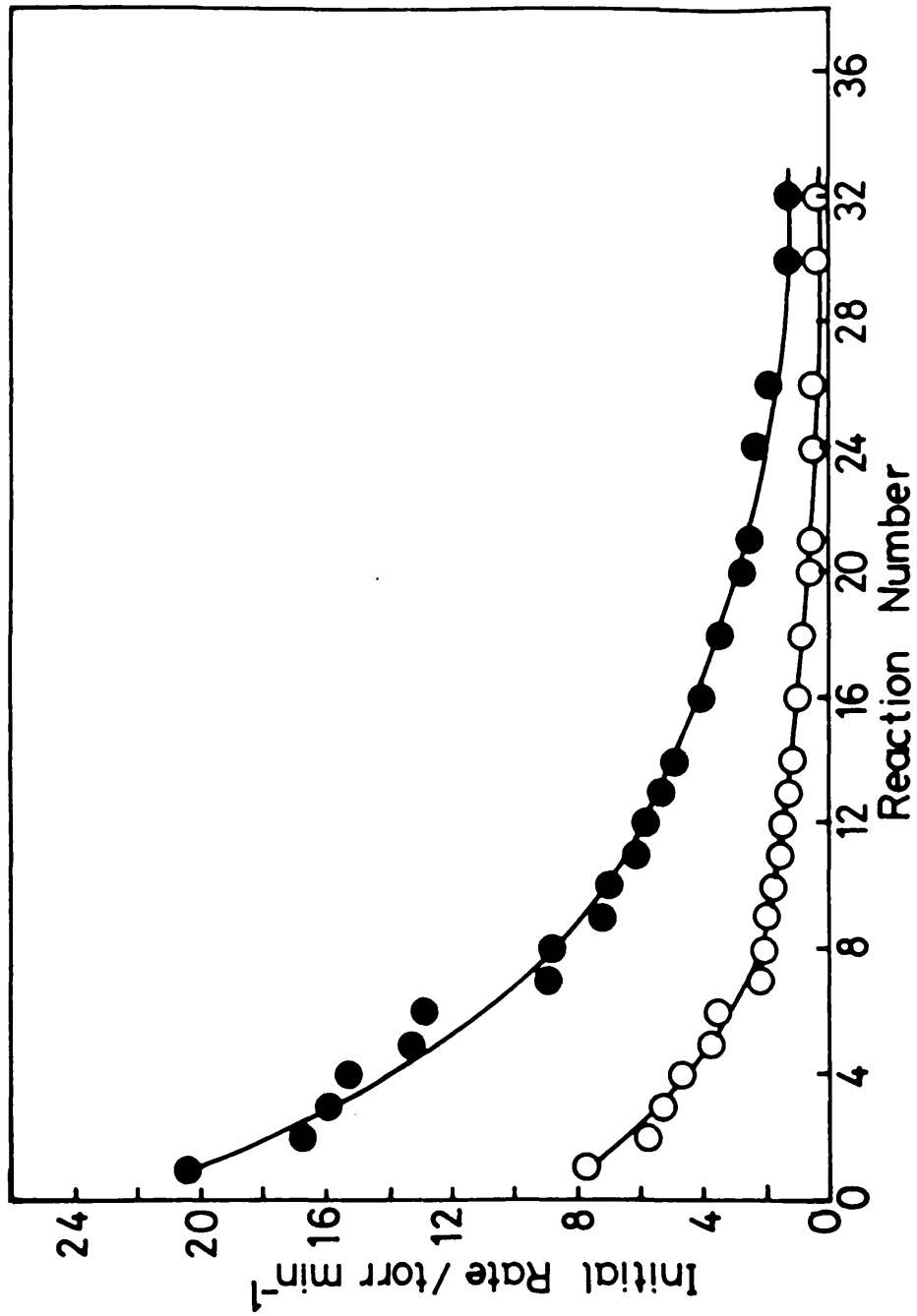
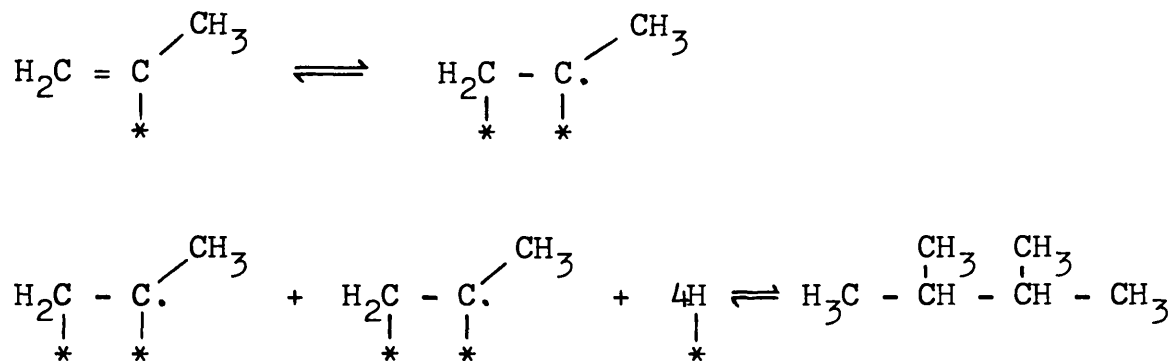


Figure 62. - Deactivation process for the first (●) and the second (○) stage of reaction over a 0.10g sample of rhodium/alumina catalyst.  
 $(P_{C_3H_4})_0 = 12.0$  torr       $(P_{H_2})_0 = 36.0$  torr

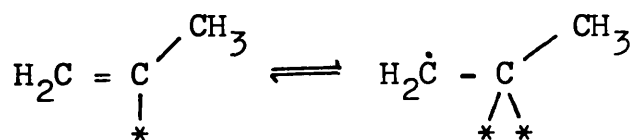
Analysis of the reaction products during the hydrogenation of allene over alumina-supported rhodium and palladium catalysts showed that during the first stage of reaction the main product was propylene, with small amounts of propane. After the acceleration point ( $-\Delta P_a$ ) the main process occurring was the further hydrogenation of propylene to propane (figures 19, 33). Analysis of the reaction products during the hydrogenation of allene over alumina-supported iridium catalyst showed a slightly higher production of propane than propylene during the first stage of reaction. Again, after the acceleration point the main process occurring was the further hydrogenation of propylene to propane (figure 28). With all three catalysts (iridium, rhodium and palladium) traces of a dimer of allene were detected by gas chromatography during the analysis of the reaction products. The formation of this dimer of allene was only detected when the pressure fall in the reaction was  $\geq -\Delta P_a$ . The identity of the dimer was not accurately determined. From the chromatographic analysis it was concluded that the dimer was a  $C_6$ -branched chain alkane. Unfortunately, the chromatographic column used did not separate  $C_6$ -branched saturated hydrocarbons and the product identification was not accurately established.

The mechanism of hydropolymerisation of allene has been explained by considering that the adsorbed propenyl half-hydrogenated species may exist as a free radical form (138).

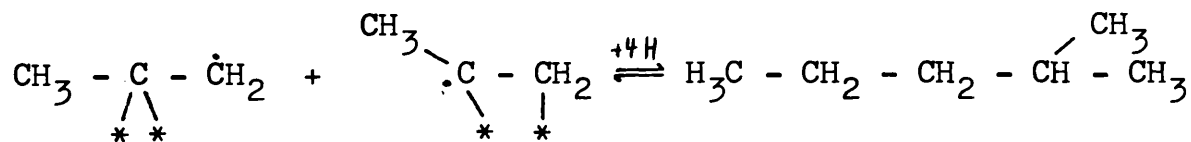
A possible mechanism of the formation of the C<sub>6</sub>-branched saturated hydrocarbons is presented below.



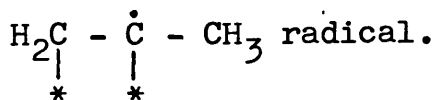
The formation of 1-methylpentane is also possible through the formation of a free radical as shown below.



and



As n-hexane was not observed as a product of allene hydrogenation the existence of the  $\text{H}_2\dot{\text{C}} - \text{C} \begin{array}{l} \diagdown * * \\ - \text{CH}_3 \end{array}$  free radical is considered to be less probable than the



The hydrogenation of allene is clearly a selective reaction, since propylene and propane were both produced. The variation of the selectivity during the deactivation process and the course of reaction were investigated for allene hydrogenation over alumina-supported iridium, rhodium and palladium catalysts. While the selectivity increased slightly during the deactivation process for rhodium (figure 35), it decreased during a series of hydrogenation reactions in the case of palladium (figure 21). The selectivity was independent of reaction number for the iridium catalyst. The selectivity was independent of pressure fall for rhodium and palladium catalysts and decreased slightly with the progress of the reaction in the case of iridium (figures 20, 29, 34).

The breakdown of selectivity occurs when propylene hydrogenation becomes important and this occurred at the onset of the second stage of reaction for all three catalysts (rhodium, iridium and palladium). Because of the very high activity encountered in the second stage it was impossible to locate the exact point at which the highly selective conditions broke down, but the amount of allene present was always very low.

Factors governing the relative yields of propylene and propane are both thermodynamic and mechanistic in origin (23). Results presented in sections 4.2, 4.3 and 4.4 permit and insight into the relative importance of the

two factors to selective behaviour of the catalyst during allene hydrogenation and are discussed in detail in the ensuing sections.

## 5.2 Behaviour of [<sup>14</sup>C]Propylene Adsorbed on Supported-Rhodium Catalysts

The results in section 4.2 show that, whereas the uptake of carbon monoxide ceased after reaching a "plateau" value, propylene was adsorbed by the catalyst over the entire pressure range used. Thus, propylene adsorption showed two distinct regions; a steep primary region followed by a linear secondary region.

The results presented in figures 44 and 46 show that the extent of adsorption of propylene is almost the same on both freshly reduced alumina- and silica-supported rhodium catalysts. The adsorbed [<sup>14</sup>C]propylene showed similar behaviour on both catalysts when the catalysts were evacuated and treated with non-radioactive propylene and hydrogen (figures 45 and 47). This similar behaviour suggests that either the support does not play an important role in the adsorption phenomena or alumina and silica have a similar role.

The number of propylene molecules adsorbed during the build-up of the primary region of the [<sup>14</sup>C]propylene adsorption isotherm on a 0.20g sample of the alumina-supported rhodium catalyst is  $0.51 \times 10^{19}$  molecules. Thus,

the number of propylene molecules adsorbed per rhodium atom in the catalyst is approximately one propylene molecule per nine rhodium atoms in the catalyst. This value is very low when compared with the number of adsorbed molecules of carbon monoxide per rhodium atom in the catalyst (see section 5.4). This low value may be explained by the fact that the adsorption is limited by the bulk of the adsorbed propylene molecules.

The analysis of the gas phase hydrocarbon in contact with the surface during the build-up of the adsorption isotherm on a freshly reduced catalyst showed that the species retained by the catalyst during the primary adsorption of propylene is a dissociatively adsorbed species. The number of propane molecules formed during the build-up of the primary region of the [ $^{14}\text{C}$ ]propylene adsorption isotherm on a 0.20g sample of the alumina-supported rhodium catalyst is  $0.14 \times 10^{19}$  molecules. From this value the "average composition" of the adsorbed species in the primary region was calculated as being  $\text{C}_3\text{H}_{5.4}$ . It was assumed that the amount of catalyst hydrogen available for hydrogenation is negligible, that is, that the vacuum/heat treatment of the catalyst was effective in removing most of the hydrogen adsorbed on the metal following the activation procedure. It has been reported previously (53) that the amount of catalyst hydrogen available for hydrogenation is negligible.

Analysis of the gas phase during the build-up of

the adsorption isotherm on a steady state catalyst showed that there was no formation of propane. This is in agreement with the observation that no primary region, in which the species are dissociatively adsorbed, was formed during the build-up of the adsorption isotherm on a steady state catalyst.

The [ $^{14}\text{C}$ ]propylene adsorption isotherm obtained with carbon monoxide precovered freshly reduced catalyst showed (figure 59) that, although carbon monoxide preadsorption presented the adsorption of primary adsorbed propylene on the metal, the extent of the secondary adsorption was only slightly affected. If it is assumed that the carbon monoxide is specifically adsorbed on the metal, the above observations suggest that the [ $^{14}\text{C}$ ]propylene primary adsorption occurs directly on the exposed metal and the turning point in the propylene adsorption isotherm corresponds to monolayer coverage of the metal with hydrocarbon.

The experimental results presented in section 4.2.3.3 show that the effect of deactivation on the [ $^{14}\text{C}$ ]propylene adsorption isotherm was to progressively reduce the fraction of the primary adsorbed propylene which can be removed by hydrogen at ambient temperature. Thus, in the steady state none of the primary adsorbed propylene can be hydrogenated from the surface. With the catalyst in its steady state the [ $^{14}\text{C}$ ]propylene isotherm did not show a primary region,

but the secondary region remained almost the same. These results indicate that the hydrogenation of propylene is associated with the secondary region. It should be noted that, although the hydrogenation of propylene is associated with the secondary region, the plot of the turning point of the primary region, at different stages during the deactivation, against the catalytic activity at the same points on the deactivation curve showed a linear relationship (figure 50).

The nature of the secondary adsorbed species was examined indirectly by analysing the gas phase during the build-up of the adsorption isotherm. The secondary adsorbed species may be considered to be associatively bonded, since no propane was detected in the gas phase during the build-up of the secondary region of the isotherm either on a freshly reduced or on a steady state catalyst. Evacuation of the reaction vessel removed ~30% of the secondary adsorbed species on a steady state catalyst. The remaining adsorbed species were irreversibly bonded to the catalyst as molecular exchange with gaseous propylene did not occur (table 15).

Hydrogen had a significant effect on the removal of species adsorbed on the catalyst. The results (section 4.2) showed that hydrogen removed species from both the primary and secondary regions, although a fraction of the adsorbed [<sup>14</sup>C]propylene was always retained by the catalyst as a

strongly adsorbed species.

As the actual rate of hydrogenation varies with the amount of primary adsorbed propylene the participation of this species in the hydrogenation process must be considered. The mechanism for catalytic hydrogenation of unsaturated hydrocarbons on metals, proposed by Thomson and Webb (79), is based on a hydrogen transfer between an adsorbed hydrogen-deficient hydrocarbon species and an associatively adsorbed alkene or alkyne, rather than on the direct addition of hydrogen to an associatively adsorbed hydrocarbon.

Previous results (136) from [ $^{14}\text{C}$ ]tracer studies of deactivation phenomena during a series of acetylene hydrogenations showed that as the catalyst became progressively deactivated the fraction of the primary adsorbed acetylene and primary adsorbed ethylene became less. It was suggested that this dissociatively adsorbed species acted as the hydrogen transfer medium as proposed by Thomson and Webb.

The similarity between the results observed previously with acetylene and the results of the present work lead to the suggestion that the hydrogenation of allene is also associated with the secondary adsorbed species, which are associatively adsorbed as an overlayer on dissociatively adsorbed hydrocarbon. Unfortunately, the allene adsorption isotherms could not be determined and the above suggestion is based only upon the similarities between the

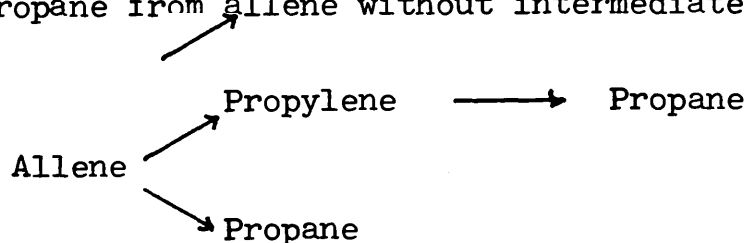
[<sup>14</sup>C]propylene adsorption studies during allene hydrogenation and previous studies of [<sup>14</sup>C]ethylene adsorption during acetylene hydrogenation (136).

The process of deactivation, in which the amounts of the propylene adsorbed on the primary region progressively decreases, may also be explained in terms of the hydrogen-transfer mechanism by considering that in the deactivation process the concentration of M - C<sub>3</sub>H<sub>x</sub> active sites progressively diminishes, either by their participation in the hydropolymerisation reaction or from their further dissociation to more hydrogen deficient hydrocarbonaceous species.

### 5.3 Allene Hydrogenation in the Presence of [ $^{14}\text{C}$ ]Propylene

It has been generally accepted that in the catalytic hydrogenation of alkynes and other di-unsaturated hydrocarbons the selectivity is dependent upon a thermodynamic and a mechanistic factor (138). The thermodynamic factor is based upon the assumption that the same surface sites are responsible for both alkene and alkyne adsorption. Thus it takes into account the difference in strength of adsorption between the alkene and the di-unsaturated hydrocarbon. The mechanistic factor takes into account the parallel reactions of alkene and di-unsaturated hydrocarbon to form the respective alkane. That is, it depends upon the specific properties of the catalyst.

In the hydrogenation of allene two possible types of selectivity may occur simultaneously. The first type is the formation of propylene in the gas phase which then readsorbs to form propane. The second type arises with the production of propane from allene without intermediate desorption.



When [ $^{12}\text{C}$ ]allene hydrogenation was carried out in the presence of [ $^{14}\text{C}$ ]propylene the amount of [ $^{14}\text{C}$ ]propane produced during the first stage of reaction constituted only a small fraction of the total propane yield. Figure 54

shows that the yield of [ $^{14}\text{C}$ ]propane increased with conversion during the hydrogenation of allene in presence of [ $^{14}\text{C}$ ]propylene. However, the yield of [ $^{14}\text{C}$ ]propane remained a constant fraction of the total propane yield throughout the first stage of reaction (table 18).

It was also observed that the yield of [ $^{14}\text{C}$ ]propane was directly proportional to the initial pressure of added [ $^{14}\text{C}$ ]propylene.

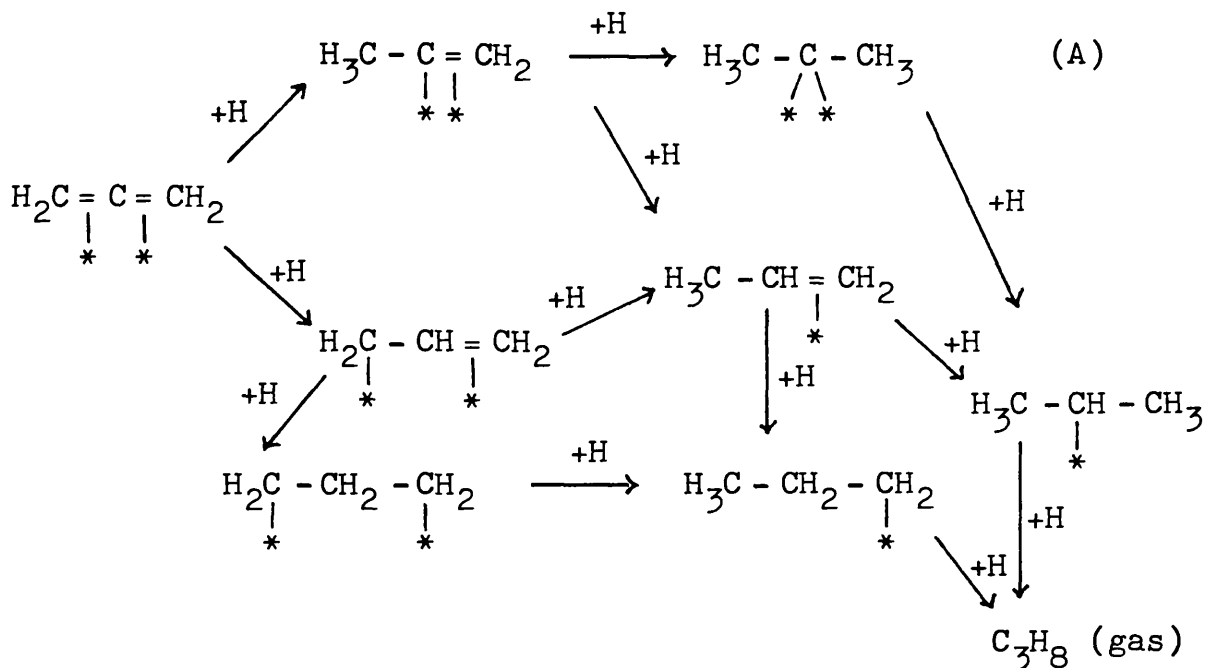
The observation that the yield of [ $^{14}\text{C}$ ]propane remained a constant fraction of the total propane yield throughout the first stage of the allene hydrogenation, and that the amounts of [ $^{14}\text{C}$ ]propane formed were directly proportional to the amount of added [ $^{14}\text{C}$ ]propylene lead to the conclusion, that the hydrogenation of [ $^{14}\text{C}$ ]propylene proceeds independently of the amount of allene in the gas phase.

The yields of [ $^{14}\text{C}$ ]propane together with the amounts of radioactive and non-radioactive propylene were used to calculate the yields of [ $^{12}\text{C}$ ]propane arising from the [ $^{14}\text{C}$ ]propylene which had undergone a desorption - readsorption cycle. It was found that the amounts of [ $^{12}\text{C}$ ]propane arising from the gas phase [ $^{12}\text{C}$ ]propylene was small when compared with the total [ $^{12}\text{C}$ ]propane yield formed during the first stage of reaction (tables 17, 19 and 21). Thus it can be concluded that the major route to the production of propane must be by a direct route from allene without intermediate desorption of propylene.

Results from the hydrogenation of allene over a carbon monoxide-poisoned rhodium/alumina catalyst showed that the hydrogenation of propylene was less affected than the hydrogenation of allene. If the formation of propane occurs only through the hydrogenation of propylene from the gas phase one would expect that the selectivity would decrease markedly over the carbon monoxide-poisoned catalyst rather than increase, as observed experimentally. The carbon monoxide induced increase in selectivity is consistent with a mechanism in which propane is produced by a direct route from allene, not involving propylene as an intermediate. A similar conclusion is reached for palladium/alumina catalysts.

During a series of allene hydrogenations over these catalysts, the acceleration point gradually disappeared during the deactivation process. This shows that the deactivation in the second stage of reaction, in which the hydrogenation of propylene is the main process, is more deactivated than the first stage. If the formation of propane occurs only through the hydrogenation of propylene from the gas phase one would expect that the selectivity would increase with reaction number, rather than decrease as observed experimentally. This, again, confirms the production of propane by a direct route from allene.

Possible routes to the direct formation of propane from allene, without intermediate desorption can be envisaged as shown in the mechanism below:



Previous results (144) from the study of allene deuteration over alumina-supported palladium led to the conclusion that the species (A) in the above reaction scheme is an important intermediate in propane formation and that a specific region of the surface may be involved in production of propane. An infrared study of allene hydrogenation (115) over silica-supported Group VIII transition metals suggests that in the initial stages of the reaction the formation of propane is via direct hydrogenation of allene without involving the desorption - readsorption of propylene.

From the amounts of [ $^{12}\text{C}$ ]propane produced direct from allene it is possible to calculate values of the "inherent" selectivity ( $S^*$ ) defined as

$$S^* = \frac{P_{\text{C}_3\text{H}_6}}{P_{\text{C}_3\text{H}_6} + P_{\text{C}_3\text{H}_8}^*}$$

where  $P_{C_3H_8}^*$  is the pressure of propane produced directly from allene. It is called 'inherent' selectivity because it depends upon the capacity, or otherwise, of the catalyst to produce propane directly from allene and it does not involve the amount of propane produced by further hydrogenation of propylene from the gas phase. It can be seen in tables 17, 19 and 21 that the inherent selectivity is independent of the progress of the reaction up to the acceleration point.

Propylene adsorption on an allene precovered catalyst, produced no propylene primary adsorption and a diminished propylene secondary adsorption. The presence of allene reduced the adsorptive capacity of the surface for propylene by ~40%, although the admission of allene to [ $^{14}C$ ]propylene precovered surface resulted in only a small decrease in the surface count rate (table 15). These results together with the results already presented in this section lead to the conclusion that propylene and allene hydrogenation occur on different sites on the surface of the catalyst.

Three different types of sites may be recognised. Type I sites are active for the direct conversion of allene to propane; type II sites are active for the hydrogenation of allene to propylene and for the hydrogenation of propylene to propane. Type III sites are active for propylene hydrogenation, but inactive for allene hydrogenation. It is possible that, as was found to be the case in the

adsorption and hydrogenation of acetylene and ethylene (47), that the type II sites may be comprised of two sets of sites, one (IIA) of which is only active for allene adsorption and hydrogenation, the other (IIB) being active in both allene and propylene adsorption and hydrogenation. However, in the absence of data relating to the adsorption of allene, in the presence and absence of propylene, no direct evidence for the existence or otherwise of these type IIA sites has been obtained.

According to this model, the observed selectivity will depend upon the relative concentration of the different types of surface sites rather than upon the different strengths of adsorption of allene and propylene. The faster rate of propylene hydrogenation when in the absence of allene, as compared with the rate when allene is present may be a reflection of a variation in availability of surface hydrogen dependent upon the surface concentrations of allene and propylene. An increase in the hydrogen availability once the allene has reacted would increase the rate of propylene reaction. Such a variation in hydrogen availability has been suggested to be important during the hydrogenation of acetylene over silica-supported iridium, palladium and rhodium catalysts (47).

#### 5.4 Carbon Monoxide Adsorption and its Effects upon Allene Hydrogenation

The adsorption of [ $^{14}\text{C}$ ]carbon monoxide on the freshly reduced alumina-supported catalysts followed the behaviour which is expected for Langmuir-type adsorption. Such behaviour has been observed on many occasions either using volumetric methods (160) or radiotracer techniques (58). It is a typical monolayer adsorption. No secondary adsorption is observed (figure 58).

The number of carbon monoxide molecules adsorbed during the build-up of the carbon monoxide adsorption isotherm on a 0.20g sample of the alumina-supported rhodium catalyst is  $2.63 \times 10^{19}$  molecules. Thus the number of carbon monoxide molecules adsorbed per rhodium atom in the total catalyst is 0.45. This value is experimentally very close to the value of 0.44 quoted by Yates et al. (153) using rhodium/alumina and other workers (167) using a rhodium/silica catalyst.

The [ $^{14}\text{C}$ ]carbon monoxide adsorption isotherm using a freshly reduced catalyst in the presence of 12.0 torr allene showed a similar shape to that obtained on the "clean" surface; the amount of [ $^{14}\text{C}$ ]carbon monoxide adsorbed on the surface of the catalyst was, however, considerably reduced, corresponding to only 13.3% of the amount adsorbed in absence of allene.

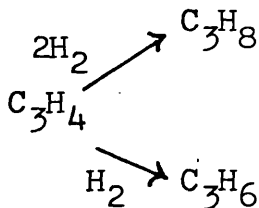
It has been shown (139) that for a random two site adsorption of allene the number of molecules adsorbed per 100 sites is limited by the bulk of the adsorbed molecules, although the proportion of truly accessible metal atoms left is quite small. Thus 100 atoms in a (110) face can adsorb 34 allene molecules, but of the 32 metal atoms not bonded to carbon only 8 are accessible to other gases such as hydrogen. The small percentage (13.3%) for the adsorption of carbon monoxide on an allene precovered catalyst surface is in reasonable agreement with the fact that, for geometrical reasons, only a fraction of the atoms left vacant by the adsorbed allene is accessible to carbon monoxide. This value compares with a value of approximately 7% for an acetylene covered rhodium-silica surface (47).

The [ $^{14}\text{C}$ ]carbon monoxide adsorption isotherm on a rhodium/alumina catalyst in its steady state, either in absence or presence of allene, showed a similar shape to that obtained on the "clean" surface, but the amount of carbon monoxide adsorbed was considerably reduced (table 22). A freshly reduced and a steady state catalyst, when in the presence of 12.0 torr of allene, adsorbs the same amount of carbon monoxide. Thus, assuming the validity of identity of the carbon monoxide and hydrogen adsorption sites on each catalyst under hydrogenation conditions, the deactivation phenomena cannot be ascribed to blocking of the hydrogen adsorption sites located on the metal.

Results presented in section 4.4 show that although a freshly reduced rhodium catalyst is completely inactive for allene hydrogenation when gas phase carbon monoxide is present, it is partially active once the carbon monoxide has been evacuated from the reaction vessel (table 23). While, at first sight, this appears to be rather surprising, since carbon monoxide adsorbs on the metal surface and only a small amount is removed by evacuation, it should be noted that exposure to allene resulted in the displacement of 13.9% of the adsorbed carbon monoxide.

The analyses of the products of allene hydrogenation over a rhodium/alumina catalyst poisoned by carbon monoxide showed that the adsorbed carbon monoxide affected the selectivity. The amount of propane produced was considerably less than that obtained with a non-poisoned catalyst (figure 60). The adsorbed carbon monoxide also affected the rate of reaction in the first stage of reaction more than the rate in the second stage of reaction.

It was concluded in section 5.3 that the formation of propylene and propane from allene occurred by independent routes:



It is apparent that the hydrogen pressure dependencies and

hence the surface hydrogen concentrations, will be different for the two routes. The direct route will be more dependent upon the surface coverage of hydrogen than that leading to formation of propylene and, in consequence, will show a greater effect from any variation in  $\theta_H$ , the surface coverage of hydrogen.

If it is considered that the effect of the carbon monoxide is to poison sites on the metal responsible for the adsorption-activation of hydrogen, then the rate of formation of propane will be more strongly influenced by the presence of adsorbed carbon monoxide than the rate of formation of propylene. Thus, it would be expected that the selectivity would be increased by the presence of adsorbed carbon monoxide in agreement with the experimental observations.

#### 5.5 Accumulative Adsorption of Carbon Monoxide on Alumina-Supported Rhodium

From the data obtained from the chemisorption of carbon monoxide on freshly reduced alumina-supported rhodium the number of molecules of carbon monoxide adsorbed per rhodium atom present in the catalyst was found to be 0.45. This value is experimentally the same as that presented by Yates et al.(153) and it is rather close to the H/M ratio, also reported by Yates et al.(153), for the same catalyst. Therefore it can be concluded, by comparison with the CO/M ratio and H/M ratio, and from the shape of the adsorption

isotherm that a monolayer of chemisorbed carbon monoxide was formed.

A striking feature of the results presented in this work is that treatment of a carbon monoxide-precovered catalyst with a mixture of hydrogen and allene or with hydrogen alone promotes further uptake of carbon monoxide. The amount of [ $^{14}\text{C}$ ]carbon monoxide adsorbed on the surface of a 0.10g sample of rhodium/alumina catalyst increased from 5973 cpm, on a freshly reduced catalyst, to 10090 cpm after various treatments with hydrogen and allene (table 25).

Enhancement of the amount of carbon monoxide adsorbed on the catalyst by coadsorption with hydrogen on polycrystalline rhodium has been reported (170), although Solymosi (171) did not observe any increase in the uptake of carbon monoxide during the coadsorption of hydrogen and carbon monoxide on a rhodium/alumina catalyst. Clearly enhancement of the amount of carbon monoxide adsorbed on the catalyst was observed in the present work. The location and nature of this enhanced uptake of carbon monoxide however, is not readily apparent.

Further reduction of the catalyst by hydrogen at room temperature could result in the creation of new surface sites and hence could increase the uptake of carbon monoxide. But the catalyst was reduced under flowing hydrogen for several hours at higher temperatures and any increase in this reduction time did not produce any increase in the uptake of carbon monoxide.

Carbon monoxide has been known to chemisorb in three forms on rhodium/alumina catalysts. These are the bridged, linear and twin types. If it is assumed that the formation of the twin type species  $[\text{Rh}(\text{CO})_2]$  is more favourable in presence of hydrogen than in its absence, or that hydrogen induces a change in the structure of the adsorbed carbon monoxide from bridged to linear form, enhancement of the carbon monoxide adsorption in the presence of hydrogen would be expected. Infrared studies of adsorbed carbon monoxide on rhodium/alumina catalysts, which had been first exposed to hydrogen, then evacuated at 300K, showed that the bands due to the twin type species were weaker than on clean catalysts (172). Therefore, it seems that adsorbed hydrogen hinders the formation of the twin type species. Comparison between infrared spectra obtained from adsorbed carbon monoxide on rhodium/alumina and from coadsorption of hydrogen and carbon monoxide showed that no significant change occurred in the appearance of the bridged carbon monoxide (171). Thus it is unlikely that a change in the structure of the adsorbed carbon monoxide induced by the presence of hydrogen was the cause of the enhanced carbon monoxide adsorption observed in this work.

A further possibility which must be considered is that the hydrogen could react with adsorbed carbon monoxide or with the products of the dissociation of carbon monoxide. This surface interaction between hydrogen and adsorbed carbon monoxide could produce a surface complex which would be

responsible for the increased carbon monoxide uptake by creating fresh surface sites.



The fresh surface sites could be created either by the formation of the surface CHO complex or by formation of a surface polymer which could effectively remove carbon monoxide from the surface.



The reaction of adsorbed hydrogen with adsorbed carbon monoxide appears to be the most probable reason for the increased carbon monoxide uptake. However, further study of this phenomenon is necessary before a complete account of the processes involved can be advanced.

## REFERENCES

References

1. Davy, H., Phil. Trans. R. Soc., 107, 77 (1817).
2. Davy, E., Phil. Trans. R. Soc., 110, 108 (1820).
3. Dulong, P.L., and Thenard, L.E., Annls. Chim. Phys., 23, 440 (1823).
4. Doebereiner, J.W., Annls. Chim. Phys., 24, 91 (1823).
5. Henry, W., Phil. Mag., 65, 269 (1825).
6. Berzelius, J.J., Annls. Chim. Phys., 61, 146 (1836).
7. Faraday, M., Phil. Trans. R. Soc., 124, 55 (1834).
8. Langmuir, I., J. Am. Chem. Soc., 38, 2221 (1916).
9. Langmuir, I., J. Am. Chem. Soc., 40, 1361 (1918).
10. Hinshelwood, C.N., Annual Reports Chemical Society, 24, 314 (1927).
11. Eley, D.D., and Rideal, E.K., Nature, Lond., 146, 401 (1940).
12. Eley, D.D., and Rideal, E.K., Proc. R. Soc., A178, 429 (1941).
13. Taylor, H.S., Proc. R. Soc., A108, 105 (1925).
14. Taylor, H.S., J. Am. Chem. Soc., 53, 578 (1931).
15. de Boer, J.H., Adv. Catal., 9, 472 (1957).
16. Thomas, I.M., J. Chem. Educ., 38, 138 (1961).
17. Brunauer, S., Emmett, P.H., and Teller, E., J. Am. Chem. Soc., 60, 309 (1938).
18. Taylor, H.S., and Williamson, A.T., J. Am. Chem. Soc., 53, 2168 (1931).

19. Trapnell, B.M.W., Proc. R. Soc., A206, 39 (1951).
20. Beeck, O., Disc. Faraday Soc., 8, 118 (1950).
21. de Boer, J.H., in 'Chemisorption', ed. W.E. Garner, Butterworths, London (1957) p.27.
22. Gundry, P.M., and Tompkins, F.C., Q. Rev., XIV, 257 (1960).
23. Bond, G.C., in 'Catalysis by Metals', Academic Press, London (1962), p.86.
24. Halsey, G., and Taylor, H.S., J. Chem. Phys., 15, 624 (1947).
25. Slygin, A., and Frumkin, A.N., Acta Phys.-Chim., URSS, 3, 791 (1935).
26. Temkin, M.I., and Pyzhev, V., Acta Phys.-Chim., URSS, 12, 327 (1940).
27. Brunauer, S., Love, K.S., and Keenan, R.G., J. Am. Chem. Soc., 64, 751 (1942).
28. Thomas, J.M., and Thomas, W.J., in 'Introduction to the Principles of Heterogeneous Catalysis', Academic Press, London (1967) p.33.
29. Brunauer, S., Deming, L.S., Deming, W.E., and Teller, E., J. Am. Chem. Soc., 62, 1723 (1940).
30. Hill, T.L., Adv. Catal., 4, 211 (1952).
31. Everett, D.H., Proc. Chem. Soc., 38 (1957).
32. Sinfelt, J.H., and Yates, D.J.C., J. Catal., 10, 362 (1968).
33. Hausen, A., and Gruber, H.L., J. Catal., 20, 97 (1971).

34. Benson, J.E., and Boudart, M., J. Catal., 4, 704 (1965).
35. Dorling, T.A., Burlace, C.J., and Moss, R.L., J. Catal., 12, 207 (1968).
36. Paneth, F.A., Z. Elektrochem., 18, 113 (1922).
37. Emmett, P.H., Catal. Rev., 7, 1 (1973).
38. Trimm, D.L., Chem. Ind. (London), p.534 (1967).
39. Campbell, K.C., and Thomson, S.J., Prog. Surf. Memb. Sci., 9, 163 (1975).
40. Aylmore, D.W., and Jepson, W.B., J. Sci. Instr., 38, 156 (1961).
41. Chènebault, P., and Schürenkämper, A., J. Phys. Chem., 69, 2300 (1965).
42. Clarke, J.T., J. Phys. Chem., 68, 884 (1964).
43. Crowell, A.D., and Farnsworth, H.E., J. Chem. Phys., 22, 1607 (1954).
44. Hughes, T.R., Houston, R.J., and Sieg, R.P., Ind. Eng. Chem. Process Design Dev., 1, 96 (1962).
45. Campbell, K.C., and Thomson, S.J., Trans. Faraday Soc., 55, 985 (1959).
46. Webb, G., and MacNabb, J.J., J. Catal., 26, 226 (1972).
47. Al-Ammar, A.S., and Webb, G., J.C.S. Faraday I, 75, 1900 (1979).
48. Roginskii, S.Z., and Keier, N.P., Dokl. Akad. Nauk., SSSR, 57, 157 (1947).
49. Roginskii, S.Z., and Keier, N.P., Izv. Akad. Nauk., SSSR, Otd. Khim. Nauk, p.27 (1950).

50. Schuit, G.C.A., and van Reijen, L.L., Adv. Catal., 10, 242 (1958).
51. Gundry, P.M., in 'Proc. 2nd Int. Congr. Catal.', Technip, Paris (1961), vol. 1, p.1083.
52. Cranstoun, G.K.L., and Thomson, S.J., Trans. Faraday Soc., 59, 2403 (1963).
53. Altham, J., and Webb, G., J. Catal., 18, 133 (1970).
54. Thomson, S.J., and Wishlade, J.L., Trans. Faraday Soc., 58, 1170 (1962).
55. Thomson, S.J., and Wishlade, J.L., J. Chem. Soc., p.4278 (1963).
56. Takeuchi, T., and Miyatani, D., Bull. Chem. Soc. Jap., 40, 58 (1967).
57. Cormack, D., Thomson, S.J., and Webb, G., J. Catal., 5, 224 (1966).
58. Al-Ammar, A.S., and Webb, G., J.C.S. Faraday I, 74, 195 (1978).
59. Norval, S.V., and Thomson, S.J., J.C.S. Faraday I, 75, 1798 (1979).
60. Norval, S.V., Thomson, S.J., and Webb, G., Appl. Surf. Sci., 4, 51 (1980).
61. Kummer, J.T., de Witt, T.W., and Emmett, P.H., J. Am. Chem. Soc., 70, 3632 (1948).
62. Parmentier, J.H., Peer, H.G., and Schutte, L., J. Catal., 22, 213 (1971).
63. Hightower, J.W., and Hall, W.K., J. Phys. Chem., 71, 1014 (1967).

64. Guzzi, L., La Pierre, B.R., Weiss, A.H., and Biron, E., J. Catal., 60, 83 (1979).
65. Derbentsev, Y.I., and Isagulyants, G.V., Russ. Chem. Rev., 38, 714 (1969).
66. Ozaki, A., in 'Isotopic Studies of Heterogeneous Catalysis', Academic Press, London (1977) p.78.
67. Bond, G.C., and Wells, P.B., Adv. Catal., 15, 91 (1964).
68. Taylor, G.F., Thomson, S.J., and Webb, G., J. Catal., 12, 150 (1968).
69. McKee, D.W., J. Am. Chem. Soc., 84, 1109 (1962).
70. Selwood, P.W., J. Am. Chem. Soc., 83, 2853 (1961).
71. Little, L.H., in 'Infrared Spectra of Adsorbed Species', Academic Press, London (1966) p.111.
72. Thomson, S.J., in 'Catalysis' (Specialist Periodical Reports), ed. C. Kemball, The Chemical Society, London (1977), vol.1, p.1.
73. Thomson, S.J., in 'Catalysis' (Specialist Periodical Reports), ed. C. Kemball, The Chemical Society, London (1980), vol.3, p.1.
74. Somorjai, G.A., Surf. Sci., 89, 496 (1979).
75. Bonzel, H.P., Surf. Sci., 68, 236 (1977).
76. Webb, G., in 'Surface and Defect Properties of Solids' (Specialist Periodical Reports), ed. M.W. Roberts and J.M. Thomas, The Chemical Society, London (1974), vol.3, p.184.
77. Touroude, R., and Gault, F.G., J. Catal., 32, 288 (1974).

78. Gault, F.G., Ledoux, M., Masini, J.J., and Roussy, G., in 'Proc. 6th Int. Congr. Catal.', ed. G.C. Bond, P.B. Wells and F.C. Tompkins, The Chemical Society, London (1977), vol.1, p.469.
79. Thomson, S.J., and Webb, G., J.C.S. Chem. Comm., p.526 (1976).
80. Weinberg, W.H., Deans, H.A., and Merrill, R.P., Surf. Sci., 41, 312 (1974).
81. Stephens, S.J., J. Phys. Chem., 62, 714 (1958).
82. Morrow, B.A., and Sheppard, N., Proc. R. Soc., A311, 391 (1969).
83. Morrow, B.A., and Sheppard, N., J. Phys. Chem., 70, 2406 (1966).
84. Prentice, J.D., Lesiunas, A., and Sheppard, N., J.C.S. Chem. Comm., p.76 (1976).
85. Sheppard, N., Chenery, D.H., Lesiunas, A., Prentice, J.D., Pearce, H.A., and Primet, M., in 'Proc. 12th Eur. Congr. Mol. Spectrosc.', ed. M. Grossmann, S.G. Elkomoss and J. Ringeissen, Elsevier, Amsterdam (1976) p.345.
86. Soma, Y., J. Catal., 59, 239 (1979).
87. Reid, J.U., Thomson, S.J., and Webb, G., J. Catal., 30, 378 (1973).
88. Al-Ammar, A.S., Thomson, S.J., and Webb, G., J.C.S. Chem. Comm., p.323 (1977).
89. Pickering, H.L., and Eckstrom, H.C., J. Phys. Chem., 63, 512 (1959).

90. Taylor, G.F., Thomson, S.J., and Webb, G., J. Catal., 12, 191 (1968).
91. Smith, D.L., and Merrill, R.P., J. Chem. Phys., 52, 5861 (1970).
92. Kesmodel, L.L., Dubois, L.H., and Somorjai, G.A., J. Chem. Phys., 70, 2180 (1979).
93. Demuth, J.E., Surf. Sci., 80, 367 (1979).
94. Ibach, H., Hopster, H., and Sexton, B., App. Surf. Sci., 1, 1 (1977).
95. Jenkins, G.I., and Rideal, E., J. Chem. Soc., p.2490 (1955).
96. Sheppard, N., and Ward, J.W., J. Catal., 15, 50 (1969).
97. Erkelens, J., and Wösten, W.J., J. Catal., 54, 143 (1978).
98. Nash, C.P., and Desieno R.P., J. Phys. Chem., 69, 2139 (1965).
99. Douglas, J.E., and Rabinovich, B.S., J. Am. Chem. Soc., 74, 2486 (1952).
100. Berndt, G.F. (personal communication).
101. Arthur, J.R., and Hansen, R.S., J. Chem. Phys., 36, 2062 (1962).
102. Hansen, R.S., and Gardner, N.C., J. Phys. Chem., 74, 3646 (1970).
103. Inoue, Y., and Yasumori, I., J. Phys. Chem., 73, 1618 (1969).
104. Bond, G.C., Catalysis, 3, 109 (1954).

105. Kesmodel, L.L., Stair, P.C., Baetzold, R.C., and Somorjai, G.A., Phys. Rev. Lett., 36, 1316 (1976).
106. Rooney, J.J., Gault, F.G., and Kemball, C., J. Catal., 1, 255 (1962).
107. Rooney, J.J., and Webb, G., J. Catal., 3, 488 (1964).
108. Rooney, J.J., J. Catal., 2, 53 (1963).
109. Dubois, L.H., Castner, D.G., and Somorjai, G.A., J. Chem. Phys., 72, 5234 (1980).
110. Sheppard, N., Pure App. Chem., 4, 71 (1962).
111. Avery, N.R., J. Catal., 19, 15 (1970).
112. Erkelens, J., J. Catal., 37, 332 (1975).
113. Cerny, S., Smutek, M., and Buzek, F., J. Catal., 47, 166 (1977).
114. Gland, J.L., and Somorjai, G.A., Adv. Coll. Interf. Sci., 5, 205 (1976).
115. Khulbe, C.P., and Mann, R.S., in 'Proc. 6th Int. Congr. Catal.', ed. G.C. Bond and F.C. Tompkins, The Chemical Society, London (1977), vol.1, p.447.
116. Gardner, N.C., and Hansen, R.S., J. Phys. Chem., 74, 3298 (1970).
117. Weinberg, W.H., Deans, H.A., and Merrill, R.P., Surf. Sci., 41, 312 (1974).
118. Dus, R., Surf. Sci., 50, 241 (1975).
119. Dus, R., and Lisowski, W., Surf. Sci., 85, 183 (1979).
120. Boudart, M., Adv. Catal., 20, 153, 1969.
121. Hattori, T., and Burwell, R. Jr., J. Phys. Chem., 83, 241 (1979).

122. Dalmai-Imelik, G., and Massardier, J., in 'Proc. 6th Int. Congr. Catal.', ed. G.C. Bond and F.C. Tompkins, The Chemical Society, London (1977), vol.1, p.90.
123. Sheridan, J., J. Chem. Soc., p.373 (1944).
124. Sheridan, J., J. Chem. Soc., p.133, 301, 305 (1945).
125. Sheridan, J., and Reid, W.D., J. Chem. Soc., p.2962 (1952).
126. Bond, G.C., and Wells, P.B., J. Catal., 4, 211 (1965).
127. Bond, G.C., Webb, G., and Wells, P.B., J. Catal., 12, 157 (1968).
128. Bond, G.C., J. Chem. Soc., p.2705 (1958).
129. Bond, G.C., and Mann, R.S., J. Chem. Soc., p.3566 (1959).
130. Bond, G.C., Dowden, D.A., and Mackenzie, N., Trans. Faraday Soc., 54, 1537 (1958).
131. Bond, G.C., and Mann, R.S., J. Chem. Soc., p.4738 (1958).
132. Bond, G.C., Newham, J., and Wells, P.B., in 'Proc. 2nd Int. Congr. Catal.', Technip. Paris (1961), vol.1, p.1177.
133. Douglas, J.E., and Rabinovich, B.S., J. Am. Chem. Soc., 74, 2486 (1952).
134. Bond, G.C., J. Chem. Soc., p.4288 (1958).
135. Bond, G.C., and Wells, P.B., J. Catal., 6, 397 (1966).
136. Al-Ammar, A.S., and Webb, G., J.C.S. Faraday I, 74, 657 (1978).
137. McGown, B.T., Kemball, C., Whan, D.A., and Scurrrell, M.S., J.C.S. Faraday I, 73, 632 (1977).

138. Webb, G., in 'Comprehensive Chemical Kinetics', ed. C.H. Bamford and C.F.H. Tipper, Elsevier, Amsterdam (1978), vol.20, p.1.
139. Bond, G.C., and Sheridan, J., Trans. Faraday Soc., 48, 658 (1952).
140. Mann, R.S., and To, E.D., Can. J. Chem., 46, 161 (1968).
141. Mann, R.S., and Tiu, D.E., Can. J. Chem., 46, 3249 (1968).
142. Mann, R.S., and Shah, A.M., Can. J. Chem., 50, 1793 (1972).
143. Bond, G.C., Webb, G., Wells, P.B., and Winterbottom, J.M., J. Catal., 1, 74 (1962).
144. Oliver, R.G., and Wells, P.B., J. Catal., 47, 364 (1977).
145. Baró, A.M., and Ibach, H., J. Chem. Phys., 71, 4812 (1979).
146. Dubois, L.H., and Somorjai, G.A., Surf. Sci., 91, 514 (1980).
147. Bradshaw, A.M., and Hoffmann, F.M., Surf. Sci., 72, 513 (1978).
148. Kroeker, R.M., Kaska, W.C., and Hansma, P.K., J. Catal., 57, 72 (1979).
149. Sheppard, N., and Nguyen, T.T., in 'Advances in Infrared and Raman Spectroscopy', ed. R.J.H. Clark and R.E. Hester, Heyden, London (1978), vol.5, p.67 and references therein.
150. Eischens, R.P., and Pliskin, W.A., Adv. Catal., 10, 1 (1958).
151. Blyholder, G., J. Phys. Chem., 68, 2772 (1964).

152. Yang, A.C., and Garland, C.W., J. Phys. Chem., 61, 1504 (1957).
153. Yates, D.J.C., Murrell, L.L., and Prestidge, E.B., J. Catal., 57, 41 (1979).
154. Yao, H.C., and Rothschild, W.G., J. Chem. Phys., 68, 4774 (1978).
155. Yates, J.T., Duncan, M.T., and Vaughan, R.W., J. Chem. Phys., 71, 3908 (1979).
156. Grant, J.T., and Haas, T.W., Surf. Sci., 21, 76 (1970).
157. Wilson, G.R., and Hall, W.K., J. Catal., 17, 190 (1970).
158. Yates, D.J.C., and Sinfelt, J.H., J. Catal., 8, 348 (1967).
159. Wankle, S.E., and Dougharty, N.A., J. Catal., 24, 367 (1972).
160. Reid, J.U., Thomson, S.J., and Webb, G., J. Catal., 29, 421 (1973).
161. Csicsery, S.M., and Pines, H., J. Chromatog., 9, 34 (1962).
162. Matucha, M., and Smolkova, E., J. Chromatog., 127, 163 (1976).
163. Schmidt-Bleek, F., and Rowland, F.S., Anal. Chem., 36, 1695 (1964).
164. Lieser, K.H., Elias, H., and Sorg, F., Z. Anal. Chem., 191, 104 (1962).
165. Bernstein, R.B., and Taylor, T.I., Science, 21, 498 (1947).

166. Reid, J.U., Ph.D. Thesis, University of Glasgow, 1971.
167. Al-Ammar, A.S., Ph.D. Thesis, University of Glasgow, 1977.
168. Bond, G.C., and Wells, P.B., J. Catal., 5, 65 (1966).
169. Reid, J.U., Thomson, S.J., and Webb, G., J. Catal., 30, 372 (1973).
170. Sexton, B.A., and Somorjai, G.A., J. Catal., 46, 167 (1977).
171. Solymosi, F., Erdöhelyi, A., and Kocsis, M., J. Catal., 65, 428 (1980).
172. Primet, M., J.C.S. Faraday I, 74, 2570 (1978).

GLASGOW  
UNIVERSITY LIBRARY  
1980